089030-9-T

COO-1705-9

3 cys

THE UNIVERSITY OF MICHIGAN

COLLEGE OF ENGINEERING
DEPARTMENT OF METEOROLOGY AND OCEANOGRAPHY

Technical Report

Sources of Trace Elements in Aerosols - An Approach to Clean Air

KENNETH A. RAHN

JOHN W. WINCHESTER
Project Director

Under contract with:

U. S. Atomic Energy Commission
Chicago Operations Office
Contract No. AT(11-1)-1705
Argonne, Illinois

Administered through:

May 1971

OFFICE OF RESEARCH ADMINISTRATION • ANN ARBOR

DISCLAIMER

THE UNIVERSITY OF MICHIGAN

COLLEGE OF ENGINEERING
Department of Meteorology and Oceanography

Technical Report

SOURCES OF TRACE ELEMENTS IN AEROSOLS - AN APPROACH TO CLEAN AIR

Kenneth A . Rahn

John W. Winchester
Project Director

ORA Project 089030

Under contract with

U. S. ATOMIC ENERGY COMMISSION
CHICAGO OPERATIONS OFFICE
CONTRACT NO. AT(11-1)-1705
ARGONNE, ILLINOIS

administered through:

OFFICE OF RESEARCH ADMINISTRATION ANN ARBOR

May 1971

spent many hours reading and editing the manuscript, as well as offering long discussions in time of need.

My typists, Mrs. G. Smith and Mrs. E. Rentschler labored long and hard on a tight schedule.

Many individuals aided in field sampling. Thanks to Mr. and Mrs. C.L. Haslett and D.C. Haslett of Niles; Dr. E.T. Petersen, R. McCready, and D. Francis of Mackinac Island State Park; R. Duston and A. Findlay of Algonquin Radio Observatory; P.A. Lange and A.C. Doan of Riding Mountain National Park; J.B. Heppes, B. Roper, and E. Sipes of Prince Albert National Park; G. Trachuk, M. Elder, and S. Marty of Jasper National Park; R.L. Vance and A.W.J. Whitford of Northern Canada Power Commission.

Lastly I would like to thank the staffs of the Ford Nuclear Reactor and Phoenix Memorial Laboratory, The University of Michigan, J.D. Jones in particular, who made my stay there so pleasant.

This work was supported in part by the U.S. Atomic Energy Commission, Contract No. AT(11-1)-1705.

TABLE OF CONTENTS

TABLE OF CONTENTS (continued)

TABLE OF CONTENTS (continued)

TABLE OF CONTENTS (continued)

LIST OF TABLES

LIST OF TABLES (continued)

LIST OF TABLES (continued)

LIST OF TABLES (continued)

LIST OF TABLES (continued)

LIST OF FIGURES

LIST OF FIGURES (continued)

LIST OF FIGURES (continued)

LIST OF FIGURES (continued)

LIST OF FIGURES (continued)

LIST OF FIGURES (continued)

LIST OF FIGURES (continued)

THIS PAGE
WAS INTENTIONALLY
LEFT BLANK

ABSTRACT

SOURCES OF TRACE ELEMENTS IN AEROSOLS -
AN APPROACH TO CLEAN AIR

by
Kenneth Albert Rahn

Co-Chairmen: A. Nelson Dingle
John W. Winchester

The objective of this research was to assess the impact of distant (anthropogenic) aerosol sources on the trace element composition of surface air in remote regions of North America. An optimized nondestructive neutron activation analytical technique was developed for determination of some 30 trace elements and was tested with three pilot studies. These studies, one of the areawide concentration variations and two of diurnal variations, also served to document some features of typical source areas. Final sampling took place at seven locations, ranging from lower Michigan to Northwest Canada.

By use of total elemental concentrations (from filter samples) and particle size distributions (from Andersen cascade impactors) the following results were achieved:

1) Sources or source process types were identified for each element at each location.
2) The relative importance of long-range transport was estimated for the different elements

3) The relative importance of various aging and removal processes on the chemical composition of the aerosol was observed.

4) Baseline concentration data were established.

5) A new assessment of the limits of composition and relative location of clean air over North America was made.

Most elements are associated with the larger aerosol particles and appear to have soil and soil dust as their main source. Remote locations show more elements of this type than do urban areas, and at a given location the soil influence was less in winter than in summer. These large-particle elements are usually light metals or rare earths, though a few other heavy metals are also in this group.

Many atmospheric elements have major non-soil sources even when observed in the most remote regions. These elements, usually associated with the smaller particles, vary more in concentration and size-distribution shape from populous to remote regions than do the soil-derived elements. They tend to be nonmetals or heavy metals, and often have relatively volatile compounds.

Multielement long-range transport can be inferred clearly in two instances, one for industrial emissions traveling probably a few hundred km to Algonquin Provincial Park, Ontario, the other for marine aerosol traveling probably a few thousand km to Fort Smith, NWT. In the latter case the aerosol appears

unchanged except for a ten-fold dilution and a loss of Cl from the smallest particles.

Gas-particle interactions are inferred for Br, but most other evolutionary processes appear to be physical in nature.

Although the more remote areas showed generally decreasing proportions of pollution products, certain elements remained anomalously high at these locations. "Clean" air, meaning air free of anthropogenically-derived aerosol particles, was therefore approached but not seen in this work.

PART I

REMOTE CONTINENTAL MEASUREMENTS

CHAPTER I

STATEMENT OF THE PROBLEM

A. Introduction

The focus of attention in this investigation is the measurement of trace elements in aerosol particle samples from surface continental air remote from urban or industrial sources. Since this problem has received little attention up to the present time, a balance has been struck between a specialized study of specific processes and a general survey intended to provide baseline data and to reveal new lines of inquiry not previously recognized. For this investigation a new neutron activation analysis procedure has been developed for obtaining high quality measurements of more than 30 trace elements in particle samples, and special sampling procedures suitable to this technique have been tested. Pilot studies in and near an urban source region have been conducted in order to permit preliminary evaluation of several possible chemical and atmospheric relationships of interest. Then a major study of surface aerosols from northern and western Canada and rural Michigan was conducted. These distinct phases of the investigation are treated in

detail in the Appendix, in Part II, and in Part I, respectively. This chapter presents some background information germane to the investigation and a full statement of the problem.

B. Limitations of Previous Investigations

Most of the previous studies of atmospheric trace elements have been confined to urban source regions. The National Air Sampling Network (U.S. Department of Health, Education, and Welfare, 1968) uses emission spectroscopy to determine 16 metals at 200 locations in the United States. Lee and Jervis (1968) analyzed Toronto air for 13 trace elements, using neutron activation.

Hashimoto and Winchester (1967) determined Se in rain and snow samples from Cambridge, Massachusetts. Lininger et al. (1966) suggest an escape of Br from particles into the air of Cambridge, Massachusetts. Kneip et al. (1969) determined several trace elements at 3 locations in New York City, and related concentration trends to seasonal and shorter-period variables.

Brar et al. (1970) determined 20 trace elements in Chicago surface air by instrumental neutron activation analysis. Lee et al. (1968) used atomic absorption spectroscopy and Andersen Samplers to measure particle size distributions of 6 metals in Cincinnati and Fairfax, Ohio. Keane and Fisher (1968) have used nondestructive neutron activation analysis to determine 7 elements in air over England.

Harrison (1970) studied the areawide distribution of Pb, Cu, and Cd in air over Northwest Indiana by means of anodic stripping voltammetry. Nifong (1970) used nondestructive neutron activation analysis to measure the particle size distribution of 29 elements, also in Northwest Indiana.

A few studies have been performed on trace elements in very remote locations. Murozumi et al. (1969) have measured Pb in Antarctic snow and ice. Chow et al. (1969) have measured Pb in air over remote Pacific Ocean locations and claim to see effects of transport from continental areas. Weiss et al. (1971) determined S and Se in a Greenland ice sheet and found S but not Se to be relatively enriched during the last century.

In contrast to the above, only a very few studies have been performed on trace elements in less remote locations subject to pollution aerosol influence. Egorov et al. (1970) studied 9 trace elements in aerosols of the USSR, at sites ranging from urban to polar. Hoffman et al. (1969) measured Na, Cu, Al, and V over the Pacific Ocean between North America and Hawaii. But little systematic multielemental work seems to exist for remote continental areas.

C. Some Properties of Aerosols

Aerosols are suspensions of solid or liquid particles and are the carriers of the trace elements of interest in this investigation. Stable atmospheric aerosols contain particles which range in size from diameters of 0.01 μm to 100 μm, or

four orders of magnitude. Particles smaller than 0.01 μm rapidly coagulate, and those larger than 100 μm are quickly removed by sedimentation. Within the stable range tropospheric lifetimes may vary from minutes to months, depending on size, water solubility, and chemical reactivity.

The distribution of an aerosol particle population is defined by

$$n(r) = dN/d(\log r)$$

where N is the total concentration of aerosol particles of radius less than r. Because of the large size range involved, the use of log r rather than r is preferred. Junge (1963) has observed that for a wide range of sizes (0.1 μm < r < 10 μm) the tropospheric aerosol over populated continental areas has an average distribution function very close to

$$n(r) = Cr^{-\beta}$$

where C is a constant and β is empirically ≈ 3. Recent work (Junge, 1969) has extended the upper limit of this dependence to r $\approx$ 100 μm.

Aerosols have a multiplicity of significant natural and anthropogenic sources. This topic is treated in detail elsewhere (Fletcher, 1966), and specific sources will be considered in later chapters.

Aerosol generation processes are often regarded to be of two basic types, dispersion and condensation. Dispersion

refers to mechanical subdivision, and tends to produce particles larger than about 0.1 μm in diameter. This lower limit may arise from the increasingly large amounts of surface free energy associated with smaller particle sizes. Condensation from the vapor phase, on the other hand, may produce particles initially of diameter less than 0.1 μm. However, in the real world aerosol particles may result from a complex series of interactions which may become more fully understood through the results of this present investigation of chemical composition.

Once generated, several processes act to modify the atmospheric aerosol population. Brownian coagulation, the theory of which was formulated by Smoluchowski (1916), is said by Junge (1963) to be the most effective mechanism for reducing the concentration of small particles in the atmosphere.

Sedimentation, or dry fallout, is determined by particle size, shape, and density. For unit density spheres of 10 μm radius, the settling velocity is about 1 cm/sec, varying with the square of the radius. For radii > 10 μm sedimentation may be the dominant removal mechanism in quiet near-surface air; for smaller particles it rapidly becomes insignificant with decreasing particle size.

Friedlander (1960) proposed a dimensional argument similar to the type used in turbulence theory to explain the observed particle-number distributions over populated continental areas. For the subrange $r \geq 0.1$ μm he invoked Brownian coagulation

and sedimentation as the only effective modification mechanisms, showing that any initial distribution with mass entering at the lower size end by coagulation and leaving at the upper end by sedimentation would eventually lead to a final steady state. This unique final steady state would have a particle-number distribution similar to the "Junge" distribution.

Junge (1963), however, explains this distribution in terms of superposition of many spectra, each arising from a single process (probably with a log-normal shape). The resultant mixture would be variable, as is actually seen, but should on the average produce a broad log-normal distribution similar to the "Junge" distribution. Junge (1969) also shows that the dynamic equilibrium proposed by Friedlander cannot generally be approached within the time scale of meteorological changes than in the troposphere.

Dry impaction may be an effective mechanism for removal of particles smaller than 10 μm. The effects of electrical charges and turbulence on this process are, however, poorly understood (Slade, 1968).

Wet removal of particles from the atmosphere may proceed by cloud droplet nucleation (rainout) or washout beneath the cloud. Rainout is particularly effective for soluble particles and those with diameters greater than a few tenths of a micron, while washout is a purely physical mechanism effective for particles with diameters > 1 μm (Fletcher, 1966).

Size Distributions. The number distribution over particle size (n(r)) and the volume distribution v(r) have been studied often for the total aerosol (Junge, 1963). Corresponding studies of mass or volume distribution for the individual chemical components are much less abundant, and represent the focus of much of this work.

Knowledge of the mass distribution over particle size (referred to below as "particle size distribution") of the elements is already recognized as important because of the particle size dependence of processes such as cloud droplet nucleation (Fletcher, 1966), deposition in the respiratory tract (Cadle, 1965), and catalysis of atmospheric reactions, including the oxidation of SO_2 (Johnstone and Moll, 1960). In addition, this work demonstrates the utility of particle size distributions for source identification and assessment of transport and removal processes.

All particle size distributions in this investigation were obtained using the Andersen Sampler (Model 0203), modified by addition of a seventh impaction stage. For some of the earlier work an in-line backup filter was also added. The principles of operation of the Andersen Sampler have been discussed elsewhere (Nifong, 1970).

The "cutoff" diameter, or the particle size for which 50 percent of the particles will be impacted on a stage, is commonly used as the minimum collection diameter. It may be calculated by the formula

$$D^2_{min} = \frac{36\mu d}{\pi\sigma V}$$

where D_{min} = minimum diameter

μ = air viscosity

σ = particle density

V = particle velocity

d = minimum width of an air streamline

Empirical calibrations of the Andersen Sampler are reported by Andersen (1966), Flesch et al. (1967), and May (quoted in Flesch et al., 1967). Their results are shown in Table I-1.

Gillette (1970) calculated the cutoff diameter for stage 7 from the above equation, and found it to be 0.40 μm.

All the above cutoff diameters apply only to the optimum sampling rate of 1.7 m^3/hr (1.0 cfm). Occasionally it is desirable to operate the impactor at higher flow rates, and the above equation shows that the cutoff diameter varies inversely as the square root of the flow rate. Figure I-1 shows these variations over some practical flow rates.

It is important to keep in mind the performance difference between the "inner" and "outer" stages of an Andersen Sampler. Stages 2-7 collect differential ranges, while stage 1 and the backup filter collect everything above and below a given size, thus being equivalent to more than one of the inner stages. Gillette (1970) has calculated how a "Junge" distribution

should be impacted by the Andersen Sampler (Table I-2). Here it is seen that stage 1 and the filter show peaks, but that the other stages collect approximately equal masses, a consequence of their cutoff radius ratios of about a factor of two from stage to stage. Thus an element with equal mass in equal log-radius increments of the aerosol will indeed show nearly a "flat" distribution in our results.

D. Analytical Techniques

The very low concentrations of individual trace elements in rural and remote surface air (10^3 - 10^{-3} ng/m^3) place a great premium on sensitivity of the analytical method. In addition, the chemical complexity of the aerosol requires extreme specificity to sufficiently reduce interferences. The large numbers of samples requiring analysis in any environmental study demand a rapid method.

To meet these conditions we have developed a computer-assisted nondestructive (instrumental) neutron activation analytical technique, optimized for analysis of airborne particles on inorganically clean filters and impaction surfaces (Appendix 2a). It combines the proven sensitivity of neutron activation with the recent advances in solid-state Ge(Li) gamma-ray detectors to allow routine detection of some 30 trace elements in most samples.

The high quality of data obtained with this technique (many elements have precisions of measurements as low as 10

percent) makes possible a detailed study of relative elemental composition both of the total aerosol and of size fractions within the aerosol. The resulting information finds much use as an indicator of atmospheric geochemical processes.

In spite of the analytical success achieved here, there is still room for much greater sensitivity. Remote measurements still are difficult because of the low concentrations involved, especially with the Andersen Sampler (Appendix 1b). Time-variation studies, where short-period samples are particularly desirable, are at present restricted to 1-2 hours per sample. Improvements in the present technique, or developments of companion techniques would be desirable.

E. Pilot Studies

Part II contains detailed descriptions of three pilot studies, each of which bears on the major remote study of Part I. The Northwest Indiana survey provided the first full-scale test of the analytical technique under heavily polluted conditions, and demonstrated the detectability and reproducibility of approximately 30 elements. These elements showed large differences in source patterns, and could be grouped according to source strengths. In addition, elemental pairings and groupings could be established based on the areawide concentration patterns. A number of elements (Na, K, Eu, Sm, Ti) were seen to have predominantly natural sources, while several others (Cu, W, Fe, Zn, Sb, Ag, Hg) showed strong, localized pollution sources.

The Niles, Michigan diurnal variations study revealed differences in patterns among the elements. Several elements, such as Al, K, and Na, showed parallel variations suggestive of elevated pollution sources at a distance. Br, on the other hand, varied with local traffic density. Several of the elements showed rapid removal at night, possibly related to involvement with nucleation during formation of local ground fog.

The Livermore, California diurnal variations study again revealed differences in behavior among the elements. Several showed patterns in accord with a local soil origin (the same elements which at Niles showed distant pollution sources), while Zn, Sb, and Br appeared to have pollution sources. Na and Cl appeared to be marine in origin.

Finally, it should be pointed out that the present investigation was carried out in cooperation with other workers in the same laboratory conducting related University of Michigan Ph.D. dissertation investigations. The completed dissertations which bear most directly on the present investigation are:

Gordon D. Nifong, Particle Size Distributions of Trace Elements in Pollution Aerosols, August 1970.

Paul R. Harrison, Area-Wide Distribution of Lead, Copper, Cadmium, and Bismuth in Atmospheric Particles in Chicago and Northwest Indiana: A Multi-Sample Application and Anodic Stripping Voltammetry, May 1970.

Completed dissertations which also relate closely to the present investigation are:

Dale A. Gillette, A Study of Aging of Lead Aerosols, February 1970.

Ronald H. Loucks, Particle Size Distributions of Chlorine and Bromine in Mid-Continent Aerosols from the Great Lakes Basin, August 1969.

The interested reader is referred to these dissertations for many findings pertinent to the present investigation.

F. Objectives of This Research

The fundamental objective of this research is to assess the impact of distant (anthropogenic) aerosol sources on the air of remote regions of North America. By observing the change of concentration and particle size distribution of the various elements in air over increasingly remote continental areas it was hoped to

1) identify sources (or source process types) for each element at each location,
2) estimate the relative importance of long-range transport among the elements,
3) observe the relative importance of various aging and removal processes on the chemical composition of the aerosol,
4) establish remote-area chemical baseline data for 1970,
5) estimate the degree of approach to "clean" air exhibited over northern North America.

TABLE I-1. Calibration of the Andersen Sampler

	50 Percent Cutoff Diameters, μm						
Stage	1	2	3	4	5	6	7
Andersen	9.2	5.5	3.3	2.0	1.0	---	---
Flesch (avgd.)	---	5.35	3.28	1.76	0.89	0.54	---
May	---	5.5	3.5	2.6	1.1	---	---

TABLE I-2. Percent of Total Mass vs. Andersen Sampler Stage for the "Junge" Distribution (after Gillette, 1970)

AS Stage	Percent of Total Mass
1	25.0
2	9.8
3	9.8
4	9.8
5	11.1
6	9.8
7	8.4
F	16.4

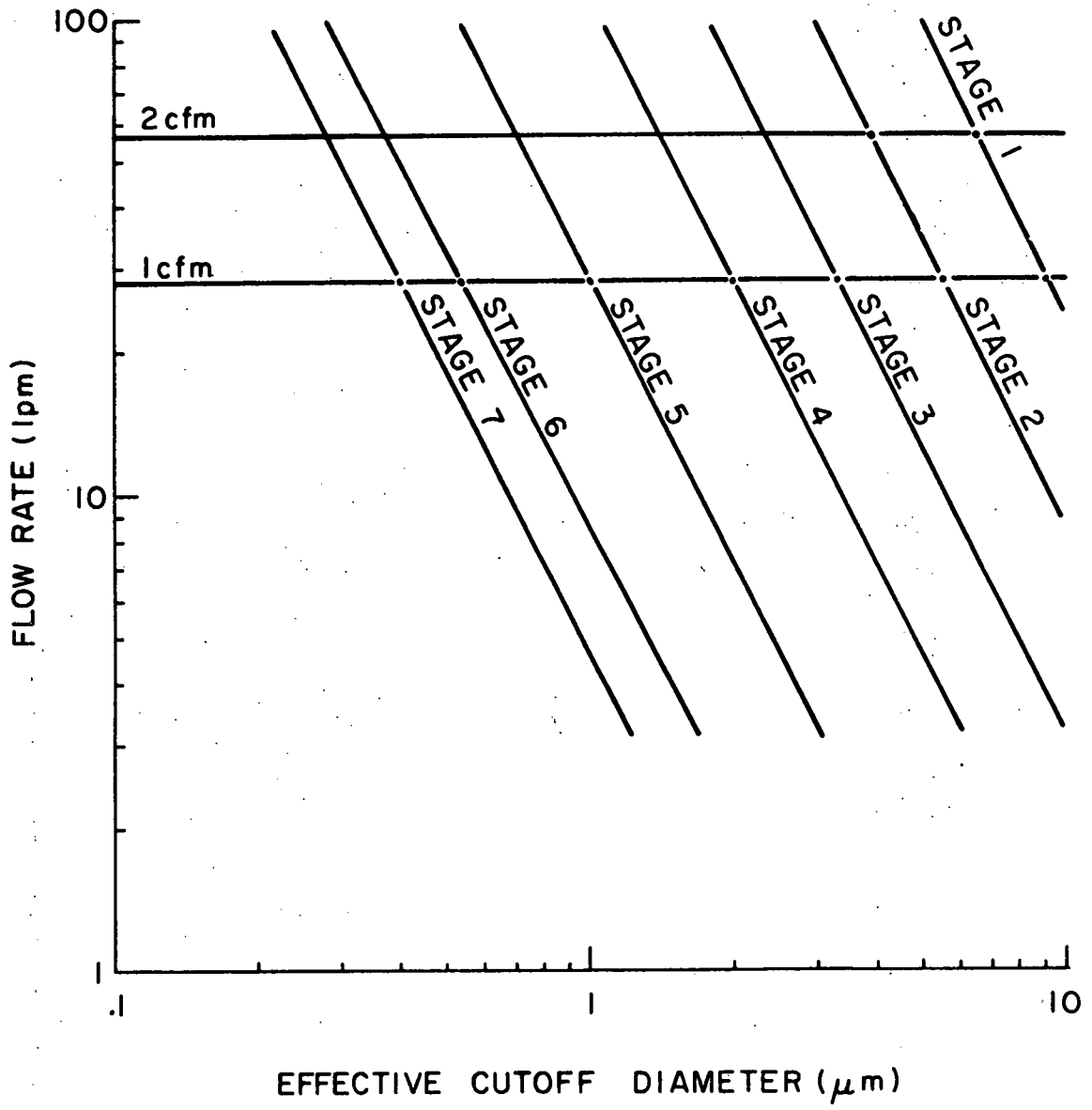

Figure I-1 Flow Rate Dependence for the Effective Cutoff Diameters of the Andersen Sampler

CHAPTER II

EXPERIMENTAL DESIGN AND SUMMARY OF RESULTS

A. Introduction

The Northwest Indiana survey, presented in Part II, provided a general picture of the areawide variation patterns of some 30 trace elements for a major industrial area. Strong sources for several of these elements (Cu, W, Cr, Zn, Sb, Br, Ag, Fe, Mn, Hg, As, and Se) were seen but were fewer in number for each element and more restricted in area of influence than had been anticipated. Several of the light metals and rare earths (Na, K, Al, Ca, Sm, and Eu) showed only weak sources, approximately as expected.

One surprising result was the height of the concentration levels at Niles. Though well outside of the Northwest Indiana urban area, Niles had levels less than an order of magnitude below the highest urban network values of most elements, including some of those with strong sources (Table VI-10). For pollution elements such as Cu, As, Se, etc., this effect was possibly due to nearby sources in the South Bend, Indiana area, but for the more common ones it seemed to reflect the presence of the same high background levels which masked the weaker Northwest Indiana sources.

Urban-industrial measurements represented only part of our ultimate experimental goals. Complementary to the Northwest Indiana study was to be a series of similar measurements in areas relatively free of anthropogenic effects. The Niles station had served as a test of the distance scale to the "background" regions, with the result that the high concentrations found here clearly dictated an upward revision of our minimum sampling separation from the tens of km of Niles-Northwest Indiana to something more like hundreds or thousands of km.

A number of results might be expected from such remote measurements. Comparison of concentration levels might reveal elements with area sources too diffuse to stand out clearly in a grid the size of that used in Northwest Indiana. Particle size measurements might afford assessment of systematic aging effects on the aerosol population, since the aerosol of remote areas could be expected to be more aged than that near major source areas. Relative contributions of natural sources (soil, for example) and pollution sources to the aerosol might also be estimated by comparisons of particle size distributions at different locations. Finally, the effect of source particle size distributions on long-range transport might be evaluated, for the smaller particles should not be removed from the atmosphere as rapidly as the larger ones.

With these as typical goals, a series of experiments was undertaken, as described below.

B. Site Selection and Sampling

Sampling was conducted in three phases, considered in detail below:

1. Mackinac Island Experiment - Site Selection

The first phase, called the Mackinac Island Experiment, took place during January and February 1970 and involved four locations in Indiana and Michigan. Two sites in East Chicago, Indiana, were chosen as heavily industrialized locations, namely Markstown Park and East Chicago Central Fire Station. The Markstown Park site is near the Lake Michigan shoreline (Figure II-1) and in particular near to the grounds of two major steel corporations. The Central Fire Station site is nearer the center of East Chicago and is surrounded by an oil refinery, a foundry, a chemical company, and a refractories operation.

The Michigan sites were Ann Arbor (roof of the School of Public Health Building, The University of Michigan) and Mackinac Island. Ann Arbor is a small city (population 100,000) with little heavy industry, chosen to be intermediate in character between East Chicago and Mackinac Island. The remote location was chosen to be Mackinac Island, Michigan, located some 500 km north of Ann Arbor.

Mackinac Island has several features which make it desirable for trace element sampling. The nearby mainland has a low population density, with the nearest heavy industry

80 km north in Sault Ste. Marie. Most of the island is the Mackinac Island State Park, from which all autos are banned, this restriction in practice limiting autos from the entire island. Thus, auto exhaust products measured by neutron activation analysis (Cl and Br) cannot here have automotive sources nearer than the town of St. Ignace, a few miles away. The low winter population of the island assures a minimum of local emissions of fossil fuel combustion products (home heating is by oil and electric heat).

The Mackinac Island State Park Commission maintains a full staff on the island during the winter, some of whom assisted with the sampling. Travel requirements to and from the site were thereby minimized and kept to a workable level.

The island is roughly 500 km NNE of the source regions of Milwaukee, Chicago, and Northwest Indiana. As suggested by the annual wind rose for Midway Airport, Chicago (Figure VI-2), the mean air trajectory starting from these sources is toward Mackinac Island. Study of the actual wind patterns during the sampling period confirms that some of the air sampled at the island may indeed have previously passed over these source regions.

2. Sampling Program

This experiment was composed of two 3-week segments. During the first of these, 7-stage Andersen Samplers (impaction surfaces of Durethene polyethylene, no backup filter) were run simultaneously at Ann Arbor and Mackinac Island. Only a

single run was made at each location, the 3-week duration being calculated from estimated atmospheric concentrations as necessary to accumulate enough aerosol mass per stage to guarantee an analytical precision of the long-lived isotopes comparable to that of the short-lived species (see Appendix 1b for remarks on problems of determination of long-lived isotopes in Andersen samples). In spite of the increased precision obtained from these longer-period samples, separate filter samples were still judged to better estimate the total elemental concentrations in the aerosol, because of their greater ease of replication and much larger aerosol masses than individual Andersen stages. To this end, three 1-week filter samples (Microsorban, 47 mm diameter) were taken in parallel with the first impactor run at Mackinac Island.

All impactor runs in this series of remote experiments were taken without backup filters. Introduction of such a filter into the system, while highly desirable because it extends the collection range down to particles of diameter well under 0.1 μm, causes a tenfold increase in the pressure drop compared to the impactor alone. Flow rates will then be very sensitive to the condition of the filter, and as it clogs the flow rate decreases. The collection properties of each stage then change, "smearing out" the observed size distributions with time.

The pumps used here (Gelman Twin Cylinder) have enough reserve vacuum to compensate for the clogging and maintain

constant flow rate, but this requires manual adjustment of a flow control, attention to two gauges, and use of a flow rate correction chart. Such an operation is quickly performed by a trained worker, but should be done at least daily. It was felt that this was too much to expect from the inexperienced volunteers at the various field locations. The backup filters were therefore eliminated, and the sampling procedure greatly simplified.

Lack of a backup filter obviously entailed the sacrifice of important information on elements normally found with a significant fraction of their mass on this stage (such as Br and V). Because these smallest particles are the ones most affected by coagulation processes, filter information would have been highly useful. In future studies this problem warrants more consideration.

During the second three-week period impactor samples were taken at each of the four locations, but no total filters were run. Details of the sampling sequence are listed in Table II-1.

3. Canadian Summer Experiment - Site Selection

The second phase of the remote sampling program extended both the scale and remoteness of the experiment, seven stations being used from lower Michigan into Northern Canada. Canada was chosen as the site of the remote locations both because of its low population density and its behavior as a source

region for air masses which subsequently move southeastward into the United States. For these reasons the air sampled in Canada's north has not recently passed over major sources of pollution, and so should show minimal anthropogenic effects.

By sampling a series of locations varying in character from semi-urban to highly remote it was considered possible that smooth patterns of concentration dropoff would be seen, which might indicate the extent to which a true continental "background" had been achieved or was achievable. Such trends would also be useful in guiding future experiments designed to measure this background.

In addition, the concentration levels themselves are significant as reference points for future measurements, serving as benchmarks against which trends with time can be determined. Though conclusions in this regard cannot be drawn from a single study, it is clearly important to establish the reference levels as soon as the technology warrants.

The seven station sites are shown in Figure II-2, and described below.

1) Niles, Michigan

This is the same station used in the Northwest Indiana study and is located on a farm in the southwest corner of Michigan. Though the immediate environs are rural, it is only 15 km north of South Bend, Indiana and 100 km ENE of Gary, Indiana. Results of the previous

experiment suggest that the site might be better classed as semiurban. It was chosen to represent a typical United States midwestern environment and was expected to give the highest concentrations of the network.

2) Mackinac Island, Michigan

This is the same site described in the preceding section.

3) Algonquin Provincial Park, Ontario

Located some 350 km north of Toronto, this site was chosen to represent continental eastern Canada. The sampler was located at the Algonquin Radio Observatory in the northeast corner of the corner of the park. A site was selected in a small meadow at the western (typically upwind) end of the observatory grounds, about 100 m from the nearest building. Access to the observatory is gained via some 80 km of gravel roads, but all roads on the grounds are paved to facilitate moving of delicate equipment and road dust fallout seemed negligible. The park as a whole is heavily forested and logging operations constitute the major activity other than recreation.

4) Riding Mountain National Park, Wasagaming, Manitoba

This park is located in southern Manitoba atop a major escarpment rising above the surrounding prairie. The sample site was at the McKinnon Creek Warden Station

at the extreme eastern extent of the park and at the base of the escarpment. The sampler was placed behind a small garage in such a position that free air circulation was maintained. To the immediate west of the site is forested park, with the prairie beginning just east of the site. The area is not densely populated, but nearly all the prairie land in the immediate vicinity is under cultivation. The nearest large cities are Winnipeg (200 km east) and Regina, Saskatchewan (300 km west). North of the park the farm land rapidly gives way to forest and lakes.

5) Prince Albert National Park, Waskesiu Lake, Saskatchewan

This park is in central Saskatchewan and is considerably more remote than is Riding Mountain, being completely north of the major farming areas. The nearest large cities are Saskatoon (150 km south) and Edmonton, Alberta (300 km west). Sampling equipment was located at Blue Bell Lookout Tower, on a hill 100 m above the surrounding country.

6) Jasper National Park, Jasper, Alberta

This is the only mountainous station of the network, the site being at Maligne Lake (2000 m above sea level). Because the warden station here is located some 50 km by road from the Jasper townsite, land line electric power is not available and a diesel generator is used instead.

The sampler was located as nearly upwind from the generator as could be determined, and about 75 m away from it. In spite of the electric power handicap, this site appeared to offer the most desirable combination of remoteness features of any comparable location in the park. The only industry near Jasper is a pulp processing plant some 30-40 km east, and though advection of effluent from this industry to Maligne Lake is possible, the circuitous route required presumably would afford much dilution.

7) Twin Gorges Hydroelectric Project, Northwest Territories

From all appearances this site is the most remote of the network and was indeed chosen for this purpose. It is at a small power dam facility 50 km north of Ft. Smith, NWT, a town of 2,500 people which is located just north of the Alberta NWT border, 60° North latitude. Population density is very low this far north, with towns being generally under 3,000 in population and separated by 100-200 km at the minimum. The next nearest town to the site is Hay River, population 3,000, about 200 km west. There is some mining activity in the area (at Pine Point, for example, 150 km west), and the Yellowknife region to the northwest is so named from its gold deposits. A smelter at Yellowknife is said to operate intermittently.

Other than the above, the area is almost completely undeveloped.

The location of the sampler here was among the best of the network. It was placed on a platform above the water intake, free from any spray and away from land by 20 m or so. Prevailing winds are light and off the lake. The site is accessible only by air, with the nearest roads being at Ft. Smith. The only local vehicular traffic is a pickup truck used for maintenance.

4. Sampling Program

As in the Mackinac Island experiment, impactors and total filters were both used. Each station followed the identical sampling sequence, namely, a 3-week Andersen Sampler run followed by four 2-week filter samples (47 mm diameter). The duration of the filter samples was lengthened to two weeks in an attempt to compensate for the lower elemental concentrations expected in these more remote areas. The 47 mm filter size was chosen because it provides greater flow rates than does the 25 mm size, as well as decreased clogging caused by dust loading. As before, the impaction surfaces were Durethene polyethylene but the filter material was now Whatman No. 41. The use of this new filter material was dictated by a combination of decreasing supply of Microsorban, and by our experiments on Whatman No. 41, which had shown it to be a completely acceptable substitute for, and in some ways even superior to the Microsorban (Appendix 1a).

The impactor sample was taken first so that the writer could make the exact flow rate adjustments (1.0 cfm is optimum) at the time of installation of equipment at a site. At the conclusion of the run, the impactor was removed by the local volunteer, sealed, and set aside until the end of the summer when it was unloaded by the writer. For the filter runs (with the same pump) the volunteer simply turned the flow rate control to maximum and left it there for the remainder of the summer, recording initial and final readings of the gauges for later computation of true flow rates and air volumes of each sample. The performance of filters, of course, is very much less dependent on the flow rate than is the Andersen Sampler (Lindeken at al., 1963), and no attempt was made to standardize flow rates other than to achieve the maximum at each location.

Table II-2 lists the sampling sequence for the different locations.

5. Canadian Winter Experiment - Site Selection and Sampling Program

Three of the summer sites were retained for a brief winter experiment (November and December, 1970). Twin Gorges (NWT) was chosen for its remoteness and ideal local qualities, while Mackinac Island and Algonquin were selected for their accessibility. At each location a 3-week Andersen sample was taken, followed by a 1-week 20x25 cm high volume filter. Problems arose in connection with the filters, however, and they were

not analyzed. At the Twin Gorges site a 4-day impactor sample with backup filter was run, after completion of the 3-week run. Sampling details appear in Table II-3.

C. Analytical

The Andersen stages were analyzed according to the usual sequence of two irradiations and four counts (Appendix 2a). No replications were made on any of these stages, though the final counts on the Twin Gorges and Jasper summer samples were each repeated because of the extremely low activities present. For the same reason counting times for the long-lived isotopes in the Andersen stages from both Canadian experiments were lengthened from 4000 seconds to 20,000 (sometimes 40,000) seconds.

The filters, on the other hand, collected such larger amounts of aerosol that they could easily be subdivided for replication purposes. For ease of handling and counting a third irradiation of 1/2 to 1 hour duration in the reactor core was added to the above sequence for the count after one day's cooling. Generally, 1/8 of a filter was used for this and for the 5-minute pneumatic tube irradiation (usually the same piece), and each of these analyses was duplicated. The remaining 3/4 filter was then irradiated for 3 hours in the core and counted after 3 weeks for the long-lived isotopes, with no replication possible here.

D. Summary of Results

Out of 31 trace elements sought, approximately 29 could be detected at most locations. Certain elements near to the limit of detection, such as In, W, and Hg, were sometimes not detected in the remote locations, suggesting local pollution sources for them in the regions where they can be seen. On the other hand, the borderline element iodine showed up most clearly in the Twin Gorges samples, possibly because of an increased marine nature of the aerosol there. The next paragraphs present a summary of the most important conclusions reached, considered in detail in the following chapters.

The major source of many atmospheric large-particle elements appears to be the soil. Most elements at most locations (at least in summer) are associated with the larger aerosol particles, suggesting a widespread dispersion-type source for them. Soil and/or humanly-generated dust seem to meet these requirements, for they are common and are injected into the atmosphere via dispersion processes (saltation for the soil and a variety of mechanisms for humanly-generated dust). The more remote locations show a larger number of elements associated with the large particles. At a given location the number of large-particle elements decreases significantly in the winter, and may be associated with the presence of local snow cover.

These large-particle elements tend to be found in refractory materials and are usually either light metals or rare earths, though a few heavy metal refractories are in this

group. Almost without exception, these large-particle elements show aerosol/soil concentration enrichments nearly equal to those of iron, an element abundant in soils. They also show a greater degree of particle size distribution shape constancy from place to place than do the other elements, at least in summer. They tend to have lower concentrations in winter than in summer, and their concentration variation over the network (summer) tends also to be much smaller than for the other elements.

Confirming evidence for their soil origin comes from the Livermore, California diurnal variations experiment (Chapter VIII), where several of these same elements showed patterns linked with wind speed and suggestive of a daily cycle of generation and removal.

On the other hand, many airborne elements appear to have major sources other than the soil. These are the elements which are associated with the smaller particles. They often have relatively volatile compounds, and tend to be heavy metals or nonmetals. Their aerosol/soil enrichments range from 10 to 10,000 times those of iron, and are much more variable with location than those of the soil elements, as are also their particle size distribution shapes. They usually show higher concentrations in winter than in summer, though this is strongly location-dependent, and their variation over the network is much greater than for the soil elements.

Evolutionary effects on alteration of size spectra due to aging are in most cases not clear-cut, possibly aggravated by

the lack of backup filters on the impactors. Cl and Br appear involved with gas-particle interactions, but the other elements do not show regular size distribution shape alterations. The uniform preferential large-particle removal of the elements in the Mackinac Island experiment suggests physical removal processes to be more important here than those based on chemical properties. The near constancy of the indium spectrum under all conditions suggests only small aging effects, though possible rapid alteration immediately upon emission into the atmosphere is not excluded.

A very strong Zn-Sb concentration coherence is seen in all experiments, which may be related to their generally similar origins and particle size distributions. A somewhat less distinct coherence is seen for In-As-Se.

The ARO samples appear to reveal the presence of a very strong single pollution source for many elements, suspected to be the nickel-zinc smelters 250 km to the west in Sudbury, Ontario. The summer vs. winter size distribution contrast is especially striking here for several elements.

TABLE II-1. Sampling Program - Mackinac Island Experiment

Location	Type Sample*	Designation	Dates	Volume, m^3
Mackinac Island	AS	MI1	13/1/70 - 3/2/70	857
	F	MI1F	13/1/70 - 19/1/70	326
	F	MI2F	19/1/70 - 26/1/70	388
	F	MI3F	26/1/70 - 3/2/70	433
	AS	MI2	3/2/70 - 23/2/70	816
Ann Arbor	AS	AA1	13/1/70 - 3/2/70	867
	AS	AA2	3/2/70 - 23/2/70	692
East Chicago	AS	CFS1	9/2/70 - 24/2/70	459
	AS	MKT1	9/2/70 - 24/2/70	459

*AS = 7-Stage Andersen Sampler

F = 47 mm diameter filter

TABLE II-2. Sampling Program - Canadian Summer Experiment

Location	Sample Type (Designation)	Dates	Vol. m^3	No. Successful Samples, Stages, and Filters	Notes
Twin Gorges	AS (TG1)	15/6-9/7	997	7	
	F (TGF1)	9/7 -23/7	1240		
	F (TGF2)	23/7-11/8	1570	4	
	F (TGF3)	11/8-25/8	1260		
	F (TGF4)	25/8-7/9	1260		
Jasper	AS (J1)	12/6-9/7	1089	6	Stage 1 lost
	F (JF1)	9/7 -20/7	796		
	F (JF2)	20/7-3/8	1080	3	
	F (JF3)	3/8 -17/8	982		4th filter not run
Prince Albert	AS (PA1)	-	-	-	AS tampered with before sampling - all stages unusable.
	F (PAF1)	6/7 -20/7	1130		
	F (PAF2)	20/7-3/8	1050	4	
	F (PAF3)	3/8 -17/8	1070		Final flow rates of filters were estimated
	F (PAF4)	17/8-31/8	1030		
Riding Mountain	AS (RM1)	15/16-6/7	665	7	Shelter roof open during Andersen Sampler possibly during first filter. Rain may have entered Andersen.
	F (RMF1)	6/7 - 20/7	968		
	F (RMF2)	20/7-3/8	900	4	
	F (RMF3)	3/8 -18/8	993		
	F (RMF4)	18/8-3/9	1050		
Algonquin	AS (ARO1)	15/6-6/7)	1600	7	As run at approx. 2 cfm
	F (AROF1)	6/7 - 20/7	1010		
	F (AROF2)	20/7-3/8	1030	4	
	F (AROF3)	3/8 -17/8	1100		
	F (AROF4)	17/8-26/10	3600		
Mackinac Island	AS (MI3)	15/6-6/7	1300	7	Pump burned out before end of first filter.
	F (MIF4)	6/7 -19/7	690	1	
Niles	AS (N1)	15/6-6/7	818	7	
	F (NF1)	6/7 -20/7	869		
	F (NF2)	20/7-17/8	930	4	
	F (NF3)	3/8 -17/8	535		
	F (NF4)	17/8-31/8	707		

TABLE II-3. Sampling Program - Canadian Winter Experiment

Location	Type Sample	Designation	Dates	Volume, m^3
Twin Gorges	AS	TG2	23/11 - 15/12	1840
	AS	TG3	16/12 - 20/12	260
Algonquin Radio Observatory	AS	ARO2	23/11 - 15/12	890
Mackinac Island	AS	MI4	30/11 - 15/12	560

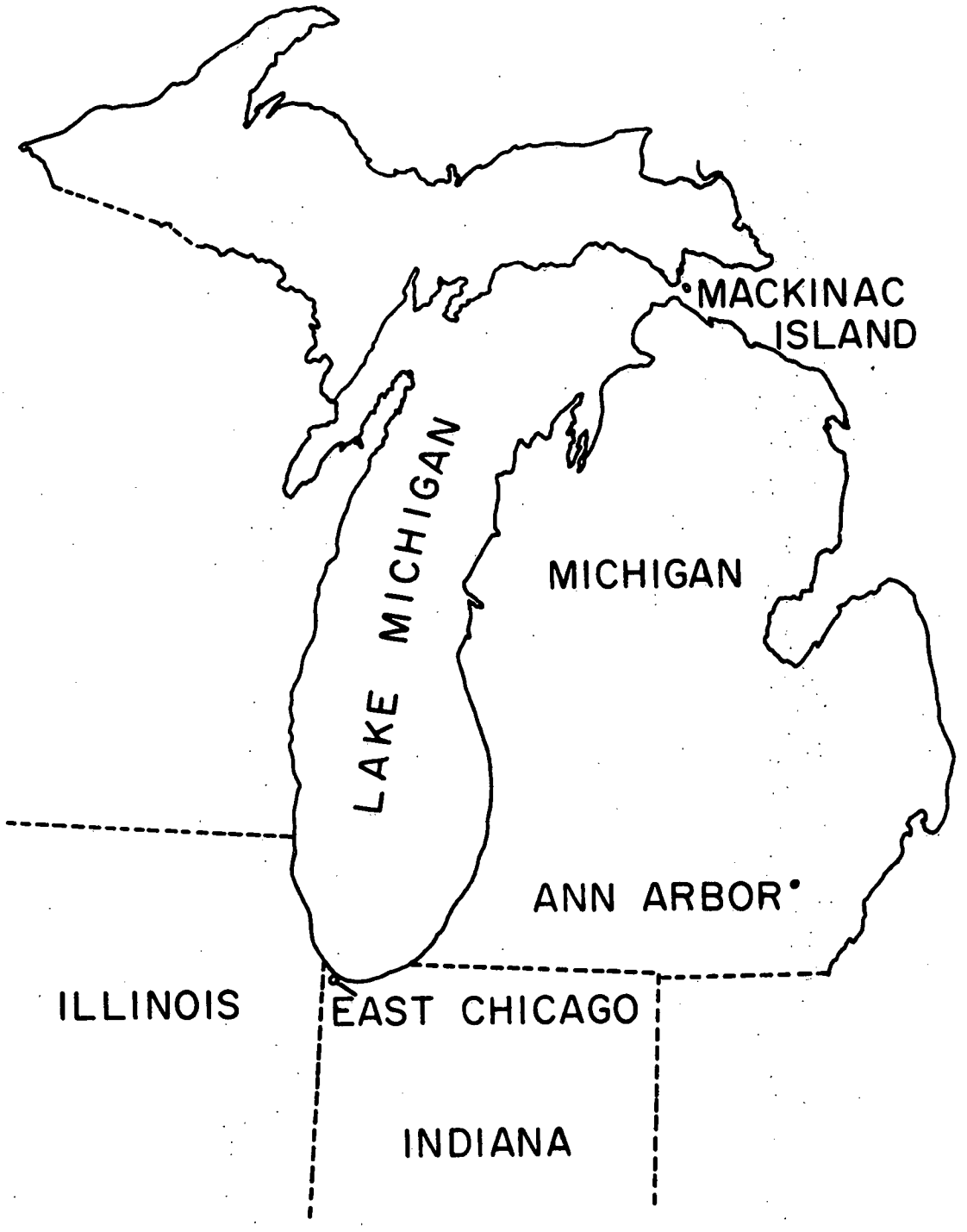

Figure II-1 Sampling Locations - Mackinac Island Experiment

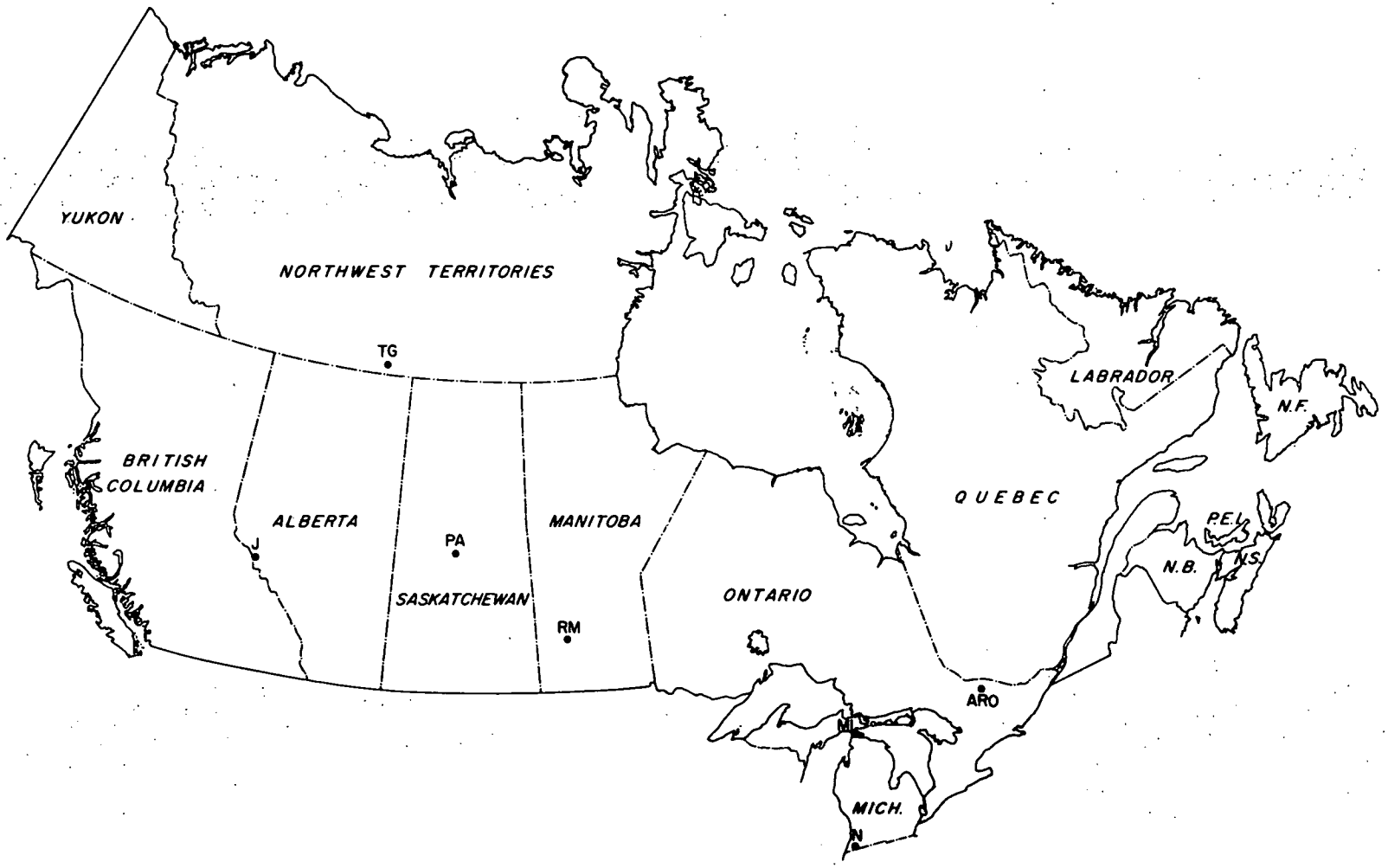

Figure II-2 Sampling Locations - Canadian Experiments

CHAPTER III

ORIGINS OF THE AEROSOL

A. Size Distribution Shape Classes

In an attempt to focus on major trends rather than on small differences among the elements at the various locations, qualitative judgments have been made by the writer concerning size distribution patterns. On the basis of the totality of results from this experiment, the observed size distributions were divided into five broad classes:

1) mass mostly associated with large particles (abbreviated "L"),
2) mass mostly associated with medium-sized particles (M),
3) mass mostly associated with small-sized particles (S),
4) "flat" mass distribution, approximately equally divided among the size ranges (F),
5) "mixed" distributions, where two or more of the first three types are present with approximately equal weights (LS, for example).

Idealized forms of each of these distributions are shown in Figure III-1. In cases where the data were inadequate to properly type the distribution of an element, it was called indeterminate (I).

The size distribution of each element in each of the 16 Andersen samples of this experiment has been assigned to one

of these categories by the writer (Tables III-1 through III-6). For comparison purposes, 20 runs of Nifong from East Chicago and Gary, Indiana (Table III-7) were similarly analyzed (Table III-8). All results are summarized in Table III-9.

B. Canadian Summer Experiment Size Distributions

Consider first the results of the Canadian summer experiment, Table III-3. Extensive groups of L-type elements appear here, while no such groups are evident for the other size classes. Table III-4 summarizes the populations of each class at each station, showing that in terms of the detectable elements (percentages given in the table for all 31 elements, whether detected or not) at a typical summer station nearly 3/4 of them were found mostly on large particles (L-type). Next in frequency but much lower (13%) are the small-particle (S-type) elements. Somewhat less abundant (9%) are the M-type elements, followed by the "flat" (F-type) elements (4%) and those with mixed (e.g., LS-type) trends (1%). This average pattern is followed closely, 5 of the 6 stations (ARO excepted) agreeing qualitatively with the above order.

The individual stations seem to fall roughly into two classes--the more remote stations of Twin Gorges, Jasper, and Riding Mountain versus the more nearby or "polluted" Algonquin, Mackinac Island, and Niles. Averages of these subgroups show distinct differences, with the remote stations having 40 percent more detectable L-type elements than the proximate

locations (bottom line, Table III-4). Individual stations show little variation from the group average.

This overall association of proximity to sources with size distributions other than L-type is confirmed by data from Nifong (Table III-8), which shows the source area of Northwest Indiana to have only half the detectable elements associated with large particles, compared to nearly 3/4 in the summer study.

The number of L-type elements appears to be smaller in winter (Tables III-1,5). This is quantized in Table III-9 where it is seen to be about one-half the total detectable.

Seasonal effects on these size distribution frequencies are summarized in Table III-10, where the percentages of L-type elements are listed by season for the three stations where direct winter-summer comparisons are available. At Mackinac Island the L-type frequency decreases by about one-half in winter; at Twin Gorges it decreases to about one-third of its summer value; and at ARO not a single element is seen with an L-type distribution in winter. Each of these three winter situations will be discussed later in more detail.

These L-type elements share a certain chemical similarity. From Table III-3, where the elements are ordered by atomic number, two broad bands of L-type elements can be seen, the light metals and the rare earths, respectively near the top and bottom of the table. They are highly reproducible in size distribution pattern, with 12 elements (Na, Mg, Al, Cl, K, Ti,

La, Ce, Sm, Eu) being L-type at all locations. In addition, Fe and Co, heavier metals, and Th, an actinide, show similar behavior.

There is a further physico-chemical contrast between the L-type elements and the others. The former have refractory compounds, especially oxides and silicates, in which forms they are often found in soils and minerals. Table III-11 lists the melting and boiling points of a number of compounds of the elements in this study, and the contrast between elements may be clearly seen. For the refractory elements important gas-phase reactions would not be expected, even in high-temperature industrial processes, in agreement with their typically-observed L-type distributions.

Conversely, several other elements have common compounds which are more volatile. In particular, the oxides of arsenic and selenium, and to a lesser degree various compounds of antimony and mercury readily volatilize. The result of such a process might be a vapor condensation onto the ambient aerosol which, if "Junge" (F-type in total mass) distributed, would produce larger concentrations of these elements in the smaller size ranges, just the shape observed for several of them.

Further inspection of Table III-3 reveals a number of elements, such as Mn, Zn, Cu, Ga, and Sb, which are L-type only in the most remote regions, suggesting that their size distributions are responding to the lack of nearby pollution sources. In this regard it is interesting to note that no elements show the reverse trend, that is, L-type distributions

only in the less remote areas.

The L-type elements appear to be more constant in size distribution pattern than the others. For example, there are 21 elements in this class at 3 or more of the 6 stations, and 15 (71%) of these are identical in type at all stations. In contrast, only 4 elements are S-type at 3 or more stations, while none of these shows the same pattern at all 6 stations.

In order to help visualize the actual variations in size distribution consistency shown by the various elements, the distributions of Al, Fe, Sm, In, and Br have been plotted for the 6 sites (Figures III-2, 3, 4, 5, 6). Indium was below the detection limit at Jasper and Twin Gorges, so is only plotted four times.

Al, Fe, and Sm, chosen as typical L-type elements, not only show a great similarity in the shape of their curves at the various locations but also show a positive correlation with each other in total concentration from station to station. Niles clearly has the highest concentrations for all three, especially over stages 2-6, while all the other stations are bunched together with values a few times lower than Niles. Inspection of the tabulated data in Appendix 3 show this same behavior to be followed by most of the other large-particle elements as well.

The indium plot is quite different from the previous ones, for its total concentration variation among stations is greater than for the L-type elements, with the ARO values being highest, greater even than those from Niles by a factor

of 2. Though not plotted, upper limits from Jasper and Twin Gorges suggest lower concentrations than at Riding Mountain, the lowest station values plotted, implying a total spread in concentration of nearly 100 times.

Bromine, though mentioned earlier to have not quite as constant a size distribution as these other elements, nevertheless shows some similarity from station to station. Each of the plots for this element shows and large- and a small-particle concentration maximum, with a well-defined dip in between. In common with indium there is quite a large variation in total concentration, the ratio between Niles and Jasper/Twin Gorges being about 50.

There are four elements which are observed to display size distributions which shift from one extreme to the other, Ga(L,S,F), Sb(L,M,S), V(L,S), and Zn(L,M,M(S)). Experimental uncertainties for Ga are large, and its variation may therefore be illusory; but it is definitely real for the others. Plots of the other three appear as Figure III-7,8,9.

The size distribution pattern of Sb at Twin Gorges is definitely L-type, while at all the others it is S- or M-type. Vanadium is strongly L-type at the western Canada locations, somewhat less so at Niles, and S-type at Mackinac Island and Algonquin. Zinc is L-type at Twin Groges, LS at Jasper, LM at Riding Mountain, and strongly M-type at the remaining three locations. Each of these three elements thus shows a shift toward small-to-medium particle dominance with increasing proximity to human activity.

On the whole, the other elements in Table III-3 show only moderate shifts in size distribution. They include Cr, Mn, Cu, As, Se, I, and W. Figures III-10 through III-13 are plots of Mn, As, Se, and Cr for the six locations. As expected, the other features of these plots are also intermediate in character.

The totality of the above observations suggests that the L-type elements originate from a widespread dispersion-type source. This idea is not incompatible with soil and the saltation process, where wind-generated airborne particles of diameters typically 100 μm impact back onto the soil, blasting loose the finer particles which take much longer to settle (Battan, 1966). These dispersion fragments may produce the L-type distribution.

On the other hand, the remaining elements appear to have sources other than the soil. The variability of their size distributions may reflect either a variety of source processes or the effect of aging. Those elements associated with small particles may have passed through a vapor condensation process, especially those elements having volatile compounds.

C. Aerosol/Soil Enrichments

The mere presence of an L-type particle size distribution for an element may not necessarily be evidence for its soil origin. Some industrial sources emit elements with this spectral shape (Nifong, 1970), and the highly soluble marine aerosol may grow from M-type to L-type by repeated cycles of cloud droplet nucleation, coalescence, and evaporation. Each of these

processes would not only cause an incorrect assignment of the element to the soil-derived group but would also mask the contributions of the other source types. Such contributions can be rather accurately assessed in this work because the number of data points provided by the multielemental method allows the discrimination of small non-soil contributions to the total aerosol.

High discrimination in turn requires good soil data. It was felt that the best soil reference is a continent-wide average (Vinogradov, 1959) rather than a few local analyses performed by us. Therefore no local soil samples were analyzed.

Using this average soil composition, a scheme was devised whereby the soil contribution to the total concentration of a given element could be accurately corrected for, thereby possibly unmasking the anomalies due to remote (pollution) sources. The total elemental concentrations (from the filter data) at each location were averaged to give a mean summer value, representative in most cases of 8 weeks in July and August (Appendix 3 and Table III-12). For each element at each station an "enrichment factor" of aerosol concentration relative to soil concentration was calculated, according to the formula:

$$F_x = \frac{\chi_x}{C_x}$$

where F_x = enrichment factor of element X,

χ_x = aerosol concentration of X, ppm, and

C_x = soil concentration of X, ppm.

Use of trace element concentrations in soil rather than in in crustal rock was considered perferable for this calculation, because the weathering of rock to soil systematically alters its trace element content. Comparison of elemental concentrations in North American and European soils with average crustal rock values (Table III-13) reveals that while many elements are nearly equally abundant in both materials, the soluble ones like Na, Mg, K, Ca, etc., are depleted in soil (presumably due to leaching during weathering), and certain nonmetallic elements like Br, I, and As are enriched in soils (possibly from fallout of volcanic debris).

The calculation of trace element aerosol concentrations in ppm of aerosol requires a knowledge of the total aerosol mass concentration, a variable not measured in this experiment. This difficulty can, however, be overcome by assuming a reasonable aerosol concentration, calculating the enrichments, then normalizing each enrichment to that of a reference element whose principal source is known, or at least strongly suspected, to be the soil. The result of this normalization will be a set of relative enrichment factors with other soil-derived elements having values of approximately unity, independent of of their initial atmospheric concentrations.

The two logical choices of soil reference elements here are Al and Fe, for several reasons:

1) they both are abundant in soil (Table III-13);
2) they both show L-type size distribution;
3) they both are determined well by activation analysis;

4) their concentrations decrease only slowly with remoteness (Table III-12, Figures III-2,3);

5) Junge (1965) cites Fe and Al as coming principally from the soil, as do Egorov et al. (1970).

Following the lead of Egorov et al., Fe was chosen as the reference element, and all enrichments were normalized to it:

$$F_{xn} = \frac{F_x}{F_{Fe}} = \frac{\frac{\chi_x}{C_x}}{\frac{\chi_{Fe}}{C_{Fe}}} = \frac{1}{K}\frac{\chi_x}{\chi_{Fe}}$$

where F_{xn} = normalized enrichment factor of element x

$K = C_x/C_{Fe}$

This division step removes all dependence of the final or normalized enrichment on the original guess for the total aerosol concentration, making interstation comparisons nearly as valid as if the total aerosol levels had been exactly known. The one hazard introduced by this procedure is the greater importance placed on the accuracy of the Fe concentration, for any error in this number at a given location will have an equivalent effect on every other enrichment at the same location. Such perturbations may be of two types, a grossly incorrect analytical number for Fe (chances of which are minimal in our procedure) or a major pollution contribution in addition to the soil-derived fraction. This last possibility also seems slight, in spite of the fact that the Northwest

Indiana study disclosed strong Fe sources in Gary and East Chicago. The concentration map for Fe (Figure VI-10) shows that the steel mills were strong sources, but the high Fe background lowered the source/background ratio to a moderate 6/1.

Keeping in mind these possible difficulties in normalization, the results shown in Table III-14 and Figure III-14 may now be considered.

1. Large-Particle Elements

Figure III-14 is a plot of the normalized enrichments for each element at each of the 7 summer stations. The most striking feature of this plot is its vertical extent, up to an ordinate of 10,000 for Se at Mackinac Island and down to 0.2-0.3 for Ga, Ti, and Cr at several stations, a spread of nearly 5 orders of magnitude. Equally noticeable is the uneven element distribution along the vertical, with a major clustering for each station occurring near 1, the value for Fe. At every location Fe falls inside the body of this clustering, usually near the geometric center but sometimes (PA, ARO) somewhat below center. The group stability of the elements in these clusters is noteworthy (as is also the stability of elements in other parts of the plot), the lists including Na, K, Ca, Mg, Al, Sc, Th, Fe, Co, Mn, V, Ti, Ce, Eu, La, and Sm.

The correlation between these elements and the L-type elements of Table III-3 is remarkable. To a first approximation

the two groups are identical. Except for Cr, V, and Mn, every element of the above list is also an L-type element at each of the 6 stations, and these three elements only deviate at 1, 2, and 2 stations, respectively. Furthermore, there is only one L-type, Cl, which is sufficiently enriched to lie outside of this major clustering.

In summary, then, the argument for a soil dust origin of the L-type elements, though remaining circumstantial, is considerably enhanced by their common enrichment factors. These values are roughly equal to those of Fe, an element very likely to be mainly soil-derived. In addition, the other presumed soil element, Al, also lies within this group, though consistently near the bottom of the cluster.

This behavior of Al (and Ti) is of interest, for it is consistently followed at all 7 locations. The reason may be related to the presence of Al and Ti in the clay or weathered fraction of the soil, as opposed to Fe, which exists heavily in the oxide fraction (Callender, 1971). Though not adequately explained at present, the phenomenon seems real at least for Al, for it is confirmed by measurements of Egorov et al. (1970) on trace element atmospheric concentrations in the USSR.

Of the nine elements for which they present data, six (Fe, Al, Cu, Mn, Cr, and Ni (Ni done with much more sensitivity than in this work)) are also determined by our method. The concentrations of these six at several locations in the USSR

are listed in Table III-15, along with comparison figures for the geometric average of stations 1-10 of the Northwest Indiana survey, and the summer and winter averages of the remote Twin Gorges Canadian station of this chapter. The Russian numbers represent annual averages, and are seen to vary over a wide range between the polar locations and the inland cities. The polar locations, considerably farther north than even our Twin Gorges station, show lower concentrations for Fe and Al, but values nearly equivalent to Twin Gorges for Cu, Mn, and Cr. Nickel at Twin Gorges was below our detection limit and so cannot be directly compared with the Russian values. The Russian continental cities, on the other hand, appear to be unusually high in Cu, Mn, Cr, and Ni, often exceeding the Northwest Indiana values.

Table III-16 and Figure III-15 show the normalized enrichments for these elements at the eight Russian locations for which they could be computed. This figure shows the same low Al enrichment as observed in our study, at both the land and ocean stations, suggesting its generality as a natural phenomenon.

2. Small-Particle Elements

A number of elements lie consistently above the Fe cluster on the enrichment plot. On the basis of the above soil interpretation, they would seem to have some major source other than the soil. With the exception of Cl, these elements also have size distributions other than L-type. This trend is seen

most clearly beginning at enrichments of roughly 10, above which are found As, Zn, Cu, Br, Se, Sb, and Hg (sometimes also W). As seen from Table III-3, these are the elements found on medium-sized and small particles at most or all locations. The vaporphase condensation or high-temperature dispersion processes implied here suggest pollution sources for these elements.

Confirming evidence for this idea again comes from Nifong (1970). His measurements of particle size distributions for these elements in Northwest Indiana showed strong small-particle enrichments for Zn, Br, As, Sb, and Hg.

3. Comparison with Northwest Indiana Source Results

It is interesting to pursue the degree of correlation between the elements showing large enrichments and those with strong sources in Northwest Indiana. By the coefficient of variation criterion of Figure VI-29, the ten elements with strongest sources would be Cu, W, Sb, Zn, Cr, Br, Ga, Fe, Ag, and Ce. The end of this list coincided with a natural break in the plot, beyond which the elements were considered to have only medium and weak sources. Conspicuously absent from this list, however, are Hg, As, and Se, which appear in the upper portion of the enrichment plot and thus would seem to have strong sources. On the other hand, elements such as Cr, Ce, and Fe which have strong sources in Northwest Indiana do not appear enriched on the plots, so in this respect the overlap between the two experiments seems incomplete and inconclusive.

There are two possible explanations for this lack of agreement. First, the list of strong sources for Northwest Indiana should be considered to be a minimum list, primarily because the southwest wind of the sampling period advected the steel industry plumes out over Lake Michigan and rendered direct sampling of steel mill effluents impossible. In spite of this, most of the elements still showed their maxima at Markstown Park (station 6), the station nearest to the steel mills, and it is likely that more direct sampling of this effluent would have revealed other elements to have strong sources here. Second, the elements Hg, As, and Se may become relatively more enriched with advection away from the source because their small-particle size distribution causes less rapid removal by natural processes. In this vein, Nifong has found the size distribution of the effluent in the vicinity of the sinter plant at Inland Steel to be heavily weighted toward the largest particles, particles which would fall out rapidly and so could not transport the effects of the source over any great distance. It thus may be more than coincidence that the three elements Fe, Cr, and Ce, which are on the strong source list but not highly enriched at some distance away, all have this large-particle distribution. Of these, at least Fe and Cr were found by Nifong to show this extreme large-particle component at the sinter plant.

D. Network Concentration Variations

The large-particle elements appear as a group to have lower concentration variations over the network than do the

other elements. Table III-17 shows that the average Niles/Twin Gorges concentration ratio for 7 typical L-type elements is about 4 times lower than the corresponding ratio for 5 S- and M-type elements.

Another way of presenting this behavior is in terms of the enrichment plot. Specific groups of elements showing or expected to show similar behavior were formed and plotted, as listed below:

1) Na, K, Al; Ce, La, Sm, Eu (Figure III-16)
2) The halogens Cl, Br, and I (Figure III-17)
3) The heavy metals Cu, V, and Ga (Figure III-18)
4) Se, As, In (Figure III-19)
5) Zn, Sb (Figure III-20)

As anticipated, the common metals Na, K, and Al behave quite similarly, with no apparent pattern. In this way they are joined by the rare earths Ce, La, Sm, and Eu, except that Eu is unusually enriched at Niles.

The halogens are more complicated. Bromine shows evidence of being a pollution element directly related to population density, for it decreases smoothly in enrichment from the most populated to the most remote environments. Chlorine, on the other hand, is much more nearly constant over the network, except for a low point at Algonquin. Iodine is different still, showing a definite enrichment maximum at Twin Gorges and a fairly constant but 4-fold lower profile at the other stations, which seems to decrease further at Niles. The explanation of this enrichment maximum at the northernmost

station may be related to an increased marine nature of the aerosol there, a possibility raised by results of winter sampling at this location and considered in Chapter IV. Though all three halogens show definite enrichments, Cl seems to pose the biggest interpretation problem. As noted earlier, it is the only element to be both consistently associated with large particles and enriched by more than an order of magnitude over the soil. The possibility of a sea-salt origin of the extra Cl will be considered.

Even though the absolute values of the enrichments of the heavy metals Cu, V, an Ga suggest different origins for them (V and Ga from soil, Cu from pollution), their enrichment patterns from station to station are roughly parallel, having highest values at Mackinac Island, Algonquin, and Niles. Parallelism is also shown by Se, As, and In, but to a much greater extent than for Cu, V, and Ga, and with more pronounced maxima at Mackinac Island and Algonquin. The parallelism here is really quite striking, and attests to the commonness of sources that might be suggested by the similar size distributions of these elements. In contrast, it was also noted that Zn and Sb, while having similar size distributions to Se, As, and In, have enrichment profiles which are somewhat different from them but very close to one another. This closeness may be caused by a nearly complete source identity within the two groups, but with only a partial overlap between group sources.

E. Seasonal Trends

Evidence useful for separating source types by seasonal concentration trends is rather complicated and mixed. The summer and winter Canadian experiments contained three stations in common (Twin Gorges, Algonquin, and Mackinac Island), and direct comparison of total concentrations are best made using the totals of the Andersen sample results (Table III-18, Figure III-21).

The Mackinac Island case is the most straightforward. The soil-derived elements are nearly all more abundant in summer, in keeping with the effect of exposed soil vs. snow cover. The small value of this summer/winter concentration ratio is surprising, though, between 1 and 2 in most cases. Only in the anomalous cases of Ca and Mg, where the values are about 5, are any soil elements significantly above 2.

On the other hand, the ratios for the pollution elements seem to be usually less than 1, indicating higher winter concentrations. This probably reflects the influence of meteorological rather than source variables, for snow cover and decreased insolation reduce mixing heights in winter while the industrial outputs should remain about the same. Using the average of the elements Zn, As, Se, Cu, and In, this meteorological factor seems to be about 2 in value. When reapplied to the soil elements, it suggests that their soil-derived component is really about 3 times higher in summer, more nearly what is intuitively expected.

The Algonquin data do not show these easily interpretable trends. Pollution and soil-derived elements are interspersed, indicating a more complex situation. The other data from here bear this out, and Algonquin will be treated later in much more detail.

The Twin Gorges data shows the greater dispersion expected from the larger analytical uncertainties here, and like Algonquin appears to be another unusual case. Particularly noteworthy are the high summer values for Al, Sc, Mn, and Ce, soil elements subject to small analytical uncertainties, and equally low values for Na, Cl, and Fe. The high winter enrichments of Na and Cl are associated with an apparent influx of marine air in the winter; this unusual situation will again be discussed later.

F. Other Evidence for Source Type

Chapter VIII reports on a diurnal variations experiment from Livermore, California, where the daily patterns of Al, Mn, Fe, V, and Sc were adequately explained only by the soil hypothesis. Their concentrations correlated closely with wind speed, rising sharply after sunrise and falling after sunset, a pattern quite unlike that previously observed for these same elements at Niles, Michigan (Chapter VII), and there attributed to the effects of elevated pollution sources at a distance.

Gillette and Blifford (1970), in a series of measurements of trace element concentrations with height in the troposphere

conclude that the close correlation of Ti, K, and Ca with Si (even over a Pacific offshore site) supports the idea of their soil origin. Nifong (1970) found evidence that Al and the rare earths had substantial "background" sources around Northwest Indiana, and that at least for Al the pollution sources appeared to contribute extra mass mainly in the vicinity of 1 μm particle diameter (stage 5 on the Andersen Sampler).

TABLE III-1. Particle Size Distribution Shapes-
Mackinac Island Experiment

	MI1	AA1	MI2	AA2	CFS1	MKT1
Na	M	L	M	L	L	L
Mg	L	L	M(I)	L	L	L
Al	L	L	L	L	L	L
Cl	L	L	L	L	L	L
K	F(S)	L(S)	S	M	L	L
Ca	L	L	L	L	L	L
Sc	L	L	L	L	L	L
Ti	L	L	L	L	L	L(M)
V	S	S	S	S	MS	S(M)
Cr	M	L	S(F)	L	L	L
Mn	S	S	S	M	ML	M
Fe	M	L	M	L	L	L
Co	L	L	F	L	L	L
Ni	I	I	I	I	I	I
Cu	M	L	M(S)	L	M(L)	M
Zn	M	L	S	L	M	M
Ga	S	L(S)	S	S(I)	M	S
As	S	S	S	M(S)	M	M
Se	S	S	S	M(S)	M	S
Br	S	S	S	M	M	S
Ag	I	I	I	I	I	I
In	M	S	M	M	M	M
Sb	S	S	S	M	M	M
I	S	I	S	LS(I)	I	I
La	L	M	M(S)	L	M	M
Ce	L	L(S)	S	L	L(M)	M
Sm	L	L(S)	M(S)	L	M	L
Eu	L	L	L(M)	L	L	I
W	L	L	S	I	I	I
Hg	I	S	S	I	M	I
Th	L	M	M(I)	L	M	L

TABLE III-2. Particle Size Summary
Mackinac Island Experiment

	MI1	AA1	MI2	AA2	CFS1	MKT1	Total
L	13	18	6	17	13	13	80 (43%)
M	6	2	8	7	12	8	43 (23%)
S	8	8	14	2	0	4	36 (19%)
F	1	0	1	0	0	0	2 (1%)
Mixed	0	0	0	1	2	0	3 (2%)
I	3	3	2	4	4	6	22 (12%)
Total	31	31	31	31	31	31	186 (100%)
*L/(Tot-I) Percent	46	64	21	63	48	52	49

*Large-particle fraction of detectable elements

TABLE III-3. Particle Size Distribution Shapes
Canadian Summer Experiment

	TG1	J1	RM1	ARO1	MI3	N1
Na	L	L	L	L	L	L
Mg	L	L	L	L(I)	L	L
Al	L	L	L	L	L	L
Cl	L	L	L	L	L	L
K	L	L	L	L	L	L
Ca	L	L	L	L	L	L
Sc	L	L	L	L	L	L
Ti	L	L	L	L	L	L
V	L	L	L	S	S	L
Cr	L	L	L	L	F	L
Mn	L	L	L	M	M(L)	L(F)
Fe	L	L	L	L	L	L
Co	L	L	L	L	L	L
Ni	I	I	I	L(I)	I	I
Cu	L	I	L	M	F(I)	F(I)
Zn	L	L(S)	L(M)	M	M	M(S)
Ga	L	L	L	F	S	L
As	M	I	S	M	S	S(M)
Se	I	S(M)	S(L)	M	S	S
Br	S(L)	S(L)	L(S)	S	S	S(M)
Ag	I	I	I(L)	I	I	I
In	I	I	M	M	M	M
Sb	L	S(M)	M	M	S	S
I	LS	S	I	I	S	I
La	L	L	L	L	L	F
Ce	L	L	L	L	L	L
Sm	L	L	L	L	L	L
Eu	L	L	L	L	L	L
W	L(I)	I	L	I	I	F
Hg	I	L	L(S)	S(I)	LS	L(I)
Th	L	L	L	L	L	L

TABLE III-4. Particle Size Summary - Canadian Summer Experiment

	TG1	J1	RM1	ARO1	MI3	N1	TG1+J1+RM1	ARO1+MI3+N1	Total
L	23	21	24	17	15	19	68 (73%)	51 (55%)	119 (64%)
M	1	0	2	7	3	2	3 (3%)	12 (13%)	15 (8%)
S	1	4	2	3	7	4	7 (7%)	14 (15%)	21 (11%)
F	0	0	0	1	2	3	0 (0%)	6 (6%)	6 (3%)
Mixed	1	0	0	0	1	0	1 (1%)	1 (1%)	2 (1%)
I	5	6	3	3	3	3	14 (15%)	9 (10%)	23 (12%)
Total	31	31	31	31	31	13	93	93	186
*L/(Tot-I) Percent	88	84	86	61	54	68	86	61	73

*Large-particle fraction of detectable elements

TABLE III-5. Particle Size Distribution Shapes - Canadian Winter Experiment

	TG2	ARO2	MI4	TG3
Na	M	M	M	M
Mg	M	I	L	M
Al	L	M	L	L
Cl	M	M	L	M
K	M	M	L	M
Ca	M	M	L	L(M)
Sc	L	M	L	-
Ti	I	I	L	I
V	M	S	S	M
Cr	L	M	S	-
Mn	M	M	S	M
Fe	LM	M	M	-
Co	L	M	M	-
Ni	I	I	M	-
Cu	M	M	F	M
Zn	M	M	M	-
Ga	M	M	S	I
As	M	M	S	M
Se	M	S	S	-
Br	M	S	S	M
Ag	I	I	I	-
In	M	M	M	I
Sb	M	S	S	-
I	M	S	S	M
La	L	M(L)	L	L
Ce	L	M	M	-
Sm	M	M	L	L
Eu	I	M	I	I
W	I	I	I	M
Hg	I	I	S	-
Th	L	I	LM	-

TABLE III-6. Particle Size Summary - Canadian Winter Experiment

	TG2	ARO2	MI4	Total
L	7	0	9	16 (17%)
M	17	19	7	43 (46%)
S	0	5	10	15 (16%)
F	0	0	1	1 (1%)
Mixed	1	0	1	2 (2%)
I	6	7	3	16 (17%)
Total	31	31	31	93 (100%)
$\frac{*L}{(Total-I)}$, %	28	0	32	21

*Large-particle fraction of detectable elements

TABLE III-7. Andersen Sampler Runs of Nifong (1970)

Run(s)	Location	Volume, m^3
2-4	Open hearth	107
7-10	Sinter	150
15-17	ECCFS	120
20	MKT	40.8
21	MKT	37.5
23-26	FS	162
31-34	GA	154

ECCFS = East Chicago Central Fire Station

MKT = Markstown Park, East Chicago

FS = Field School, East Chicago

GA = Gary Airport

TABLE III-8. Particle Size Summary - Selected Nifong Runs

Run(s)	2-4	7-10	15-17	20	21	23-26	31-34	Total
L	10	13	11	10	6	11	12	73 (34%)
M	3	0	3	4	6	0	2	18 (8%)
S	8	7	6	6	5	11	5	48 (22%)
F	0	0	0	1	0	0	0	1 (1%)
Mixed	2	2	0	0	1	0	3	8 (4%)
I	8	9	11	10	13	9	9	69 (32%)
Total	31	31	31	31	31	31	31	217 (100%)
L (Tot-I)	%43	59	55	48	33	50	54	49

Table III-9. Particle Size Summary - All Experiments

	Mackinac Island (Winter)	Canadian (Summer)	Canadian (Winter)	Average	NW Indiana Nifong, Selected
L*	49	73	21	53	49
M*	26	9	56	25	12
S*	22	13	19	18	32
F*	1	4	1	2	1
Mixed*	2	1	3	17	5
Total**	164	163	77	--	148

*As percent of determinable elements

**Total number of determinations

TABLE III-10. Seasonal Particle Size Comparison - Percentage of Determinable Elements with L-type Distributions

	Jan-Feb 1970	June-July 1970	Nov-Dec 1970
TG	--	88	28
MI	33	54	32
ARO	--	61	0

TABLE III-11. Melting and Boiling Points of Selected Chemical Compounds

Compound	T_m (°C)	T_b (°C)	Compound	T_m (°C)	T_b (°C)
$SbBr_3$	97	280	Al_2O_3	2045	2980
$SbCl_3$	73	283	La_2O_3	2315	4200
Sb_2O_3	656	subl.1550	MgO	2800	3600
As_2O_3	315	---	Mn	1244	2097
$CaAl_2Si_2O_8$ (nat anorthite)	1551	---	$MnCl_2$	650	1190
			MnO_2	-0,535	---
$CaSO_4$	1450	---	HgO	d 500	---
CaO	2580	2850	HgS	subl. 583	---
Cr_2O_3	2435	4000	KCl	776	subl.1500
CoO	1935	---	KBr	730	1380
Cu	1083	2595	$SeBrCl_3$	190	---
Cu_2O	1235	-0,1800	$SeCl_4$	subl. 170-196	d 288
$CuSO_4$	200	d 650	SeO_2	subl. 315-317	---
CaAs	1238	---	NaCl	801	1413
GaSe	960	---	NaBr	755	1390
InAs	943	---	TiO_2	1830 -1850	2500-3000
In_2O_3	---	volat.850	V_2O_5	690	d 750
Fe	1535	3000	WO_3	1473	---
Fe_2O_3	1565	---	Zn	419	907
$FeCl_3$	282	315	ZnO	1975	---
Al	600	2467	$ZnCl_2$	262	732

TABLE III-12. Total Elemental Concentrations (ng/m^3) - Canadian Summer Experiment

	TG	J	PA	RM	ARO	MI	N
Na	18	36	43	56	69	44	120
Mg	16	53	60	130	40	470	160
Al	66	145	150	330	240	230	580
Cl	9	13	11	28	4	35	46
K	54	106	112	175	170	150	340
Ca	40	150	130	360	160	1150	650
Sc	0.044	0.082	0.12	0.16	0.14	0.12	0.49
Ti	5	8	9	12	15	11	35
V	0.21	0.33	0.42	0.73	1.9	1.8	3.6
Cr	0.59	0.32	1.1	0.92	1.9	0.91	3.8
Mn	1.5	5.3	5.9	8.7	12	9.2	41
Fe	71	220	180	270	310	250	950
Co	0.042	0.059	0.085	0.11	0.16	0.17	0.34
Ni	<2	<2	<2	<2	5	<3	<7
Cu	0.9	3.8	0.9	4.4	7.9	10	15
Zn	3.8	5.2	13	15	40	22	130
Ga	0.026	0.042	0.035	0.056	0.14	0.15	0.35
As	0.31	0.27	0.32	0.45	4.7	3.2	4.6
Se	0.043	0.033	0.063	0.18	0.63	0.67	0.89
Br	0.54	2.0	2.9	3.1	5.7	7.2	94
Ag	<0.15	<0.15	<0.2	<0.2	<0.4	<0.5	<0.7
In	0.0013	<0.003	0.0020	0.0029	0.039	0.024	0.017
Sb	0.13	0.13	0.16	0.21	0.60	0.40	1.9
I	0.20	0.21	0.13	0.18	0.27	<0.2	<0.5
La	0.091	0.12	0.10	0.19	0.30	0.17	0.76
Ce	0.24	0.25	0.32	0.31	0.69	0.41	1.6
Sm	0.013	0.017	0.018	0.035	0.051	0.030	0.11
Eu	0.0017	0.0037	0.0036	0.0082	0.0090	0.0080	0.019
W	0.016	0.035	<0.03	<0.05	0.041	0.30	0.12
Hg	0.06	0.17	<0.3	0.41	0.19	0.38	0.61
Th	0.052	0.036	0.040	0.058	0.056	0.018	0.11

TABLE III-13. Elemental Concentrations in Crustal Rock, Soil, and Sea Water

	Crustal Rock Abundance ppm(1)	Avg. Soil Abundance ppm(2)	Sea Water Abundance g/ton(1)	Sea Salt Abundance ppm(1)
Na	28,300	6,300	10,556	324,000
Mg	20,900	6,300	1,272	39,200
Al	81,300	71,300	0.1	3
Cl	130	100	18,980	584,000
K	25,900	13,600	380	12,000
Ca	36,300	13,700	400	12,000
Sc	22	7	0.00004	0.0012
Ti	4,400	4,600	0.005	0.15
V	135	100	0.005	0.15
Cr	100	200	0.002	0.06
Mn	950	850	0.0008	0.025
Fe	50,000	38,000	0.0034	0.105
Co	25	8	0.0001	0.003
Ni	75	40	0.005	0.15
Cu	55	20	0.002	0.06
Zn	70	50	0.015	0.45
Ga	15	30	0.0005	0.015
As	1.8	5	0.003	0.09
Se	0.05	0.01	0.004	0.12
Br	2.5	5	65	2,000
Ag	0.07	(0.1)	0.0002	0.006
In	0.1	---	---	---
Sb	0.2	---	0.0002	0.006
I	0.5	5	0.05	1.5
La	30	(40)	0.0003	0.009
Ce	60	(50)	0.0004	0.012
Sm	6.0	---	---	---
Eu	1.2	---	---	---
W	1.5	---	0.0001	0.003
Hg	0.08	0.01	0.00003	0.0009
Th	7.2	6	0.000005	0.00015

(1) Mason (1966)

(2) Vinogradov (1959)

TABLE III-14. Aerosol-Soil Normalized Enrichments - Canadian Summer Experiment

	TG	J	PA	RM	ARO	MI	N
Na	1.5	0.98	1.4	1.3	1.3	1.1	0.76
Mg	1.3	1.4	2.0	2.9	0.8	11	1.0
Al	0.49	0.34	0.46	0.65	0.42	0.45	0.32
Cl	47	22	23	41	5	51	18
K	2.1	1.3	1.7	1.9	1.5	1.7	1.0
Ca	1.5	1.9	2.0	3.8	1.4	13	1.9
Sc	3.3	2.1	3.6	3.2	2.5	2.6	2.8
Ti	0.58	0.29	0.41	0.38	0.40	0.42	0.30
V	1.1	0.57	0.87	1.1	2.4	2.7	1.4
Cr	1.6	0.28	1.1	0.68	1.2	0.67	0.76
Mn	0.95	1.1	1.5	1.5	1.8	1.6	1.9
Fe	1	1	1	1	1	1	1
Co	2.8	1.3	2.2	2.0	2.5	3.0	1.7
Ni	<26	<8.6	<10	<7.4	15	<11	<6.8
Cu	24	33	9.7	32	47	76	30
Zn	40	17	54	44	100	67	100
Ga	0.46	0.24	0.24	0.27	0.58	0.70	0.48
As	33	9.3	13	13	110	97	37
Se	2300	570	1300	2600	7700	10,000	2700
Br	58	69	120	88	140	220	760
Ag	<790	<260	<420	<290	<500	<760	<280
In	6.8	<5.2	4.2	4.1	47	36	6.8
Sb	340	110	170	150	370	300	380
I	21	7.2	5.4	5.3	6.5	<6	<4
La	1.2	0.52	0.54	0.65	0.92	0.63	0.76
Ce	2.5	0.86	1.3	0.88	1.7	1.2	1.3
Sm	1.2	0.48	0.62	0.82	1.0	0.75	0.72
Eu	0.74	0.53	0.62	1	0.92	1.0	6.4
W	5.8	4.0	<4.2	<5	3.3	30	3.2
Hg	3200	2900	<6200	5900	2200	5800	2400
Th	4.6	1.0	1.4	1.4	1.2	0.45	0.72

TABLE III-15. Elemental Concentrations in the USSR

Location	Latitude	Comments	Fe*	Al*	Cu*	Mn*	Cr*	Ni*
Cape of Desire (Novaya Zemlya)	75	Polar Island	4.3	1.7	0.61	0.25	0.34	0.38
Dickson Island		Polar	24	8.3	2.9	1.1	---	1.3
Salehard	67	Polar, Inland	21	7.9	2.9	1.7	1.6	2.4
Sevastopol	45	On Black Sea	160	130	14	14	6.7	15
Petropavlovsk, Kamchatka	53	City on Okhotsk Sea, Pacific Ocean	390	86	---	12	2.7	5.9
Magadan	60	City of Okhotsk Sea, Pacific Ocean	410	86	13	21	6.0	7.2
Tien Shan		Continental City	---	---	2500	380	94	97
Novosibirsk	55	Continental City	---	---	---	200	120	150
Novosibirsk	55	Continental City	---	---	660	430	120	72
Tashkent	42	Continental City	---	---	110	140	92	160
Tashkent	42	Continental City	---	---	1500	270	140	160
Semipalatinsk	51	Continental City	---	---	---	170	59	68
Indian Ocean, N. Lat.	--	----------	180	120	12	7.9	7.2	2.9
Indian Ocean, S. Lat.	--	----------	7.0	12	2.1	0.24	0.23	0.35
NW Ind. Stas. 1-10	42	Highly polluted urban	6500	1900	380	180	54	<50
TG, Summer (Winter)	60	Most remote of 7 Stations	71/ (810)	66/ (38)	0.9/ (2.2)	1.5/ (0.7)	0.59/ (1.1)	<2/ (<2)

*Concentration, ng/m^3

TABLE III-15. Normalized Enrichments in the USSR

Element	Novaya Zemlya	Dickson Island	Salehard	Sevas-topol	Petropav-lovsk	Magadan	Indian Ocean North	Indian Ocean South
Al	0.23	0.18	0.14	0.38	0.17	0.083	0.029	0.66
Cr	19	---	17	12	1.7	2.4	14	4.0
Mn	3.8	2.0	3.4	3.6	1.6	1.9	2.0	2.4
Fe	1	1	1	1	1	1	1	1
Ni	88	48	150	91	22	14	22	47
Cu	290	260	190	150	190	52	130	400

TABLE III-17. Niles/Twin Gorges Concentration Ratios

Large-Particle Elements	Concentrations* (ng/m^3)		N/TG Ratio
	Niles	Twin Gorges	
Fe	950	71	13
Al	580	66	8.8
Sc	0.49	0.044	11.1
Sm	0.11	0.013	8.5
Cr	3.8	0.59	6.4
Ce	1.6	0.24	6.6
Na	120	18	6.7
	Geometric Average		8.4
Small-Particle Elements			
Br	94	0.54	170
As	4.6	0.31	15
Sb	1.9	0.13	15
Se	0.89	0.043	21
Zn	130	3.8	34
	Geometric Average		31

*Data from Table III-12.

TABLE III-18. Seasonal Concentration Comparisons - TG, ARO, MI

	TG1 Summer	TG2 Winter	TG1/TG2	ARO1 Summer	ARO2 Winter	ARO1/ARO2	MI3 Summer	MI4 Winter	MI3/MI4
Na	49	290	0.17	65	99	0.66	48	96	0.50
Mg	41	37	1.1	47	33	1.4	370	70	5.3
Al	170	38	4.5	240	250	1.0	250	180	1.4
Cl	7.8	310	0.025	6.9	21	0.33	15	11	1.4
K	83	41	2.0	140	44	3.2	190	75	2.5
Ca	120	48	2.5	120	38	3.2	880	200	4.4
Sc	0.065	0.016	4.1	0.11	0.033	3.2	0.12	0.089	1.3
Ti	14	2.7	5.2	12	5.1	2.4	12	12	1.0
V	0.32	0.37	0.87	1.3	2.5	0.52	1.4	0.88	1.6
Cr	2.5	1.1	2.3	0.88	1.3	0.68	1.1	1.2	0.9
Mn	3.1	0.73	4.2	9.5	7.1	1.3	8.1	7.1	1.1
Fe	96	810	0.12	230	300	0.77	240	250	1.0
Co	0.087	0.037	2.4	0.11	0.086	1.3	0.4	0.26	0.54
Ni	---	---	---	---	---	---	---	---	---
Cu	0.84	2.2	0.38	4.9	13	0.38	1.8	8.7	0.21
Zn	4.1	2.8	1.5	36	30	1.2	23	32	0.72
Ga	0.026	0.18	0.14	0.12	0.11	1.1	0.19	0.095	2.0
As	0.22	0.77	0.29	4.7	2.2	2.1	5.1	8.0	0.64
Se	0.038	0.164	0.59	0.43	0.34	1.3	0.38	1.2	0.32
Br	1.1	2.7	0.41	2.9	3.7	0.78	6.0	5.7	1.1
Ag	---	---	---	---	---	---	---	---	---
In	<0.0018	0.0039	<0.46	0.074	0.071	1.0	0.011	0.061	0.18
Sb	0.078	0.085	0.92	0.71	0.28	2.5	0.54	0.38	1.4
I	0.24	0.35	0.69	0.11	0.26	0.42	0.17	0.37	0.46
La	0.20	0.10	2.0	0.33	0.065	5.1	0.29	0.17	1.7
Ce	0.45	0.11	4.1	0.58	0.16	3.6	0.35	0.38	0.92
Sm	0.024	0.020	1.2	0.050	0.012	4.2	0.035	0.021	1.7
Eu	0.0039	0.0064	0.61	0.0086	0.0040	2.1	0.0058	0.0047	1.2
W	<0.027	0.12	<0.23	0.043	0.045	1.0	0.062	0.038	1.6
Hg	0.34	0.048	7.1	0.19	0.19	1.0	0.46	0.90	0.51
Th	0.076	0.030	2.5	0.044	0.0071	6.2	0.033	0.028	1.2

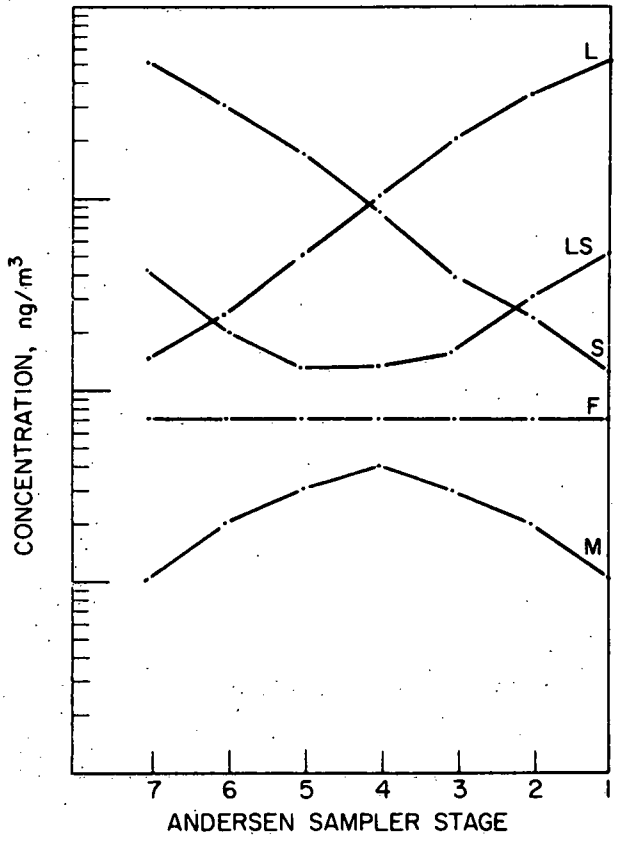

Figure III-1 Idealized Particle Size Distribution Shapes

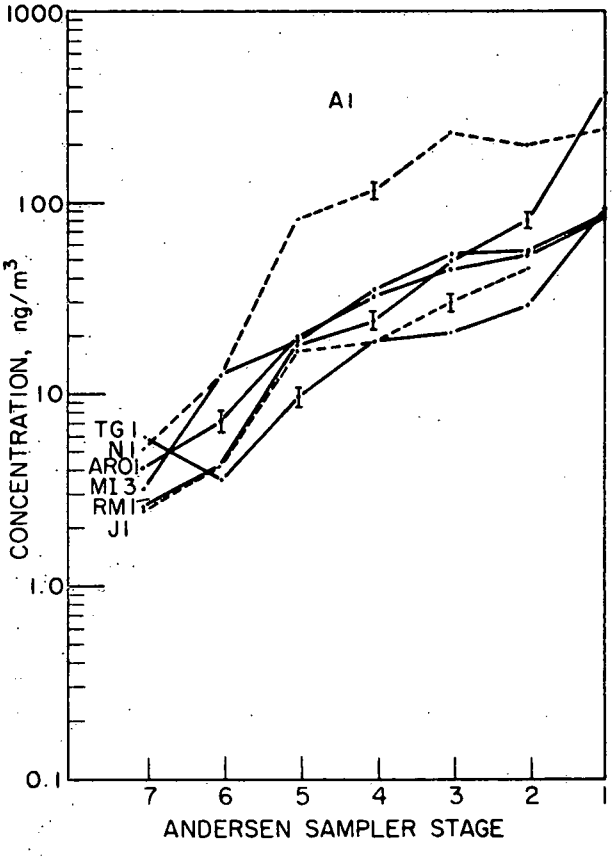

Figure III-2 Particle Size Distributions of Al, Canadian Summer Experiment

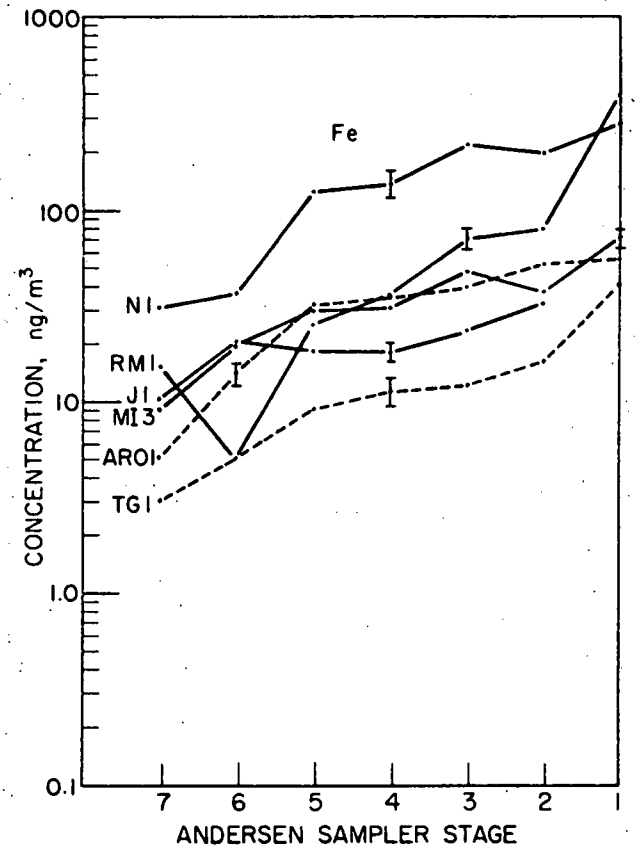

Figure III-3 Particle Size Distributions of Fe, Canadian Summer Experiment

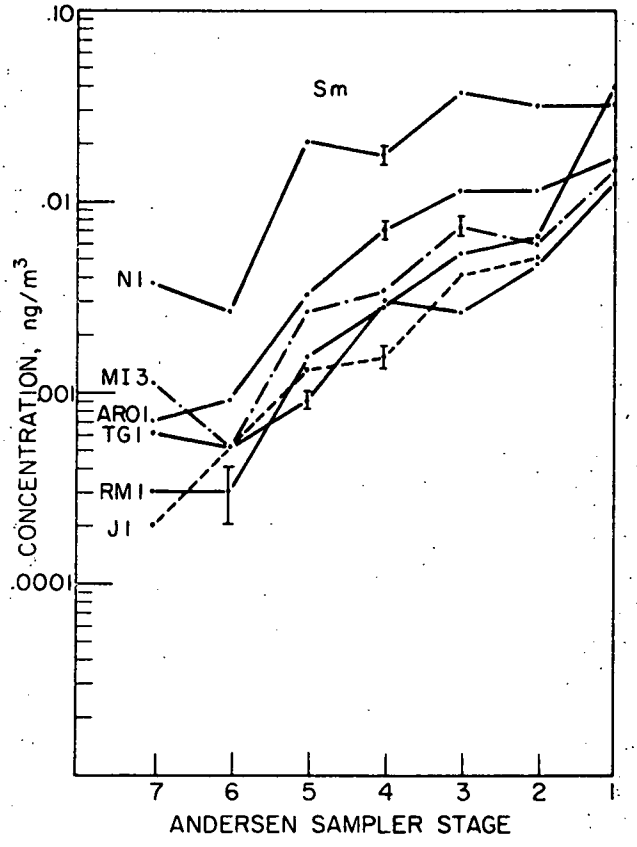

Figure III-4 Particle Size Distributions of Sm, Canadian Summer Experiment

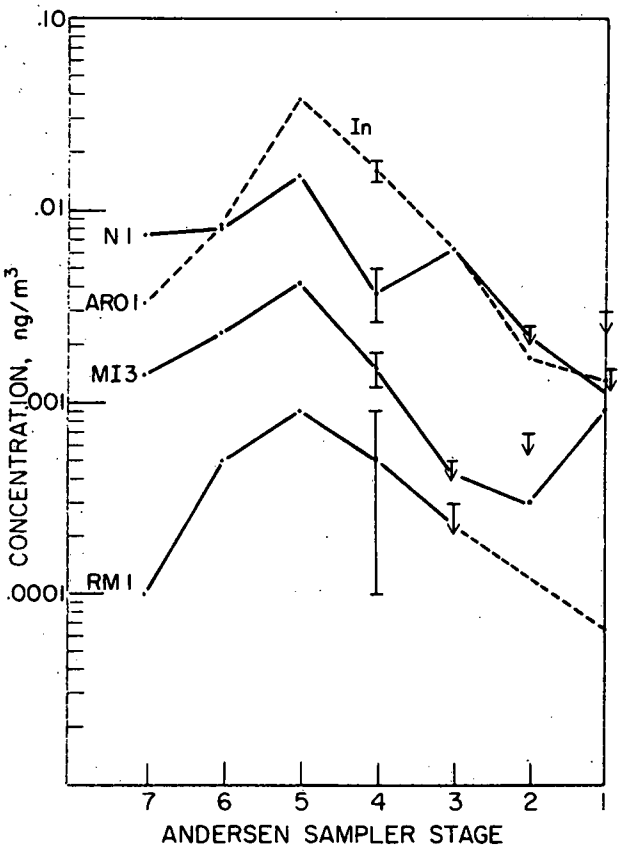

Figure III-5 Particle Size Distributions of In, Canadian Summer Experiment

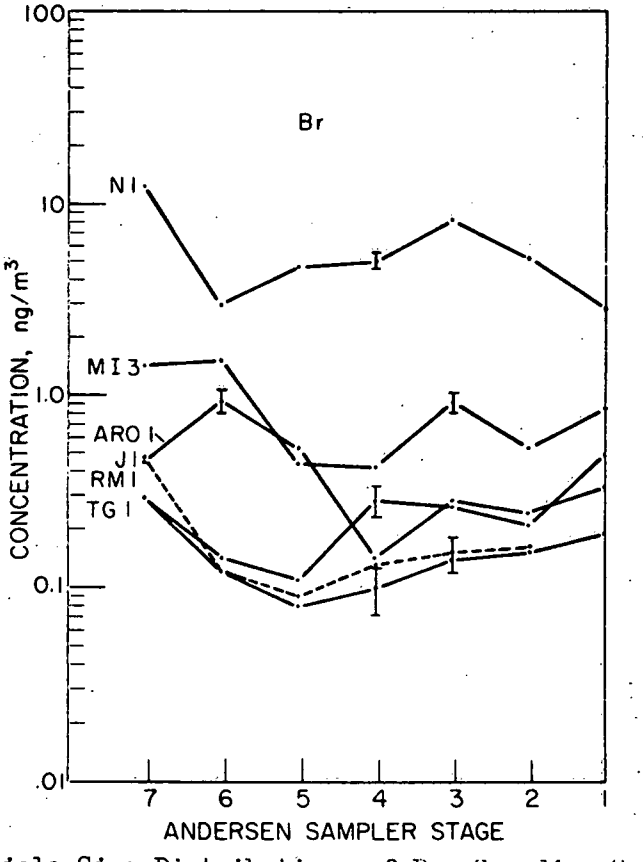

Figure III-6 Particle Size Distributions of Br, Canadian Summer Experiment

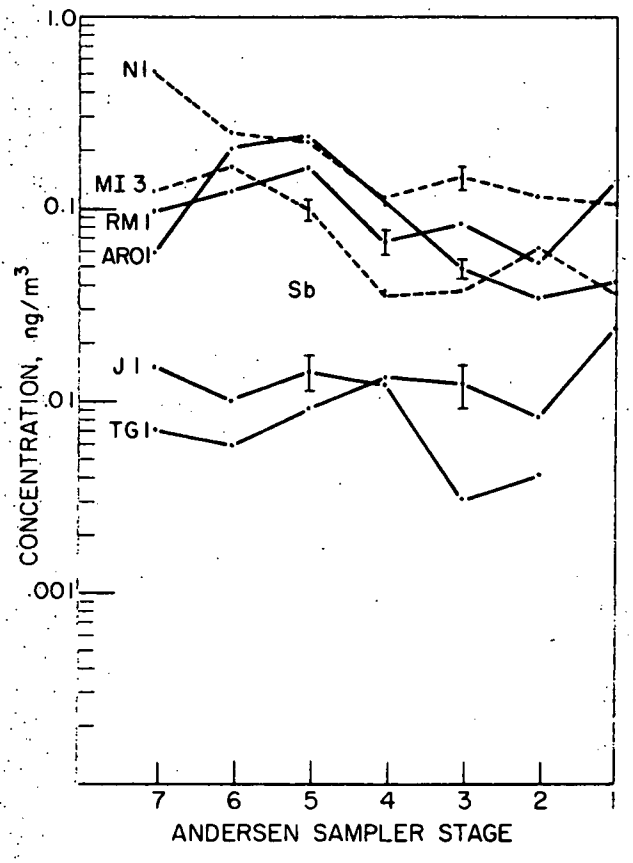

Figure III-7 Particle Size Distributions of Sb, Canadian Summer Experiment

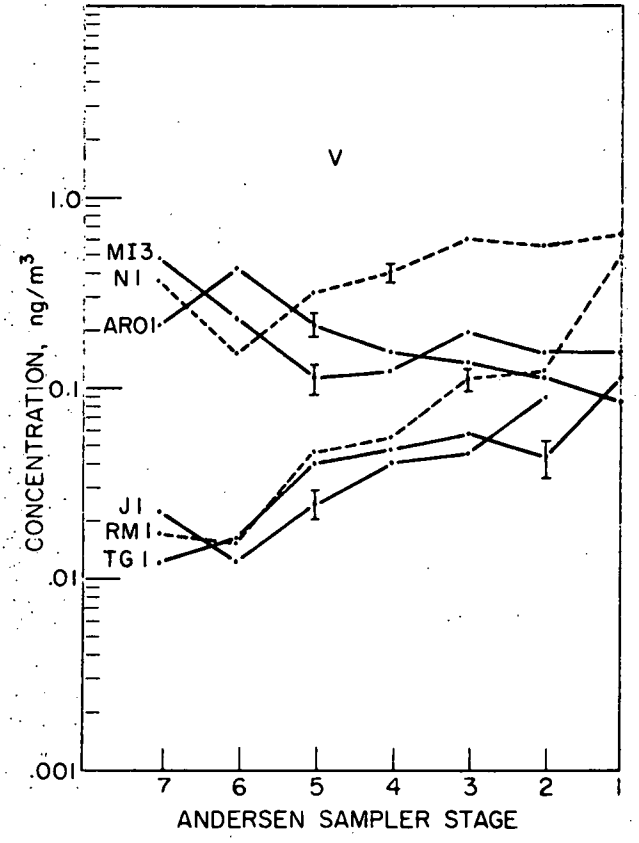

Figure III-8 Particle Size Distributions of V, Canadian Summer Experiment

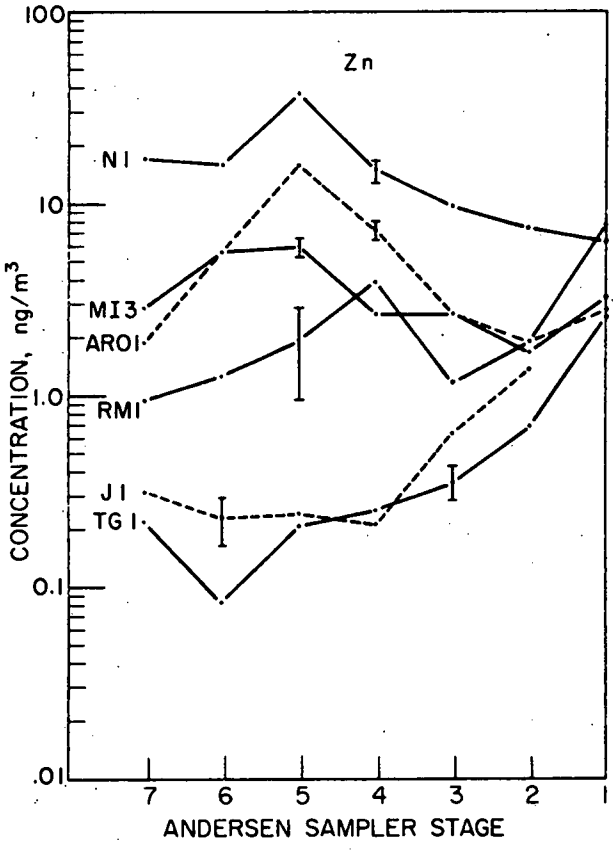

Figure III-9 Particle Size Distributions of Zn, Canadian Summer Experiment

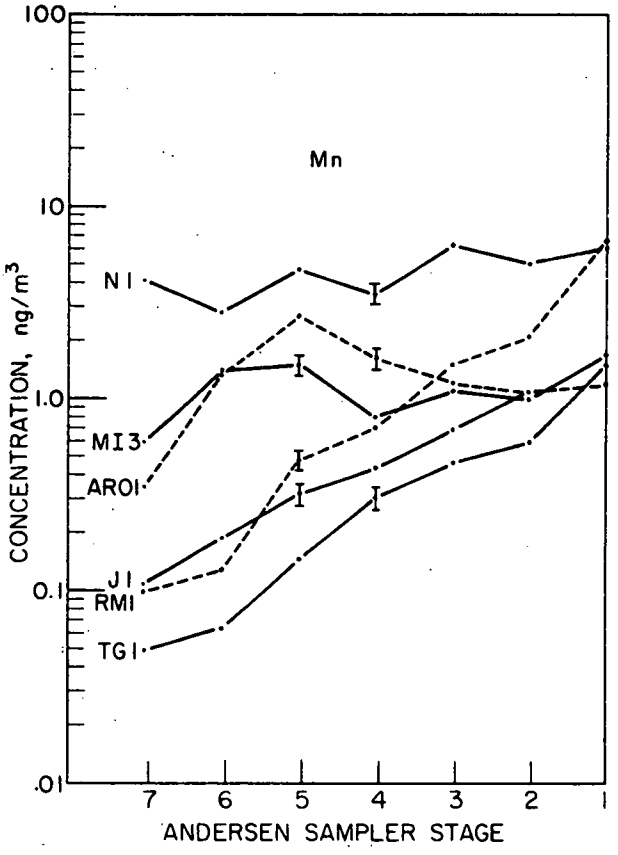

Figure III-10 Particle Size Distributions of Mn, Canadian Summer Experiment

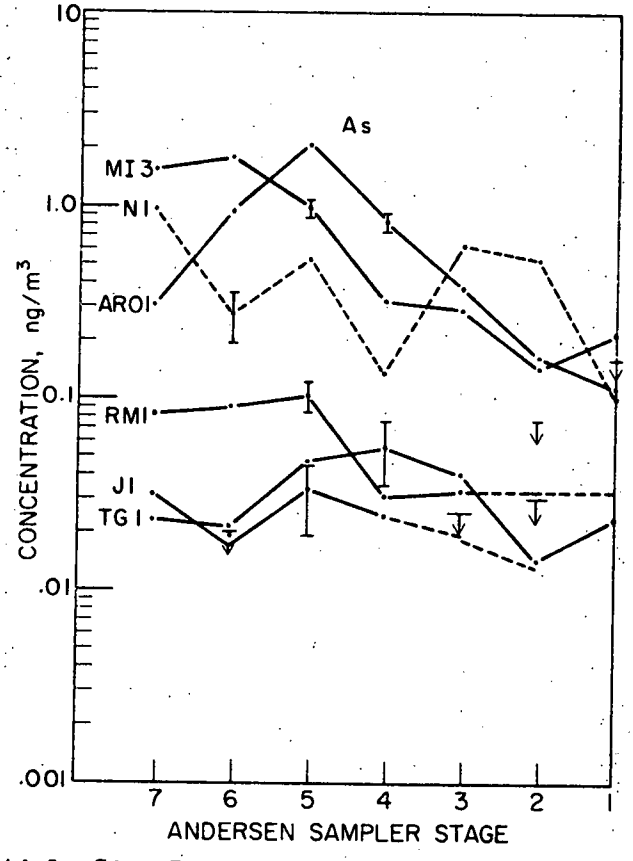

Figure III-11 Particle Size Distributions of As, Canadian Summer Experiment

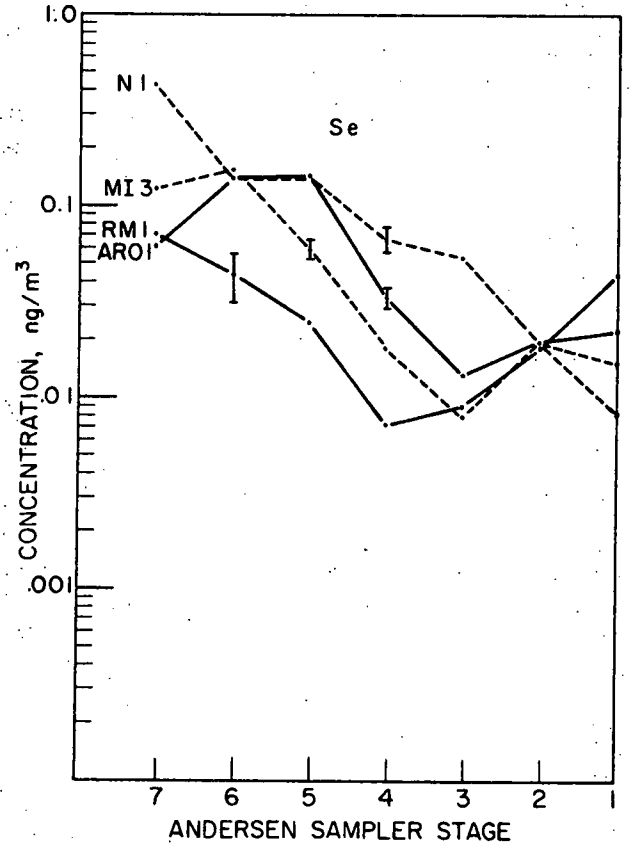

Figure III-12 Particle Size Distributions of Se, Canadian Summer Experiment

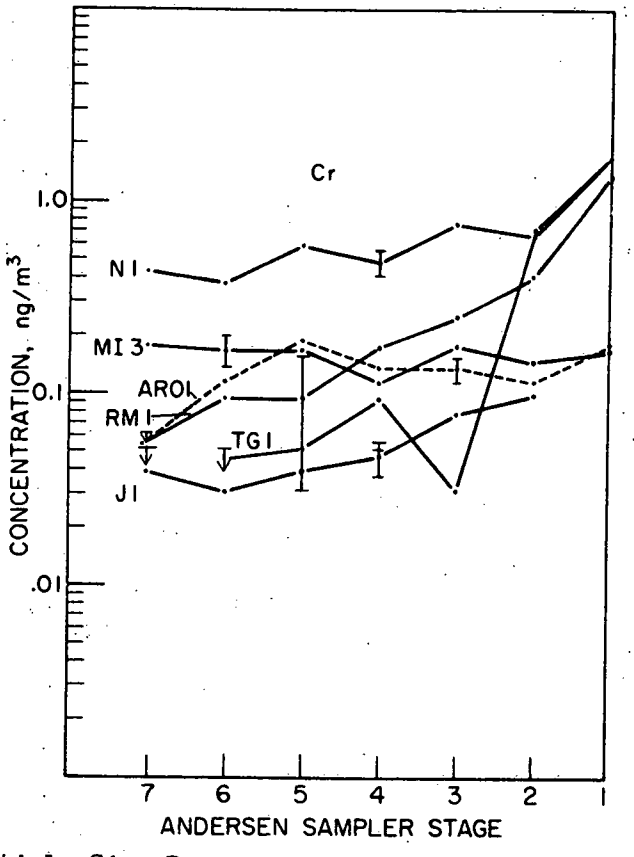

Figure III-13 Particle Size Distributions of Cr, Canadian Summer Experiment

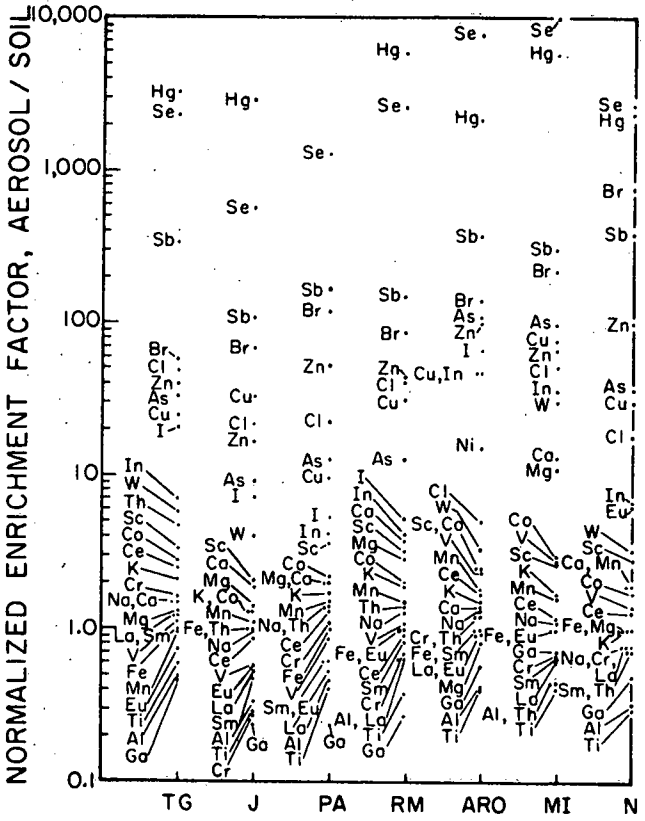

Figure III-14 Normalized Enrichment Factors, Canadian Summer Experiment

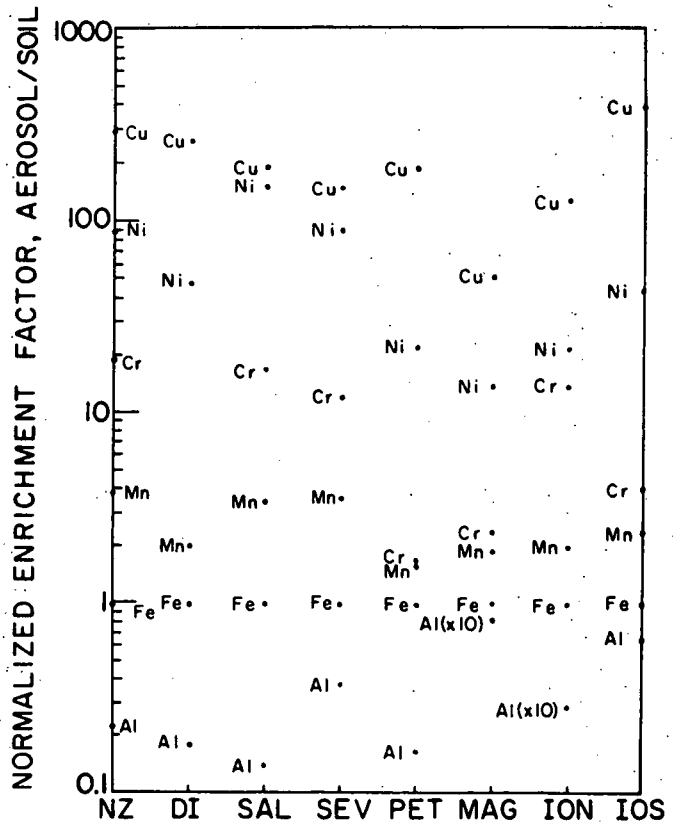

Figure III-15 Normalized Enrichment Factors, USSR

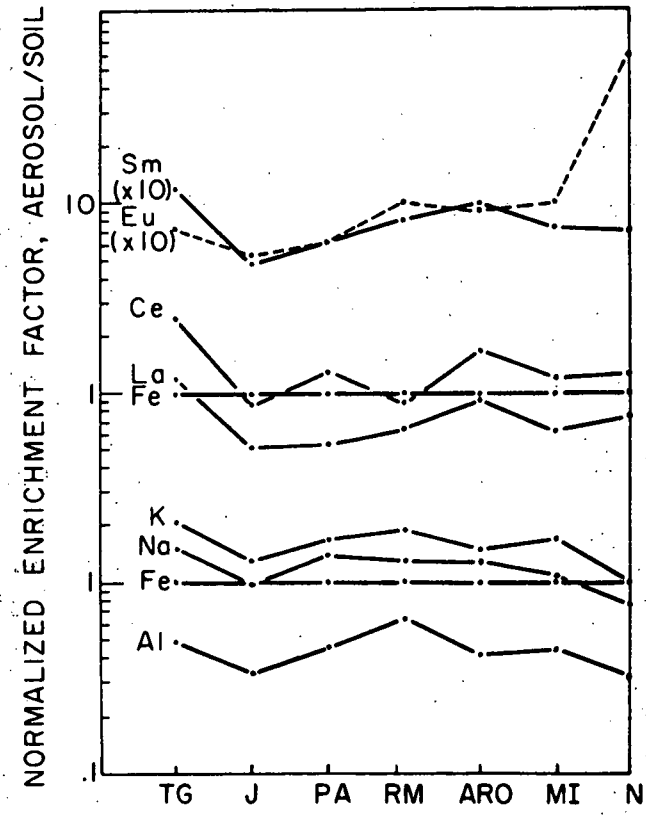

Figure III-16 Normalized Enrichment Factors, Canadian Summer Experiment

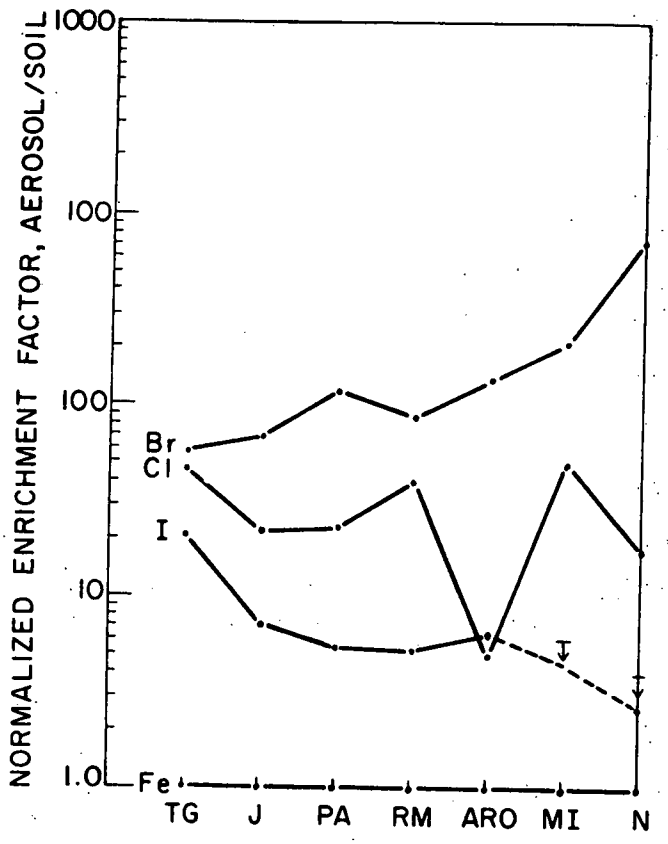

Figure III-17 Normalized Enrichment Factors, Canadian Summer Experiment

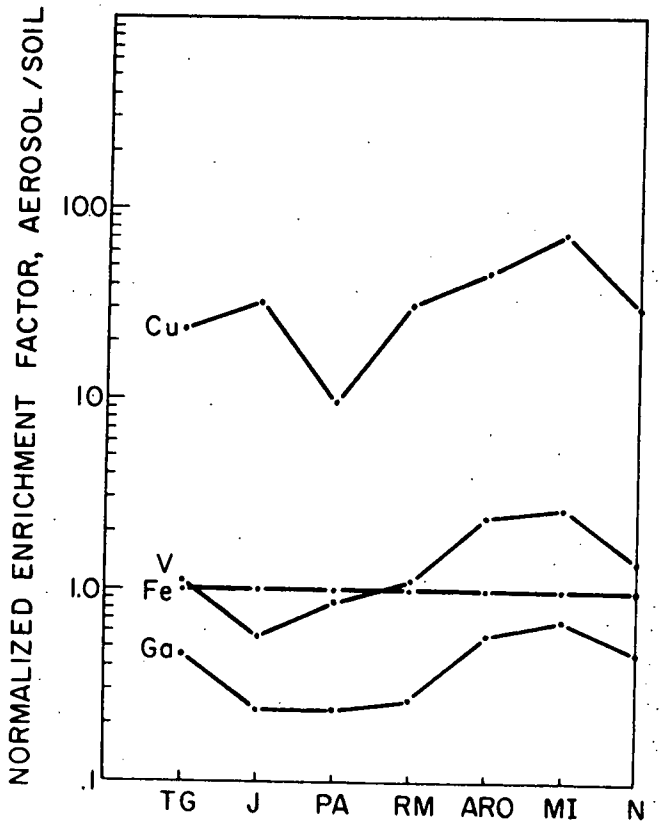

Figure III-18 Normalized Enrichment Factors, Canadian Summer Experiment

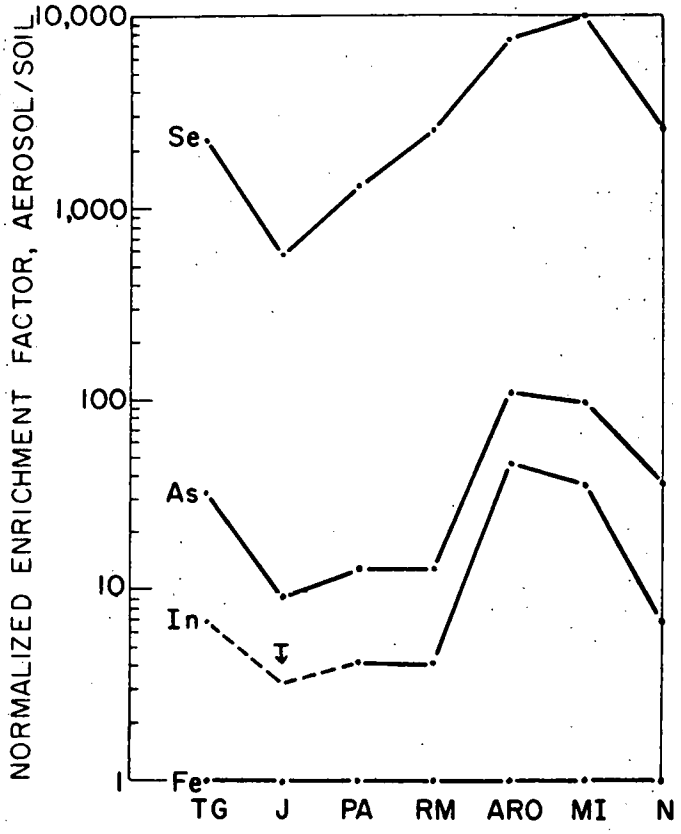

Figure III-19 Normalized Enrichment Factors, Canadian Summer Experiment

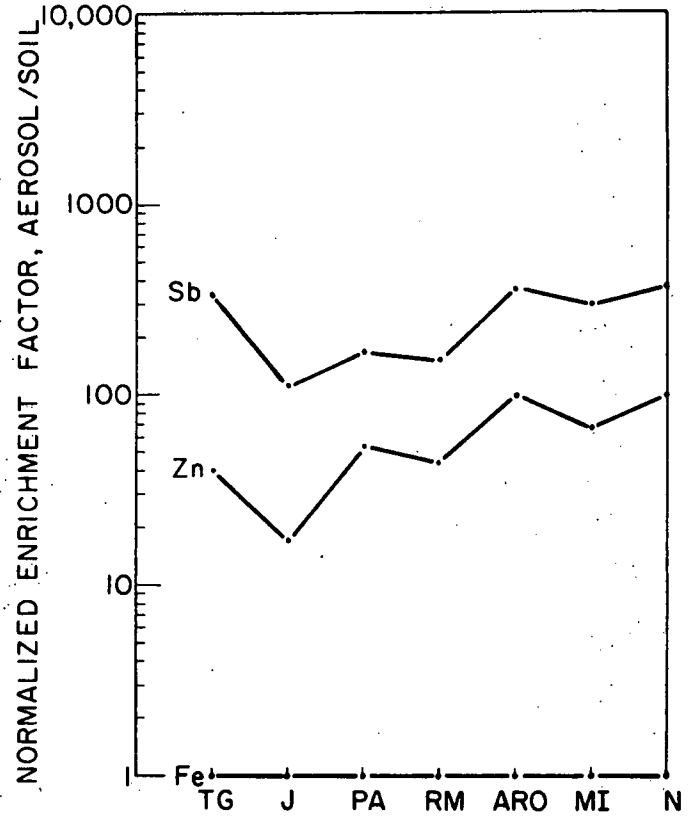

Figure III-20 Normalized Enrichment Factors, Canadian Summer Experiment

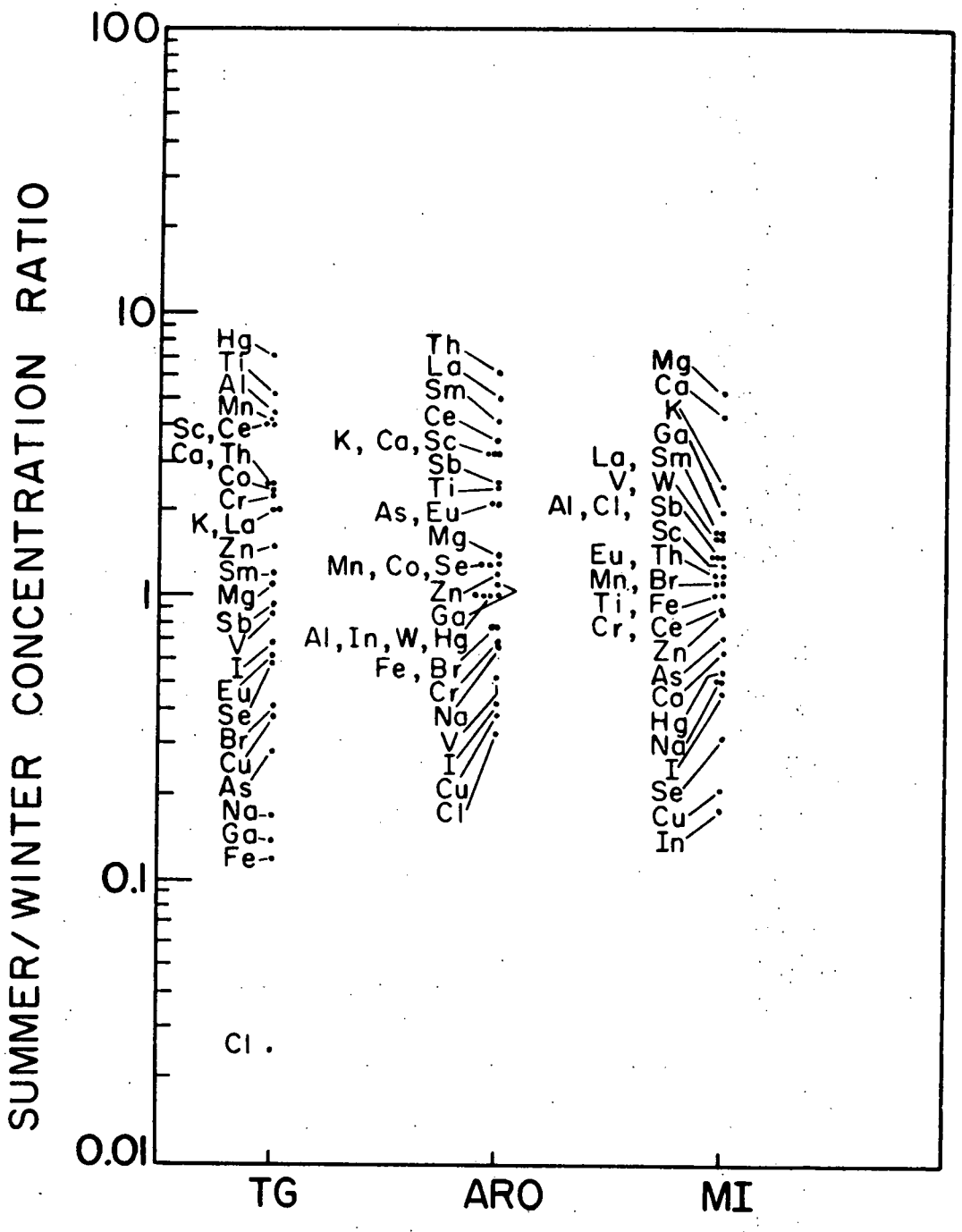

Figure III-21 Seasonal Concentration Ratios, TG, ARO, MI

CHAPTER IV

EVOLUTION OF THE AEROSOL

A. Summary of Implications

Aerosol particle size distributions may be modified by coagulation, sedimentation, impaction, rainout, washout, vapor-phase transfer, and cycling through condensation-evaporation stages in cloud processes. Of these, only coagulation is impossible to observe here, because the particles affected are too small to be caught by the Andersen Sampler without backup filter. The following paragraphs summarize by process the implications of the data of this investigation; the remainder of this chapter presents the relevant observations in detail.

Sedimentation and Impaction

Effects of sedimentation and impaction are most clearly implied in the Mackinac Island experiment, though only indirectly. A systematic preferential depletion of large particles is seen for nearly all elements between source regions (East Chicago and Ann Arbor) and Mackinac Island. When quantified, this removal is seen to be nearly independent of elemental chemical properties, suggesting purely physical removal mechanisms such as sedimentation and impaction (possibly also washout).

The Twin Gorges winter samples (TG2 and TG3) reveal marine aerosol which has penetrated some thousands of kilometers inland. Because the Na size spectrum remains nearly unaltered from that of fresh marine aerosol, it is speculated that physical removal processes have been largely ineffective in the 0.4 - 4 μm diameter size range, even over a period of days.

On the other hand, removal processes may be effective over a period of hours for locally wind-generated aerosol, as suggested by the Livermore, California experiment (Chapter VIII). The similar variations of wind speed and concentrations of several elements there may be due to saltation of very large particles during the day followed by rapid fallout of these same particles as the wind decreases at night. However, particle size data were not obtained in this experiment, making these conclusions somewhat tentative. Sedimentation velocities should allow such rapid fallout for the largest particles, for a 10 μm diameter particle has a fall velocity of 1 cm/sec, which varies with the square of the diameter.

The Niles, Michigan diurnal variations experiment (Chapter VII) suggests that large-particle elements may be preferentially removed during ground fog, possibly due to their activation as condensation nuclei, growth, and removal by sedimentation/impaction.

Rainout and Washout

Little can be said here, except as concerns the case of indium. This element always has the M-type distribution, no

matter how remote or proximate the location, suggesting that at least this size range is nearly unaffected by every modification process, including rainout and washout.

Vapor-Phase Transfer

The major source of continental Br may be auto exhaust (Loucks and Winchester, 1969). Br is rarely observed to have a parallel size distribution with Pb (as measured by Gillette, 1970). Br often shows an S-type distribution extending well into the larger size range, suggesting a vapor-phase transfer mechanism. Coagulation seems to be excluded here because of the sizes involved.

The clearest evidence for vapor-phase processes comes from the Twin Gorges winter samples. Iodine bears a nearly r^{-1} relation to Na, the expected result if the I were surface-distributed on the Na-containing particles. Cl follows Na in the larger sizes, with nearly the sea-salt ratio, but is heavily depleted in the smaller-sized particles. Br also shows major differences from its summer spectrum, but does not quite follow Na in shape.

B. Physical Removal in the Mackinac Island Experiment

The specific size distribution results from the first 3-week period of the Mackinac Island experiment (January) will now be considered (samples AA1 and MI1). Because the nature of the argument to be developed involves the data from many

elements, they will be presented in some detail. The Ann Arbor size distributions are plotted in Figures IV-1 through IV-4, with like distribution shapes grouped together for quick comparison. The Mackinac Island results are handled similarly in Figures IV-5 through IV-9. Tables IV-1,2 present total concentrations for both phases of the experiment.

Ann Arbor Size Distribution Patterns

In Ann Arbor the majority of the elements are found with L-type shapes, and within this large group there are second-order gradations. For example, Sc, Fe, Zn, Al, and Cu are strongly associated with the larger sizes, while La appears with somewhat smaller particles and Ga and K have pronounced small-particle components. But the overall trend is clear and suggests the source processes for these elements to be of the dispersion type. The soil and industrial sources are immediate possibilities.

Mackinac Island Patterns

The size distribution patterns of the simultaneous Mackinac Island sample are more complex but apparently not independent of the Ann Arbor trends. There are considerably fewer elements associated with the largest particle sizes but each one that is is similarly found at Ann Arbor.

The four elements Fe, Cr, Cu, and K are here either flat in size distribution or somewhat M-type in shape, and again each of these had an L-type shape at Ann Arbor.

Na, Zn, and In peak similarly in the smaller intermediate sizes, while Mn, As, Br, V, I, Sb, Se, and Ga have S-type patterns. Again there is a definite relation between the two locations, for with the exception of Na and Ga these elements were in the same Ann Arbor group (S). (Iodine was determined only for some stages at Ann Arbor, but the four reported values point to a strong small-particle association.)

Mackinac Island - Ann Arbor - East Chicago Comparison

During the second 3-week period (February) simultaneous Andersen samples were taken in all four locations. The repeated samples at the Michigan locations show size distributions highly similar to the first 3-week period (Table III-1). There are some elements, though, such as Cu, K, and the rare earths Ce, La, and Sm, which show peaks at smaller particle sizes than before, but the size distributions of the majority of elements closely resemble those of the first period, and the elements may be placed into the same size group. For example, the large-particle group still contains Sc, Ca, Cl, Ti, and Th, while Mn, As, Se, V, Hg, I, In, Zn, Br, and Sb are still associated with small particles. A comparison of the two Ann Arbor samples confirms these constant tendencies for this location also. There is no case of an element shifting radically from small to large particles or in the opposite direction from the first sample to the second at the same location.

The two East Chicago Andersen runs again show a remarkable similarity to the Michigan runs. The particle size trend

of a given element is generally very similar at all four sites, but with the expected higher concentrations in East Chicago.

Figures IV-10 through IV-17 present comparative particle size distribution plots for eight elements at each of the four locations. The three urban locations appear much more similar to each other both in total concentration and size distribution than they are to Mackinac Island, and differences between the urban locations are not usually great.

Fe and Al are shown as representatives of soil-derived elements which may also have pollution sources, and again show the preferential association with large particles noted for the first 3-week period. Manganese is similar, except that it shows stronger tendencies than iron. Bromine, usually considered to originate primarily from transportation sources, shows a possible industrial source near the Central Fire Station as revealed by the concentration peak at stage 4 (rarely seen for Br but shown by several other elements there), but at the other stations shows the usual S-type pattern. (Note that the "industrial" Br does not show up at Markstown Park, suggesting that it is not from the steel industry.) In general, the urban Mackinac Island concentration ratios of Br at the three urban locations are among the highest for the elements of this experiment, probably a reflection of the unusually low values at Mackinac Island.

The other four elements shown, Zn, Sb, As, and In, behave similarly to the above examples, but for Zn there appears to

be a strong dispersion source in Ann Arbor, suggested by Nifong (1970) to be fly ash from power plants and incinerators. This is the only case where we have observed a pure L-type shape for Zn. The majority of source processes seem to give rise to M- and S-type patterns for this element.

Indium is interesting because of the high degree of similarity among its size distributions, more so than for the other elements. This is treated in more detail below.

The arsenic plot is unusual for its similarity of concentrations between Mackinac Island and the other locations. This cannot be some effect of its size distribution alone, for the same S-type distribution is shown by a number of other elements with much larger concentration differences between locations. It also appears not to be related to volatility, since Hg is also volatile and shows larger urban/Mackinac Island ratios. The other (most likely) explanation is that of a source of As near Mackinac Island, possibly in the industrialized Sault Ste. Marie area.

In summary, then, the addition of the East Chicago stations seems to add little to the total picture being developed other than higher concentrations and the knowledge of the degree of similarity between source and remote regions.

Mackinac Island - Ann Arbor Comparisons

A detailed comparison of the Ann Arbor size distributions with those of Mackinac Island during the same period reveals a

remarkable regularity of large-particle preferential enrichment at Ann Arbor (or large-particle preferential depletion at Mackinac Island). This seems to be valid for nearly all the elements, independent of their chemical nature, supposed formation process, or observed particle size distribution, and holds true to a comparable extent during both sampling periods. Figures IV-18 through IV-22 show some representative Mackinac Island-Ann Arbor comparisons for the first 3-week period. Typical elements are Al and Fe. Aluminum, a large-particle element at both locations, has the bulk of its extra mass at Ann Arbor on stages 1-4, while stages 6-7 are more nearly equal and stage 5 is essentially the same at both locations. Other large-particle elements showing similar behavior include Na, Cu, Cr, and Fe. Iron is noteworthy for the sharp divergence of behavior at stage 4. Arsenic, though heavily associated with small particles at Mackinac Island and much less so at Ann Arbor, nevertheless show this same relative enrichment, also beginning sharply at stage 4. As mentioned earlier, this behavior may be partially caused by a local source. Br shows this effect less strongly, while V, Mn, and Se have nearly identical patterns at both sites.

In an attempt to quantify the above observations, the Ann Arbor/Mackinac Island concentration ratio was calculated for each element on each stage, then normalized to stage 7 as 1.0. For each stage the geometric mean ratio over 23 elements (Mg, I, Ga, W, Hg, Th, omitted because of large uncertainties) was

determined, with the results shown in Figure IV-23 and Tables IV-3,4. Figure IV-23 shows that the mean normalized stage ratios show the same increasing trend with increasing particle size during both sampling periods, but the enrichments are larger during the second of these.

In order to learn whether this enrichment pattern was a function of the size distribution shape itself, the above sequence was repeated for 3 elemental subgroups, roughly those containing S-type elements, F-type elements, and L-type elements. The geometric mean normalized concentration ratios for these cases are given in Tables IV-5,6, and displayed in Figure IV-24, where it appears that the enrichment pattern is size-distribution independent.

The explanation for this phenomenon is not immediately clear. The fact that most elements show both concentration dropoffs and equal alterations of their size-distribution shapes between Mackinac Island and Ann Arbor suggests a combination of dilution plus removal. The removal process seems to act on a certain fraction of the particles in a given size range, independent of their chemical nature. Examples of such physical processes are dry impaction, fallout, and washout. Cloud droplet nucleation per se would not change the spectra in this way, for its effect may depend on the solubility of the individual particles, and should show up in preferential removal of large soluble particles compared to small insoluble ones. The observed large particle removal

is in agreement with cloud droplet nucleation tendencies, but there seems to be little solubility effect seen here.

C. Vapor-phase Redistribution of Bromine

In inland areas the major source of both atmospheric Pb and Br appears to be combustion of leaded gasolines (Gillette, 1970; Loucks and Winchester, 1969). The ethyl fluid additive contains Pb, Cl, and Br, with Pb approximately 2 g/gallon and mass ratios Br/Cl = 1.15 and Br/Pb = 0.39. The major emission product is believed to be PbBrCl. If this is correct, the initial particle size distributions of Pb andBr should be identical.

The size distribution of atmospheric lead is well-known (Gillette, 1970), and appears not to change significantly with aging of the aerosol. Approximately 50 percent of the Pb is found on the backup filter, with the other 50 percent divided roughly equally among the impaction stages.

Our size spectra for Br show definite and fairly reproducible differences from the typical Pb spectra. Bromine tends more to an S-type distribution at many of the more populated locations, especially where aging of some hours' duration may be involved. However, because of the lack of a backup filter and direct Pb measurements here, any conclusions must be highly tentative.

Consider the various Br spectra of this experiment (Figures III-6 and IV-14,22,25). Runs N1, MKT1, MI1, MI2, MI3, MI4, ARO1, and ARO2 show definite S-type tendencies, with well-defined maxima on the later impaction stages. This behavior

is explainable either in terms of coagulation or vapor-phase transport, except for the cases where particle sizes are affected which are too large to be influenced by coagulation (MI1, MI2, MI4, ARO2). Since Br is known to be lost from automotive combustion aerosols (Lininger et al., 1966; Winchester and Duce, 1967), such a vapor-phase transfer mechanism seems a strong possibility here. Nifong (1970) also finds evidence that Br quickly becomes associated with particles of diameter 1-2 μm (Andersen stages 4-5).

The summer Br spectra from the western Canadian locations are highly similar to one another and different from the previously-discussed examples. Each has a broad minimum at stages 5 and 6, with the large-particle end nearly as high as the small-particle end. This behavior at stage 7 can be understood in terms of vapor-phase transfer from smaller combustion aerosols, but the reasons for the increase in concentration at the larger sizes are not clear. These first stages cannot reflect soil contributions, for the aerosol/soil enrichment factor even at these remote locations is too high (50-100). Industrial processes seem to be eliminated because of the remoteness and lack of confirming observations by Nifong (1970) anywhere in Northwest Indiana.

A possible explanation may be multiple cycles of cloud droplet nucleation, coalescence, and evaporation. Several nuclei would then be combined into one for each cycle, and the result of several cycles would be a considerably enlarged nucleus. Inorganic bromine compounds tend to be soluble,

thus favoring their participation in such processes before eventual removal from the atmosphere.

D. Constancy of Indium Particle Size Distributions

Indium is the only element observed in this study to invariably exhibit an M-type distribution. Its reproducibility is even better than this alone would indicate, for the Andersen stage with maximum concentration is always that corresponding to particle diameters of about 1 μm, usually stage 5. The extent of this similarity can be seen from Figures IV-26,27 and Figures III-5, IV-17.

Measurements of Nifong (1970) generally confirm this observation, though they show a wider range of behavior nearer to sources. Specifically, indium occasionally peaked on stages 6 or 7, and more frequently on the backup filter.

This size distribution regularity suggests that indium has only one or a very few major source processes. The small size may indicate a high-energy dispersion source rather than a condensation type, but this source cannot be the soil.

More importantly, the In spectra do not appear to vary significantly with remoteness, perhaps because the sources are widespread and none of the sampling sites was really remote from them. It may also be explained in terms of the peak position of 1 micron diameter being in just the size range which is affected significantly by neither coagulation nor precipitation processes. In any event, In spectra do not appear to be highly altered through aging.

E. Aging Effects on a Marine Aerosol

The winter aerosol at Twin Gorges, NWT, is remarkable. Because of its unusual aspects all elemental size spectra are shown (Figures IV-28 through IV-32).

Most of the size distributions are nearly as expected. Al, Co, Cr, Th, Sc, Ce, and La are strongly L-type. Fe, K, Ca, Sb, Mn, and Sm are nearly L-type, but with a peak on stage 4 or 5. Cu, V, Zn, As, Ga, In, and Se are M-type.

The surprise comes in the Na and Cl spectra (Figure IV-32). Sodium, with its very large peak at stages 4 and 5, is here unlike any element seen before, and in particular unlike any of the other Na spectra of this experiment (Figures IV-33,34). The resemblance to the ARO2 spectrum is fortuitous, as will be developed later. Chlorine is very similar to sodium, especially at the larger particle sizes, again being different from its norm (Figures IV-35,36). Mg and Br show some resemblance to Na and Cl, each deviating from its more normal pattern.

This Na pattern (which because of its analytical precision will serve as the reference shape) strongly resembles the shape of Cl and Br in fresh Hawaiian marine air (Duce et al., 1967) (Figure IV-40), and leads to the inference that actual marine aerosol is being observed here. [Note that in Figure IV-40 stage A represents the largest particles. The particle diameter at the Na maxima (1.5 μm) is also quite close to the comparable Cl figures of Duce et al. (4 μm). This Cl/Na

behavior is apparently reproducible, reappearing in Andersen sample TG3 (Figure IV-37).

Further confirmation for the marine aerosol idea comes from the seasonal variations, which show Cl and Na enriched over their summer values by 40 and 5.9 times, respectively, while a soil element like Al is 4.5 times lower than its summer level (Figure III-21). In addition, the Cl/Na ratio increases from a summer value of 0.16 to 1.1 in winter, approaching the sea water value of 1.8.

If the sea-salt origin of the Na and Cl here is accepted, other ideas immediately follow. First, the aerosol has undergone an order-of-magnitude dilution since its generation, for typical Na concentrations near the ocean are a few $\mu g/m^3$, while the total Na here is 290 ng/m^3. This dilution may involve mixing with more continental air containing the L- and M-type elements observed here.

Secondly, though some of the marine aerosol may have been removed from the atmosphere during transit, the apparent near preservation of its original shape suggest this to be a small effect, since removal processes may be size-dependent. In view of the small particle sizes of this aerosol, minimal removal seems physically reasonable.

Other elemental ratios are of interest. Table IV-7 shows that the Mg/Na ratio is nearly the same as the sea water value, suggesting along with its size distribution that it is of marine origin. Next to Na, Mg is the most abundant cation in sea water (Table III-13). The Br/Na ratio is slightly above

that for sea water, possibly because of a longer mean atmospheric residence time of Br or because of pollution sources. The I/Na ratio is 260 times greater than the sea water value, consistent with the well-known iodine marine aerosol enrichment (Winchester and Duce, 1966).

But the Cl/Na ratio is of greatest interest (Figures IV-38,39; Table IV-8). In the larger particles it is very close to the sea water ratio of 1.8, and the somewhat lower ratio for stage 1 can easily be accounted for by soil-derived Na admixture. In the smallest particles Cl/Na is far below the sea water ratio and suggests Cl loss from small particles in the atmosphere during aging. (Previous observations (Chapter VIII; Junge, 1963) have noted a Cl loss with time in filter samples taken without size discrimination.) Since the travel distances from the open ocean may be thousands of kilometers the aging times may be days or longer, depending on specific air trajectories of sampled air. Apparently there is little change in the Cl/Na ratio in larger particles during this time.

TABLE IV-1. Elemental Concentrations
Mackinac Island Experiment

	MIl (ng/m^3)	AAl (ng/m^3)	AAl/MIl
Na	78	360	4.6
Mg	15-35	90	3.6
Al	140	570	4.1
Cl	16	450	28
K	80	200	2.5
Ca	110	440	4.0
Sc	0.098	0.50	5.1
Ti	12	53	4.4
V	1.0	3.4	3.4
Cr	1.6	7.8	4.9
Mn	10	41	4.1
Fe	410	1300	3.2
Co	0.16	0.61	3.8
Ni	--	--	--
Cu	9.9	150	15
Zn	23	420	18
Ga	0.17	0.82	4.8
As	6.4	4.9	0.77
Se	0.31	0.90	2.9
Br	5.9	80	14
Ag	0.09-0.22	0.41	2.7
In	0.01	0.037	3.7
Sb	0.56	2.7	4.8
I	0.47	--	--
La	0.16	1.9	12
Ce	0.39	1.9	4.9
Sm	0.021	0.10	4.8
Eu	0.005	0.016	3.2
W	0.08	0.57	7.1
Hg	<0.21	0.6	>2.9
Th	0.019	0.10	5.3

TABLE IV-2. Elemental Concentrations — Mackinac Island Experiment

	MI2 (ng/m^3)	AA2 (ng/m^3)	CFS1 (ng/m^3)	MKT1 (ng/m^3)	MI2/MI2	AA2/MI2	CFS1/MI2	MKT1/MI2
Na	110	1300	950	750	1.0	12	8.6	6.8
Mg	42	220	520	460	1.0	5.2	12	11
Al	160	700	960	1000	1.0	4.4	6.0	6.3
Cl	14	1700	1500	920	1.0	120	110	66
K	81	260	320	400	1.0	3.2	4.0	5.0
Ca	150	800	1300	1200	1.0	5.3	8.7	8.0
Sc	0.10	0.77	0.72	0.68	1.0	7.7	7.2	6.8
Ti	12	62	48	68	1.0	5.2	4.0	5.7
V	1.3	5.8	30	41	1.0	4.5	23	32
Cr	1.3	5.6	18	24	1.0	4.3	14	18
Mn	9.6	36	75	84	1.0	3.7	7.8	8.8
Fe	330	1200	2100	2500	1.0	3.6	6.4	7.6
Co	0.13	0.47	1.3	1.0	1.0	3.6	10	7.7
Ni	--	--	--	--	--	--	--	--
Cu	6.6	60	24	340	1.0	9.1	3.6	52
Zn	29	1000	750	480	1.0	35	26	17
Ga	0.14	0.85	1.3	1.2	1.0	6.1	9.3	8.6
As	4.5	7.4	10	8.8	1.0	1.6	2.2	2.0
Se	0.74	1.5	1.4	1.6	1.0	2.0	1.9	2.2
Br	5.3	73	96	80	1.0	14	18	15
Ag	--	0.19	--	--	--	--	--	--
In	0.018	0.083	0.31	0.073	1.0	4.6	17	4.1
Sb	1.1	4.4	27	12	1.0	4.0	25	11
I	0.42	--	10	3.7	1.0	--	24	8.8
La	0.26	1.0	2.5	10	1.0	3.8	9.6	38
Ce	0.48	1.8	2.5	7.9	1.0	3.7	5.2	16
Sm	0.067	0.92	0.16	0.39	1.0	14	2.4	5.8
En	0.0062	0.033	0.037	0.06	1.0	5.3	6.0	9.7
W	--	<0.8	0.36	0.56	--	--	--	--
Hg	0.11	0.28	2.3	1.2	1.0	2.5	21	11
Th	0.029	0.097	0.23	0.27	1.0	3.3	7.9	9.3

TABLE IV-3. Normalized Concentration Ratios, AA1/MI1

	7	6	5	4	3	2	1
Na	1.0(0.2)	1.2(0.3)	0.55(0.10)	1.7(0.3)	2.9(0.5)	4.5(0.8)	6.4(1.2)
Mg	1.0(2.1)	1.4(2.8)	2.1(2.7)	5.1(5.1)	2.1(2.5)	3.7(6.6)	3.2(4.4)
Al	1.0(0.3)	0.66(0.12)	0.37(0.07)	0.94(0.14)	1.3(0.3)	1.6(0.3)	1.9(0.4)
Cl	1.0(0.4)	4.3(4.4)	0.86(0.32)	1.2(0.3)	2.8(0.5)	2.9(0.5)	3.2(0.6)
K	1.0(0.2)	0.68(0.13)	0.42(0.09)	1.0(0.2)	1.4(0.3)	1.0(0.2)	1.8(0.3)
Ca	1.0(0.7)	1.7(1.2)	0.92(0.38)	1.7(0.6)	2.7(0.9)	2.3(0.8)	6.0(1.6)
Sc	1.0(0.5)	1.8(0.8)	0.9(0.2)	2.6(0.6)	3.4(0.9)	2.8(0.5)	6.0(3.2)
Ti	1.0(1.3)	8.6(9.8)	1.2(0.9)	4.4(2.6)	6.2(3.8)	3.4(1.3)	4.9(1.8)
V	1.0(0.2)	1.1(0.2)	0.81(0.16)	1.0(0.2)	1.3(0.3)	1.4(0.3)	1.9(0.4)
Cr	1.0(0.3)	1.0(0.2)	1.0(0.2)	2.5(0.7)	2.4(0.5)	3.7(1.3)	4.3(0.8)
Mn	1.0(0.2)	1.9(0.5)	1.2(0.2)	2.0(0.5)	1.6(0.4)	1.7(0.3)	3.0(0.5)
Fe	1.0(0.4)	1.0(0.3)	1.3(0.3)	3.7(0.7)	6.1(1.2)	6.0(1.1)	15(3)
Co	1.0(0.6)	0.72(0.55)	0.47(0.26)	1.3(0.7)	2.4(0.9)	1.3(0.6)	2.1(0.9)
Ni	--	--	--	--	--	--	--
Cu	1.0(0.2)	0.87(0.21)	0.57(0.16)	2.1(0.4)	3.9(0.9)	7.9(1.9)	73(16)
Zn	1.0(0.2)	0.98(0.17)	1.4(0.3)	4.9(0.9)	12(3)	14(3)	26(5)
Ga	1.0(0.3)	1.5(0.8)	0.54(0.62)	1.9(1.1)	1.8(1.0)	3.0(2.1)	2.7(3.1)
As	1.0(0.3)	0.89(0.25)	0.98(0.25)	5.0(1.7)	5.5(2.5)	4.2(2.9)	11(10)
Se	1.0(0.4)	1.3(0.4)	1.1(0.4)	1.3(0.9)	3.4(4.2)	2.0(2.2)	1.1(1.2)
Br	1.0(0.3)	1.2(0.3)	0.96(0.20)	2.3(0.6)	2.3(0.5)	2.1(0.6)	2.9(0.9)
Ag	--	--	--	--	--	--	--
In	1.0(0.6)	0.88(0.27)	0.50(0.19)	0.79(0.39)	0.93(0.37	0.41(0.26)	0.30(0.28)
Sb	1.0(0.2)	1.4(0.3)	0.99(0.26)	1.30(0.3)	1.3(0.3)	0.96(0.36)	0.96(0.30)
I	1.0(0.4)	0.62(0.36)	2.7(3.0)	3.4(4.0)	0.54(0.68)	1.5(2.0)	0.68(0.76)
La	1.0(1.0)	0.61(0.64)	0.42(0.28)	0.28(0.08)	0.24(0.06)	0.094(0.037)	0.14(0.07)
Ce	1.0(0.8)	0.92(1.00)	0.30(0.20)	0.58(0.25)	0.88(0.23)	0.83(0.40)	1.1(0.5)
Sm	1.0(1.9)	0.57(0.61)	0.18(0.07)	0.12(0.05)	0.17(0.04)	0.14(0.04	0.25(0.08)
Eu	1.0(1.0)	0.33(0.58)	0.27(0.36)	0.52(0.46)	0.72(0.49)	0.35(0.26)	1.0(1.2)
W	1.0(3.2)	2.5(3.6)	2.2(2.6)	1.4(1.3)	5.0(4.2)	4.2(2.9)	13(14)
Hg	1.0(1.2)	0.53(0.67)	0.59(0.76)	0.24(0.30)	0.15(0.21)	0.18(0.19)	0.53(0.69)
Th	1.0(1.7)	1.0(1.7)	0.67(0.60)	1.4(0.8)	2.8(1.7)	0.83(0.59)	3.3(2.5)

TABLE IV-4. Normalized Concentration Ratios, AA2/MI2

	7	6	5	4	3	2	1
Na	1.0(0.3)	0.56(0.11)	1.1(0.2	4.1(0.7)	11(3)	31(6)	75(15)
Mg	1.0(1.4)	0.7(1.0)	1.4(0.8)	1.8(3.8)	1.6(2.7)	11(16)	7.7(4.5)
Al	1.0(0.2)	0.58(0.09)	1.2(0.2)	2.6(0.4)	3.0(0.5)	3.2(0.6)	5.3(0.8)
Cl	1.0(1.0)	0.8(0.7)	1.5(0.6)	6.0(2.0)	5.9(1.0)	12(3)	17(3)
K	1.0(0.2)	1.9(0.4)	3.7(0.7)	2.8(0.5)	2.0(0.4)	2.4(0.4)	5.0(1.1)
Ca	1.0(0.6)	0.40(0.18)	0.47(0.20)	0.76(0.24)	2.4(0.7)	1.6(0.5)	2.6(0.8)
Sc	1.0(0.5)	1.2(0.5)	2.2(0.5)	3.9(0.7)	16(3)	5.5(1.3)	10(2)
Ti	1.0(1.5)	0.33(0.56)	0.19(0.22)	0.17(0.10)	0.73(0.35)	0.88(0.51)	0.86(0.47)
V	1.0(0.3)	1.0(0.2)	1.7(0.4)	1.2(0.2)	1.3(0.2)	1.3(0.3)	1.9(0.4)
Cr	1.0(0.6)	6.1(1.1)	13(3)	27(9)	21(5)	12(3)	34(9)
Mn	1.0(0.2)	1.1(0.2)	4.1(0.8)	3.7(0.6)	2.4(0.4)	2.8(0.6)	4.5(1.0)
Fe	1.0(0.3)	1.2(0.2)	2.7(0.5)	4.2(0.8)	6.5(1.0)	7.4(1.3)	12(2)
Co	1.0(0.2)	3.3(0.8)	4.1(0.8)	5.1(1.3)	8.6(1.9)	7.2(1.4)	12(3)
Ni	--	--	--	--	--	--	--
Cu	1.0(0.4)	1.3(0.4)	2.9(0.8)	5.9(1.7)	8.3(2.2)	14(5)	52(18)
Zn	1.0(0.2)	3.1(0.5)	12(2)	60(13)	170(40)	240(60)	290(60)
Ga	1.0(0.7)	9.4(9.5)	1.4(2.0)	1.4(0.6)	0.93(0.81)	1.4(2.0)	4.2(5.0)
As	1.0(0.3)	0.58(0.14)	2.1(0.4)	1.7(0.8)	0.82(0.76)	1.9(1.4)	5.6(4.0)
Se	1.0(0.2)	6.4(1.2)	14(3)	8.2(3.1)	5.8(2.6)	1.7(2.1)	8.0(5.0)
Br	1.0(0.3)	0.97(0.28)	3.2(0.6)	4.9(1.1)	4.1(0.8)	4.3(0.8)	9.1(1.7)
Ag	--	--	--	--	--	--	--
In	1.0(0.3)	0.67(0.13)	1.4(0.2)	1.5(0.6)	1.8(0.8)	1.3(1.1)	3.1(3.0)
Sb	1.0(0.2)	5.7(1.0)	9.5(2.3)	9.9(1.8)	16(3)	9.0(1.5)	10(2)
I	1.0(0.4)	1.2(0.6)	10(16)	9(11)	9(13)	10(9)	7(5)
La	1.0(0.3)	1.3(0.9)	1.6(0.6)	2.3(0.8)	2.4(0.7)	3.1(1.5)	6.5(4.5)
Ce	1.0(0.2)	20(21)	4.9(1.0)	6.5(1.4)	13(3)	11(3)	18(5)
Sm	1.0(0.3)	1.3(0.6)	3.4(0.4)	13(3)	41(7)	91(17)	220(40)
Eu	1.0(1.0)	0.94(0.96)	1.1(1.3)	1.2(1.2)	2.8(2.7)	4.3(5.2)	7(11)
W	1.0(1.1)	2.2(2.7)	9(12)	10(14)	7.8(6.5)	26(37)	260(250)
Hg	1.0(0.8)	1.7(1.2)	2.4(2.8)	0.5(0.5)	0.5(1.0)	6.7(6.5)	0.8(0.8)
Th	1.0(1.2)	0.45(0.57)	0.16(0.10)	2.9(1.6)	1.3(0.7)	2.7(1.3)	3.8(1.4)

TABLE IV-5. Normalized Concentration Ratios by Subgroup, AA1/MI1

	7	6	5	4	3	2	1
			Small-Particle Elements				
Br	1.0	1.2	0.96	2.3	2.3	2.1	2.9
As	1.0	0.89	0.98	5.0	5.5	4.2	11
Sb	1.0	1.4	0.99	1.3	1.3	0.96	0.96
Se	1.0	1.3	1.1	1.3	3.4	2.0	1.1
V	1.0	1.1	0.81	1.0	1.3	1.4	1.9
Geom. Avg.	1.0	1.2	1.0	1.8	2.4	1.9	2.3
			Large-Particle Elements				
Ca	1.0	1.7	0.92	1.7	2.7	2.3	6.0
Al	1.0	0.66	0.37	0.94	1.3	1.6	1.9
Cl	1.0	4.3	0.86	1.2	2.8	2.9	3.2
Sc	1.0	1.8	0.9	2.6	3.4	2.8	6.0
Ti	1.0	8.6	1.2	4.4	6.2	3.4	4.9
Geom. Avg.	1.0	2.4	0.79	1.9	2.9	2.5	4.0
			"Flat" Elements				
Co	1.0	0.72	0.47	1.3	2.4	1.3	2.1
K	1.0	0.68	0.42	1.0	1.4	1.0	1.8
La	1.0	0.61	0.42	0.28	0.24	0.094	0.14
Fe	1.0	1.0	1.3	3.7	6.1	6.0	15
Geom. Avg.	1.0	0.74	0.57	1.1	1.5	0.93	1.7

TABLE IV-6. Normalized Concentration Ratios by Subgroup, AA2/MI2

	7	6	5	4	3	2	1
			Small-Particle Elements				
Br	1.0	0.97	3.2	4.9	4.1	4.3	9.1
As	1.0	0.58	2.1	1.7	0.82	1.9	5.6
Sb	1.0	5.7	9.5	9.9	16	9.0	10
Se	1.0	6.4	14	8.2	5.8	1.7	8.0
V	1.0	1.0	1.7	1.2	1.3	1.3	1.9
Geom. Avg.	1.0	1.8	4.3	3.8	3.3	2.8	6.0
			Large-Particle Elements				
Ca	1.0	0.40	0.47	0.76	2.4	1.6	2.6
Al	1.0	0.58	1.2	2.6	3.0	3.2	5.3
Cl	1.0	0.8	1.5	6.0	5.9	12	17
Sc	1.0	1.2	2.2	3.9	16	5.5	10
Ti	1.0	0.33	0.19	0.17	0.73	0.88	0.86
Geom. Avg.	1.0	0.59	0.84	1.5	3.5	3.1	4.6
			"Flat" Elements				
Co	1.0	3.3	4.1	5.1	8.6	7.2	12
K	1.0	1.9	3.7	2.8	2.0	2.4	5.0
La	1.0	1.3	1.6	2.3	2.4	3.1	6.5
Fe	1.0	1.2	2.7	4.2	6.5	7.4	12
Geom. Avg.	1.0	1.8	2.8	3.4	4.0	4.5	8.5

Table IV-7. Comparison of Aerosol Elemental Ratios with Sea Water Values

Ratio	Aerosol (TG2), Winter	Sea Water
Mg/Na	0.13	0.12
Cl/Na	1.1	1.8
Br/Na	0.01	0.006
I/Na	1.2×10^{-3}	4.6×10^{-6}

TABLE IV-8. Cl/Na Ratios – Winter Samples TG2, TG3

Stage	1	2	3	4	5	6	7	F
TG2	0.63	1.3	1.6	1.5	<0.62	<0.01	0.08	--
TG3	0.42	1.3	1.7	1.6	<0.025	<0.094	-2.7	1.4

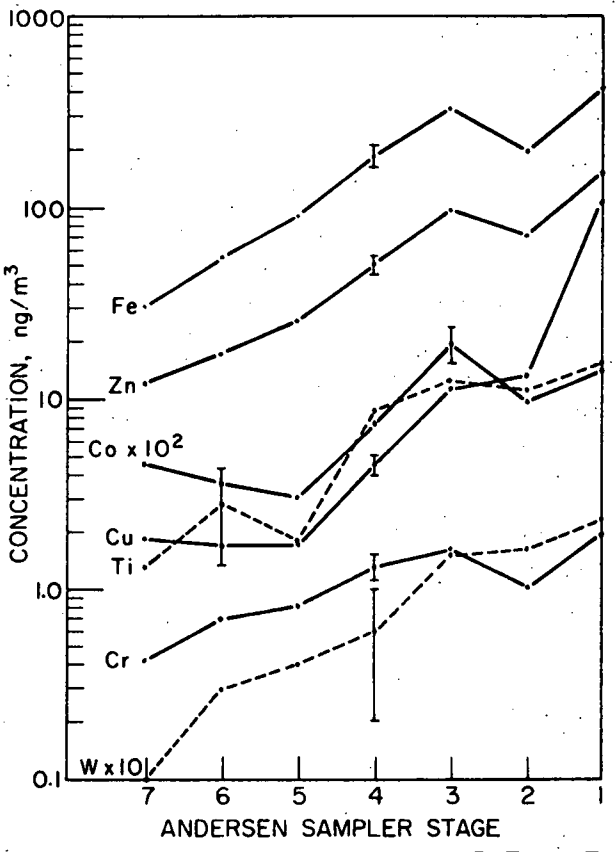

Figure IV-1 Andersen Sample AA1 - L-Type Elements

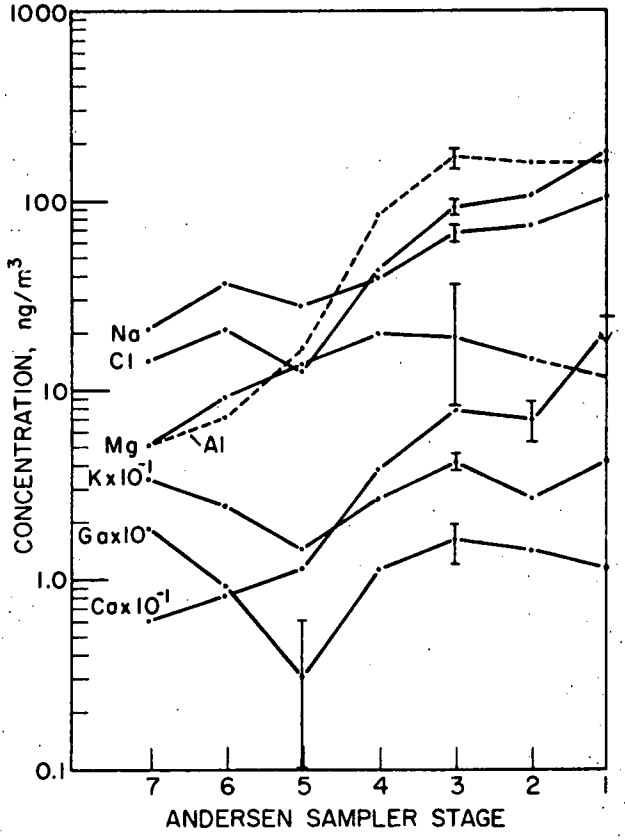

Figure IV-2 Andersen Sample AA1 - L-Type Elements

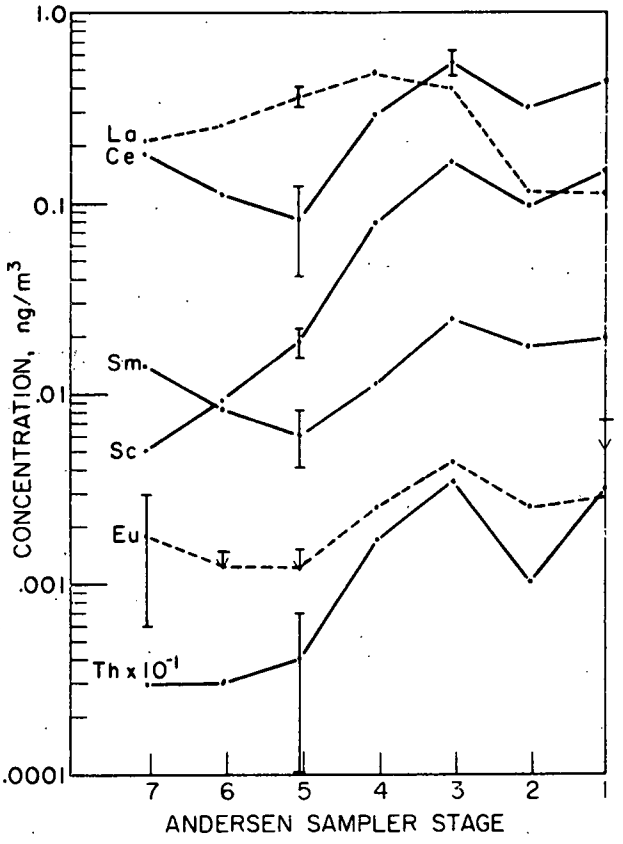

Figure IV-3 Andersen Sample AA1 - L- and M-Type Elements

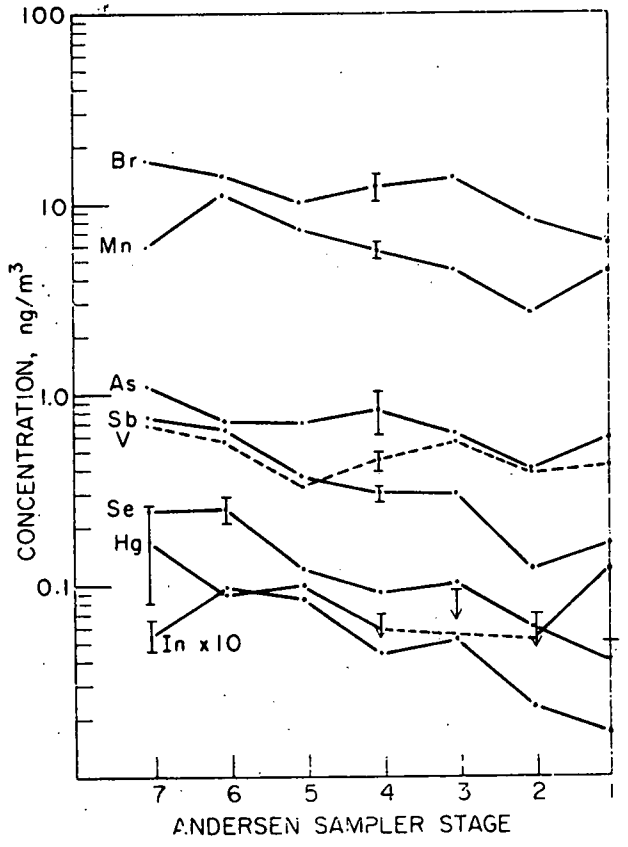

Figure IV-4 Andersen Sample AA1 - S- and M-Type Elements

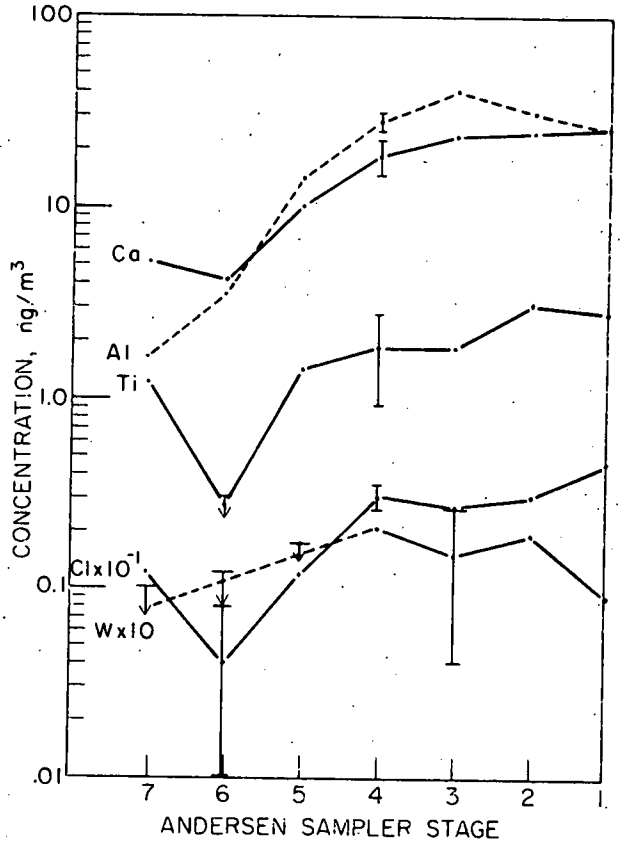

Figure IV-5 Andersen Sample MI1 - L-Type Elements

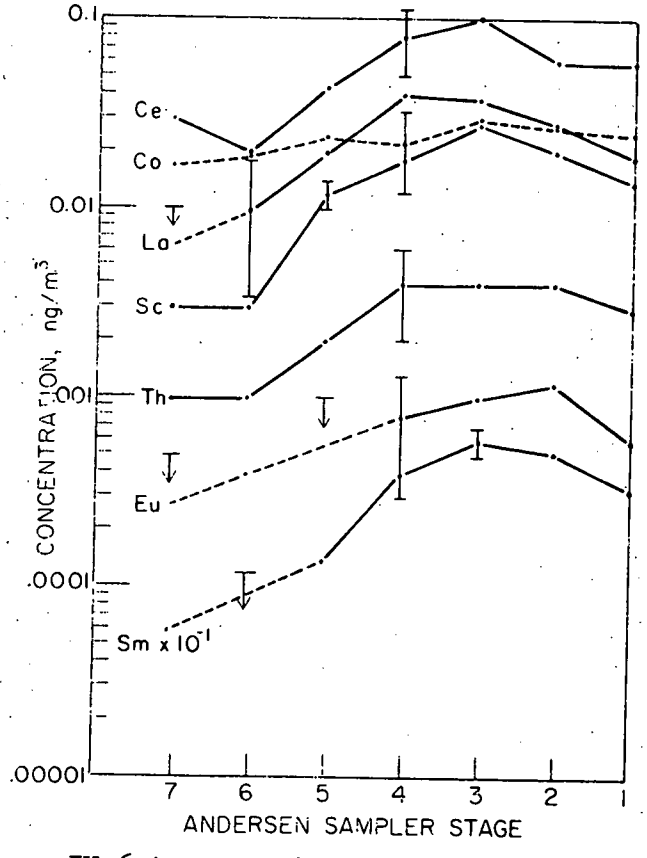

Figure IV-6 Andersen Sample MI1 - L-Type Elements

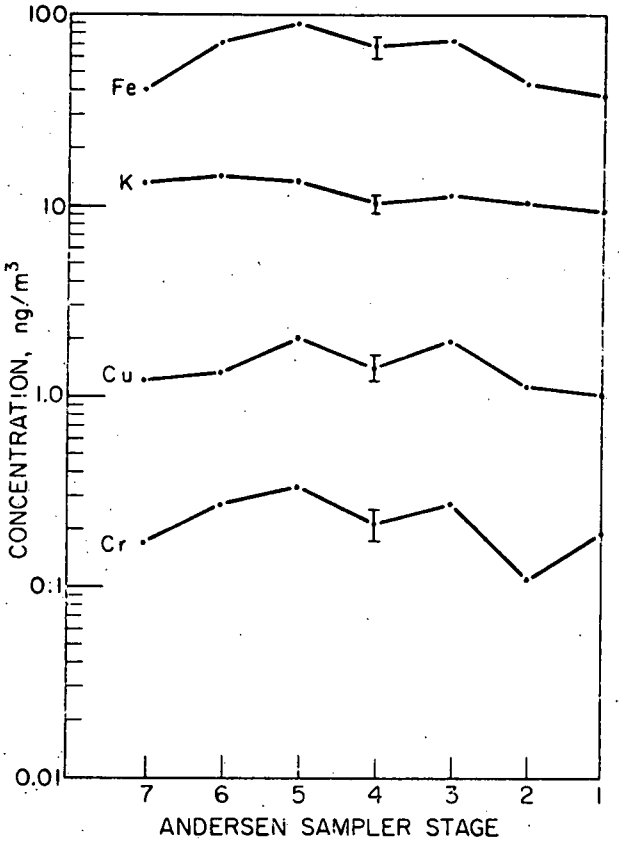

Figure IV-7 Andersen Sample MI1 - F- and M-Type Elements

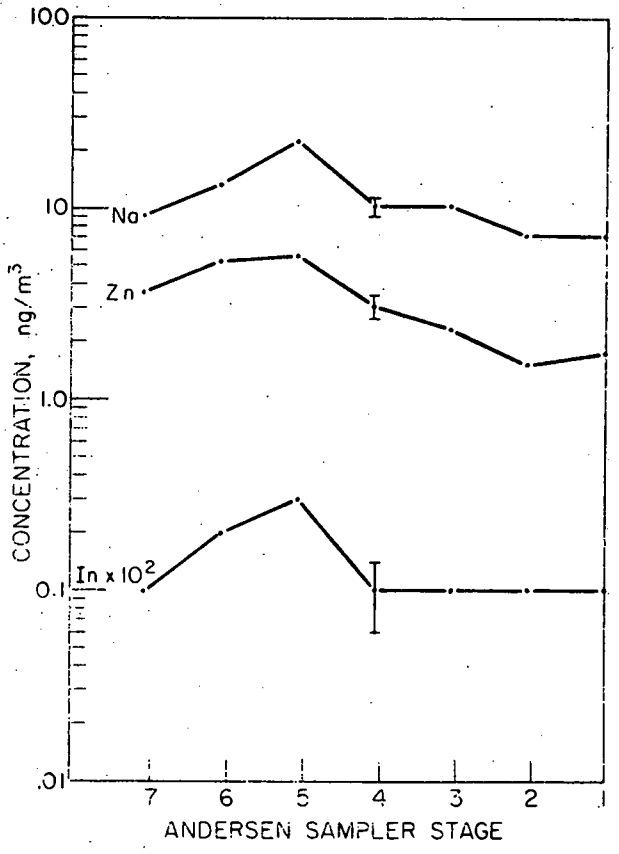

Figure IV-8 Andersen Sample MI1 - M-Type Elements

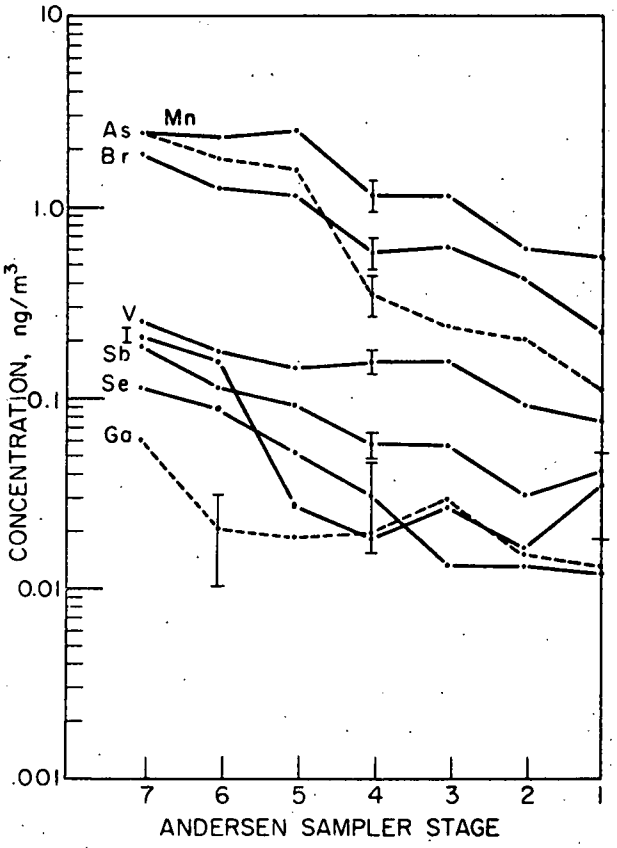

Figure IV-9 Andersen Sample MI1 - S-Type Elements

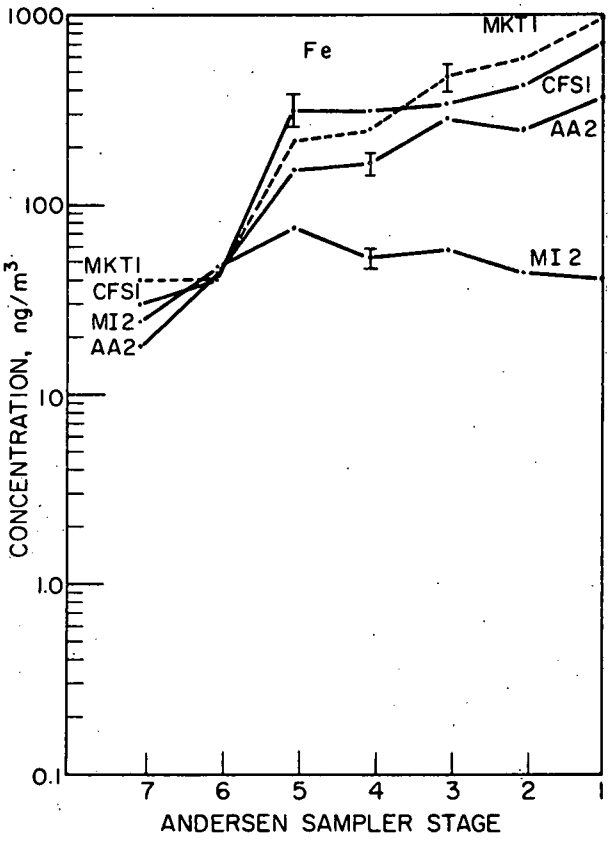

Figure IV-10 Mackinac Island - Ann Arbor - East Chicago Comparison - Fe

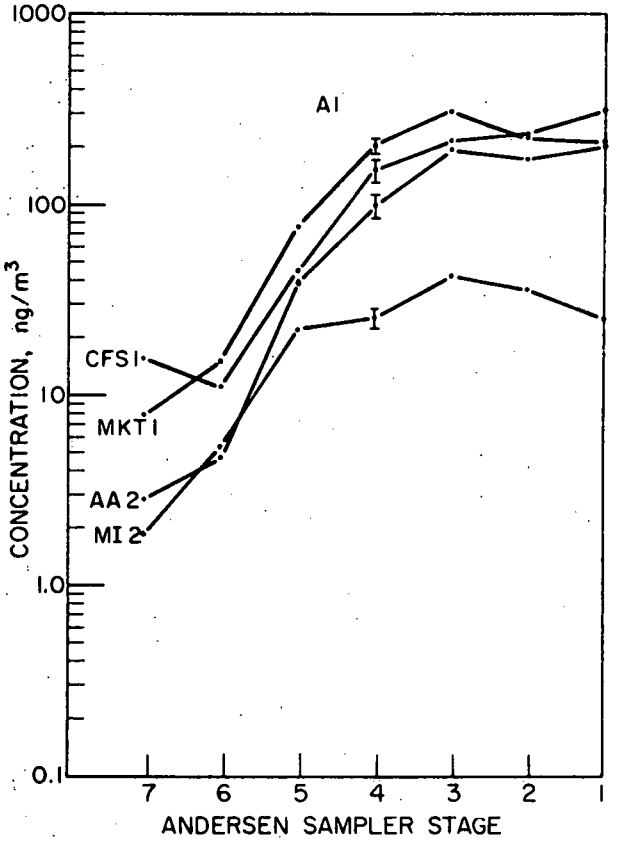

Figure IV-11 Mackinac Island - Ann Arbor - East Chicago Comparison - Al

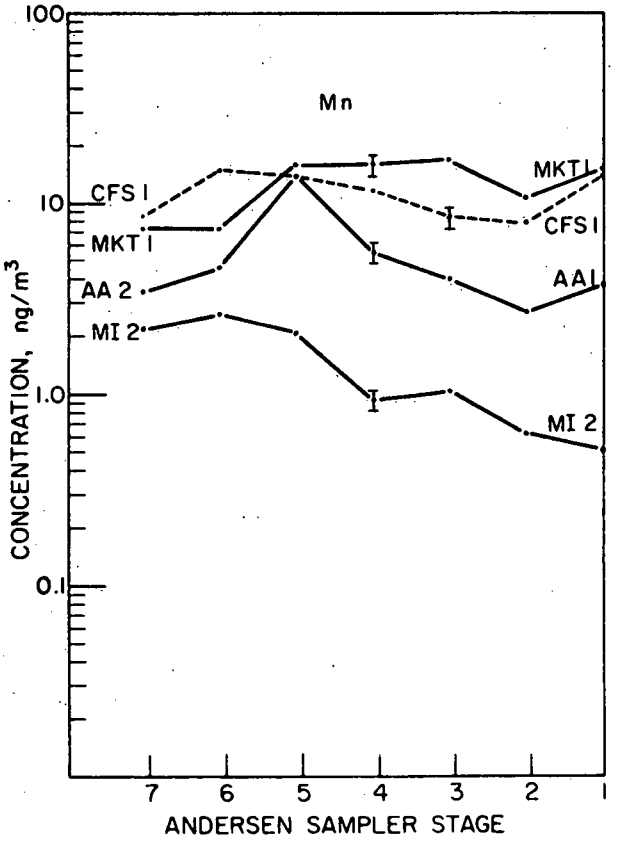

Figure IV-12 Mackinac Island - Ann Arbor - East Chicago Comparison - Mn

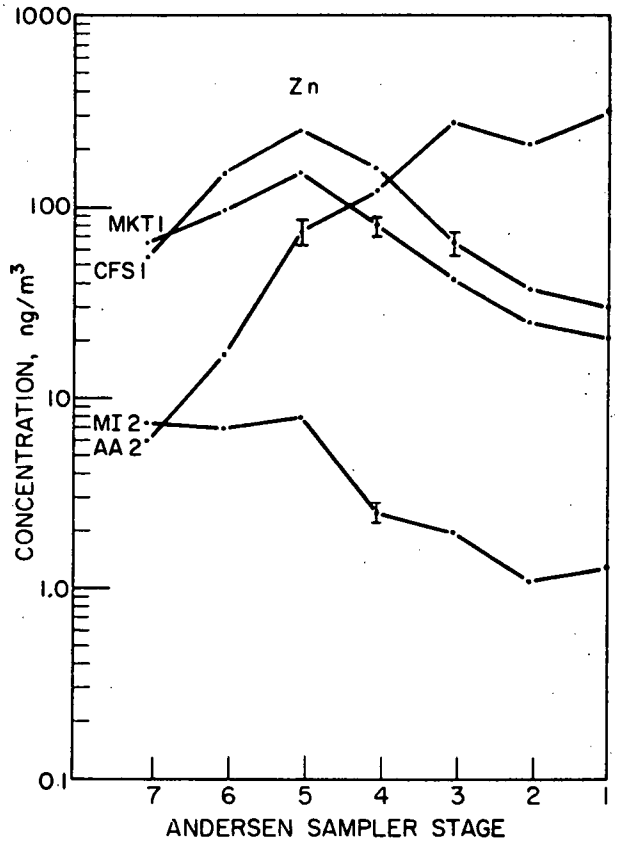

Figure IV-13 Mackinac Island - Ann Arbor - East Chicago Comparison - Zn

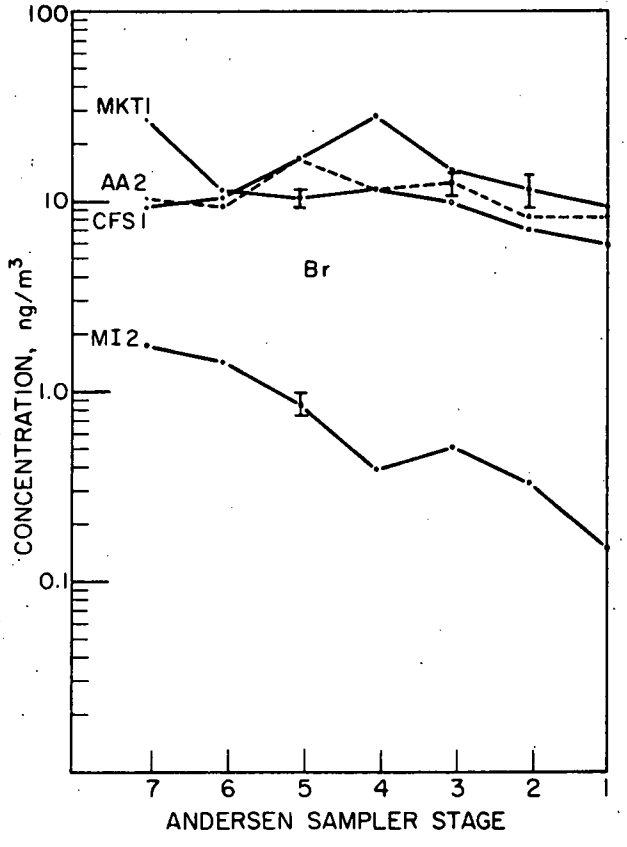

Figure IV-14 Mackinac Island - Ann Arbor - East Chicago Comparison - Br

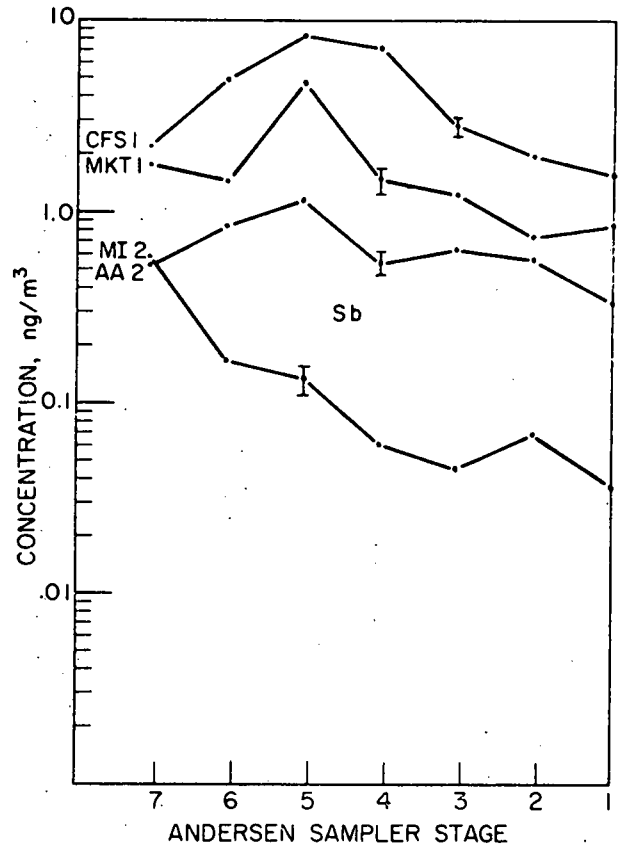

Figure IV-15 Mackinac Island - Ann Arbor - East Chicago Comparison - Sb

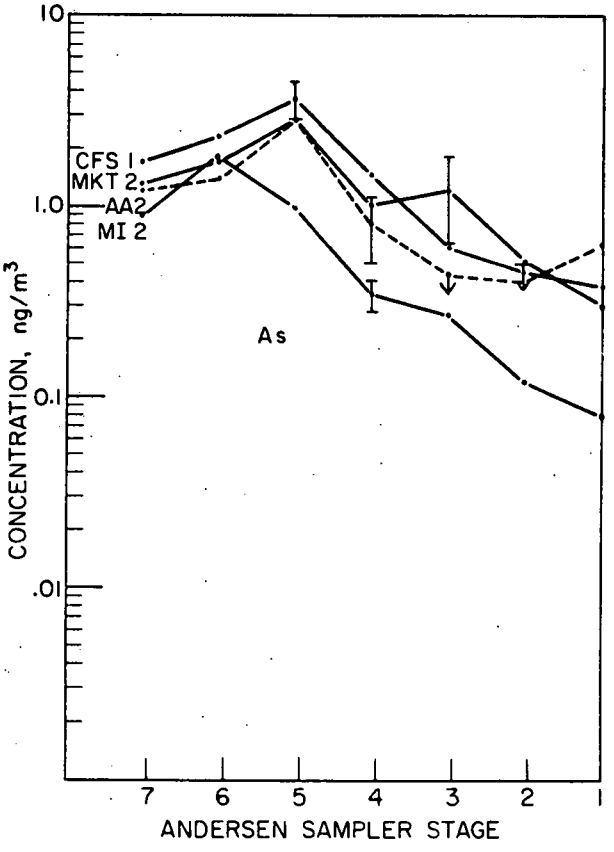

Figure IV-16 Mackinac Island - Ann Arbor - East Chicago Comparison - As

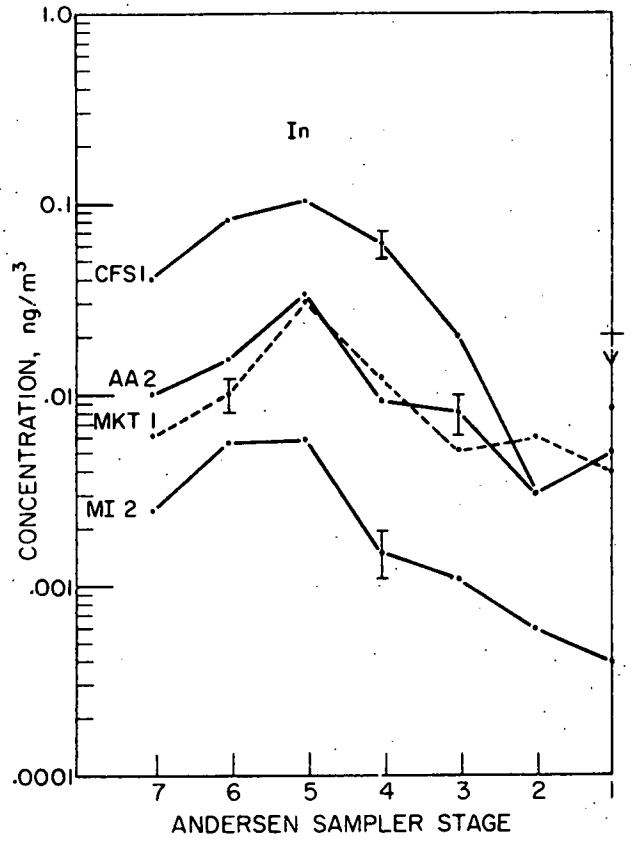

Figure IV-17 Mackinac Island - Ann Arbor - East Chicago Comparison - In

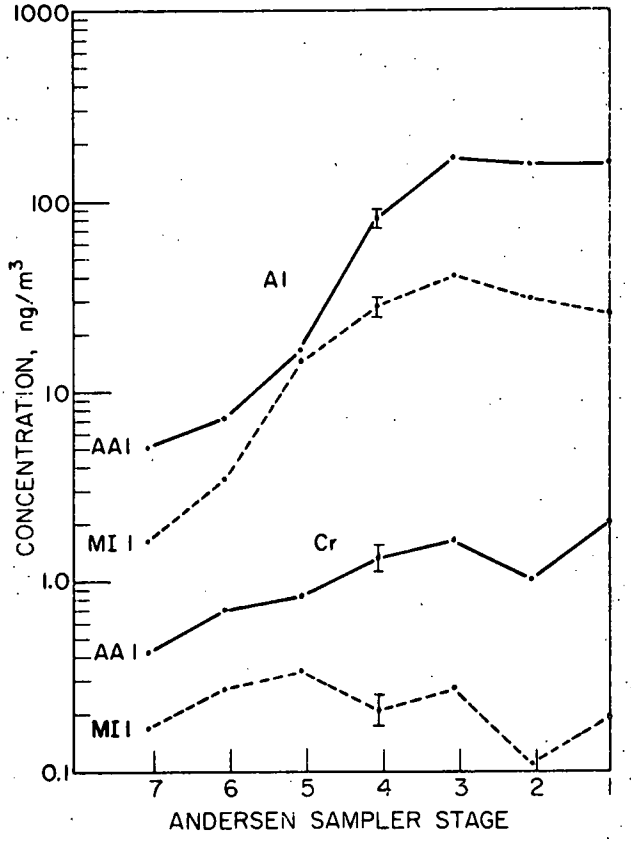

Figure IV-18 AA1 - MI1 Comparison - Al, Cr

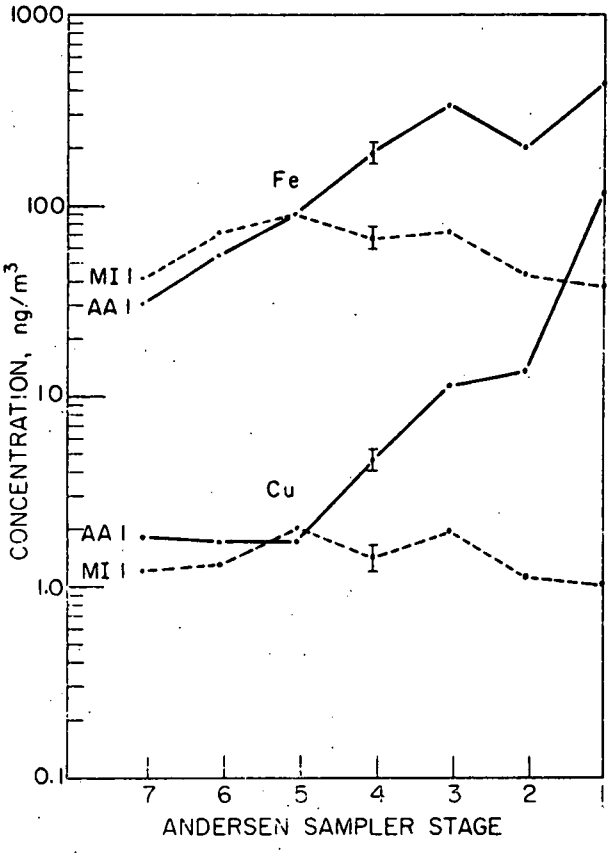

Figure IV-19 AA1 - MI1 Comparison - Fe, Cu

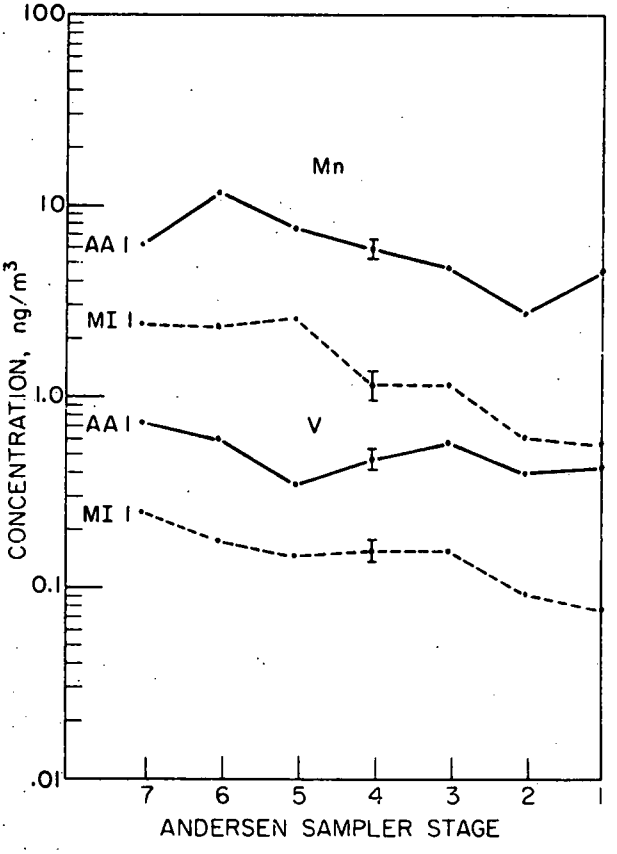

Figure IV-20 AA1 - MI1 Comparison - Mn, V

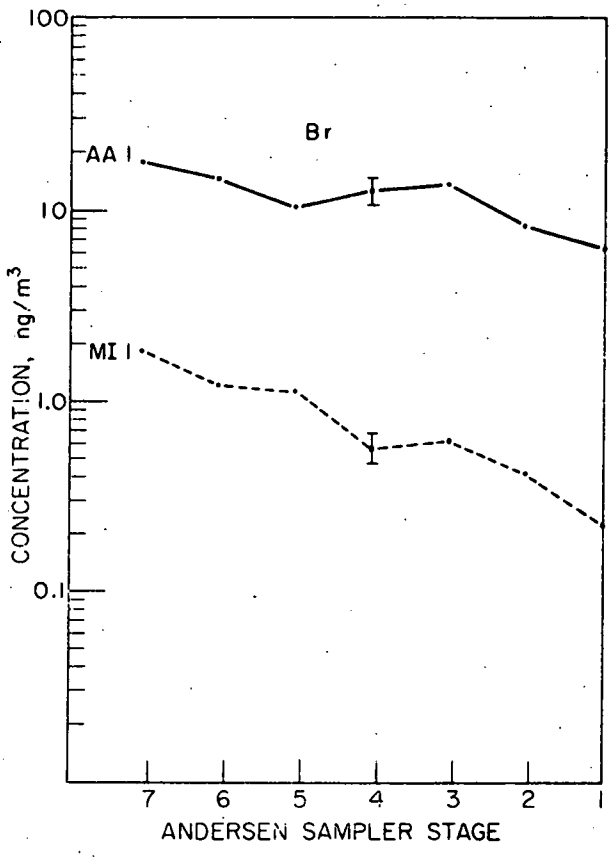

Figure IV-21 AAl - MIl Comparison - As, Se

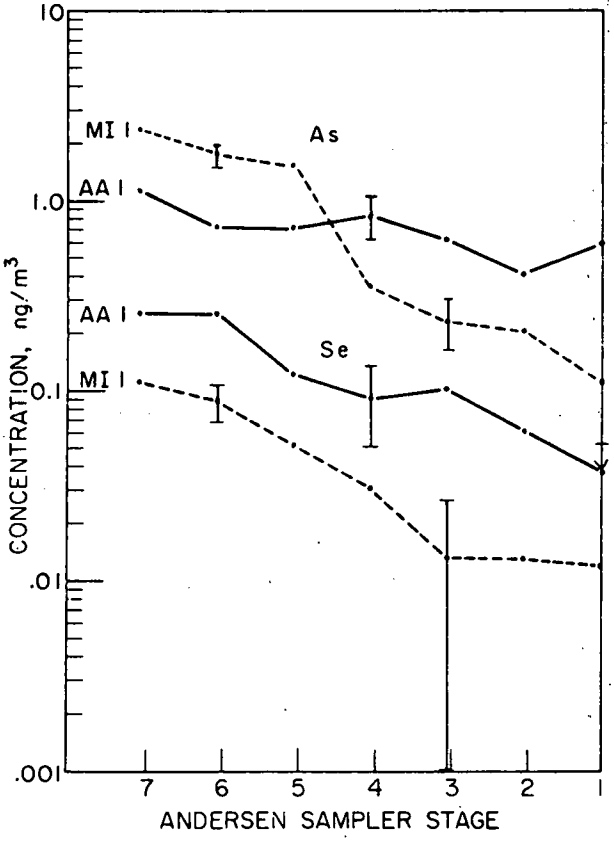

Figure IV-22 AAl - MIl Comparison - Br

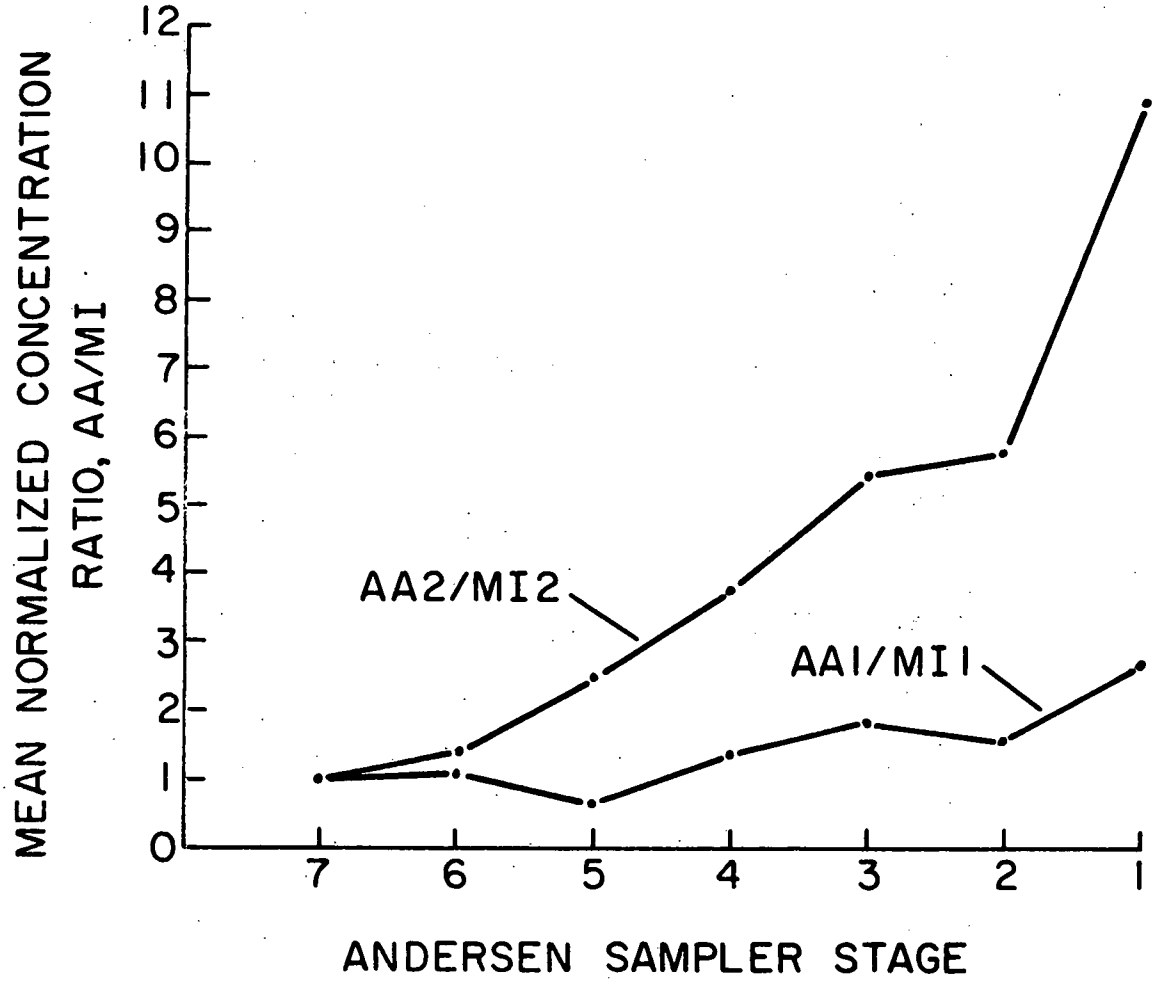

Figure IV-23 Mean Normalized Concentration Ratios, AA/MI

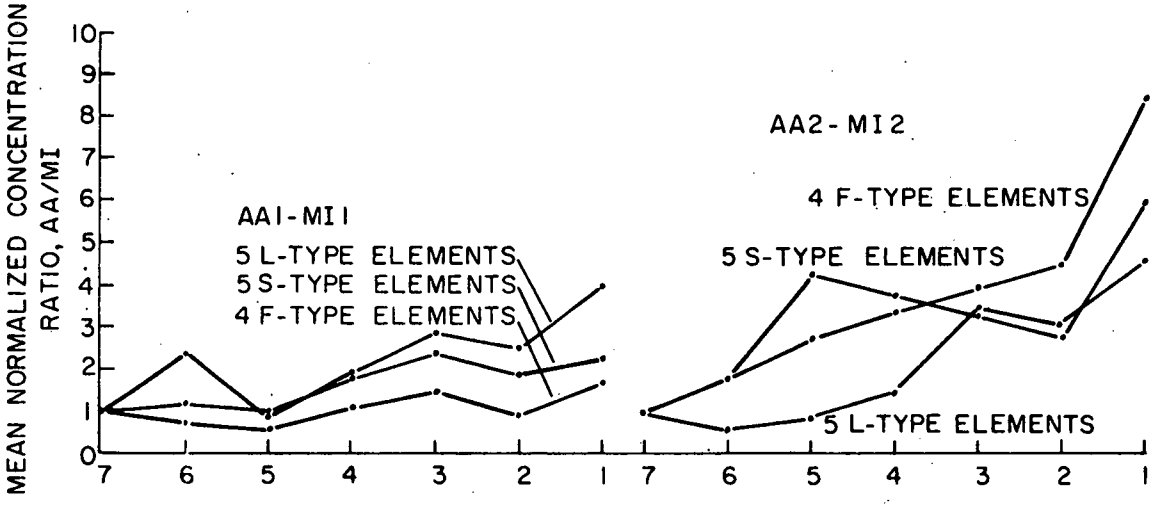

Figure IV-24 Mean Normalized Concentration Ratios by Subgroup, AA/MI

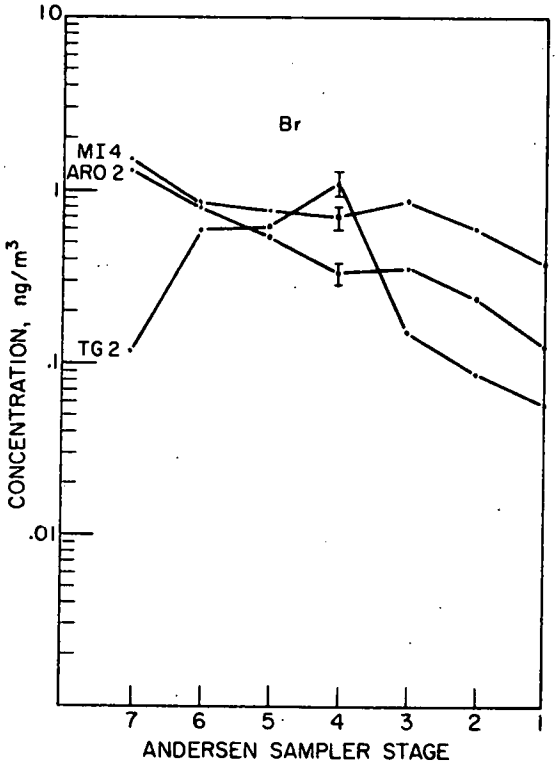

Figure IV-25 Br Spectra - Canadian Winter Experiment

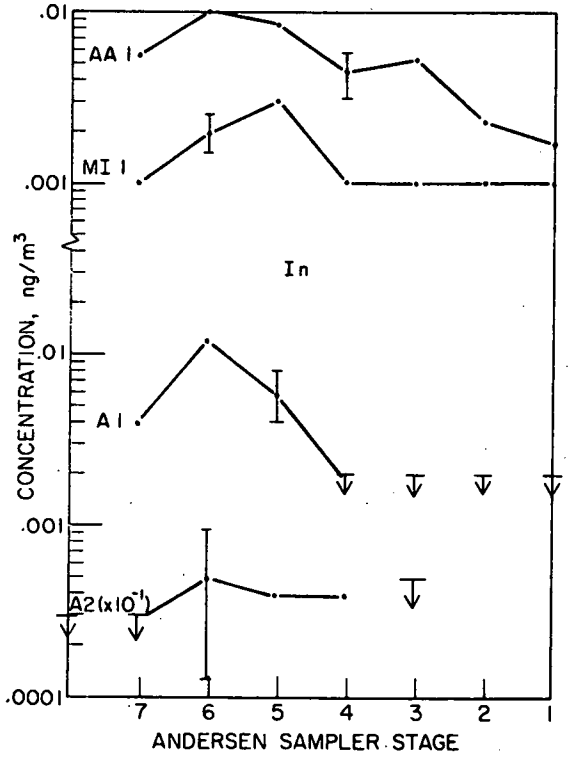

Figure IV-26 Miscellaneous In Spectra

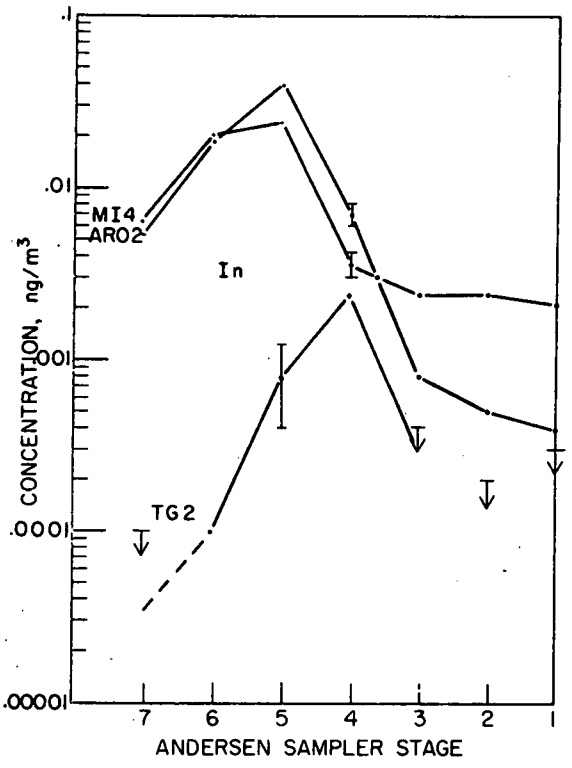

Figure IV-27 In Spectra - Canadian Winter Experiment

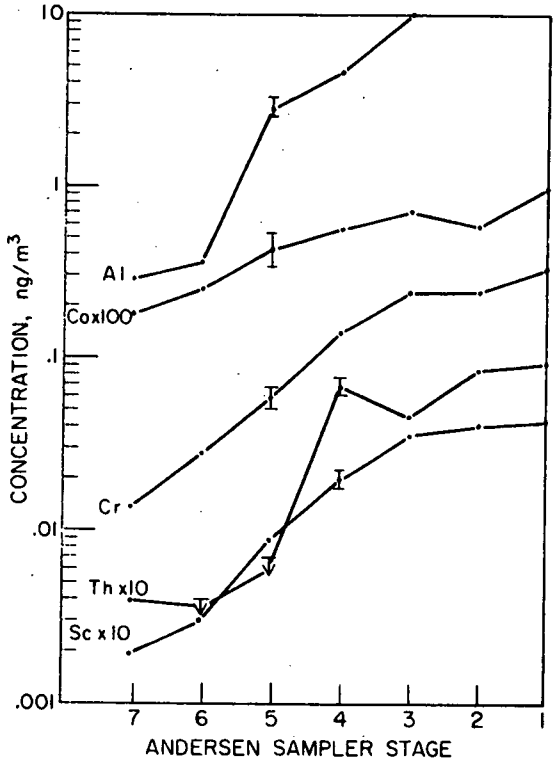

Figure IV-28 Andersen Sample TG2 - L-Type Elements

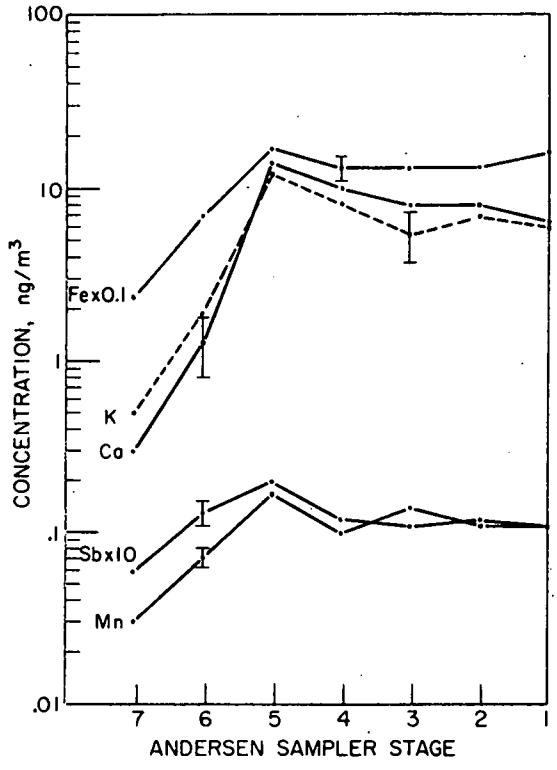

Figure IV-29 Andersen Sample TG2 - L-Type Elements

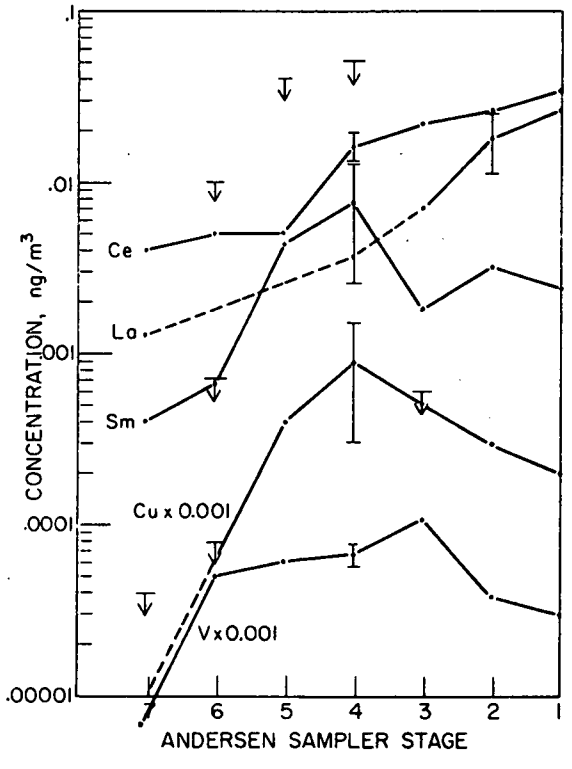

Figure IV-30 Andersen Sample TG2 - L- and M-Type Elements

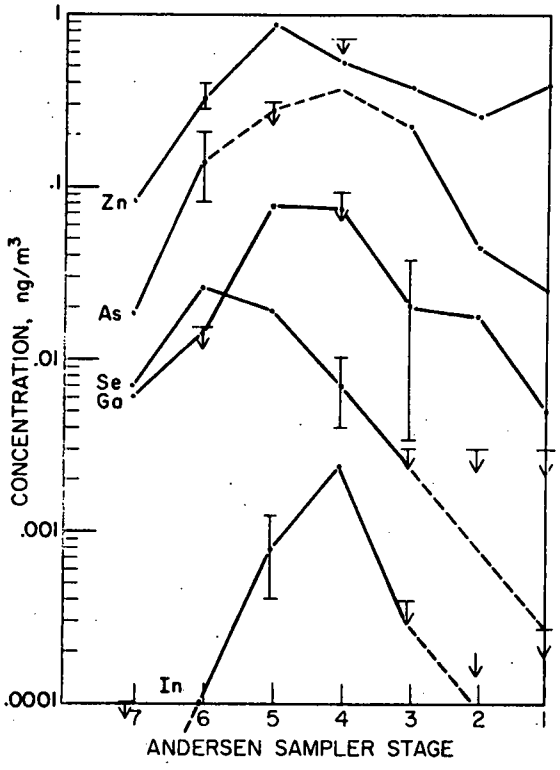

Figure IV-31 Andersen Sample TG2 - M-Type Elements

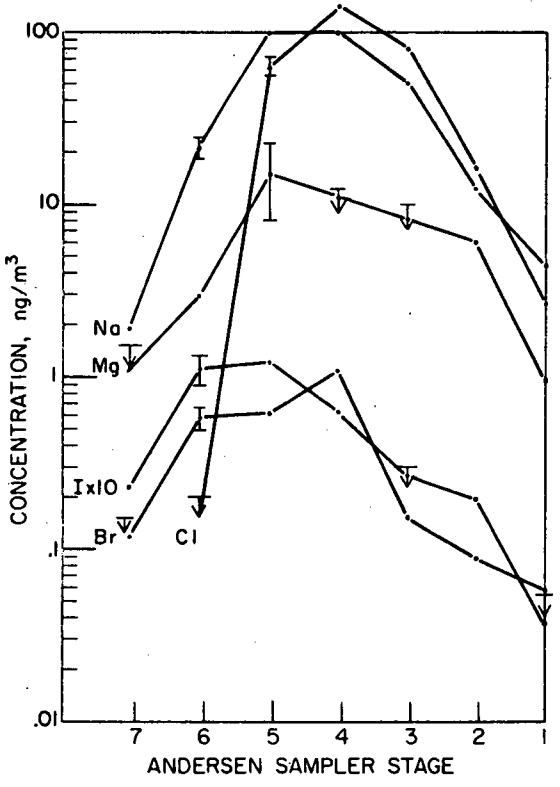

Figure IV-32 Andersen Sample TG2 - M-Type Elements

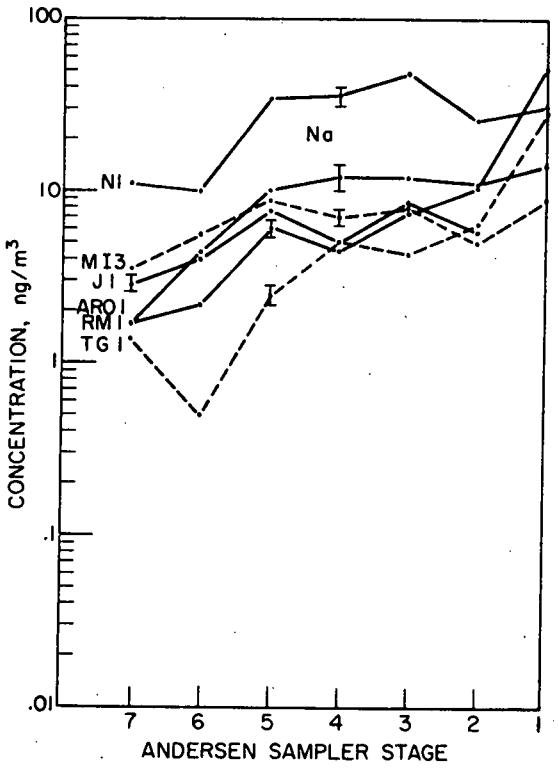

Figure IV-33 Na Spectra - Canadian Summer Experiment

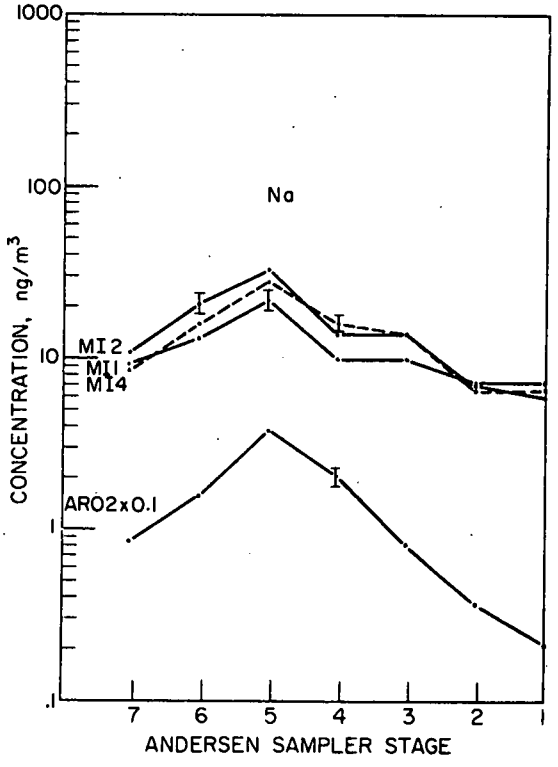

Figure IV-34 Na Spectra - Winter Samples

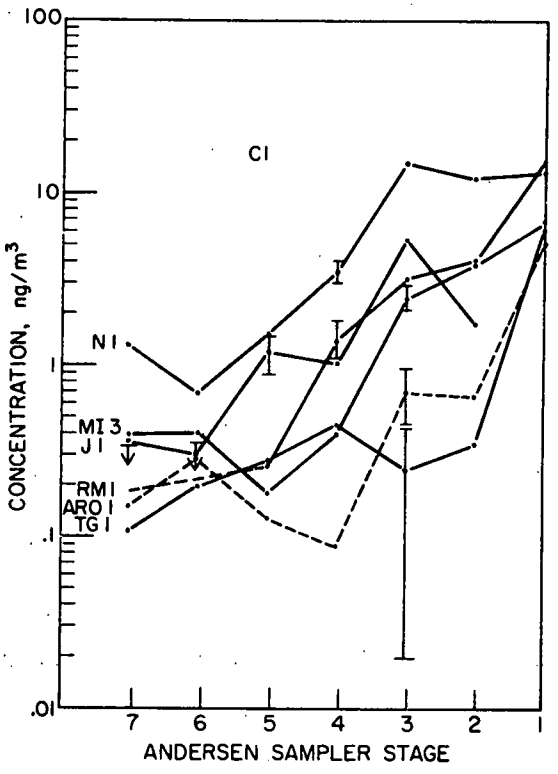

Figure IV-35 Cl Spectra - Canadian Summer Experiment

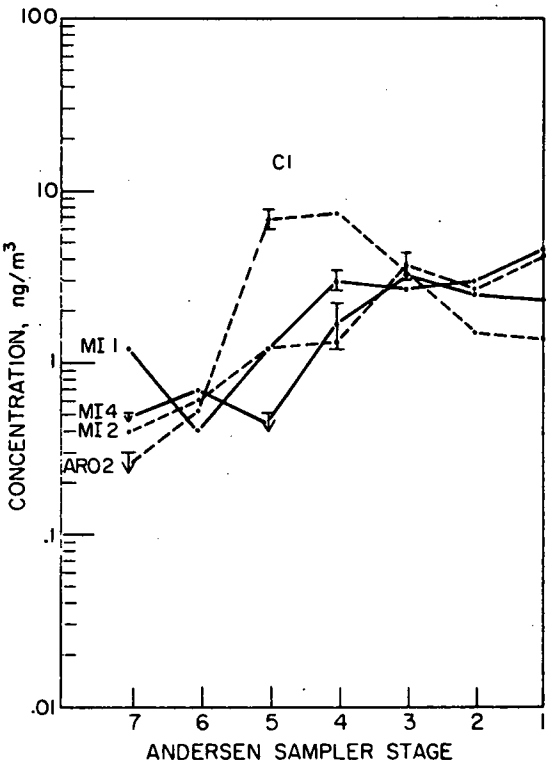

Figure IV-36 Cl Spectra - Winter Samples

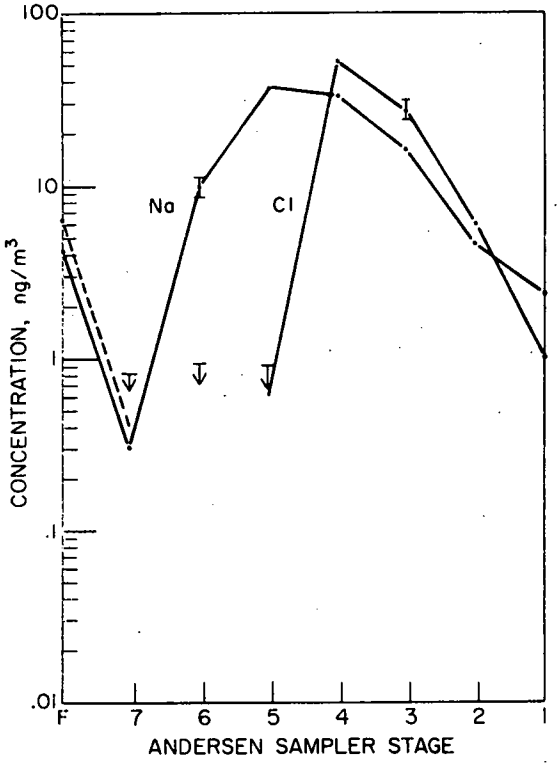

Figure IV-37 Na - Cl Comparison - TG3

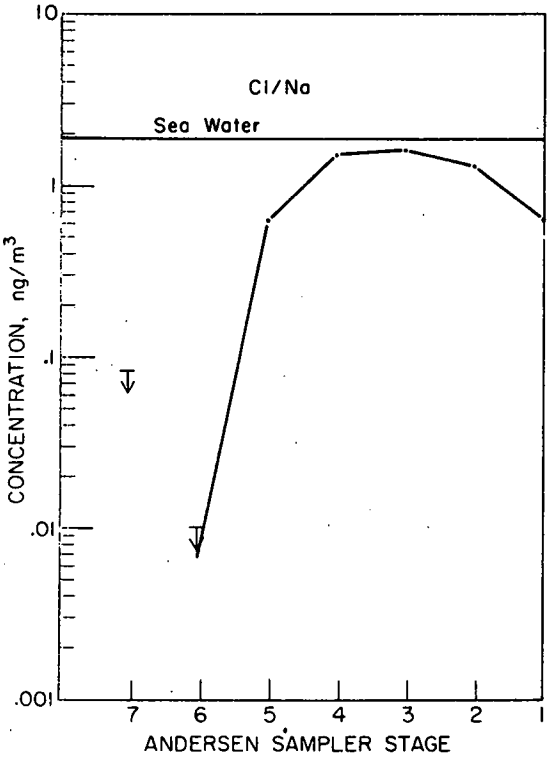

Figure IV-38 Cl/Na Ratios - TG2

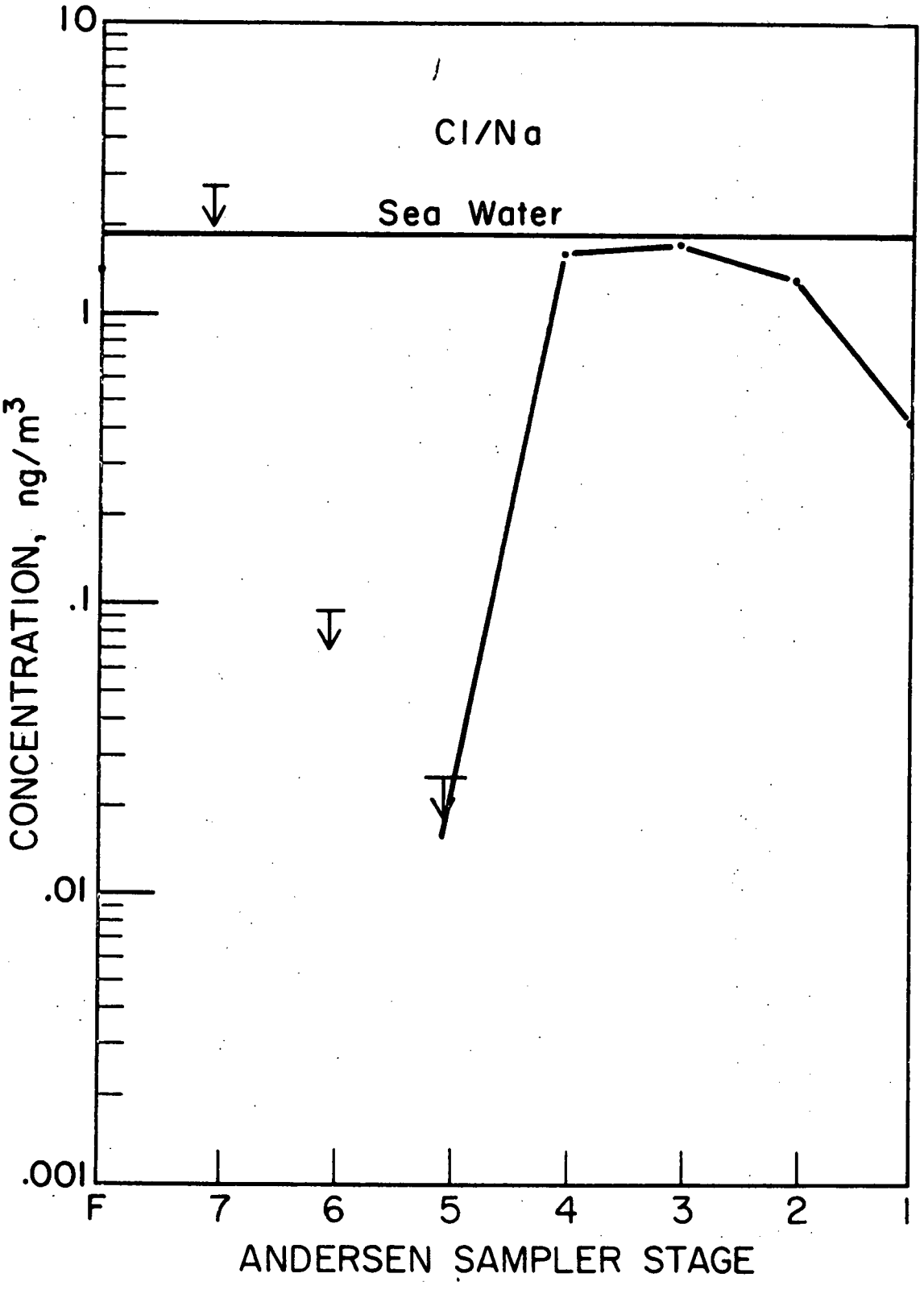

Figure IV-39 Cl/Na Ratios - TG3

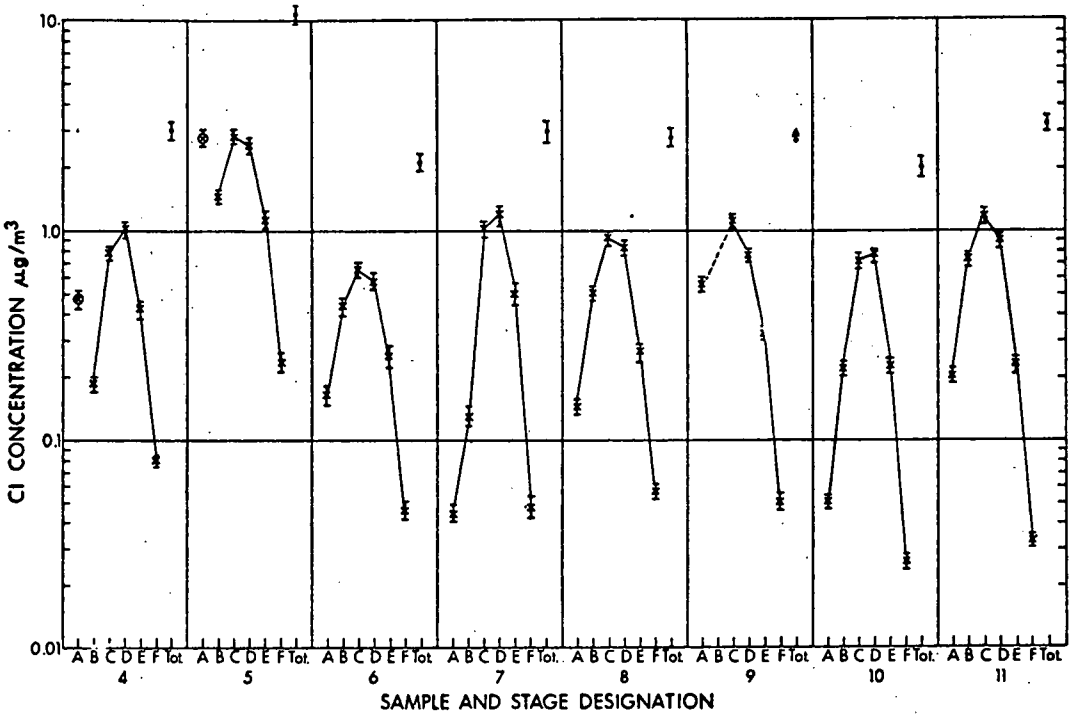

VARIATION OF ION RATIOS

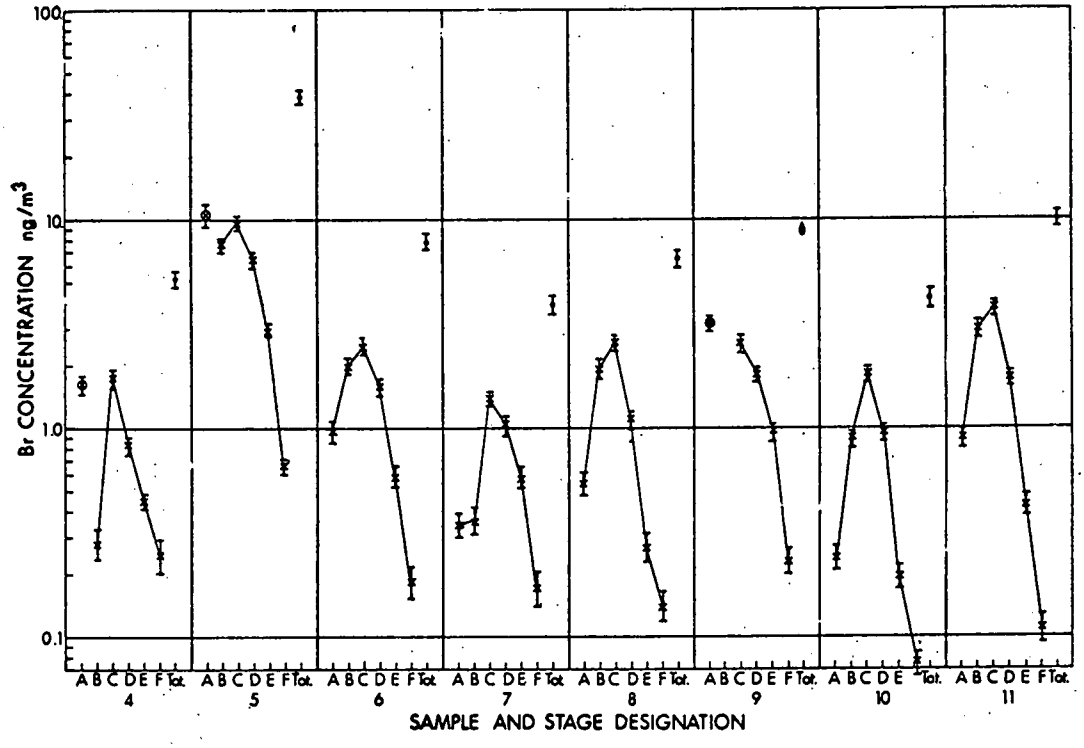

Figure IV-40 Cl and Br Particle Size Distributions in Fresh Marine Aerosol (after Duce et al., 1967)

CHAPTER V

SPECIAL ELEMENTAL CORRELATIONS

A. ARO: A Strong Pollution Source in a Clean Area

Summer

The summer Andersen sample at Algonquin (ARO1) reveals an unusual parallelism in size distribution patterns for the elements Zn, Mn, As, Cu, Se, Sb, and In (Figure V-1). Each shows a strong maximum at stage 5 or vicinity, falling off by up to an order of magnitude on either side. Though M-type distributions are common for these elements in summer (Table III-3), this degree of parallelism in a single sample is unique. Also, the number of M-type elements here is by far the highest of the summer stations (Table III-4). Of the above elements, Zn and Se are highly enriched here, and As and In are the most highly enriched of any location in the network (Table III-14).

Most of the other elements are normal in pattern. Figure V-2 shows that Fe, Al, Na, and K are clear-cut L-types, while Cr has an apparent LM combination.

Winter

The winter Andersen sample (ARO2) shows nearly identical spectra for 5 of the 7 M-type elements listed above (Se, Sb vary slightly and are shown in Figure V-6), but this list is

augmented by Fe, Al, Na, K, Cr, Ga, and possibly Sm (Figures V-3,4). Several other elements (Cl, Ce, Co, Sc, Th, Eu) show peaks on larger particle sizes (Figure V-5), but not a single element can be considered L-type. Though a somewhat similar winter situation was also seen at Mackinac Island, comparison with Figures IV-5 to IV-9 and Tables III-2,6 will show basic differences between the two sites.

S-type behavior is strongly shown by Br, V, and I, and to a lesser extent by Se and Sb (Figure V-6). This sets Se and Sb somewhat apart from the M-type elements with which they were classified in summer, but even then they also tended more toward an S-type shape than did the others (Figure V-1). The shift of V to a strong S-type shape may be from local fuel oil combustion at the Algonquin Radio Observatory. Part of the Se shift may also be explained in this way, because of its occurrence with S in fossil fuels. Some of the Se may be from background advected from the Mackinac Island vicinity, also strongly S-type (Figure III-2).

Sources: Industrial vs. Soil

A number of considerations suggest the M-type elements to be of industrial origin. Several (Zn, As, Cu, In, Se, Sb) have high aerosol/soil enrichment factors (Figure III-14, Table III-14) at all stations, and some (As, In) show their highest actual concentrations here. Harkins and Swain (1908) report detection of major amounts of As, Sb, Cu, Pb, Zn, Mn, Fe, and Al in smelter smoke, with their list bearing a striking

resemblance to the unusual elements here at ARO. Pb is of course not determined in this work, and Fe, Mn, and Al are here seen to have major soil contributions as well.

Indeed, the major heavy industry in the surrounding area is the mining and smelting of Ni-Cu-Zn ores in the vicinity of Sudbury, Ontario, some 250 km NW. There are three Ni-Cu smelters near Sudbury, as well as an electrolytic copper refinery. Both the detection of Ni in the summer filters at ARO, the only station in the network where it was above the detection limit, and its aerosol/soil enrichment factor of 15 reinforce the idea of the link between the activities at Sudbury and the non-soil elements at ARO.

The strength of the hypothesized industrial source is demonstrated by the winter particle size distributions (Figures V-3,4), where soil contributions to Fe, Al, Na, K, and Cr are overshadowed by those from the pollution source. There seems to be a delicate balance of source strengths for these elements, with the soil dominating in summer and the industrial source in winter. On the other hand, neither completely overshadows the other. The summer plots (Figure V-2) show shoulders at stage 5 for Fe, K, Na, and Cr, while the winter plots (Figure V-3) show Fe, Al, and K with higher levels at stages 1, 2, and 3 than for the more volatile, purely pollution elements.

Source Characteristics

A single source type is strongly suggested by the size distribution shapes of the M-type elements. The remarkable

number of elements with stage 5 maxima (14 of 24 in winter) and their similarity of shape indicate that they are not only from the same source but also probably associated with the same particles. The elements would appear to be volume- rather than surface-distributed in most cases, because of the unusual similarity between elements normally quite different in particle size distribution. For example, Fe and Zn have winter size distributions that differ only slightly in the first 2-3 stages (Figure V-3). The peak is at stage 5 for both, with highly similar shapes. This is to be contrasted with the results of Nifong (1970) for Northwest Indiana. These show Fe always L-type, and Zn was nearly always M- or S-type, even near strong sources. The Zn-Fe difference in Indiana can be attributed in part to source process differences, but also in part to volatility differences which made Zn a condensation aerosol. At ARO, however, the similar size distributions suggest little or no condensation to have occurred, or else systematic differences would have been seen between the refractory and the volatile elements.

The expected nature of such spectral shape differences can be seen from the equations describing an aerosol number distribution. For a number distribution $n(r) = dN/d(\log r)$, where N is the total number of particles of radius less than r, corresponding surface and volume distributions will be, respectively,

$$s(r) = 4\pi r^2 n(r)$$

$$v(r) = \frac{4}{3}\pi r^3 \, n(r)$$

These are simply related:

$$s(r) \propto \frac{1}{r} \, v(r)$$

independent of the form of n(r). Given two elements, one surface-distributed on an aerosol and the other volume-distributed in that same aerosol, the surface-distributed element will be relatively more abundant on the smaller particles.

Consider a log-normal particle-number distribution, typically the result of a dispersive process (Fletcher, 1966) and bearing a certain resemblance to the ARO spectra. If the number maximum is at radius r_o, the following equations apply:

$$n(r) = dN/r(\log r) \sim \exp \left\{ - [\log(r/r_o)]^2 \right\}$$

$$s(r) = 4\pi r^2 \, n(r) \sim r^2 \, n(r)$$

$$v(r) = \frac{4}{3} \pi r^3 \, n(r) \sim r^3 \, n(r)$$

These are plotted in Figure V-7.

If $r_{s\ max}$ and $r_{v\ max}$ are respectively the radii of maximum concentrations of surface- and volume-distributed elements, differentiation of the above equations shows that

$$r_{v\ max} = 4.5 \, r_o$$

$$r_{s\ max} = 2.7 \, r_o$$

$$r_{v\ max}/r_{s\ max} = 1.7$$

In other words, an element which is volume distributed in a log-normal particle-number aerosol will have its mass distribution maximum at a radius of 4.5 times the radius of number maximum, or about 2 Andersen Sampler stages higher. Similarly, a surface-distributed element in this same aerosol will show its concentration maximum about one Andersen stage higher than the true number maximum, or 1 stage lower than the volume-distributed element. Note that, though s(r) and v(r) are each slightly skewed toward smaller r, the overall resemblance to the log-normal n(r) is very close.

Inspection of the ARO1 and ARO2 plots for families of elements with maxima separated by one stage reveals nothing conclusive. Elements such as Fe, Al, As, and Zn show systematic but very small differences in the expected direction, but these may be due to background slope differences of L- vs M- or S-type distributions. One of three choices would then seem to be preferred. Either all the elements have vaporized, or none have, or else anti-pollution devices on the stacks have removed so many of the largest particles that the original distributions are no longer recognizable. Of these, the second seems most likely.

On the other hand, the long-range transport to ARO will allow many of the largest particles to settle out,thus tending to shape the refractory products more like the volatiles, but

this effect cannot be quantitatively evaluated without a knowledge of the original size distributions.

The question of condensation vs. dispersion origin is further resolved by work of Nifong. On the basis of size distribution data he finds Mn in Northwest Indiana to be L-distributed as expected for dispersion aerosols, and to a lesser extent the same is observed for Cu. In summer at ARO these two elements are similar to the volatiles, suggesting a dispersion source process for all.

On the other hand, the inferred r_o for the dispersion process is very small. The stage 5 maximum implies $d_{vmax} = 1.5/4.5 = 0.3$ μm, near to the lower limit of dispersive processes. This would suggest a high-energy dispersive process (such as at high temperature), implying a greater degree of vaporization than that inferred from the size distributions of typically volatile elements. At the present this dilemma remains unresolved.

B. The Coherence of Zn and Sb

Zinc and antimony show a high source correlation throughout all our measurements. In the Canadian summer study their aerosol/soil enrichments, though several times higher for antimony than for zinc, were in a nearly constant ratio for all seven stations (Figure III-20). Their particle size distributions are almost always quite similar, but with Sb usually being relatively more abundant on stages 6 and 7 (Figure V-1, for example).

The Northwest Indiana survey (Part II) revealed Zn and Sb to have the third largest linear correlation coefficient of any of the elemental parts, 0.91 ± 0.04. Visual inspection of the relevant concentration maps will verify this conclusion, for the isopleths are quite similar in appearance.

The diurnal variations study for Livermore, California (Part II) shows that Zn and Sb generally follow the trace of the other elements, except for a short excursion of some 12 hours in length when they together rose in concentration by a factor of 5 while all the others (except Na, Cl, and Br) were falling by a factor of 2. This unusual behavior suggested a simultaneous temporary emission of Zn and Sb into the atmosphere at some point upwind, which perhaps only coincidentally began after dark and ceased in early morning.

Though it is very common, the close behavioral correlation between Zn and Sb is not universal. In Ann Arbor in winter Zn and Sb almost certainly have different sources, because here the Sb has its usual size distribution (small particles) but the Zn shows a clear, strong large-particle dispersion source, the only case of its kind we have seen.

Nifong (1970) noticed in the Northwest Indiana industrial area a generally high but not universal degree of parallelism in the particle size distributions of Zn and Sb, in agreement with our more remote measurements.

The reasons for this source and size distribution coherence appear to originate from a combination of physical and

geochemical similarities between the elements. Both are classed by Mason (1966) as chalcophiles, elements favoring a sulfide rather than silicate or basic iron phase of a melt. They will thus be found together in minerals such as sphalerite, ZnS. Their similarity of volatility causes the commonness of particle size distributions observed.

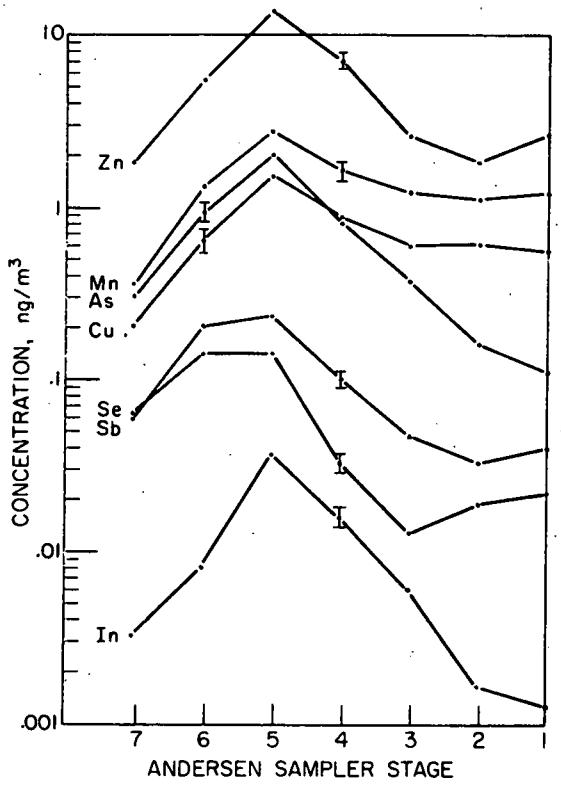

Figure V-1 Andersen Sample AR01 - M-Type Elements

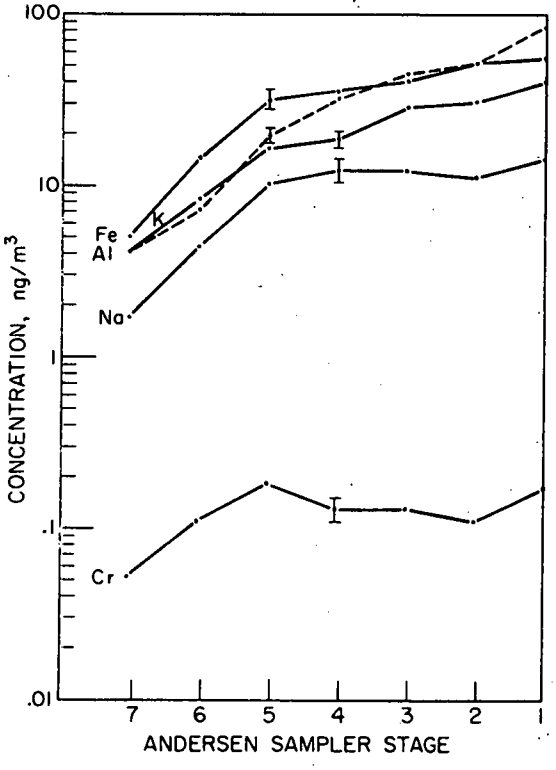

Figure V-2 Andersen Sample AR01 - L-Type Elements

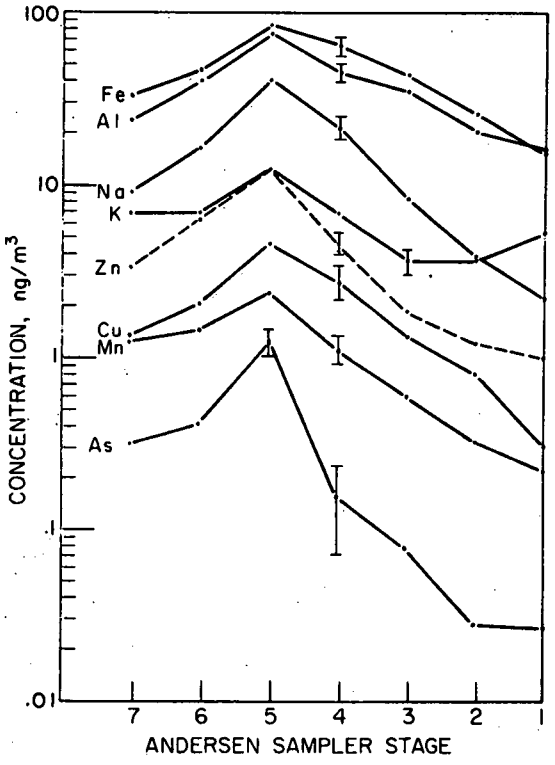

Figure V-3 Andersen Sample AR02 - M-Type Elements

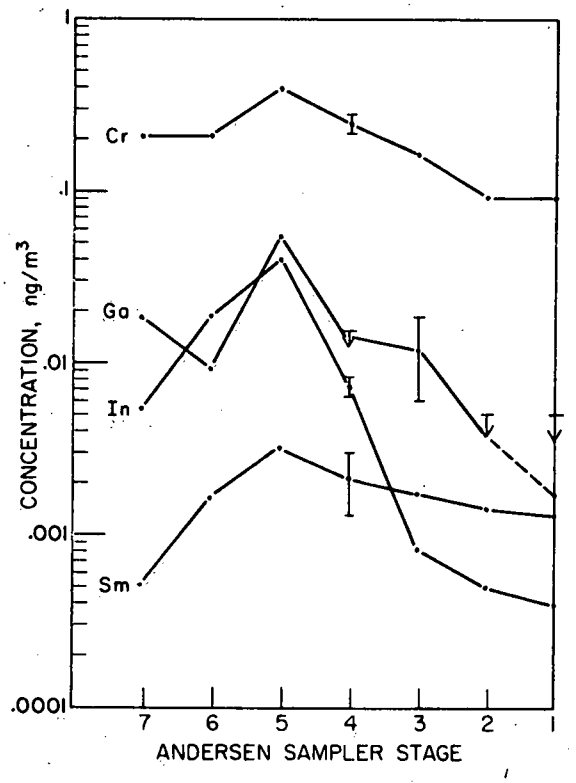

Figure V-4 Andersen Sample AR02 - M-Type Elements

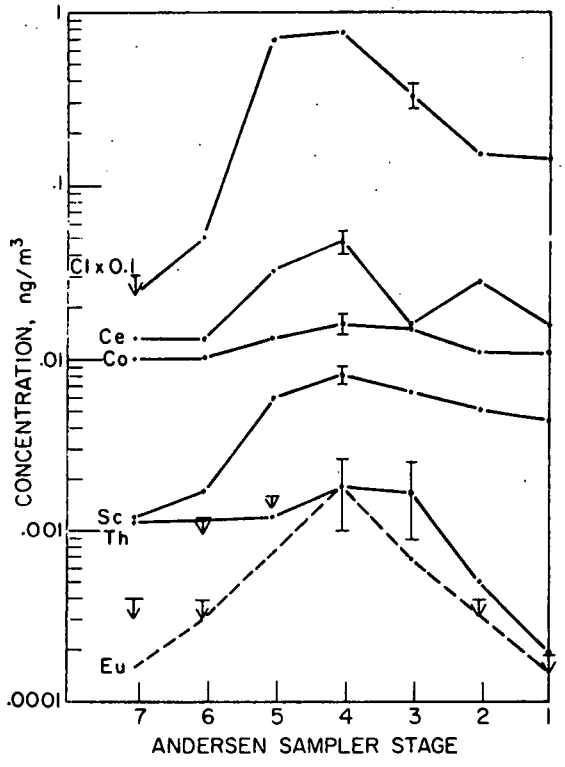

Figure V-5 Andersen Sample AR02 - M-Type Elements

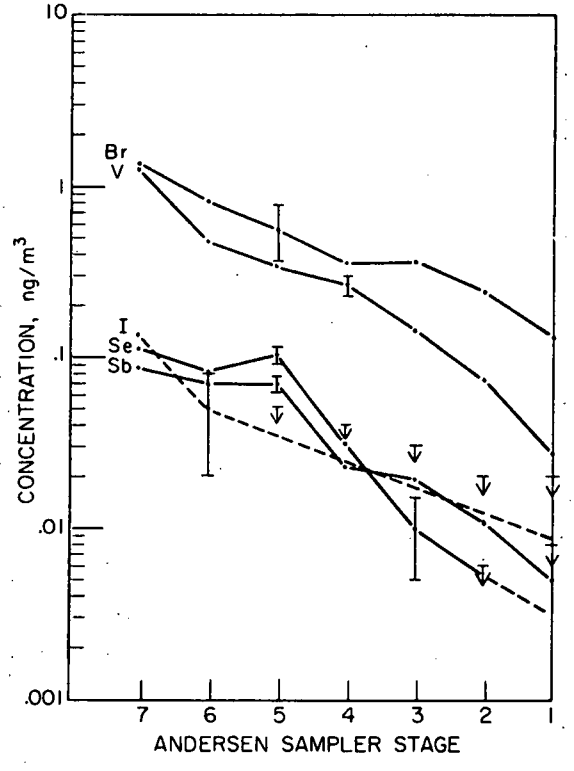

Figure V-6 Andersen Sample AR02 - S- and M-Type Elements

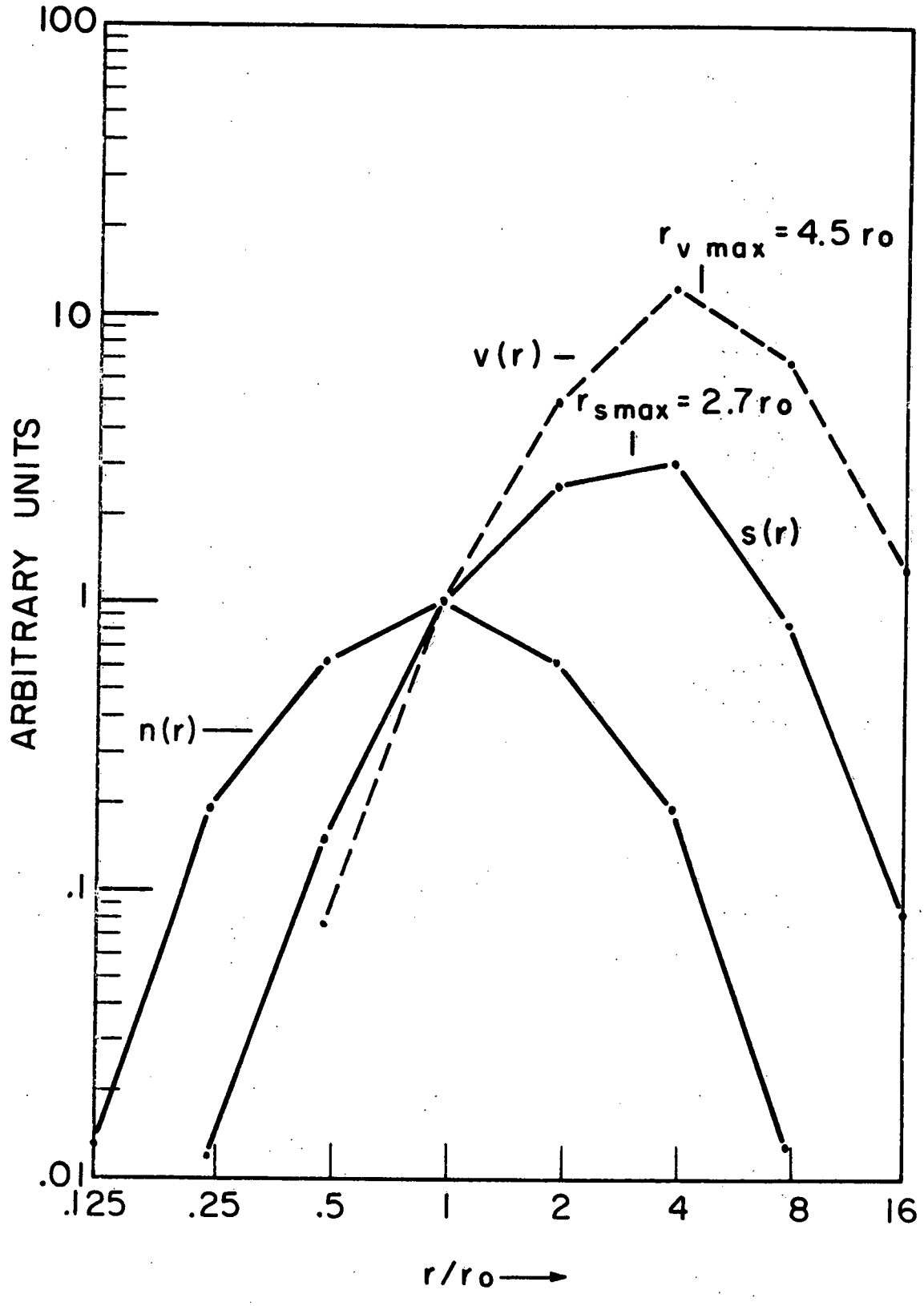

Figure V-7 Number, Surface, and Volume Distributions for a Log-Normal Number Distribution

PART II

STUDIES NEAR URBAN-INDUSTRIAL SOURCE REGIONS

CHAPTER VI

NORTHWEST INDIANA: THE STUDY OF AN INDUSTRIAL SOURCE AREA*

A. Introduction

Proper interpretation of data taken in rural and remote regions depends heavily on an understanding of conditions for the same trace elements in source regions. Since portions of many of the elements appearing in remote regions probably originate in major industrial areas, a study of at least one such source region was deemed desirable.

Few detailed data are available for most elements in cities. Some numbers are published, typified by quarterly and yearly averages of 16 elements issued by the National Air Sampling Network (U.S. Department of Health, Education, and Welfare, 1968) for about 100 urban locations, usually one per city. Our goals demand more specialized measurements—a comprehensive short-term multielement areawide survey throughout

---

*Publication of the data portion of this work is planned under the authorship of P.R. Harrison, K.A. Rahn, R. Dams, J.A. Robbins, J.W. Winchester, S.S. Brar, and D.M. Nelson. The statistical analysis portion will be published in Nuclear Techniques in Environmental Pollution. International Atomic Energy Agency, Vienna, under the authorship of R. Dams, J.A. Robbins, K.A. Rahn, and J.W. Winchester.

the whole of a major source area. A sufficiently dense sampling grid should reveal which of the elements have strong pollution sources, and perhaps afford some estimate of their nature and location. With knowledge of source patterns and general concentration levels as a starting point, comparisons with remote locations can be made more meaningful.

B. Experimental

1. Site Selection

The Hammond-East Chicago-Gary-Whiting metropolitan complex (pictured in Figure VI-1, and referred to below simply as Northwest Indiana) was chosen for the site of this study for several reasons. It is one of the nation's biggest industrial areas, with three large steel mills and four petroleum refineries situated along the Lake Michigan shoreline. Other important industries are foundries, steel fabricators, chemical plants, a cement manufacturing plant, and two sizable power utilities. The "Air Pollution Inventory" (Ozolins et al., 1968) of the area shows that particulate emission from industrial processes accounts for 76 percent of the total particulate emissions in the area. We felt that this compact clustering of major sources might provide both high concentrations and strong spatial variations of trace elements. Furthermore, the variety of source processes should tend to maximize the number of detectable trace elements, thus providing a maximum of information.

Harrison (1970) had demonstrated the existence of a very strong Cu concentration maximum in East Chicago which was

reproducibly found on each of his six sample days and was apparently a permanent feature in the area. This aroused our interest in the possibility of major sources of other trace elements in the area, perhaps related to the copper source.

2. Sampling Program

Each of the four cities runs an active air pollution monitoring program. All of the local sites are equipped with high volume pumps and 20x25 cm (8x10 in) filter holders, the ideal choice for our purposes.

For this study a network was formed by combining the facilities of the four cities with the adjoining Porter and Lake Counties, as well as Michigan City. Figure VI-3 shows the location and numerical designation for these 24 sites. Table VI-1 shows their areas of jurisdiction and name. Where possible, the stations are 2 to 3 stories above ground, but at least for station 6 this was not the case. In an effort to obtain a measure of the more distant background, a sample was taken at a rural station (No. 30, Niles, Michigan), located on a farm some 100 km ENE of the metropolitan area. The sampler here was 1.5 meters above ground, over short grass.

All filters were 20x25 cm, exposed for 24 hours starting 11 June, 1969, usually at 0000 hrs but in some cases at 0900 hrs. They were cut from Microsorban (see Appendix 1a), a polystyrene material whose high flow rate, freedom from dust loading effects, and low analytical blanks make it ideal for trace element sampling in heavily polluted areas. Its loosely

woven cottonlike constitution causes a certain portion of the unexposed edge area to tear off when removed from the filter holder, precluding exact weighing after sampling. For this reason no total suspended particulate measurements are available for this day.

Figure VI-4 shows the surface weather map for 7 AM EST, 11 June, 1969. A strong southerly air flow would be expected, and was generally observed during the period at all area meteorological stations (Figure VI-3). Other meteorological data of interest are listed in Table VI-2. As expected from the strong pressure gradient and 0.9 fractional cloud cover, the wind traces were rather steady, hourly extremes of speed and direction at East Chicago being 6 to 18 mph and 180 to 220°, respectively.

3. Analytical

The procedure used here was nearly the same as described in Appendix 2a, except for the addition of a third irradiation of two hours duration in the reactor core. The usual sequence of four counts was followed, and the entire scheme is shown in Table VI-3.

It had appeared from previous analyses that replication was advantageous when maximum accuracy was the goal. Because of the pilot study nature of this project and the desire to try to evaluate realistically all possible sources of error, every analysis was performed from two to four times, on

different sections of the filter, and the results (Appendix 4) represent mean values of these replications. Standard deviations given in parentheses were determined from the dispersion of these individual analyses, and represent approximately the 60 to 70 percent confidence level. Uncertainties contributing to the reported deviations include filter subdivision, spatial neutron flux variation during irradiation, counting geometry and statistics, filter-impurity inhomogeneities, and possible inhomogeneities of air flow through the filter.

C. Results

Twenty-eight elements were detected in nearly all the 25 samples, while two other elements (Ag and Ni) could be detected only in a limited number of samples. The mean values and standard deviations are listed in Appendix 4. No values for Cl are given because of prohibitively high impurity levels in the polystyrene filter used (see Appendix 1a), while the concentrations of the elements I and Au were below the detection limit of urban samples. In subsequent sampling on Whatman No. 41 filter paper and in less polluted areas both Cl and I have been regularly determined.

The concentrations of the elements detected range from 18,000 ng/m^3 for S down to 0.04 ng/m^3 for In. In order of decreasing maximum concentration the list reads: S, Fe, Co, Cu, Al, Mg, K, Zn, Na, Mn, Br, Ti, Cr, Sb, V, Ce, As, La, W,

Ag, Hg, Se, Ga, Sc, Co, Th, Sm, Eu, and In. Reproducibilities are reflected in the standard deviations of Appendix 4, generally in the 10 to 30 percent range but larger for elements whose concentrations were in the neighborhood of the urban detection limit (S, In, W, Ga, As, Mg, Ag, Ni). Further information on sensitivities and reproducibilities is given in Appendix 2a.

D. Discussion

1. Source Strengths and Locations

A study of the concentration maps (Figures VI-5 through VI-28) given for 24 of the elements will reveal subjective differences in the areawide distributions (results for Ga, In, W, As, Ti, and Ni, were not plotted because of their large uncertainties). As an aid to visualizing patterns and comparing element to element, concentration isopleths have been drawn in a geometric series at 50 percent of the maximum concentration, 25 percent, 12 percent, 6 percent, and 3 percent. From these and from Appendix 4, it can be seen that some elements such as K, Ti, Al, Na, Eu, and Sm only show minor concentration variations throughout the entire 25 station network, reflected in isopleths with little pattern regularity. On the other hand, certain others such as Cu, Fe, Zn, Sb, Cr, W, and Br show much larger variations, with their isopleths revealing well-defined and often similar concentration patterns. This correlation of large concentration variations with patterned isopleths suggests that the latter group of elements

may possess distinct and recognizable sources in Northeast Indiana.

In an attempt to make these arguments more quantitative, Figure VI-29 shows a plot of the coefficient of variation, S, over the area for each element. It is calculated as follows:

$$S = \frac{1}{\bar{x}} \sqrt{\frac{1}{N} \sum_{i=1}^{N} \left(x_i - \bar{x} \right)^2}$$

where N, x_i and $\bar{x}$ are respectively the number of stations, the concentration at a particular station, and the arithmetic mean concentration. Although this measure cannot be used to separate the elements into well-defined groups it can be seen that the elements Cu, W, Sb, Zn, Cr, Br, Ga, Fe, Ag, Ce, and Mn show large variations indicative of important local sources while the concentrations of the elements Sm, Na, Eu, Al, Ti, and K vary only to a comparatively small extent over the area. Many of the elements Hg, Th, In, As, V, Ca, La, Co, Mg, S, Se, and Sc, which show intermediate values of the coefficient of variation, may have local sources in the area, but these sources either appear to be less important individually as compared to the background or more evenly distributed.

It is interesting to note that among the elements showing pronounced enrichment in the area, only a limited number of different concentration patterns are found, indicating that although different sources are present, a given group of sources may be primary for several elements. This is clearly seen in

Figure VI-30 where the elements are plotted next to the location of their maximum concentration. Most of the elements with large concentration gradients have their maximum at station 6 in East Chicago, near which the heaviest industry is located, in particular two large steel mills. Maxima for Fe, Zn, Cr, W, As, and Co, which might be linked with the steel production, are found in this location, with Sb and Ag having maxima in the immediate neighborhood. The Ca maximum and the high Mg concentration at this station may originate from the large amounts of dolomite used in the steel production as well as from a neighboring cement plant. The elements Ga, Hg, Mn, Ce, La, Sc, and Th also have high concentrations at this location. At station 13 in Gary in the immediate vicinity of another steel mill, several of the latter elements show a secondary maximum, examples being Fe, Cr, As, Co, W, Ce, Mn, Ca, and Mg. Station 1 in Hammond, situated near the shoreline, shows a primary maximum for Mn, Mg, Sc, Na, K, and Ti and a secondary maximum for Al, La, Sm, Eu, Ce, Th, Ca, Mg, Co, Fe, S, and Se. The industrial process to which the very high copper concentration in East Chicago can be linked is not obvious. A secondary copper maximum is experienced at station 23 in Chesterton.

Another way to approach the problem of elemental sources is by comparing the mean particle composition in the most heavily industrialized area to the composition in the outlying areas. Because some elements show concentration variations of

an order of magnitude or more, geometric rather than arithmetic means were preferred for use. These have the feature of suppressing the effect on the mean of an isolated high value while retaining equal weight for very low values. Table VI-4 gives the geometric mean concentrations over all stations, over stations 1-10, and over stations 14-25. A comparison between the means in the industrialized versus the semi-rural neighborhood indicates the presence of sources in the former area for roughly the same elements as mentioned before, namely Cu, Sb, Zn, Cr, Br, Fe, Ag, Ce, Mn, Ca, Mg, La, Sc, Co, Th, and In.

There are three groups of elements where observed atmospheric elemental ratios may help confirm the nature of the source. For example, Table VI-5 compares the concentration ratios of the rare earths Ce, La, Eu and Sm, in air particulates to their concentration ratios in a number of sediments which are believed to be reasonably representative of the minerals used in industry and for the soil contribution to the aerosol. The agreement with the geometric mean concentration over all stations is very good. For the heavily industrialized area (stations 1-10) the elements La and Ce, which appear to have local sources, are slightly enriched.

The most important emission sources of Ca and Mg in the area are the cement and steel industries and the combustion of coal. Table VI-6 provides the Ca-Mg ratio in dolomite, used in these industries, and for the particulate emissions from coal.

and fuel oil combustion. The Ca-Mg ratio in the aerosol is close to the dolomite value because this represents more than 65 percent of the emissions for both elements (Winchester and Nifong, 1969). It is, however, increased by the contribution of fly ash which is enriched in Ca relative to Mg.

Because S and Se originate primarily from the combustion of coal and fuel oil, the Se/S ratio in these materials should be indicative of the ratio of the material when emitted into the air. Table IV-7 summarizes these ratios. According to the pollution inventory of Winchester and Nifong (1969) the sulfur pollutants from coal are about four times the levels resulting from oil. Thus, the Se/S ratio of 2.2×10^{-4} found in the air particulates agrees with the source ratio.

This agreement may be partially fortuitous, though, because of two cancelling factors. The combustion product SeO_2 is only a vapor above 315°C, and a smaller percentage of it than of S should be emitted into the atmosphere. (Weiss et al. (1971) confirm this idea from measurements of Se and S in Greenland ice, where S but not Se has increased during the last hundred years.) On the other hand, a larger percentage will condense and be caught, as shown by Pillay and Thomas (1969), who found that on the average 44 percent of the selenium in the air is captured by a filter paper having good efficiency down to 0.1 μm, while this fraction is generally lower for sulfur.

Repeated smaller-scale sampling in this area (Nifong, 1970) has revealed considerably higher concentrations for several elements at stations 6 and 9 and nearer the shoreline steel mills. Two suggestions follows:

a) Absolute concentration maxima reported here may be lower than the average for this area. The reasons for this may be twofold. The unusually steady and brisk south-southwest wind during the sampling period caused a situation of high ventilation, producing lower-than-normal concentrations of those elements having nearby sources. Secondly, the wind direction was such as to transport a large fraction of the shoreline steel and cement plant emissions directly out over the lake, making downwing sampling impossible. Since the steel and cement manufacturing industries emit respectively about 85 percent and 12.5 percent of the industrial particulate emissions in this area Ozolins et al., 1968), this wind direction may have caused the observed concentrations to be significantly lower than normal.

b) Higher concentrations found in the immediate neighborhood of open hearth and sintering plants confirm the previous suggestion that the source of several elements is linked with the steel production (Nifong, 1970).

Inspection of the concentration maps for those elements with large variations often reveals a solitary maximum surrounded by stations all having much lower values, with no clear-cut plume. This pattern is not shared by the total particulate (Figure VI-31) and presumably reflects a point source for the element in question. The presence of such large concentration changes between stations often separated by as little as 2 km may be attributed in part to the extremely steady prevailing wind during the sampling period, but more probably represents the grosser features of a permanent fine structure on a scale smaller than that revealed by the present network. A follow-up study with more closely-spaced stations would be desirable.

2. Elemental Areawide Pair Correlations

It was pointed out previously that a first view of the isopleths reveals that a number of elements which are expected to have common sources in East Chicago show very similar distribution patterns. It is interesting to note that the distributions of Cr, Fe, and Ce, as reflected in the isopleths, are quite similar to each other, as are those of Sb and Zn, Sc and Co, and Sm and Eu. It may also be worthwhile to compare the distribution of the elements S and Se which are known to have common sources (burning of coal and fuel oil). Although the analytical results for sulfur are of low quality and bear a large uncertainty, the two sets of isopleths still show some

similarity. To find possible objective correlations between the elements, their sources and their atmospheric behavior, a statistical analysis of the data was performed (Dams et al., 1970), with the results as summarized below.

Linear correlation coefficients were computed between all possible pairs of elements as follows:

$$r_{xy} = \frac{\overline{x\,y} - \bar{x}\,\bar{y}}{\sqrt{\overline{x^2} - (\bar{x})^2}\sqrt{\overline{y^2} - (\bar{y})^2}}$$

where x and y represent the concentrations of both elements to be correlated. Standard deviations of the correlation coefficients were calculated from the analytical standard deviations of x and y as follows:

$$\sigma_{r_{xy}} = \sqrt{\sum_{i=1}^{N}\left(\frac{\delta r}{\delta x_i}\right)^2 \left(\delta x_i\right)^2 + \sum_{i=1}^{N}\left(\frac{\delta r}{\delta y_i}\right)^2 \left(\delta y_i\right)^2}$$

The use of this expression for $\sigma_{r_{xy}}$ of course assumes that x and y are independent variables and is thus not strictly correct. Nevertheless it provides a measure of the extent of uncertainty in the computed correlation coefficients based on assumed independent errors in measurement of x and y.

Table VI-8 summarizes the most significant correlations in order of decreasing significance. Out of 435 computed correlation coefficients, 25 are larger than 0.795 and 105 are larger than 0.60, with no significant negative correlations being found. Inspection of this table reveals the highly

interesting fact that most of the significant correlations are between elements having only moderate and weak sources, and not between those with strong sources. In fact, out of the list of strong-source elements (Cu, W, Sb, Zn, Cr, Br, Ga, Fe, Ag, Ce, and Mn) as derived from Figure 29 above, the elements Cu, W, Br, Ga, and Ag do not correlate with any other element well enough to appear in Table VI-8. Of those that do, Cr does not correlate highly with any other of these strong-source elements. Of the remaining elements, the most important correlation is between the Zn-Sb pair, which not only has the third highest correlation coefficient but is composed of two elements with very strong sources. This pair of elements has later been observed to display great similarities in particle size distribution, time variation, and areawide concentration on a continental scale (see Chapters III,V, and VIII).

Figures VI-32 and VI-33 graphically illustrate two of the best correlating pairs of elements, namely Co-Sc and Zn-Sb. The least squares linear fit and the boundaries as obtained from the analytical standard deviations of the concentrations are shown, and it is apparent that most of the stations fall within these boundaries. As an example of two "background" elements (both showing little variation over the network) the graph of Sm-Eu is also shown (Figure VI-34). Though the correlation coefficient here is only 0.77, a fact probably due to

the larger analytical uncertainties for these elements, more than 70 percent of the stations fall within the statistical uncertainty and the significance of a linear correlation can be accepted.

The fact that elements with strong sources do not correlate well with one another likely means that their sources are different. An interesting question is the extent of this difference - whether a low correlation coefficient necessarily means that they have only a very small source overlap. To identify possible perturbing effects on the correlation coefficient of points with strong sources for only one of the two elements (where the elemental ratio is markedly different from the geometric mean ratio over the network) a point regression technique was applied. For the pairs of elements with a correlation coefficient of at least 0.70, the linear correlation coefficient was calculated by successively deleting most stations for which the concentration relationship deviates greatly from the calculated linear fit. In Table VI-9 those calculations which are improved considerably by deleting one or two stations are summarized.

It is obvious from this table that the correlations of Fe with several other elements increases strongly when station 13 is deleted, which suggests that this station should be near a source of Fe. This notion is quickly confirmed by the concentration map for Fe, Figure VI-10, where the concentration at station 13 is seen to be some 5-6 times above the values

at the surrounding stations. As compared to the other elements, this increase in concentration is unusually high. Some of the other elements, such as Cr, Zn, Sb, and Br, also show local maxima here, but only Br matches Fe in intensity of enrichment, and that is probably coincidentally due to the nearness of the traffic of downtown Gary to this station (Br does not show a strong enrichment at station 6, also near to the steel industry, either in this experiment or in the Mackinac Island experiment of the next chapter). Figure VI-35 illustrates the strength of this Fe source, for the Fe concentration is seen to be 3 times higher here than expected from the linear fit for Fe-Co. Station 13 also appears to be anomalously high in magnesium, for when deleted from the Ca-Mg calculation their correlation coefficient also increases significantly (Figure VI-36). Although the analytical uncertainty of the magnesium concentration is large, Ca and Mg seem to correlate linearly.

In agreement with these observations, station 13 is indeed known to be near to a large steel mill, which is just north of it on the lake shore.

On the basis of the above observations Figure VI-37 was drawn, showing the linear correlations (station 13 deleted) of the elements presumably linked with industries located in the East Chicago area. Although not all the large intercorrelations are shown on this figure, it is obvious that correlations larger than 0.85 are very frequent in this group. It

is apparent that most elements of this group are strongly correlated with Fe. Since iron is known to be a major component of the particulate emissions of the steel mills, it is believed that most of the elements are linked with the local steel and supporting industries. Side elements in this figure, such as V and In, may however have other important sources in the area. The elements Cu and to some extent Ag seem to have a separate major source which cannot from this study alone be correlated with the steel manufacturing.

In order to further investigate possible similarities between groups of elements a "cluster analysis" was performed, described elsewhere (Dams et al., 1970). This attempted to delineate groups of elements from their variation patterns, and resultant groups included Co-Sc-Th-Ce and Cr-Zn-Sb with high reliability scores, as well as In-Mn-Fe-Mg-Ca-La-V and Cu-Ag showing a more loose linkage. It is perhaps significant that all these elements were also found to have sources within the industrialized area. As expected on the basis of the coefficients of variation the elements Na-K-Sm-Eu, apparently not associated with industrialized sources, form a cluster.

3. Meteorological Effects

There do not seem to be clear-cut meteorological effects noted in this study, partially because the wind direction was such as to blow the greatest mass of particulate material over the lake where downwind effects could not be studied. In spite

of this hindrance, however, some effect of wind direction may be evident in the general NNE orientation of isopleths of elements which show large concentration gradients, such as Cu, Zn, Cr, Sb, and Fe. On the other hand, it is impossible solely on the basis of a one-day study to rule out the possible coincidental alignment of sources with wind direction. There is some hint of strong concentration gradients on the downwind side of sources, especially for Cu, but this is not clearly defined.

The presence of strong maxima for steel-related elements at stations 6, 9, and 13, which for this day were upwind of the mills, is here tentatively interpreted as arising from re-entrainment of surface dust previously having fallen out from the effluent of the mills. Turbulent backwash of the plumes seems highly unlikely both because of the stack heights and upwind distances involved.

4. Total Suspended Particulate

A correlation of elemental concentration patterns with the variation of total suspended particulate over the network would be highly desirable. As mentioned above, such correlation is not directly possible for this sampling day because of the use of polystyrene filter material. It is possible, though, to approximate the distribution of total particulate by using data from Harrison (1970) for a day of similar wind, June 6, 1968. These data (Figure VI-31) reveal a maximum

variation of 2.4x over the network, but a somewhat anomalous maximum near station 2 in Hammond. (Inspection of Harrison's data for other days commonly reveals broad maxima centered over northern East Chicago or vicinity, the region here found to contain the maxima of most individual elements. These data also suggest that the range of total particulate may vary from 1.5-4 over the network.)

The significance of this data is of course that the total particulate of an area, having originated with a variety of sources, tends to show much smoother areawide variations than do the individual elements. It should not be used as a guide for these elements, for it may be very misleading.

5. Control Station

Originally it was hoped that the "control" station at Niles would be of some value in assessing long-range effects such as differential transport of the elements, but relatively high concentrations were found there for S, Se, Cu, Sb, As, and Ga (Table IV-10). These may be partially ascribed to the influence of South Bend, Indiana, some 15 km to the south, but may more generally represent normal variations in the trace element background of the region. In any event, we were surprised by these high concentrations in a region that appeared quite rural and removed from immediate pollution sources.

Subsequent measurements (Chapters III, IV) have disclosed that most of the elements listed above as being unusually

enriched at Niles (S, Se, Sb, and As) almost invariably are found in the atmosphere principally associated with the small particles (Cu and Ga less frequently so) which would not fall out rapidly during transport. Thus the possibility exists that their high concentrations at Niles may indeed result from advection from some distant source area, but with South Bend so close this may not be required.

E. Conclusions

In summary, then, a number of conclusions can be drawn from this study. Northwest Indiana shows a variety of elemental source strengths, with a number of elements strongly enriched locally, but a comparable number having little variation over the network. The pollution-derived elements seem to be the heavier metals (Cu, Sb, Zn, Cr, Fe, Ag, Ce, Mn, Br), while the "background" elements are often the light metals and rare earths (Na, K, Ti, Eu, Sm).

Most elements show their strongest sources with the steel industry, a conclusion which is in agreement with the large quantities of particulate matter emitted by this industry in the area.

Several of the pollution-derived elements show strong correlation in their areawide distributions, especially Zn and Sb.

A number of other elements show strong sources which do not appear to be steel-industry related. Examples are Cu, Ag, Br, and V.

The number of strong sources for a given element is very small, at least to the degree of resolution offered by the present network.

Variation of total particulate over the area is much smoother than the variation of most individual elements, because the total particulate effectively integrates the various elemental patterns.

The background at the Niles control station was not as low as expected for a number of elements, most of which are pollution-derived and usually present on small particles. A true "background station" should apparently be located much farther from the Northwest Indiana area than is Niles.

TABLE VI-1. Station Key

HAMMOND

1. Water Works
2. Goldblatt's
3. City Hall

WHITING

4. Fire Station
5. South Side School

EAST CHICAGO

6. Marktown
7. Central Fire Station
8. Roxanna School
9. Field School
10. Franklin School

GARY

11. Airport
12. Ivanhoe
13. Fire Station
14. Williams School
15. Kuny School
16. Wirt

LAKE COUNTY

17. Highland
18. Hobart
19. Crown Point

PORTER COUNTY

21. Ogden Dunes
22. South Haven
23. Chesterton
24. Valparaiso

OTHER

26A. Michigan City
30. Niles, Michigan

TABLE VI-2. Summary of Meteorological Data

Location	Sky Cover*	Avg. Wind Speed mph	m/s	Prevail. Direct.**	$T_{max.}$ °C	$T_{min.}$ °C	Precipitation mm
O'Hare Field	.9-.9	10.4	4.6	170	31	16	1
Univ. of Chicago	---	---	---	---	33	17	---
Midway	.9-.8	13.6	6.1	180	33	18	Trace
East Chicago	---	10.7	4.8	200	--	--	---
Michigan City	---	10.8	4.8	170	--	--	---

*Sunrise-sunset and sunset-sunrise

**Measured in degrees East of North

TABLE VI-3. Irradiation and Counting Scheme

Filter Area (cm^2)	Air Volume (m^3)	T_{irr}	Reactor Location	Flux (n/cm^2-sec)	T_{cool}	T_{count}	Isotopes Measured
0.8	5	5 min	Pneum	2.0×10^{12}	3 min	400 sec	^{28}Al; ^{52}V; ^{66}Cu; ^{51}Ti; ^{37}S ^{49}Ca;
					15 min	1000 sec	^{27}Mg; ^{80}Br; ^{38}Cl; ^{128}I; ^{56}Mn; ^{24}Na; ^{116m}In
1.6	10	2-5 hrs	Core	1.5×10^{13}	18-36 hr	2000 sec	^{42}K; ^{64}Cu; ^{69m}Zn; ^{82}Br; ^{76}As; ^{72}Ga; ^{122}Sb; ^{140}La; ^{153}Sm; ^{152m}Eu; ^{187}W; ^{198}Au;
13.0	80	2-5 hrs	Core	1.5×10^{13}	20-30 da	4000 sec	^{46}Sc; ^{51}Cr; ^{59}Fe; ^{60}Co; ^{58}Co; ^{65}Zn; ^{75}Se; ^{110m}Ag; ^{124}Sb; ^{141}Ce; ^{203}Hg; ^{233}Pa

TABLE VI-4. Geometric Mean Concentrations in Air Particulates

Element	Geometric Means ng/m^3 air		
	All Stations 1-25	Stations 1-10 Industrialized	Stations 14-35 Semi-rural
S	10,000	11,500	9,000
Ca	2,800	3,950	2,150
Al	1,950	1,850	2,000
V	7.4	9.3	6.4
Cu	180	380	120
Ti	175	190	170
In	0.06	0.07	0.045
Br	66	94	45
Mn	130	180	100
Mg	1,100	1,350	900
Na	285	285	275
Sm	0.34	0.34	0.33
Zn	270	510	175
Sb	6.3	12.4	4.2
W	0.65	0.8	0.5
Ga	0.85	0.75	0.95
Eu	0.09	0.10	0.085
As	4.4	4.2	4.3
K	1,150	1,250	1,100
La	2.4	3.4	1.9
Co	1.1	1.5	0.9
Fe	3,900	6,500	2,500
Sc	1.6	2.1	1.35
Cr	21	54	11
Hg	2.0	2.5	1.9
Se	2.2	2.6	2.1
Th	0.42	0.57	0.35
Ce	3.8	6.1	2.5
Ag	<1.5	1.9	<1
Ni	<30	<50	<25

TABLE VI-5. Comparison Between Rare Earth Ratios in Air Particulates and in Sediments

Element Ratio	Correlation Coefficient	Concentration Ratio Air Particulates		Concentration Ratio		
		All Stations 1-25	Stations 1-10	North American Shales[1]	Sandstone[2] Glauconite	Limestone[3] Lannon
Ce/La	0.81±0.04	1.6	1.8	2.0	2.7	--
Ce/Eu	0.76+0.13	42	60	38	59	--
Ce/Sm	0.51±0.12	11	18	11	12	--
La/Eu	0.68±0.17	27	33	20	21	30
La/Sm	0.62±0.14	7	10	5.6	4.3	8.2
Eu/Sm	0.77±0.13	0.27	0.30	0.29	0.20	0.27

[1]Composite of 40 American shales, Haskin et al. (1966)

[2]Glauconite bearing sandstone, Haskin et al. (1966)

[3]Limestone from Milwaukee, Wisconsin, Haskin et al. (1966)

TABLE VI-6. Comparison between Ca-Mg ratios in Air Particulates and Industrial Sources

	Air Particulates (ng/m^3) (Geometric Means)		Limestone** Dolomite (Percent)	Ash Analyses** of U.S.A. Bituminous Coals (Percent)	Particulate Emission From Fuel Oil Combustion* (Percent)
	All Stations	Stations 1-10 Industrialized			
Ca	2,800	3,950	31	1-15	0.4
Mg	1,100	1,350	18	0.2-2.5	0.3
Ratio Ca/Mg	2.5	2.9	1.7	5-6	1.3

*Winchester and Nifong (1969)

**Lewis and Crocker (1969)

TABLE VI-7. Comparison Between Ratio Se/S in Air Particulates and Combustion Material

Element	Concentration in Air Particulates ng/m^3		Average Concentrations %*	
	All Stations 1-25	Industrialized N.W. Indiana Stations 1-10	Coal	Crude Oil
S	10,000	11,500	2.4%	---
Se	2.2	2.6	---	---
Se/S Ratio	2.2×10^{-4}	2.3×10^{-4}	3×10^{-4}	0.5×10^{-4}

*Pillay et al. (1969)

TABLE VI-8. Linear Correlation Coefficients Between Trace Elements in Air Particulates

Elements		Linear Correlation Coefficient	Stand. Dev. on Linear Correlat. Coefficient	Ratio Geometric Means
X	Y	r_{XY}	$\sigma_{r_{XY}}$	$\frac{\bar{X}_g}{\bar{Y}_g}$
Co	Sc	0.96	0.03	6.8×10^{-1}
Sc	Th	0.92	0.09	3.8
Zn	Sb	0.91	0.04	4.3×10^{1}
Co	Th	0.89	0.08	2.6×10^{-1}
Sc	Ce	0.85	0.04	4.2×10^{-1}
Eu	K	0.85	0.10	7.9×10^{-5}
Sm	K	0.85	0.07	2.9×10^{-4}
Zn	Co	0.84	0.07	2.5×10^{2}
Fe	Ce	0.84	0.04	1.0×10^{3}
Th	Ce	0.84	0.07	1.1×10^{-1}
Mn	Ce	0.84	0.06	3.4×10^{1}
Ca	Co	0.84	0.04	2.6×10^{3}
La	Sc	0.83	0.06	1.5
Co	Fe	0.83	0.05	2.8×10^{-4}
La	Th	0.83	0.07	5.8
Fe	Sc	0.82	0.05	2.4×10^{3}
Mn	Fe	0.82	0.06	3.4×10^{-2}
Co	Cr	0.82	0.04	5.1×10^{-2}
Mg	Fe	0.82	0.11	2.8×10^{-1}
In	Mn	0.81	0.19	4.4×10^{-4}
La	Ce	0.81	0.04	6.4×10^{-1}
Fe	Th	0.80	0.07	9.2×10^{4}
Zn	Cr	0.80	0.04	1.3×10^{1}
Zn	Fe	0.80	0.06	6.9×10^{-2}
Co	Ce	0.80	0.05	2.9×10^{-1}

TABLE VI-9. Linear Correlation Coefficients of Trace Elements After Deletion of One or Two Sampling Stations

Elements Correlated		Correlation Coefficients		Sampling Station(s) Deleted
		Original	After Station Regression	
Fe	Zn	0.80	0.92	13
Fe	Cr	0.78	0.94	13, 10
Fe	Sc	0.82	0.91	13
Fe	Co	0.83	0.94	13
Fe	Ce	0.84	0.90	13, 2
Fe	Th	0.80	0.91	13
Fe	Ca	0.74	0.84	13, 10
Mg	Ca	0.74	0.87	13
La	Ca	0.72	0.83	2, 7
La	Co	0.77	0.85	2
La	Th	0.83	0.90	2
La	V	0.73	0.80	2
La	Sc	0.83	0.89	2
Zn	Th	0.78	0.87	7
Zn	W	0.73	0.88	7, 1
Th	W	0.74	0.82	1
V	Sb	0.73	0.83	7

TABLE VI-10. Concentrations at Maximum, Minimum, and Control Station

Element	Concentrations ng/m^3			Concentration Ratios	
	Maximum	Minimum	Niles	Max/Min	Max/Niles
S	18,000(10,000)	3,00(3,000)	11,000(5,000)	6(9)	1.6(1.0)
Fe	13,000 (3,000)	1,420(120	1,900 (100)	9,7(3)	7.2(2.0)
Ca	7,000 (700)	1,410 (200)	1,000 (200)	5.0(0.7)	7.0(1.5)
Cu	4,000 (200)	25 (4)	280 (20)	160 (30)	14(1.5)
Al	3,100 (300)	1,375 (70)	1,200 (70)	2.3 (0.3)	2.6(0.3)
Mg	2,700 (1,000)	530 (300)	500 (300)	5.1 (3)	5.4(3)
K	1,860 (110)	730 (90)	720 (50)	2.5 (0.4)	2.4(0.3)
Zn	1,550 (200)	100 (12)	160 (20)	16 (2)	9.6(1.4)
Na	500 (50)	160 (20)	170 (20)	3.1 (0.4)	2.9(0.4)
Mn	390 (50)	63 (3)	62 (3)	6.2 (1)	6.3(1.0)
Br	300 (30)	26 (2)	38 (6)	12 (1.5)	8.1(2)
Ti	280 (50)	120 (25)	120 (25)	2.3 (0.7)	2.3(0.7)
Cr	113 (20)	6.2 (0.8)	9.5(0.8)	18 (3)	12(2)
Sb	31 (3)	2.2 (0.2)	6.0(0.3)	14 (2)	5.3(0.7)
V	18.1(1.5)	4.01 (1.0)	5.0(0.3)	4.5 (1.2)	3.6(0.4)
Ce	13 (1.5)	1.4(0.1)	0.82(0.06)	9.3 (1)	16(4)
As	12(2)	2(1)	4.6 (2)	6 (4)	2.6(1.2)
La	5.9(0.4)	0.9(0.3)	1.3 (0.3)	6.6(2.5)	4.5(1.0)
W	5.6(1)	0.3(0.3)	0.4(0.2)	19(19)	14(7)
Ag	5(2)	0.5	1	10	5
Hg	4.9(0.9)	0.8(0.3)	1.8(0.3)	6.1(3)	2.6(0.7)
Se	4.4(1.2)	0.8(0.5)	2.5(0.5)	5.5(3)	1.5(0.6)
Ga	3.5(1.0)	0.25(0.15)	0.9(0.4)	14(10)	3.9(1.2)
Sc	3.1(0.3)	0.92(0.1)	1.2(0.1)	3.4(0.4)	2.6(0.3)
Co	2.6(0.6)	0.47(0.06)	0.95(0.1)	5.5(1)	2.7(0.7)
Th	1.3(0.4)	0.17(0.02)	0.27(0.08)	7.6(2)	3.1(1.0)
Sm	0.65(0.20)	0.17(0.02)	0.24(0.03)	3.8(1.5)	2.0(0.4)
Eu	0.17(0.03)	0.06(0.01)	0.055(0.02)	2.8(0.5)	3.0(0.5)
In	0.15(0.06)	0.03(0.03)	0.04(0.03)	5(5)	3.7(3)

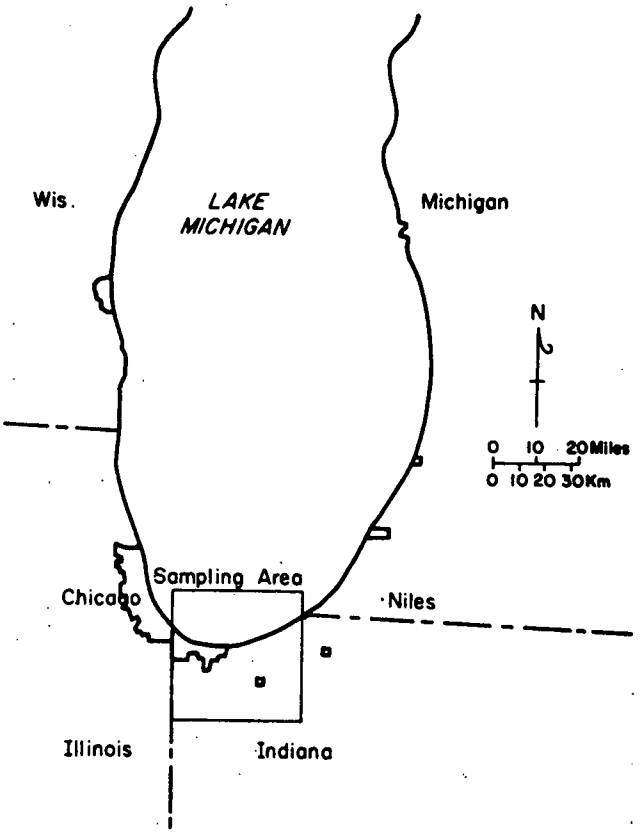

Figure VI-1 Map of Southern Lake Michigan

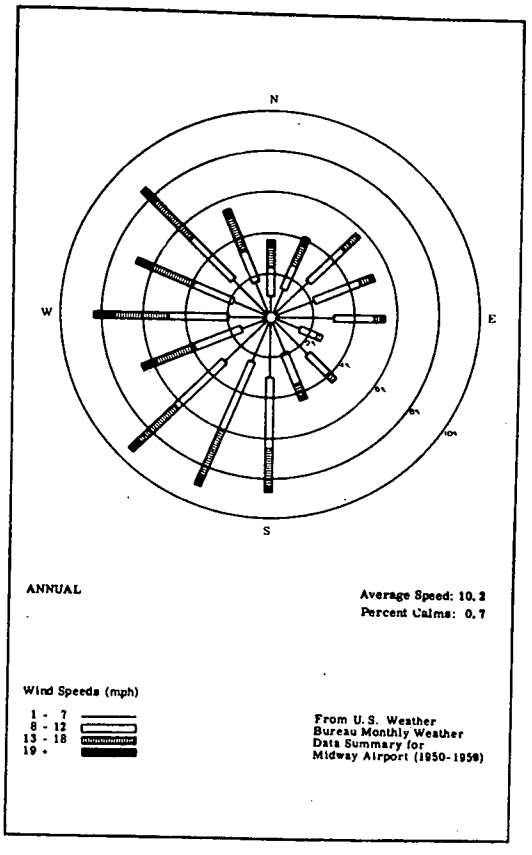

Figure VI-2 Wind Rose for the Chicago - Northwest Indiana Area

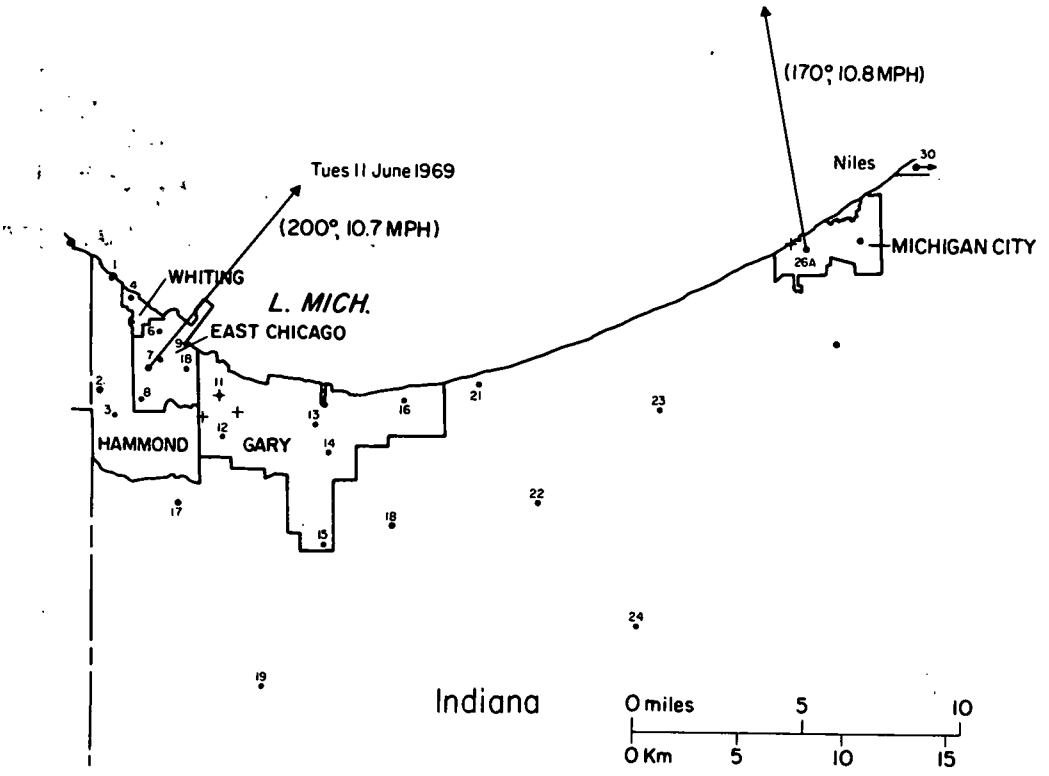

Figure VI-3 Map of Sampling Area with Numbers and Locations of Sampling Sites and Wind Direction for 11 June 1969

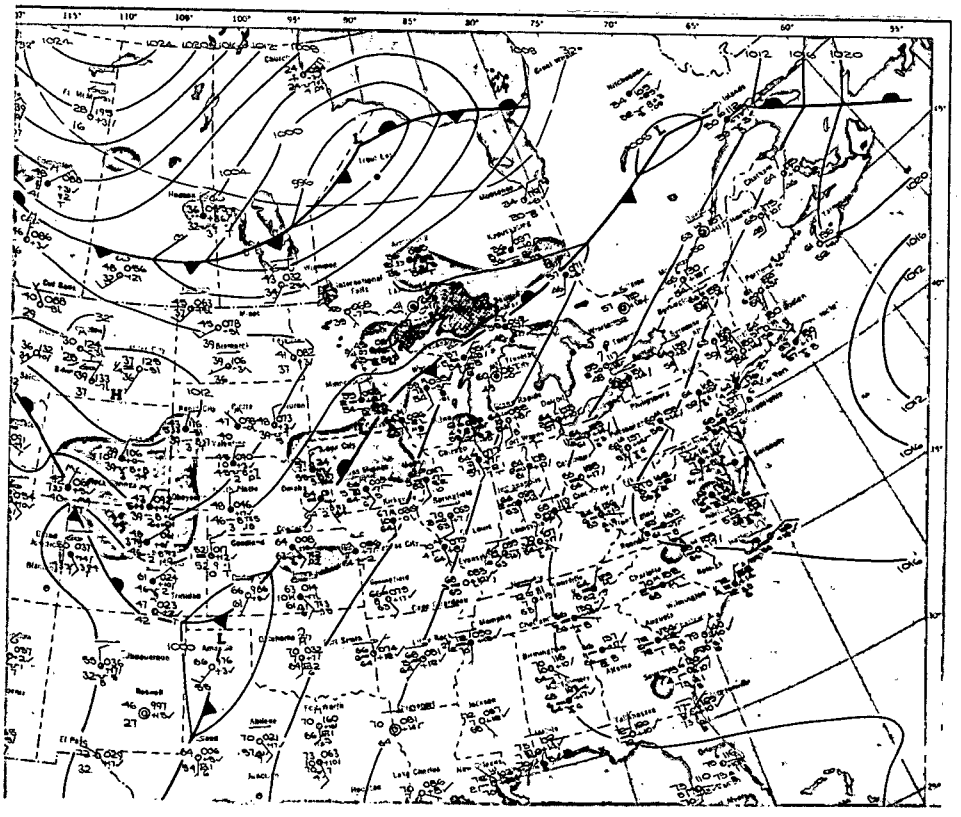

Figure VI-4 Weather Map of Northeast U.S.A. for 0700 11 June 1969

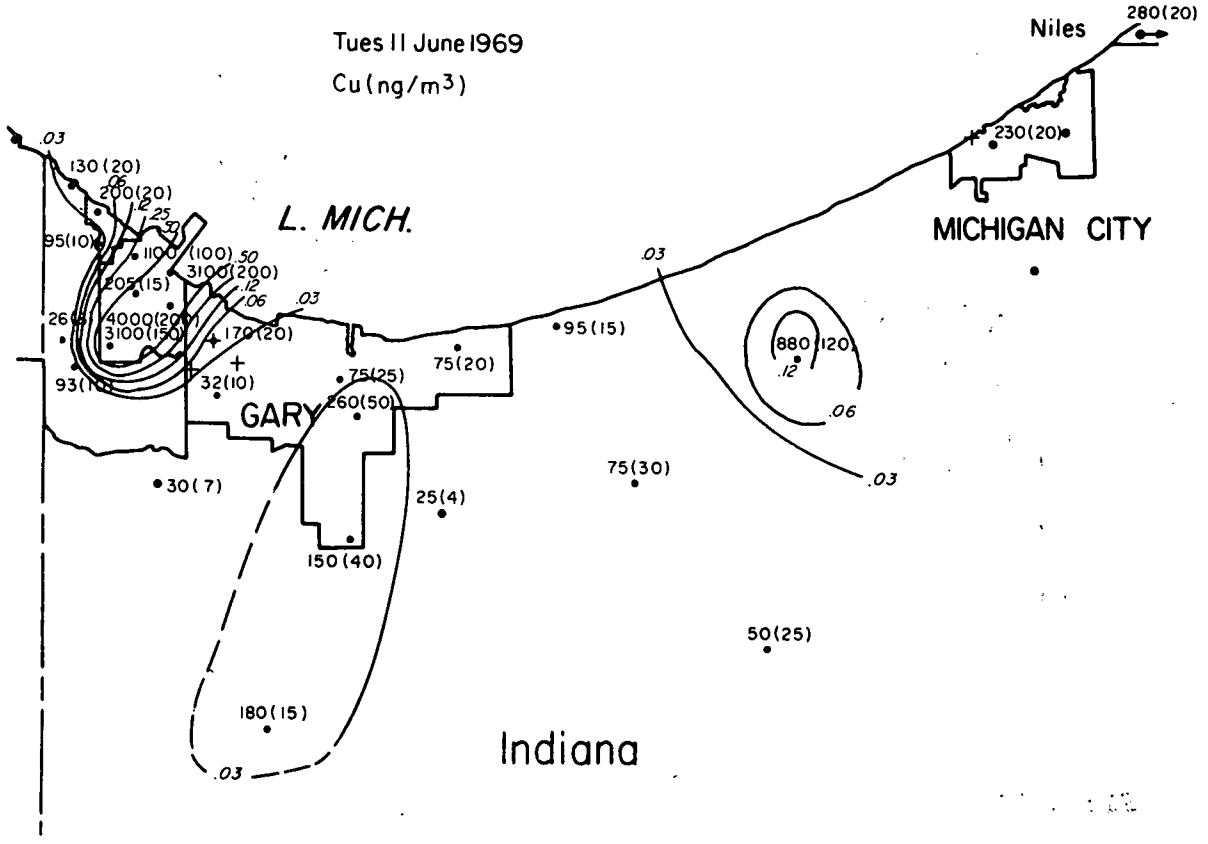

Figure VI-5 Concentration Distribution of Copper

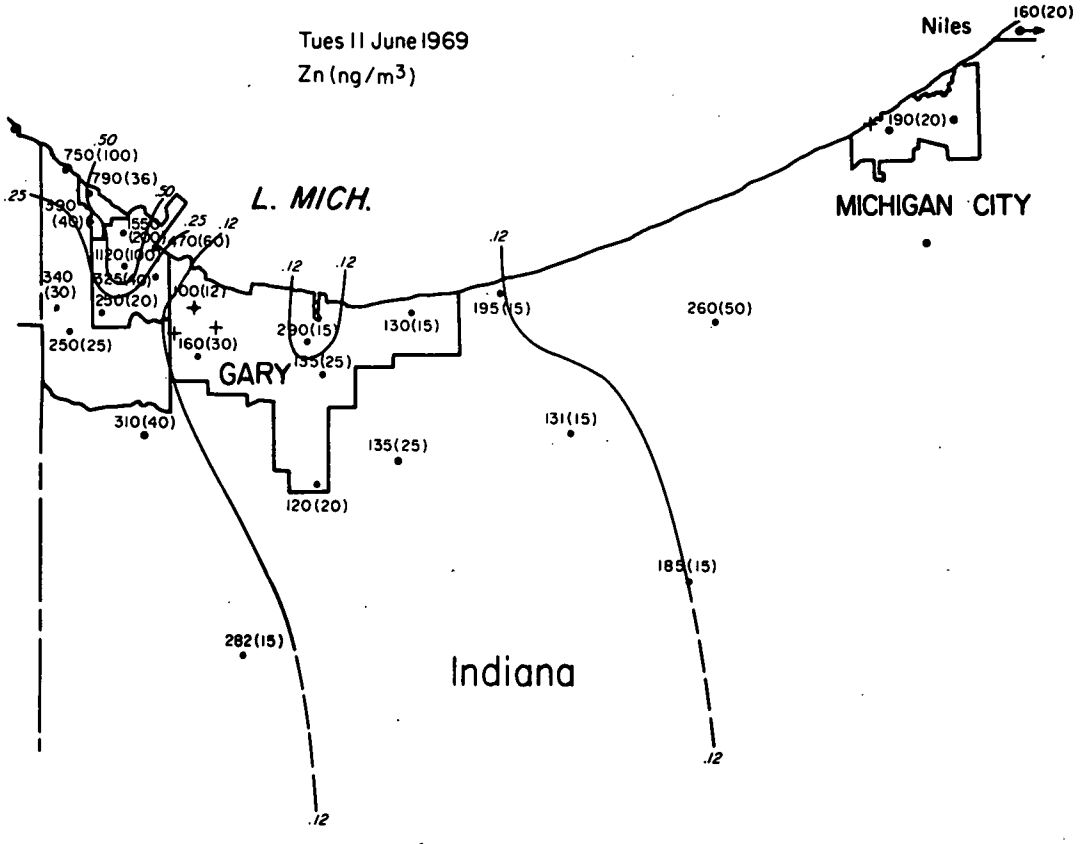

Figure VI-6 Concentration Distribution of Zinc

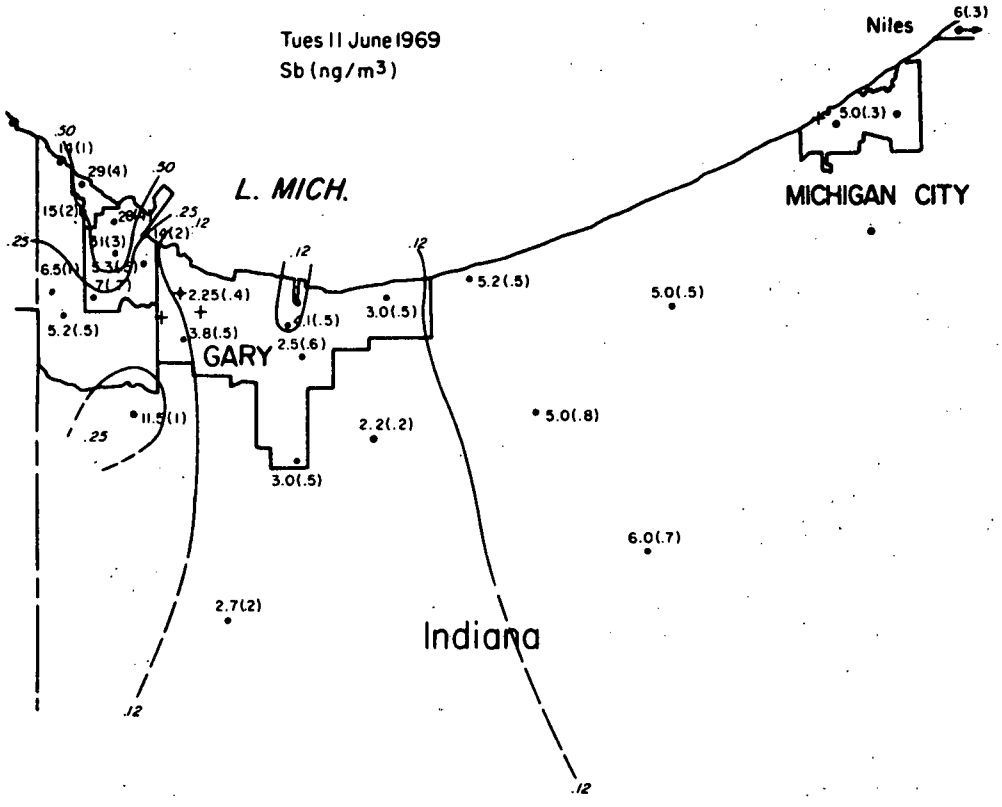

Figure VI-7 Concentration Distribution of Antimony

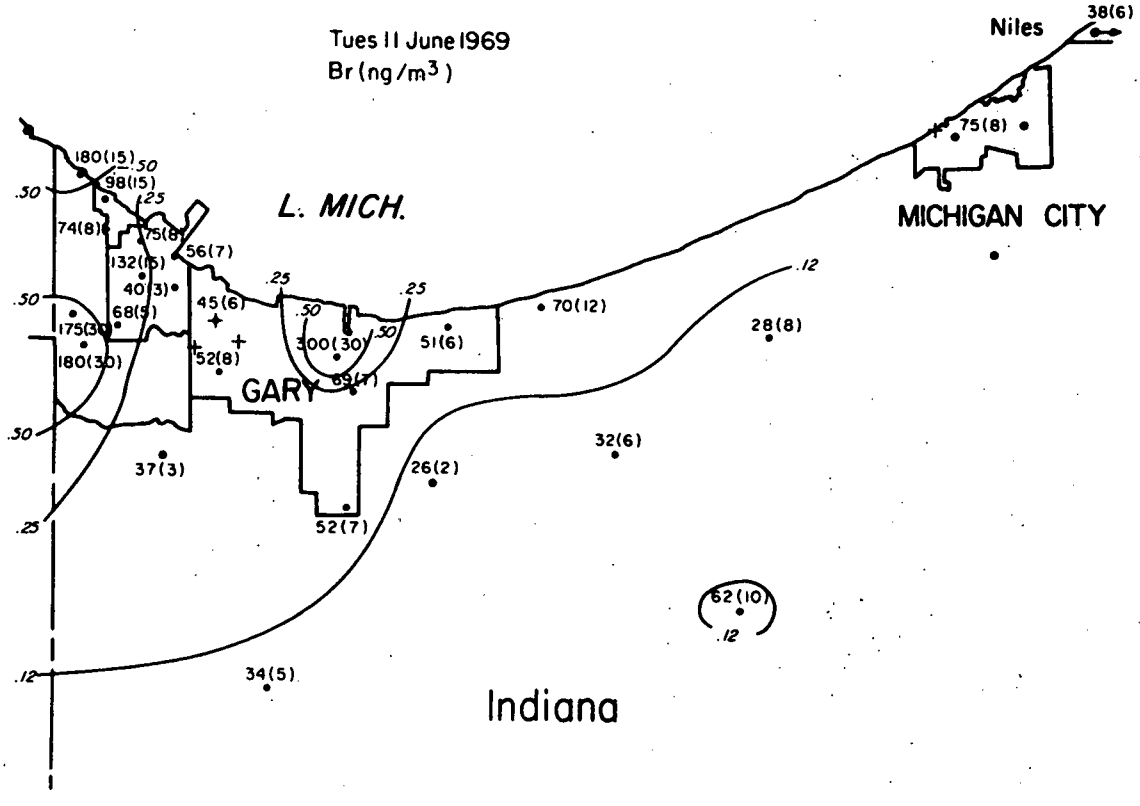

Figure VI-8 Concentration Distribution of Bromine

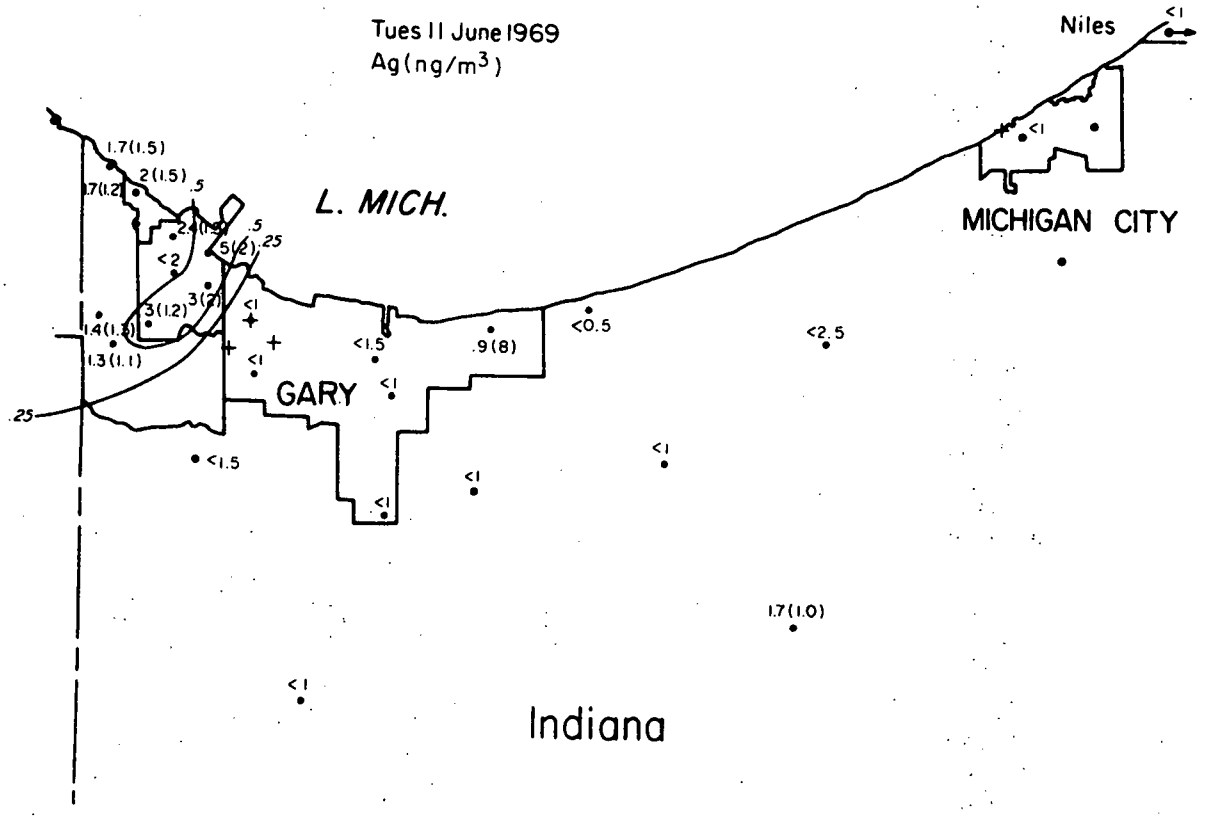

Figure VI-9 Concentration Distribution of Silver

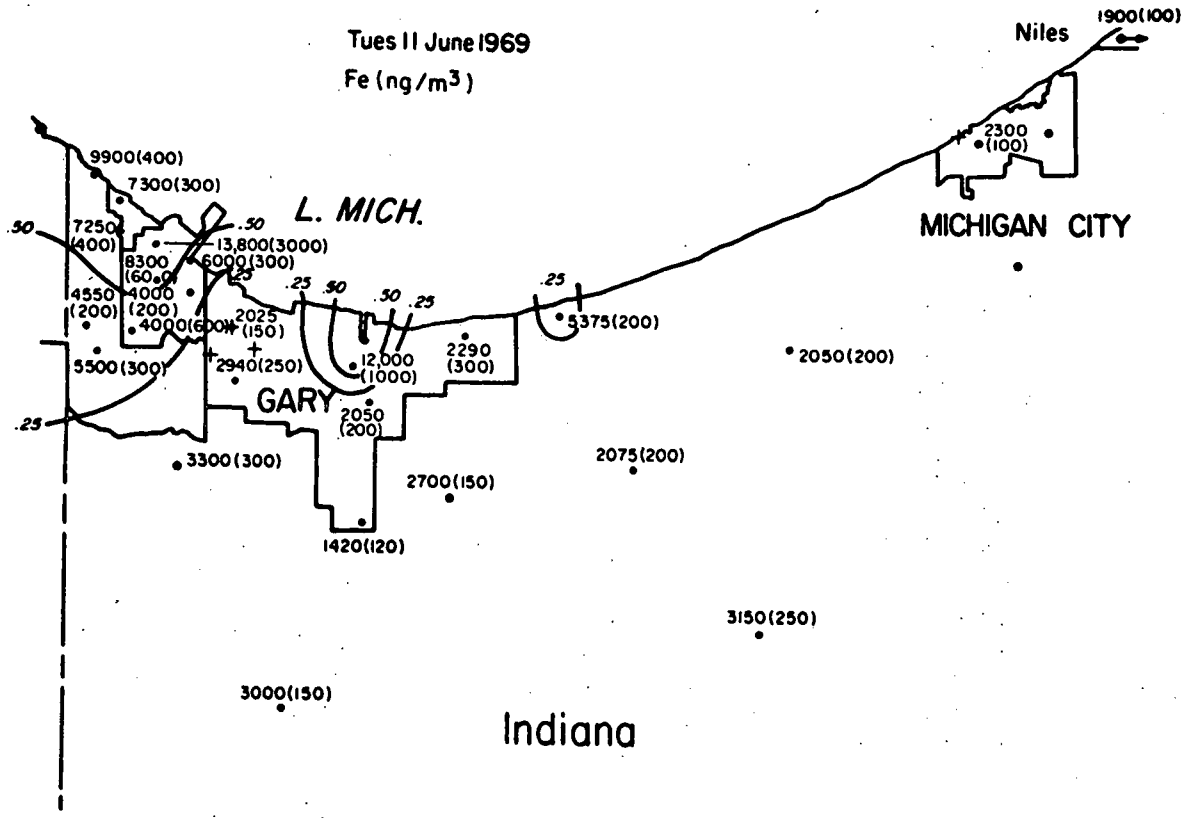

Figure VI-10 Concentration Distribution of Iron

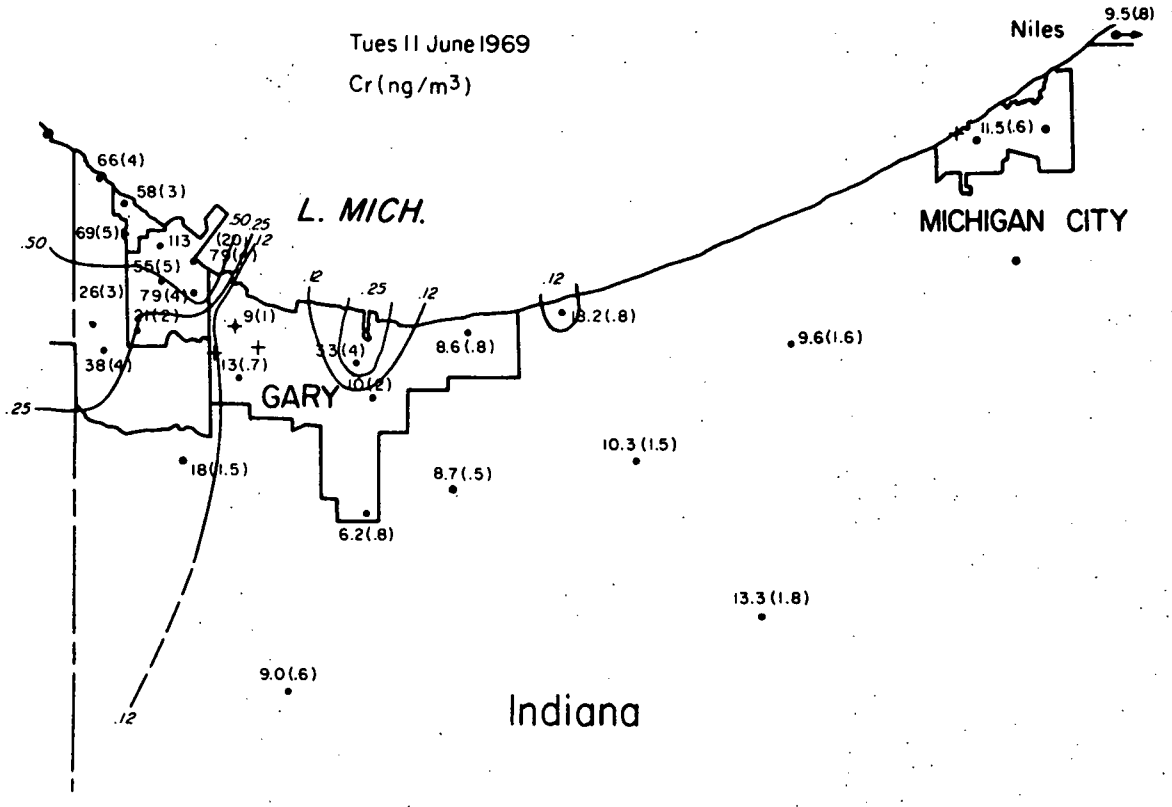

Figure VI-11 Concentration Distribution of Chromium

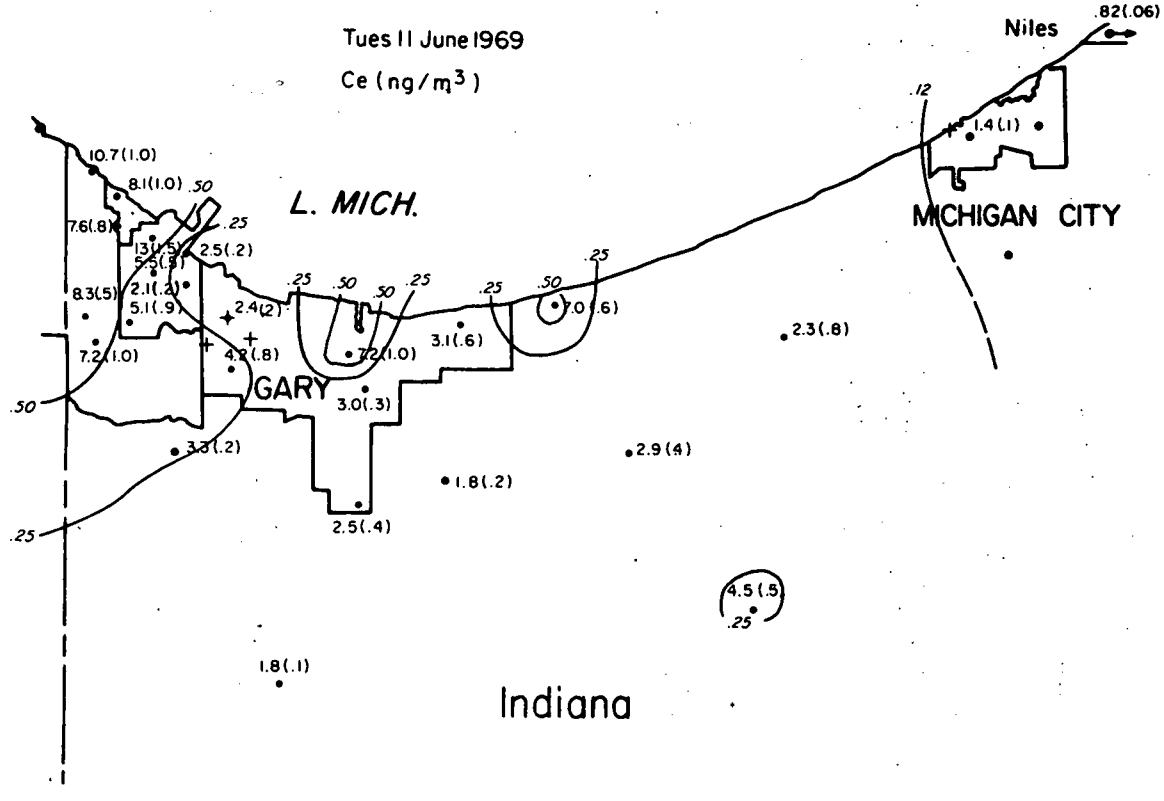

Figure VI-12 Concentration Distribution of Cerium

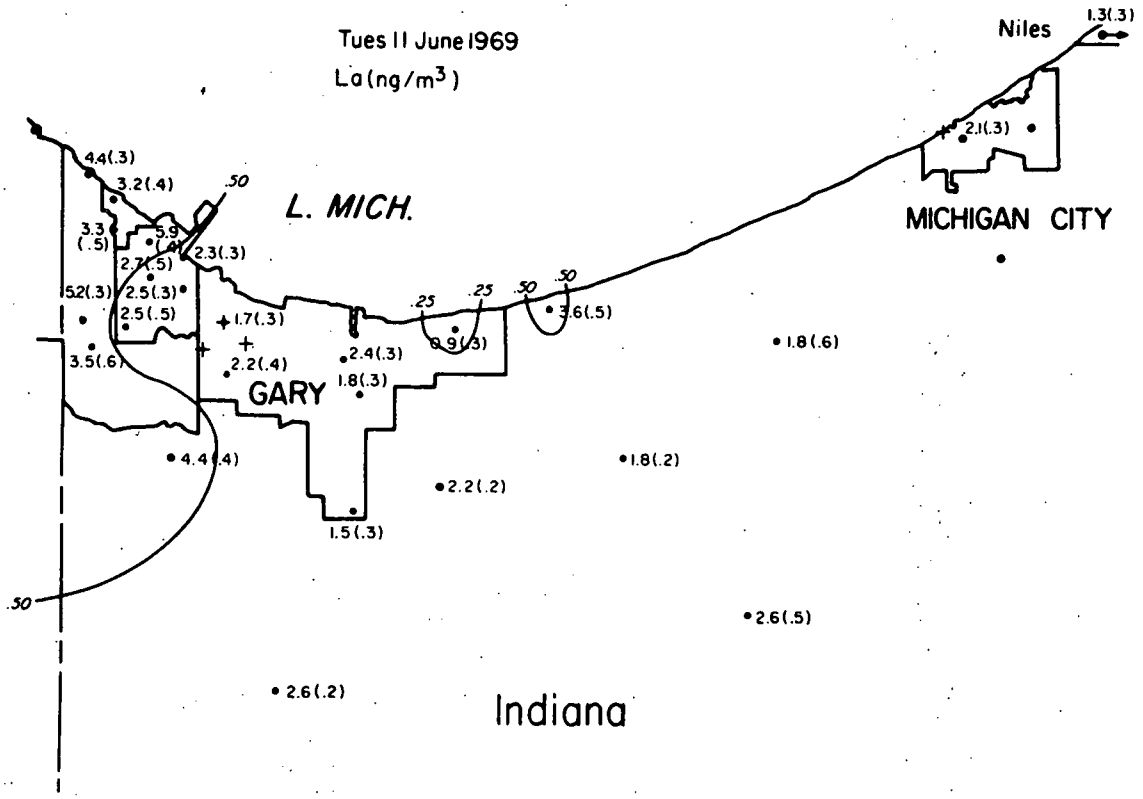

Figure VI-13 Concentration Distribution of Lanthanum

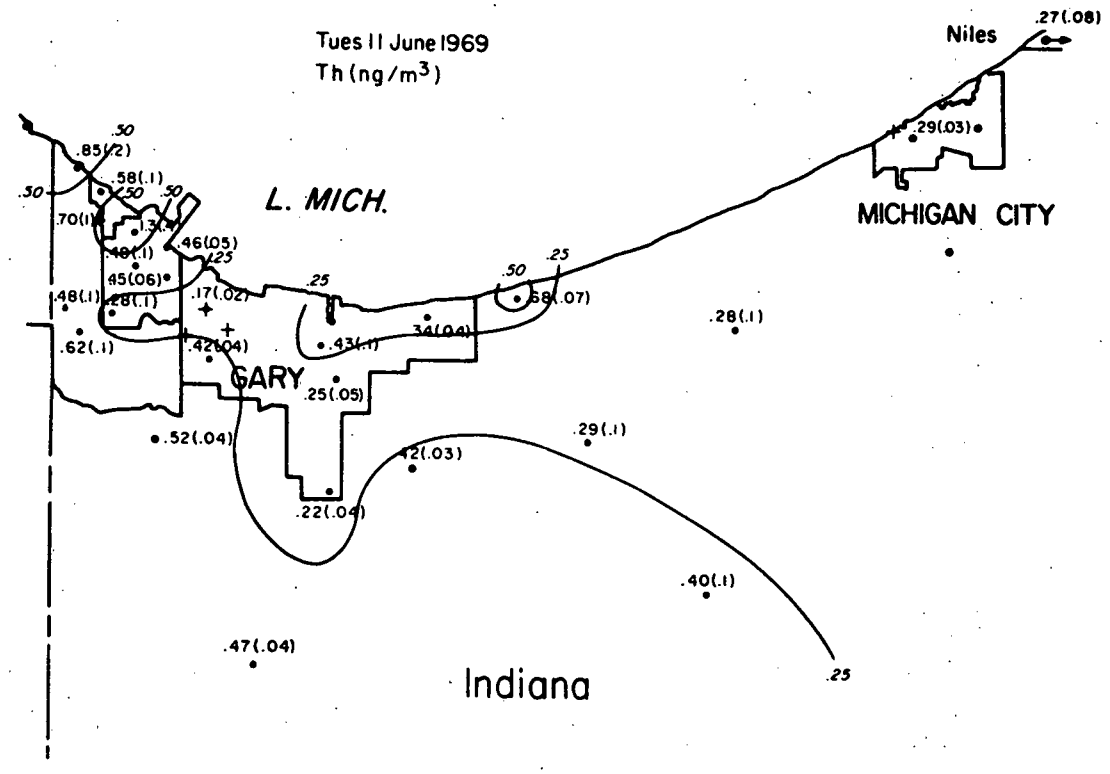

Figure VI-14 Concentration Distribution of Thorium

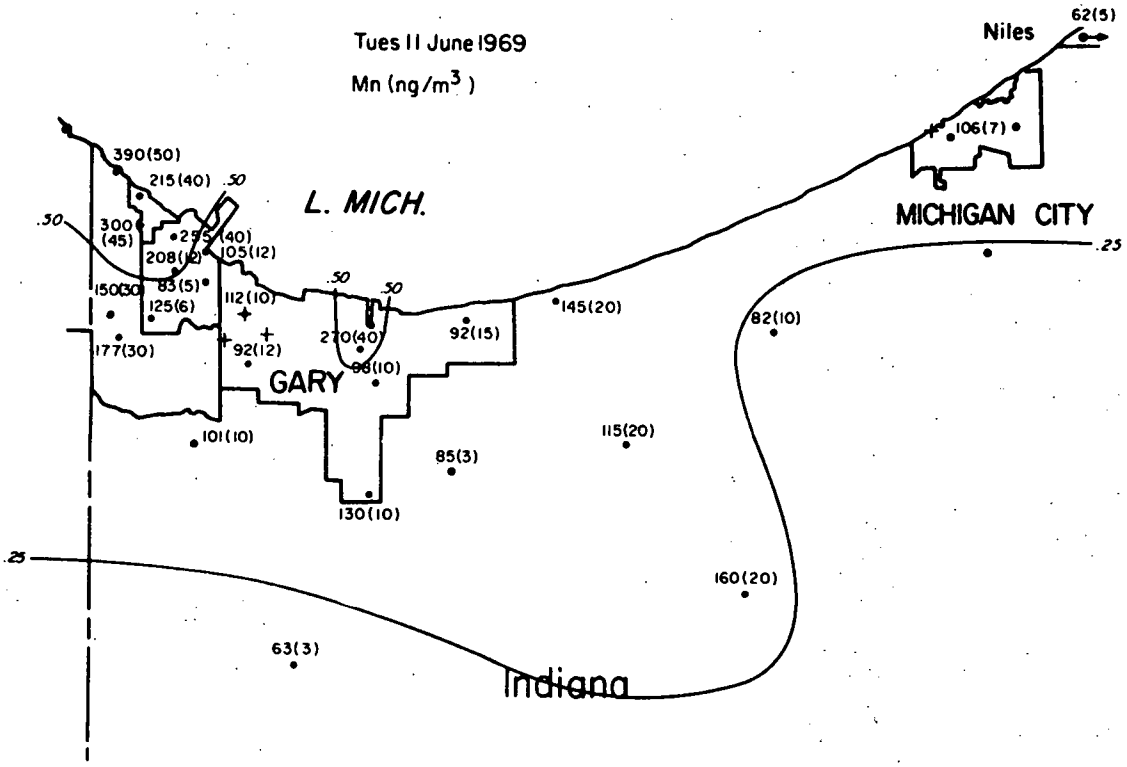

Figure VI-15 Concentration Distribution of Manganese

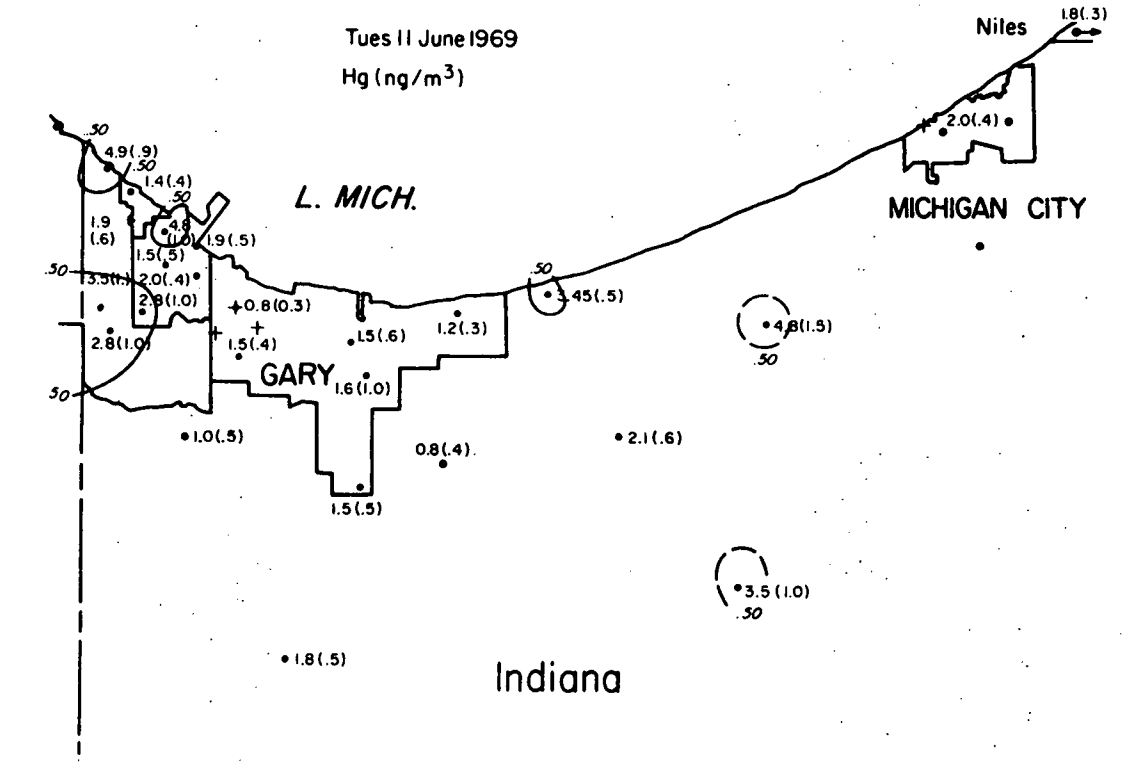

Figure VI-16 Concentration Distribution of Mercury

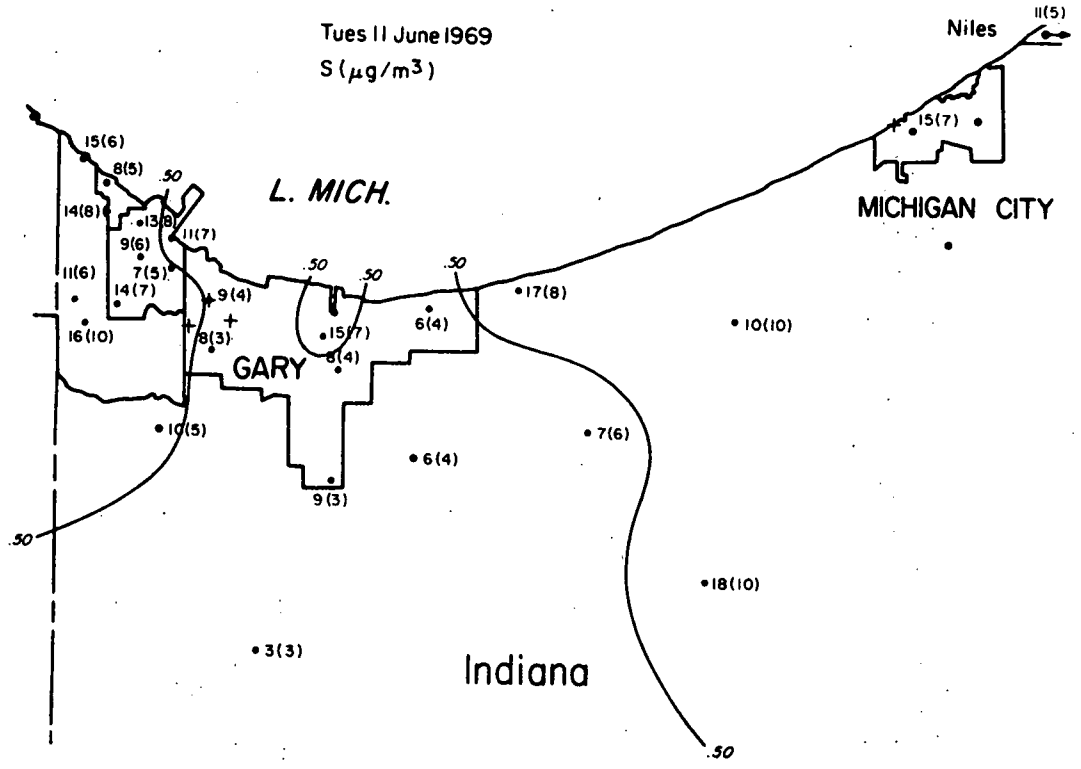

Figure VI-17 Concentration Distribution of Sulfur

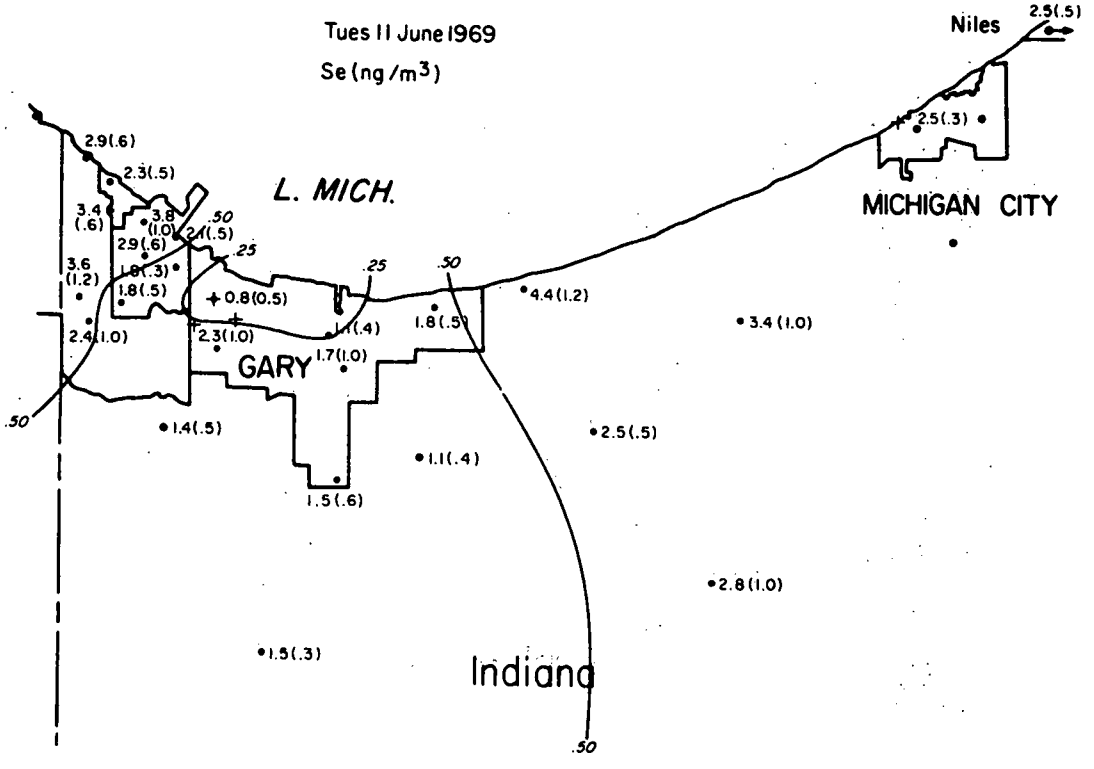

Figure VI-18 Concentration Distribution of Selenium

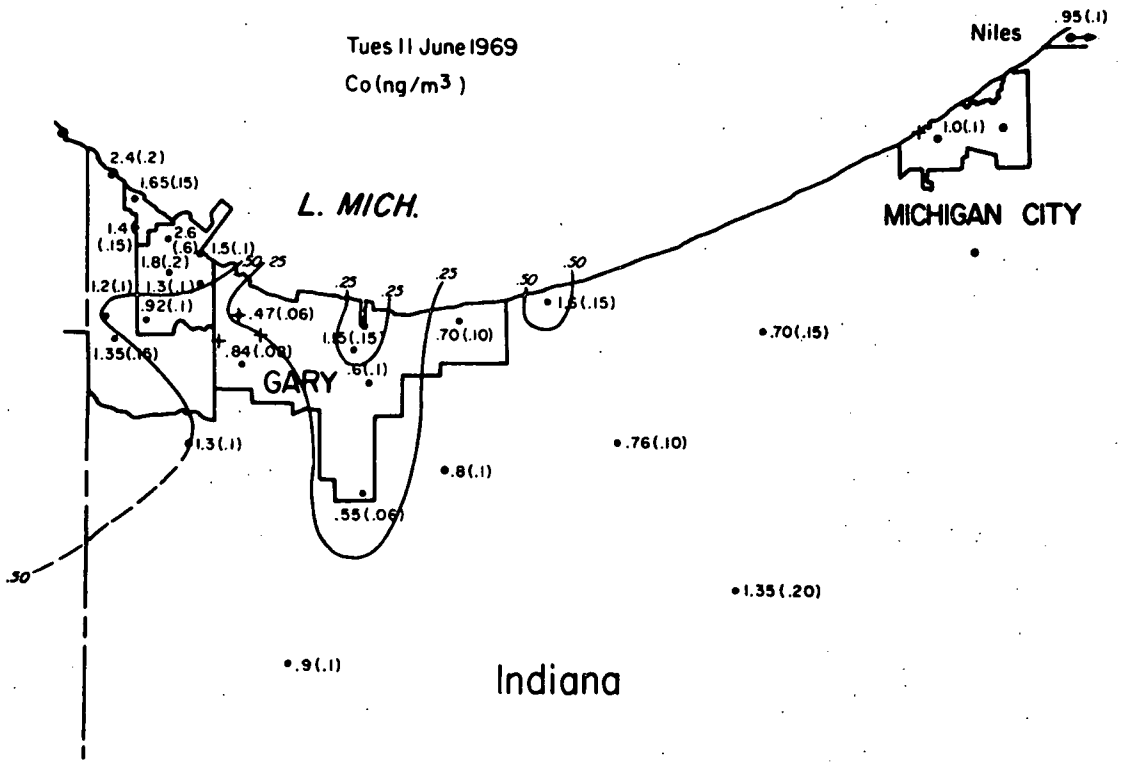

Figure VI-19 Concentration Distribution of Cobalt

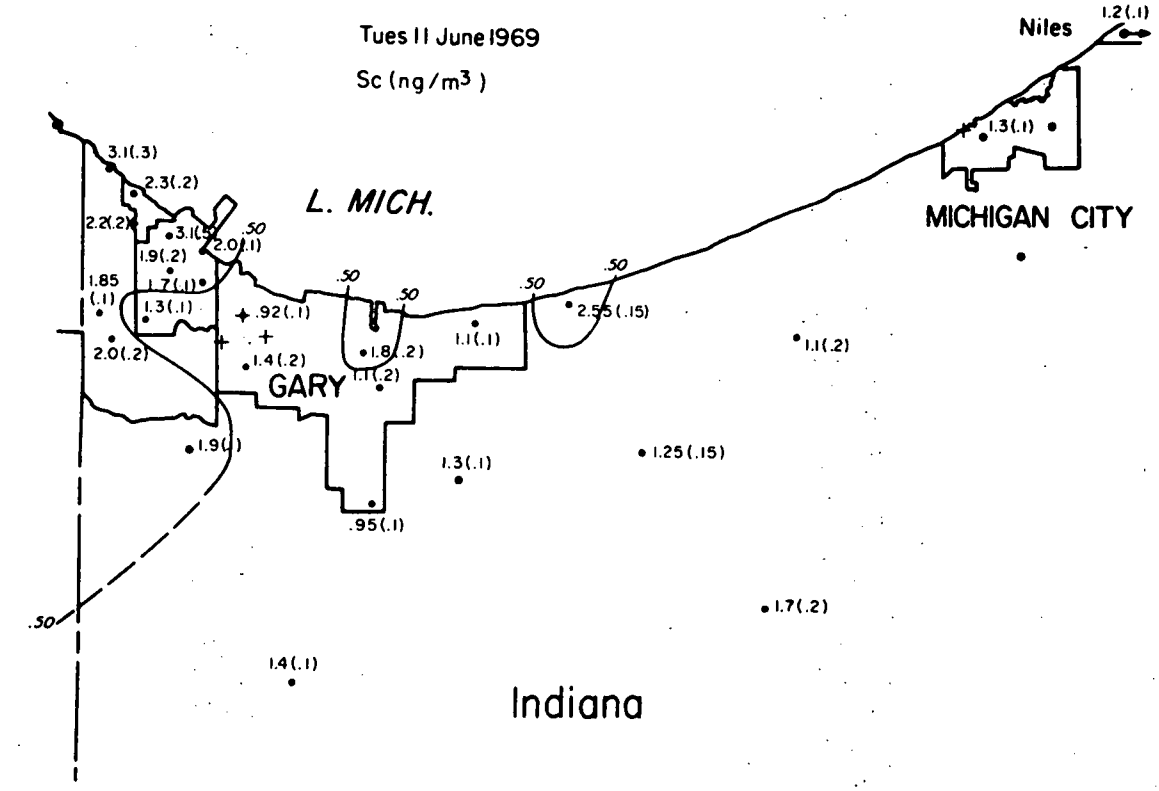

Figure VI-20 Concentration Distribution of Scandium

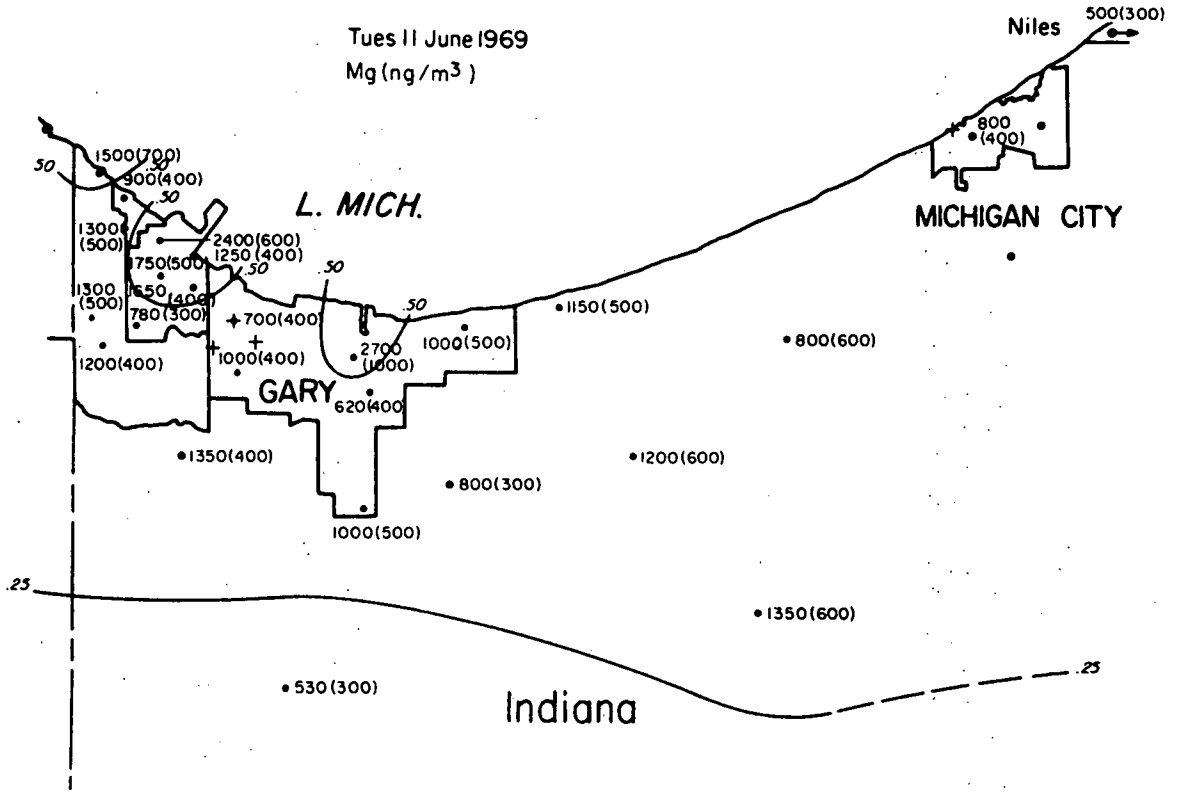

Figure VI-21 Concentration Distribution of Magnesium

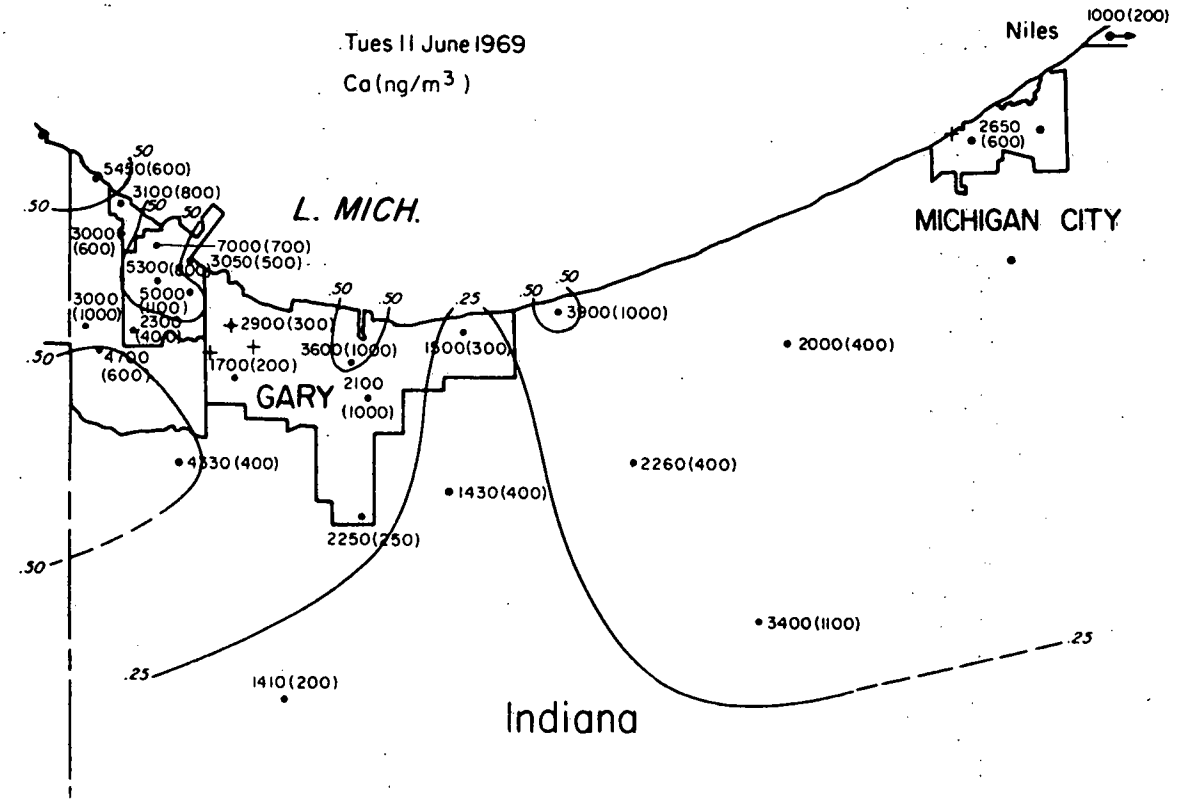

Figure VI-22 Concentration Distribution of Calcium

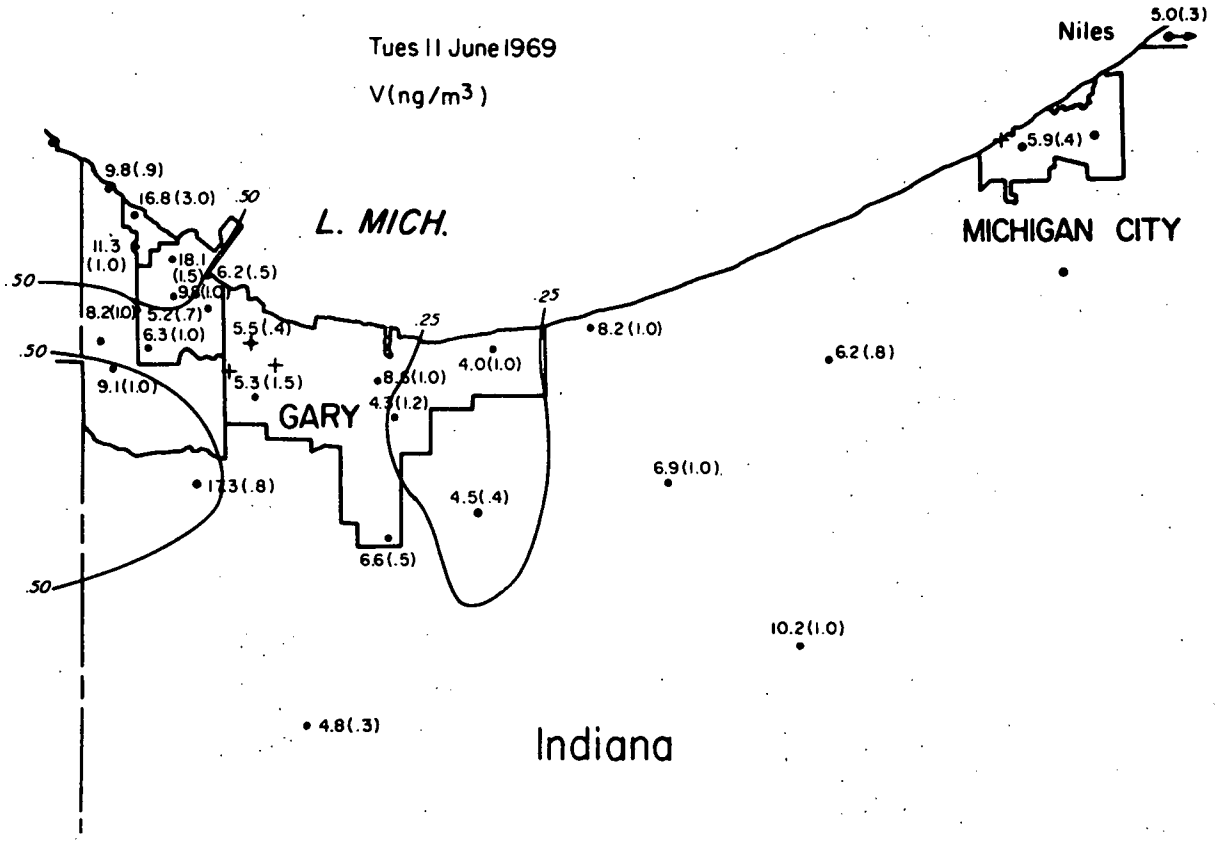

Figure VI-23 Concentration Distribution of Vanadium

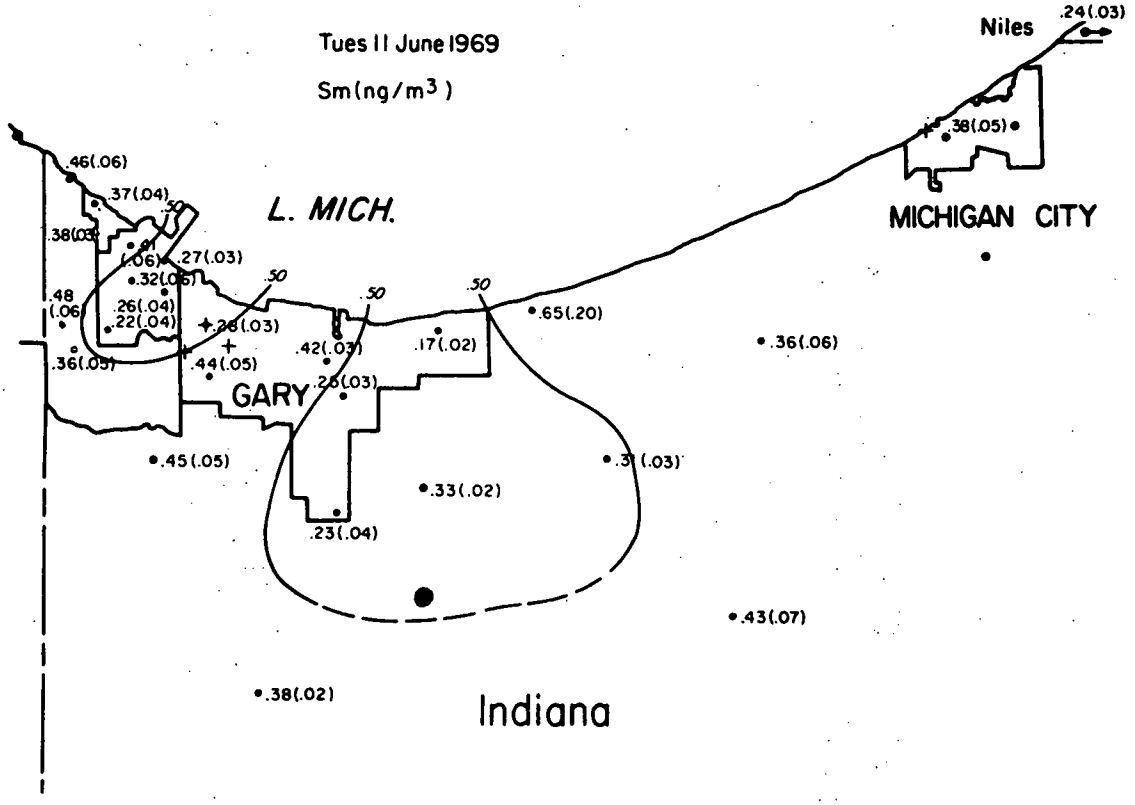

Figure VI-24 Concentration Distribution of Samarium

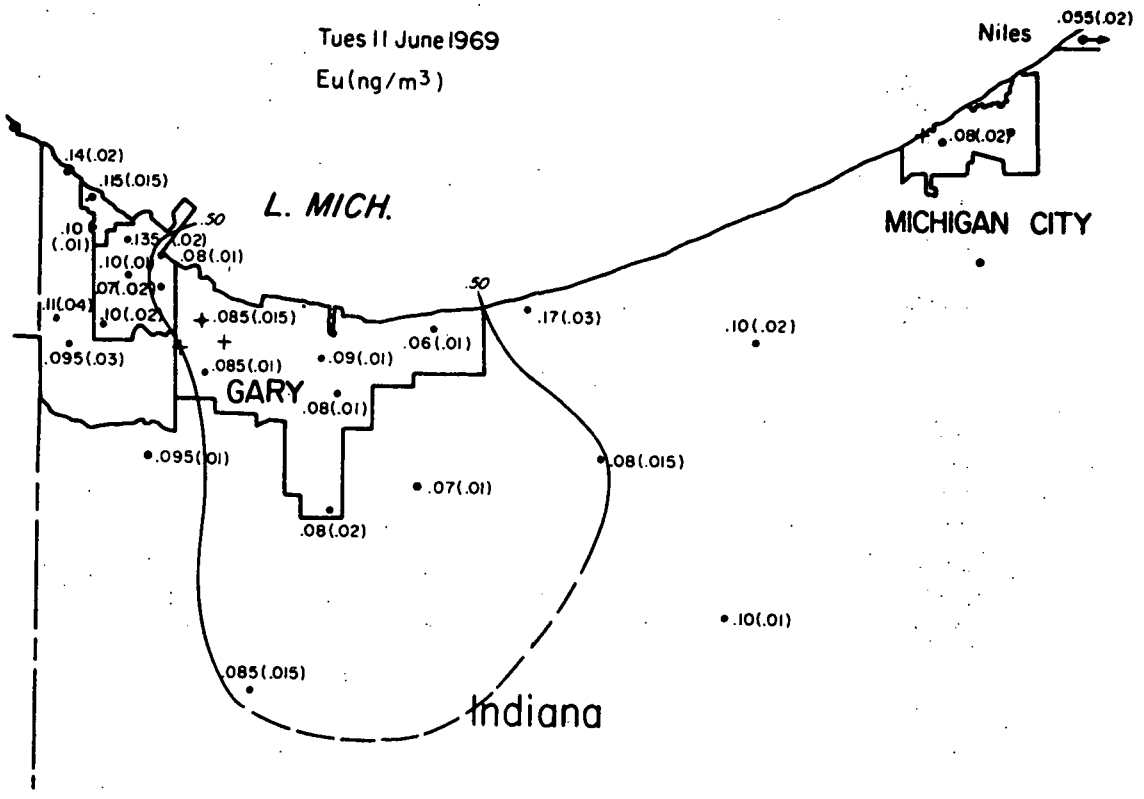

Figure VI-25 Concentration Distribution of Europium

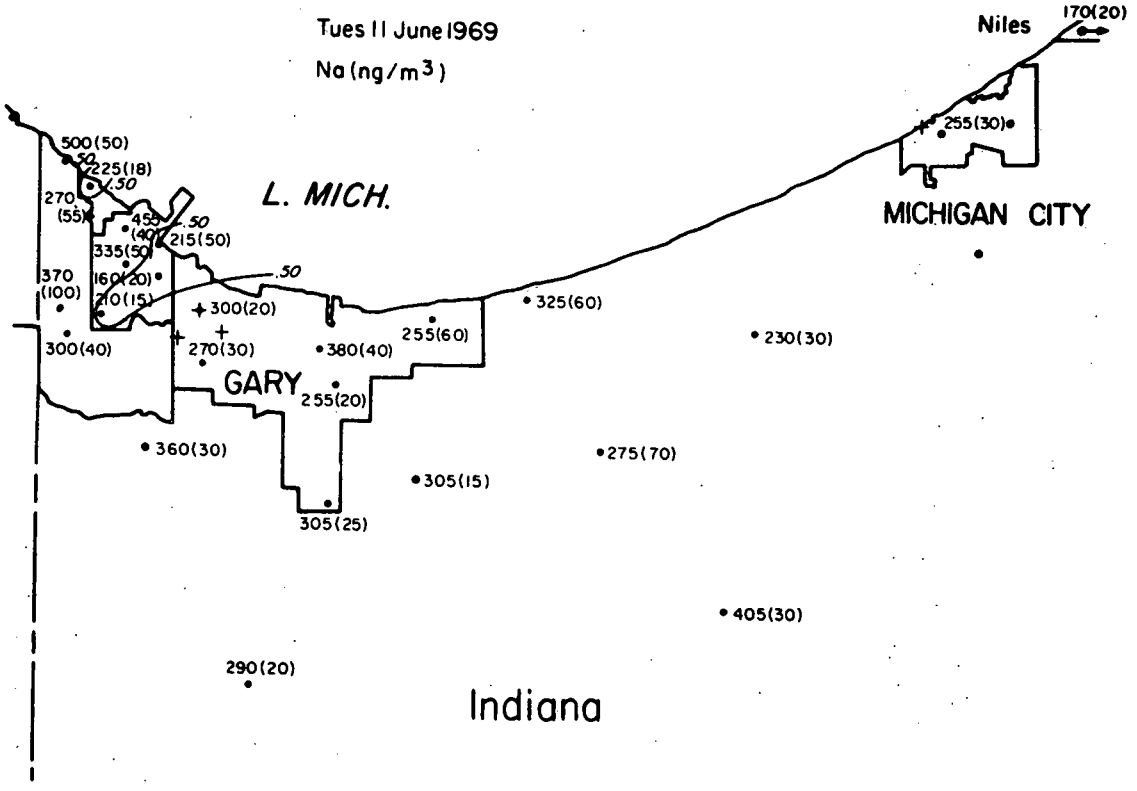

Figure VI-26 Concentration Distribution of Sodium

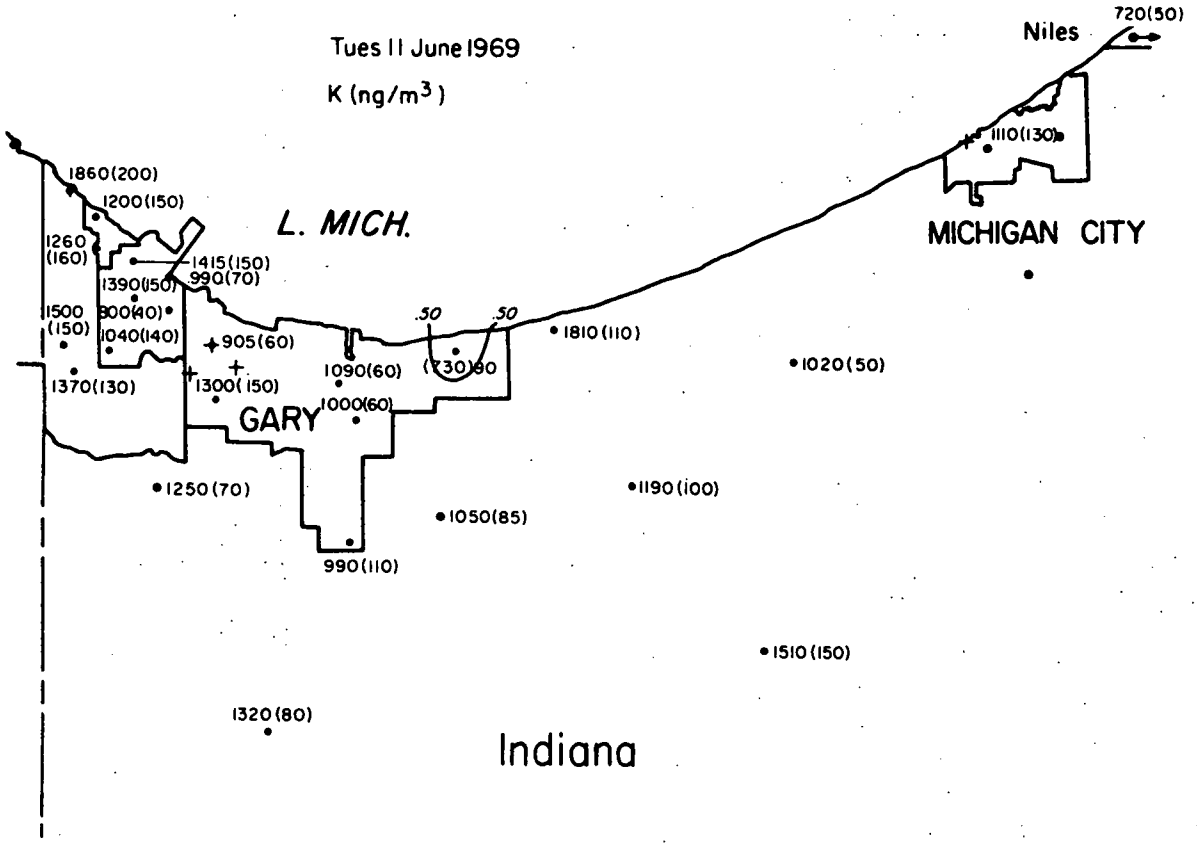

Figure VI-27 Concentration Distribution of Potassium

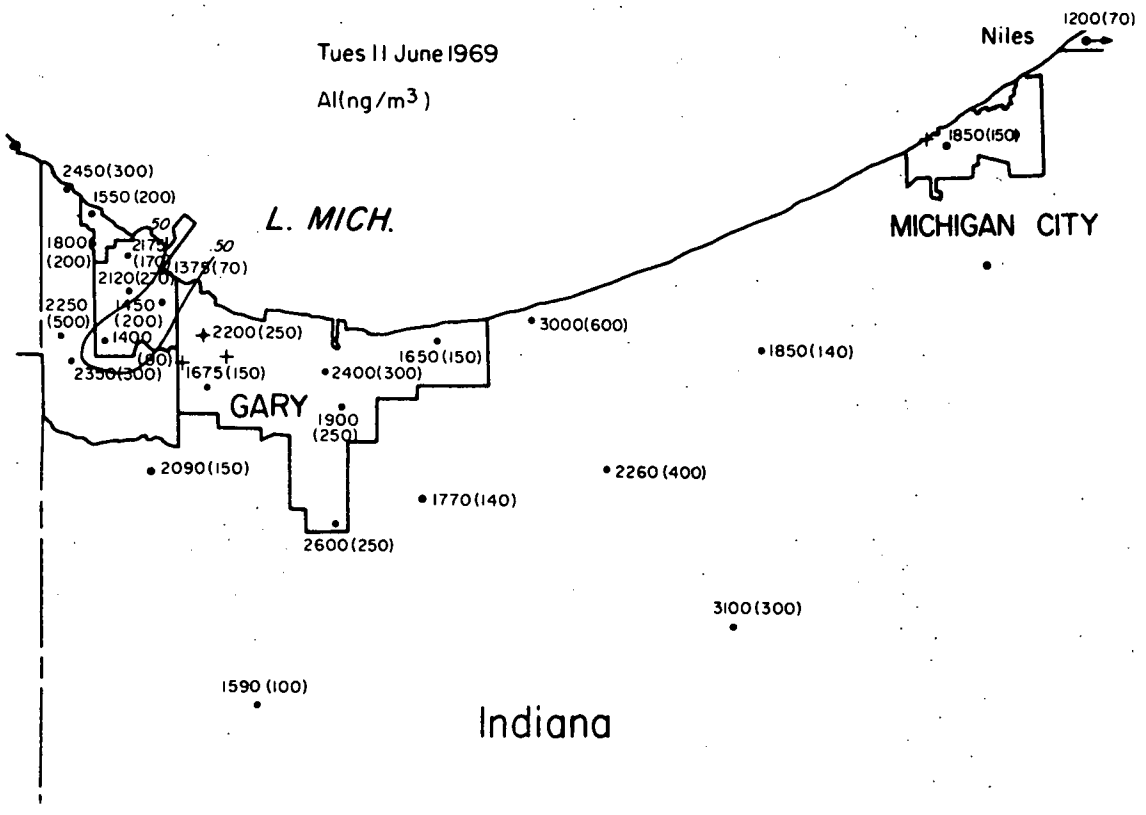

Figure VI-28 Concentration Distribution of Aluminum

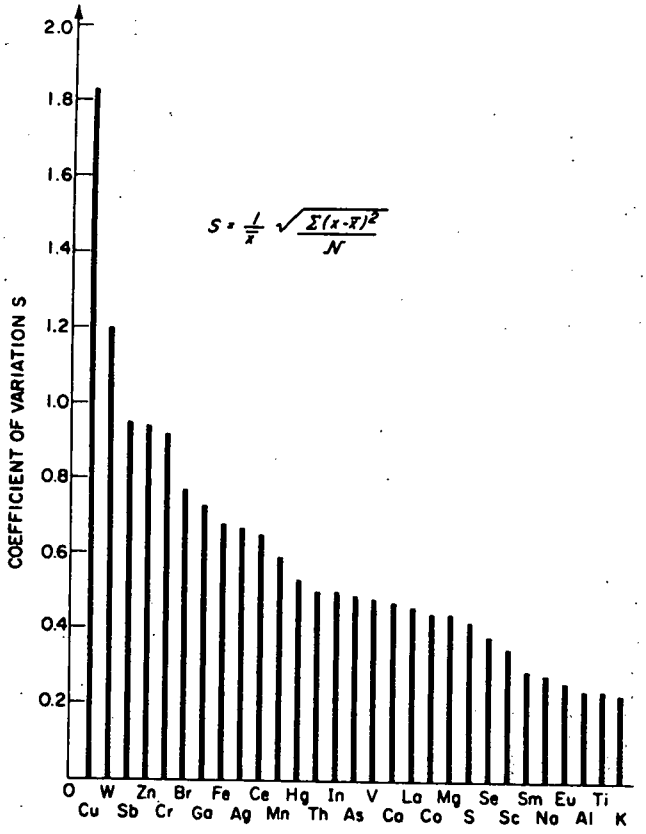

Figure VI-29 Coefficient of Variation

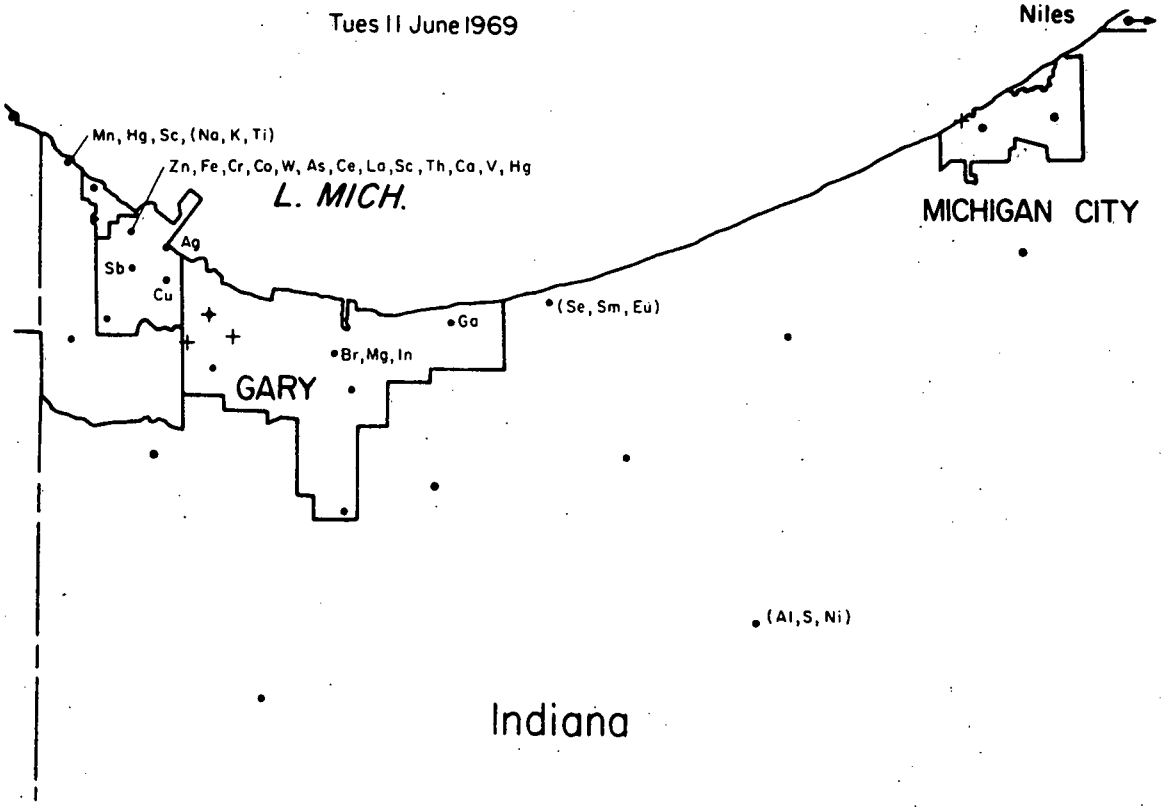

Figure VI-30 Locations of Maximum Concentrations of the Elements

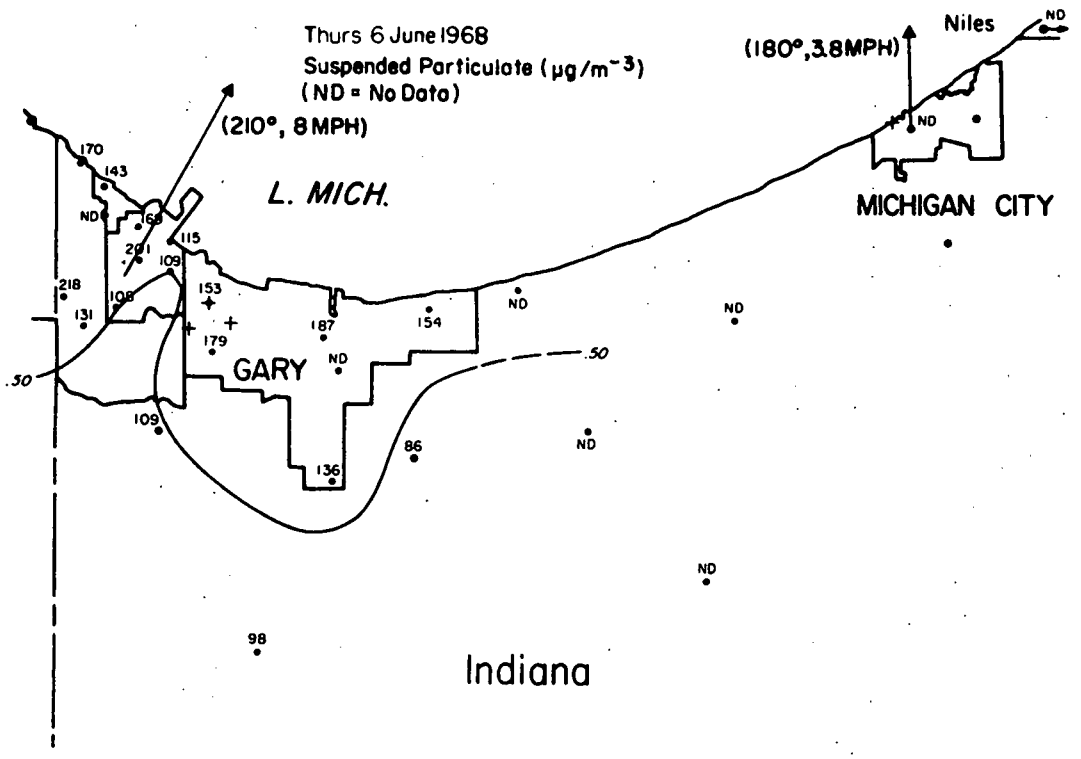

Figure VI-31 Concentration Distribution of Suspended Particulate and Wind Direction for 6 June 1968

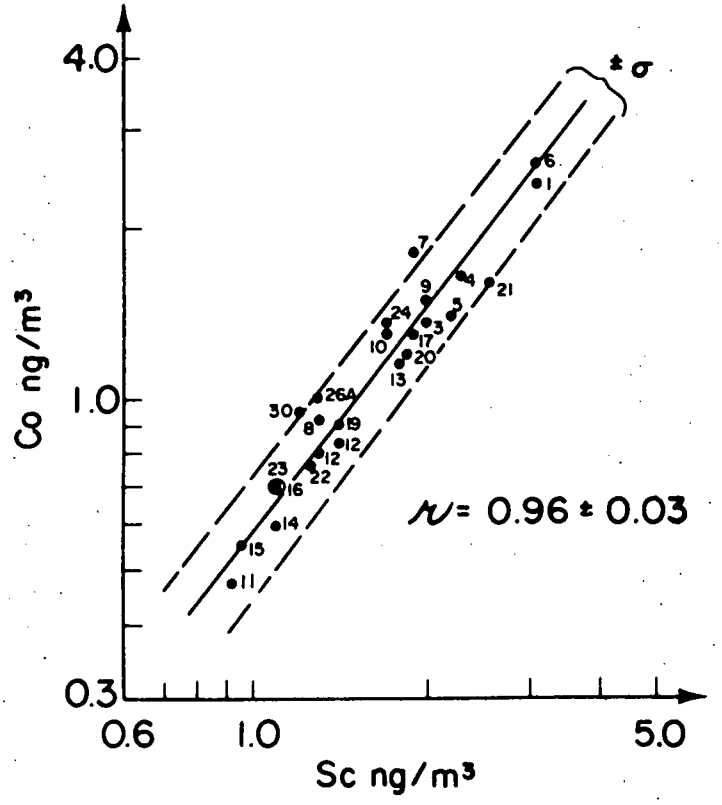

Figure VI-32 Concentration Correlation of Co/Sc Over All 25 Sampling Stations

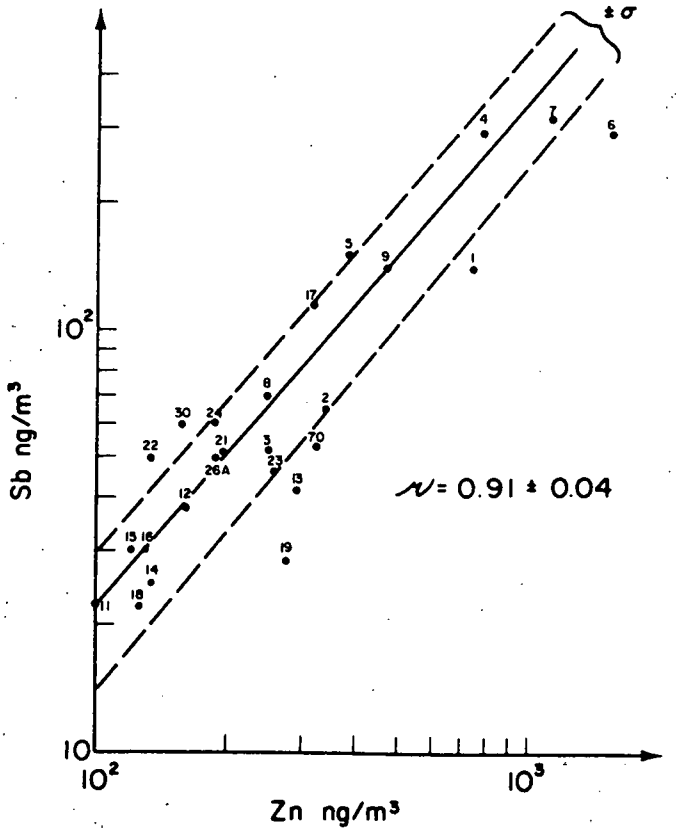

Figure VI-33 Concentration Correlation of Zn/Sb Over All 25 Sampling Stations

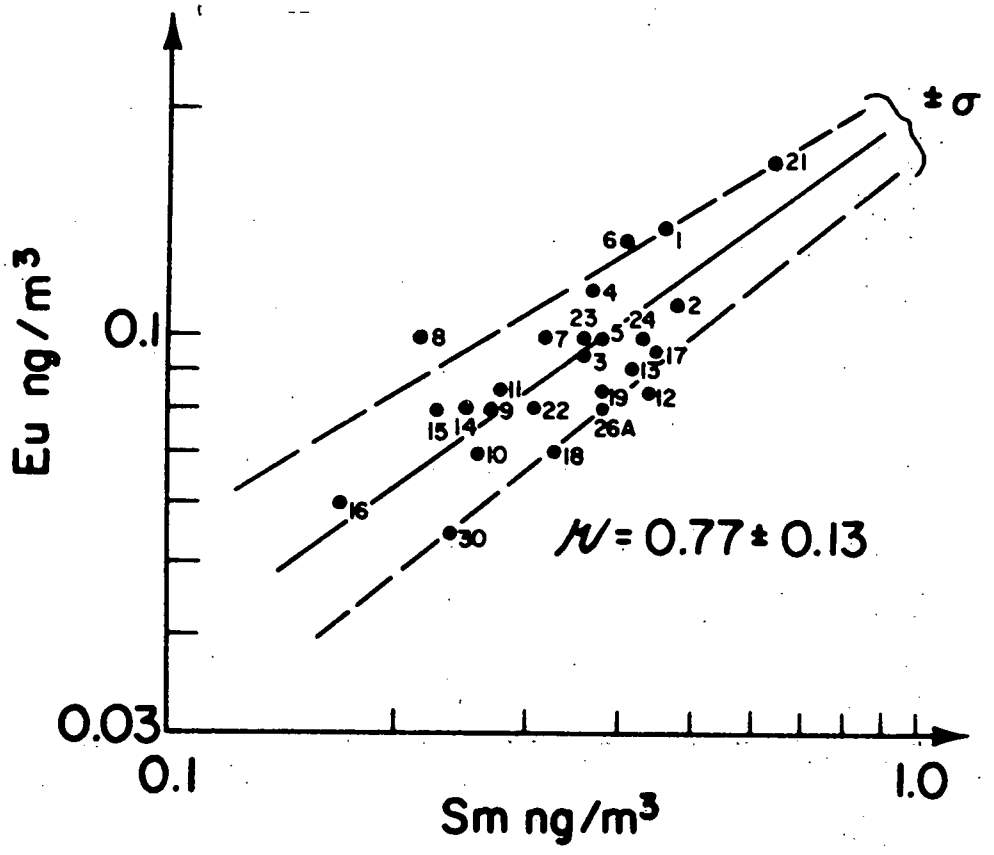

Figure VI-34 Concentration Correlation of Sm/Eu Over All 25 Sampling Stations

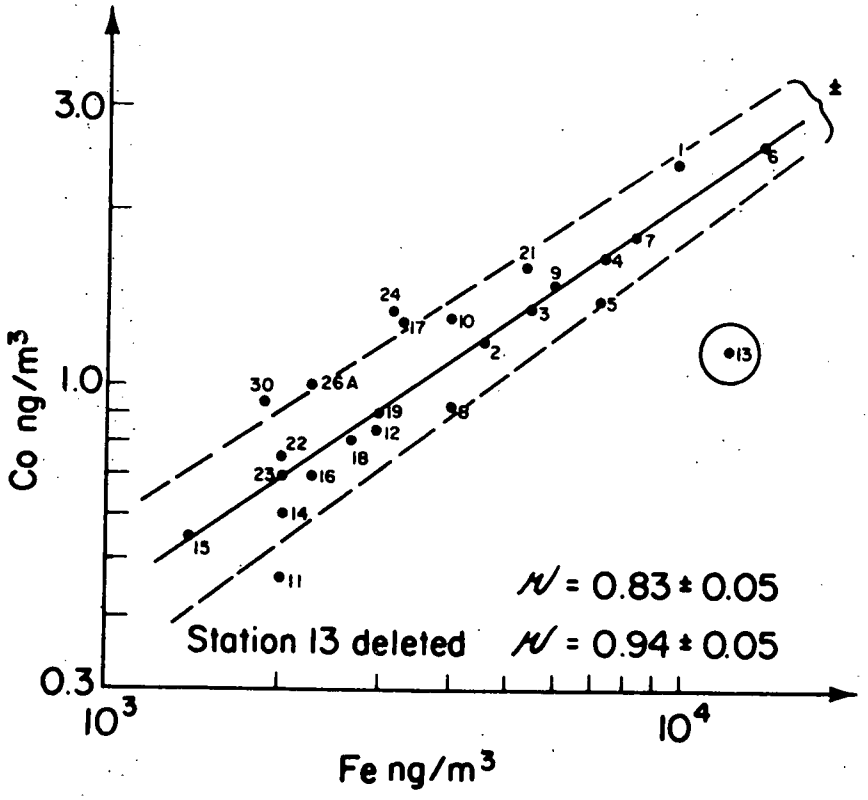

Figure VI-35 Concentration Correlation of Co/Fe Over 24 Sampling Stations, Station 13 Deleted

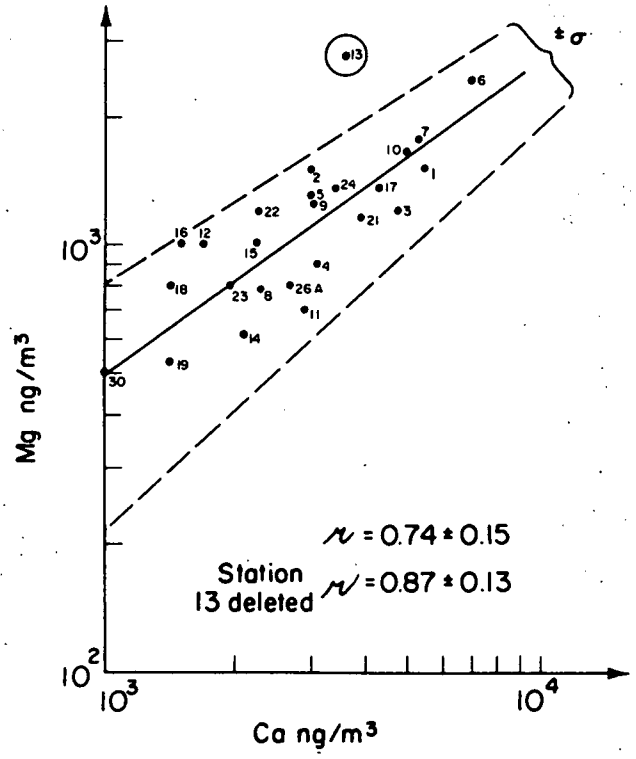

Figure VI-36 Concentration Correlation of Ca/Mg Over 24 Sampling Stations, Station 13 Deleted

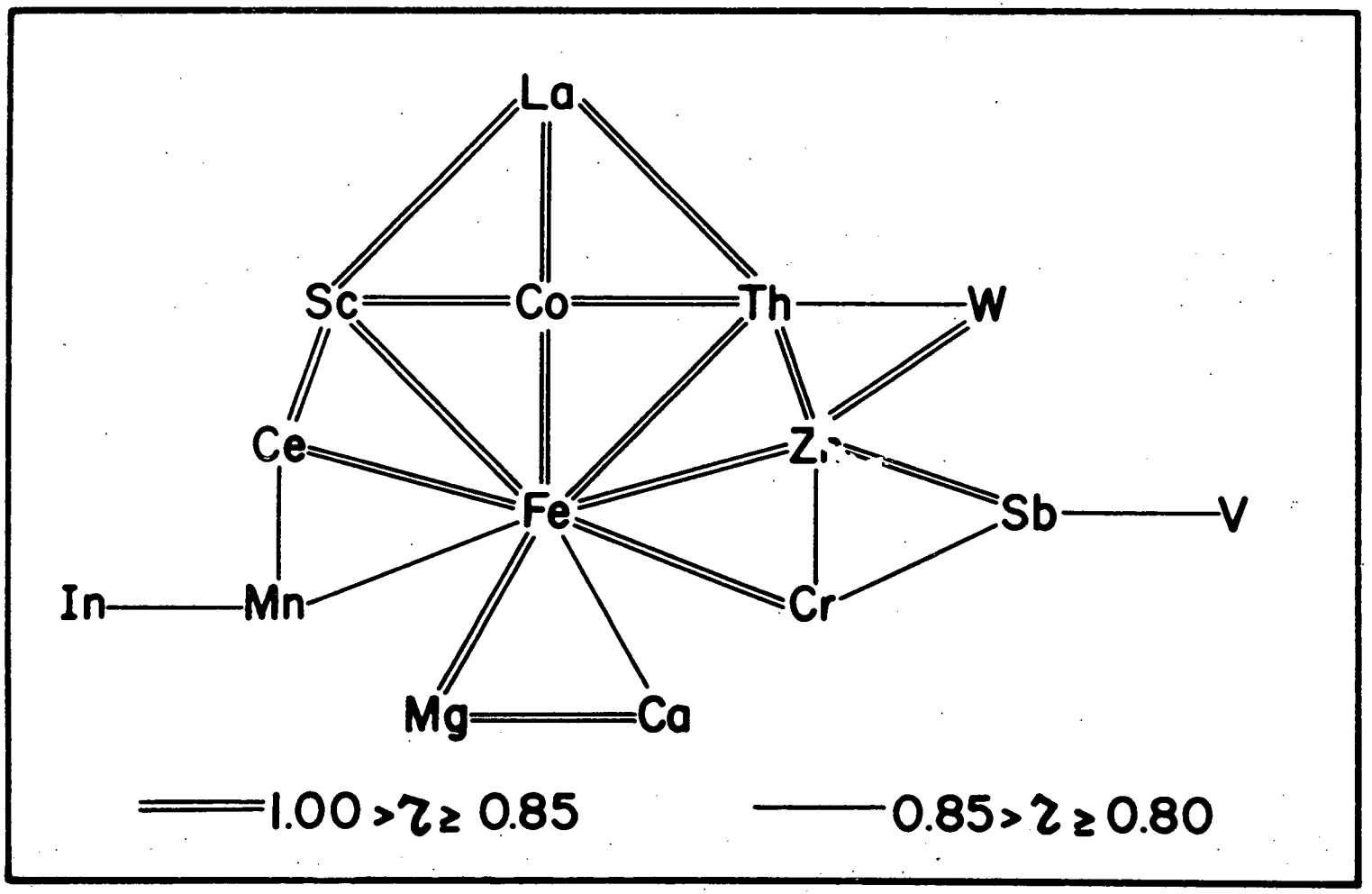

Figure VI-37 Map of Elemental Correlations Over 24 Sampling Stations,

Station 13 Deleted

CHAPTER VII

DIURNAL VARIATIONS I - NILES, MICHIGAN

A study of the diurnal concentration variations of atmospheric trace elements has recently been begun as part of a larger study of their general atmospheric behavior. Previous investigations of daily patterns of pollution concentrations have been both theoretical (Hewson, 1960; U.S. Department of Health, Education, and Welfare, 1965) and empirical (Commins, 1967; Munn, 1959; Summers, 1966; Weisman, 1969; U.S. Department of Health, Education, and Welfare, 1968) where in the latter cases soiling index, smoke, sulfur dioxide, nitrogen oxides and total particulate have served as indicators. To our knowledge, however, daily variations of individual trace elements have not yet been reported. Previous studies have all been in urban areas, whereas a rural setting was chosen for this investigation in an attempt to minimize the effects of source processes and urban micrometeorology relative to the mesometeorology.

This study was made possible by the recent development by the authors of a technique for nondestructive neutron activation analysis of aerosols collected on a high purity

*This work will be published in Atmospheric Environment under the authorship of K.A. Rahn, R. Dams, J.A. Robbins, and J.W. Winchester.

filter (Dams et al., 1970) in which up to 33 elements may be determined from 24-hour samples, many of which are recognized as being of pollution origin. Diurnal studies require sample lengths as short as possible, and the extreme sensitivity of this technique allows the determination of at least 15 elements in samples collected for as short a time as 90 minutes. In an effort to better correlate time variation patterns from element to element, particle size distributions were measured simultaneously.

Sampling

Sequential 90-minute filter samples were taken throughout the period, using a polystyrene material (Dams et al., 1971) which combines good filtering performance with reasonably high purity. A high flow rate per unit surface area was achieved through the combination of a high vacuum pump (Gelman twin cylinder) and 25 mm diameter filter holders. Such a system produces flow rates through the polystyrene of 12 $l\text{-}min^{-1}\text{-}cm^{-2}$, as opposed to the figure of 4.5 $l\text{-}min^{-1}\text{-}cm^{-2}$ obtained with a high volume sampler (20 x 25 cm filter and low vacuum pump). Each sample consisted of aerosols from approximately 4 m^3 of air.

Particle size distribution of the elements were determined by use of an Andersen Cascade Impactor, which separates aerosols into 7 fractions ranging from radii of roughly 8μm down to 0.1 μm. Highly pure polyethylene sheets were used as impaction

surfaces and analyzed in the same manner as the filters. A backup polystyrene filter (25 mm diameter) was used to catch the smaller particles. Because of the low flow rate of this instrument (28 $l\text{-}min^{-1}$) only one size distribution sample was taken throughout the experiment. All samples were taken in a ventilated instrument shelter 1.5 meters above ground, over short grass.

Sampling was performed in a rural area 5 km west of Niles, Michigan and 15 km north of South Bend, Indiana. It is approximately 45 km east of Lake Michigan and 100 km northeast of the heavily industrialized Northwest Indiana area. Samples were taken during 34 hours on 21 and 22 August, 1969, when the entire north central and northeastern U.S. was under the influence of a broad Canadian high pressure area. Winds during this period varied from calm at night to 6.5 m/sec during the afternoon, and the extreme stability of the air mass prevented any clouds from forming. Light ground fog was observed during the early morning hours of the second day. Figures VII-1 and VII-2 give some of the meteorological conditions recorded at ESSA WBAS South Bend, Indiana. Figures VII-3 and VII-4 show surface weather conditions for 7 AM EST on both sampling days.

Analysis

The technique as described earlier (Dams et al., 1970) was applied. The complete filter (25 mm diameter) or the

complete polyethylene sheet was irradiated twice with slow neutrons in the Ford Nuclear Reactor at The University of Michigan, first for 5 minutes, later for 4 hours. Each sample was counted 4 times, at 3 and 15 minutes after the first irradiation, and 20 hours and 20 days after the second irradiation. Counting was performed with a 30 cm^3 Ge(Li) high resolution gamma ray detector coupled to a 4096 channel pulse height analyzer. A digital computer program was used to integrate photopeaks of the sample, compare them with standard spectra, subtract blank values, calculate concentrations of the elements in air and standard deviations on the obtained results.

Results

The results are summarized in Table VII-1. They reveal that 15 elements could be determined in nearly all of the samples, namely Al, V, Br, Na, K, Mn, Ti, Sm, Eu, La, Sc, Zn, Fe, Co, and Cr. A half dozen others (Sb, As, Ga, Mg, Cu, and Ce) could only be determined in some samples. Due to their incompleteness the results for the latter 6 elements are not very useful and are not given in Table VII-1. The behavior of a number of representative elements is shown in Figure VII-5. Particle size distributions of 18 elements are summarized in Table VII-2 and 9 of of these are plotted in Figures 6 and 7. Standard deviations are given in parentheses. If high count rates were obtained these standard deviations may be as low as 10 percent. Because of the short sampling times the concentrations of several elements were at or near the limit of

detection, and standard deviations of these results are much higher. On some stages of the Andersen impactor only an upper limit could be set for the concentration of several elements.

Discussion

It is obvious that very large variations occur in the concentrations of several elements during a 24-hour period. The behavior of aluminum, shown in Figure VII-5, is representative of a number of other elements such as Ti, Mg, Sc and the rare earths, Sm, Eu, and La. Concentration variations by a factor of up to 10 occur within a few hours. A number of other elements such as Na, K, Fe, Co, and Cr show less prominent variations, on the order of 2.5 rather than 10. The behavior of Mn seems to be in between these two extreme groups.

How can this consistent behavior pattern for a large number of elements be understood? Smoke, SO_2, NO, NO_2, CO, total oxidants, total hydrocarbons and visibility measurements have also shown consistent diurnal patterns, but with average variations of at most a factor of three (Commins and Walter, 1967; Munn and Katz, 1959; Summers, 1966; Weisman et al., 1969; USPHS, 1968). Being urban measurements, these variations were mostly related to variations in local source processes and city ventilation. In the present case, one deals with a rural area, and measures primarily distant sources, and diurnal meteorological variations should thus be more important. The pattern found is indeed consistent with the predicted variations of ground-level concentrations from elevated sources (HEW, 1965).

With the previous considerations in mind the following tentative explanation is offered. Particulate pollutants released at stack height during the fair weather nocturnal temperature inversion conditions tend to remain at stack height until after sunrise. Daylight hours bring ground heating and generation of turbulent motions which build rapidly upwards until the pollutant layer is reached some one to three hours after sunrise. Eddy transport of these pollutants to the surface (Hewson fumigation type I) causes the steep morning peak. Continued increase of the maximum mixing level until the midafternoon further dilutes concentrations, after which the lowering mixing level and increasing thermal stability initiates the gradual concentration increase of late afternoon and early evening.

The concentration levels of evening, being effectively cut off from elevated sources by the temperature inversion, might be expected to decrease slightly during the night. Instead, they are in most cases observed to drop rapidly during the early morning hours, often reaching the lowest levels of the sampling period. Our hypothesis is that local ground fog at the sampling site was the primary agent responsible for this decrease, due to fog droplet nucleation, probably predominantly by the giant particle component of the aerosol population, followed by enhanced sedimentation and/or impaction of the enlarged droplets. Though fog was not recorded at the more urban South Bend Airport, the temperature there decreased to within

two degrees of the dewpoint, and the relative humidity reached a maximum of 93 percent at the 4 AM and 8 AM observations (Figure VII-1).

Confirmation of this idea comes from the observation that in general those elements showing the largest concentration variations share two characteristics, namely relatively deep morning minima and masses concentrated on larger particles. This relation can be verified from the plots of Al and V, and is also noted for Ti, Mg, Sc, La, Eu, and Sm. On the other hand, elements like Na, K, Cr, Co, and Mn, showing smaller diurnal variations, are more equally distributed over the 0.1 to 10 μm size range.

We then visualize the fog formation as involving the larger and more soluble aerosols (i.e., those orindarily collected on the first stages of the impactor), rapidly growing to a quasi-equilibrium radius of some 5 to 10 μm. Because the droplet concentration in typical fogs (100-500 cm^{-3}) is large relative to the giant aerosol number density in continental aerosols (1 cm^{-3}) (Junge, 1963) but small relative to the large particle component of the same (1000 cm^{-3}), it is possible that a majority of the giant particles and a minority of the large particles served as nucleating agents. Removal of these droplets would preferentially decrease concentrations of those elements primarily in giant aerosols.

Certain of the observed elements show diurnal patterns suggestive of local sources. Br is the clearest example, the

probable source being automotive exhaust from the road some 50 meters distant. Distinct traffic maxima are observed about 6-7 AM, 3-5 PM, and 11-12 PM, very nearly the time of Br maxima. Further evidence comes from the measured particle size distribution of Br, where 65 percent of its mass is found on the backup filter (Table VII-2). This is in agreement with the very small, condensation aerosol nature of auto exhausts, and indicates the fresh nature of most of the Br (Loucks and Winchester, 1970).

The diurnal variation of Zn is not very consistent with the other elements, which may be partially due to the low quality of the analytical results for this element. It may however also be correlated with its predominant distribution on small particles, probably due to formation via a condensation process.

The steep morning peak makes th V pattern somewhat different from those of the other elements. The most important source of V is known to be fuel oils, but because of the August date this does not seem to provide a sufficient explanation. Heating of commercial establishments may be related to the steep morning peak, however. In addition, a considerable fraction (30 percent) of this element is found on the very small particles, pointing toward a condensation formation process and recent age for its Aitken component.

Conclusion

The obtained results demonstrate that nondestructive neutron activation analysis can very favorably be applied to the study of diurnal variations of trace elements in the atmosphere. The 15 elements which can be measured after sampling times as short as 90 minutes in a rural area show distinct variations in diurnal behavior and should be indicators enough for the behavior of most other trace elements. It seems that the application of this technique in studies of simultaneously measured total concentration variations and particle size distribution of airborne particulates should lead to significant advances in the understanding of source processes and identification of dilution and removal mechanisms. The observed size distribution patterns remote from the source may not only reflect differing source processes but may also result in a tendency toward different atmospheric behavior patterns. This specific investigation was, however, only of an exploratory nature and further experiments under different meteorological conditions are under way in order to expand upon the tentative conclusions reported here.

TABLE VII-1. Diurnal Behavior of Fifteen Elements

Begin Sampling Time Total Sampling Time	ng/m^3 Element					
	8 h 10 80 min	9 h 30 90 min	11 h 00 90 min	12 h 30 90 min	14 h 00 90 min	15 h 30 90 min
10^{-3}xAl	2.9(.3)	1.9(.2)	2.1(.2)	0.65(.07)	0.88(.09)	1.1(.1)
V	11(1)	8.8(.9)	6.2(.7)	1.7(.3)	2.6(.3)	2.0(.4)
Br	160(16)	105(11)	77(8)	48(5)	160(16)	125(12)
Na	540(50)	310(57)	580(50)	300(30)	300(60)	280(55)
K	---	840(80)	1040(100)	460(50)	550(50)	650(60)
Mn	64(6)	31(3)	49(5)	20(2)	29(3)	27(3)
Ti	260(75)	185(60)	73(65)	67(45)	<47	39(50)
Sm	---	0.30(.04)	0.30(.03)	0.055(.025)	0.15(.04)	0.22(.03)
Eu	---	0.045(.02)	0.07(.02)	<0.02	0.05(.02)	0.025(.015)
La	---	1.7(.4)	2.1(.4)	0.5(.35)	1.0(.3)	1.5(.35)
Sc	---	1.4(.3)	2.4(.4)	0.45(.20)	0.45(.20)	1.1(.3)
Zn	---	150(40)	50(50)	95(35)	65(30)	90(30)
10^{-3}xFe	---	2.1(.6)	3.0(.6)	<0.9	1.6(.6)	1.1(.6)
Co	---	1(.8)	2(.81)	0.8(.8)	0.8(.8)	1.1(.8)
Cr	---	35(10)	25(10)	24(10)	12(10)	29(10)

TABLE VII-1 (cont'd)

Begin Sampling Time Total Sampling Time	ng/m^3 of Element					
	17 h 00 90 min	18 h 30 90 min	20 h 00 90 min	21 h 30 90 min	23 h 00 90 min	0 h 30 90 min
10^{-3}xAl	1.6(.2)	1.9(.2)	2.1(.2)	1.2(.1)	1.6(.2)	1.2(.1)
V	3.5(.4)	4.5(.5)	4.7(.5)	3.0(.5)	3.9(.6)	2.4(.5)
Br	44(5)	122(12)	121(12)	89(9)	340(34)	231(23)
Na	290(30)	320(45)	405(40)	230(50)	320(40)	345(35)
K	940(90)	560(60)	900(90)	650(60)	690(70)	640(60)
Mn	41(4)	51(5)	61(6)	51(5)	75(7)	46(5)
Ti	72(50)	155(50)	75(55)	130(55)	140(65)	150(55)
Sm	0.25(.03)	0.17(.03)	0.33(.03)	0.33(.035)	0.16(.035)	0.27(.03)
Eu	0.035(.015)	0.04(.015)	0.05(.02)	0.08(.015)	0.035(.015)	0.03(.015)
La	2.1(.35)	3.8(.4)	1.9(.3)	1.2(.3)	1.6(.3)	0.8(.3)
Sc	1.4(.3)	1.1(.3)	1.4(.3)	1.35(.3)	1.4(.3)	1.2(.3)
Zn	<50	85(30)	130(40)	220(30)	130(40)	60(40)
10^{-3}xFe	1.3(.5)	1.7(.6)	1.0(.6)	1.9(.6)	1.7(.6)	1.8(.6)
Co	1.0(.8)	1.4(.8)	1.1(.8)	1.2(.8)	0.6(.8)	0.8(.8)
Cr	25(10)	27(10)	29(8)	15(10)	37(10)	18(8)

TABLE VII-1 (cont'd)

Begin Sampling Time Total Sampling Time	ng/m^3 Element					
	2 h oo 90 min	3 h 30 90 min	5 h 00 90 min	6 h 30 90 min	8 h 00 90 min	9 h 00 90 min
10^{-3}x Al	0.56(.06)	0.39(.04)	0.51(.05)	1.3(.1)	1.8(.2)	1.3(.1)
V	2.0(.4)	1.25(.4)	1.9(.4)	6.8(.7)	15.8(1.6)	3.5(.4)
Br	91(9)	61(6)	34(4)	970(90)	120(12)	53(5)
Na	215(45)	150(50)	160(21)	230(55)	340(60)	190(21)
K	430(40)	410(40)	330(30)	600(60)	860(80)	370(40)
Mn	30(4)	28(4)	27(4)	32(3)	46(3)	40(5)
Ti	<34	<42	<30	185(75)	145(60)	78(38)
Sm	0.12(.03)	0.12(.03)	0.16(.02)	0.33(.07)	0.39(.04)	0.21(.03)
Eu	0.02(.01)	0.025(.015)	0.02(.01)	0.09(.02)	0.075(.02)	0.04(.01)
La	1.2(.25)	0.3(.3)	0.7(.2)	1.1(.3)	1.7(.3)	0.8(.25)
Sc	0.50(.20)	0.90(.20)	0.35(.20)	1.1(.3)	1.3(.3)	1.3(.3)
Zn	100(30)	150(30)	75(30)	100(30)	150(30)	55(25)
10^{-3}x Fe	0.9(.6)	1.3(.7)	0.5(.5)	1.9(.7)	1.3(.7)	0.9(.5)
Co	<0.7	0.8(.7)	0.5(1.0)	1.2(.8)	1.3(.8)	0.7(.8)
Cr	13(8)	30(10)	14(7)	21(10)	17(10)	12(8)

TABLE VII-1 (cont'd)

Begin Sampling Time / Total Sampling Time	ng/m^3 of Element					
	11 h 00 90 min	12 h 30 90 min	14 h 00 90 min	15 h 30 90 min	17 h 00 90 min	8 h 10 34h 20 min
10^{-3}xAl	0.93(.09)	1.4(.1)	1.4(.1)	1.5(.1)	2.6(.3)	1.6(.2)
V	31(.5)	3.0(.5)	2.9(.5)	4.2(.6)	5.0(.7)	5.1(.5)
Br	36(7)	36(7)	47(6)	52(8)	59(9)	141(14)
Na	360(60)	330(50)	390(40)	360(70)	480(60)	330(35)
K	690(60)	670(60)	730(70)	740(70)	810(80)	630(60)
Mn	35(4)	38(40)	71(7)	106(11)	74(11)	53(5)
Ti	125(60)	<48	68(50)	82(68)	78(68)	240(35)
Sm	0.16(.03)	0.10(.03)	0.22(.03)	0.39(.03)	0.20(.03)	0.165(.02)
Eu	0.06(.015)	0.035(.015)	0.04(.015)	0.04(.015)	0.035(.015)	0.035(.015)
La	0.5(.3)	0.3(.3)	0.8(.3)	3.0(.4)	1.1(.3)	1.25(.2)
Sc	0.9(.25)	0.7(.25)	0.8(.25)	0.7(.25)	0.8(.25)	0.9(.25)
Zn	140(40)	<60	120(30)	80(30)	130(30)	120(30)
10^{-3}xFe	0.9(.5)	<0.6	1.1(.5)	1.5(.5)	1.0(.5)	1.2(.4)
Cr	24(8)	24(8)	20(7)	23(9)	25(9)	21(7)
Co	<0.8	<0.8	<0.9	<0.8	<0.8	0.7(.5)

TABLE VII - 2. Particle Size Distributions of Eighteen Elements (ng/m^3)

Element	Backup Filter	Stage-Andersen			
		7	6	5	4
Al	100(10)	25(2.5)	71(7)	106(10)	405(40)
V	0.75(.07)	0.11(.03)	0.077(.033)	0.16(.04)	0.38(.07)
Br	63(6)	6.4(.6)	2.3(.5)	4.3(.6)	5.2(.6)
Cl	---	<11	<10	<10	14(4)
Na	46(5)	9.1(1.6)	14(2)	20(2.5)	18(2.5)
K	38(4)	22(2)	13(1.5)	24(2.5)	39(4)
Mg	<80	37(35)	35(33)	42(30)	120(40)
Mn	9.0(.9)	5.8(.6)	3.5(.3)	2.3(.2)	2.7(.3)
Ti	14(7)	<3	<6	<8	6(6)
Sm	---	0.0015(.0015)	0.002(.001)	0.01(.002)	0.02(.002)
Eu	---	0.001(.001)	0.0008(.0008)	0.0035(.001)	0.005(.001)
La	---	0.01(.01	0.01(.01)	0.05(.03)	0.09(.02)
Ce	<0.5	<0.5	<0.5	<0.5	0.75(.4)
Sc	0.02(.01)	0.01(.01)	0.01(.01)	0.06(.02)	0.12(.02)
Zn	26(5)	12(2)	10(2)	7.5(2)	3.5(2)
Co	0.08(.08)	0.06(.06)	0.06(.06)	<0.08	<0.08
Cr	2(1)	2.3(.8)	3.1(.8)	1.2(.6)	0.6(.6)
Ga	---	0.08(.05)	0.04(.04)	0.05(.04)	0.10(.04)

TABLE VII-2 (continued)

Element	Backup Filter	Stage-Andersen		
		3	2	1
Al	100(10)	532(55)	438(45)	417(42)
V	0.75(.07)	0.39(.07)	0.44(.07)	0.58(.07)
Br	63(6)	8.5(1.0)	3.7(.5)	2.1(.5)
Cl	---	24(5)	28(5)	28(5)
Na	46(5)	21(2.5)	30(4)	49(5)
K	38(4)	99(10)	92(9)	154(15)
Mg	80	110(48)	190(50)	220(56)
Mn	9.0(.9)	6.4(.6)	5.1(.5)	7.9(.8)
Ti	14(7)	7(7)	18(7)	13(7)
Sm	---	0.04(.004)	0.035(.003)	0.05(.005)
Eu	---	0.008(.001)	0.008(.001)	0.01(.0015)
La	---	0.19(.02)	0.14(.03)	0.27(.03)
Ce	0.5	0.5(.4)	0.6(.4)	1.1(.4)
Sc	0.02(.01)	0.3(.04)	0.2(.04)	0.3(.04)
Zn	26(5)	<2	<2	<2.6
Co	0.08(.08)	0.08(.08)	0.16(.10)	<0.08
Cr	2(1)	0.8(.8)	1.3(.8)	1.3(.8)
Ga	---	0.12(.06)	0.13(.05)	0.16(.05)

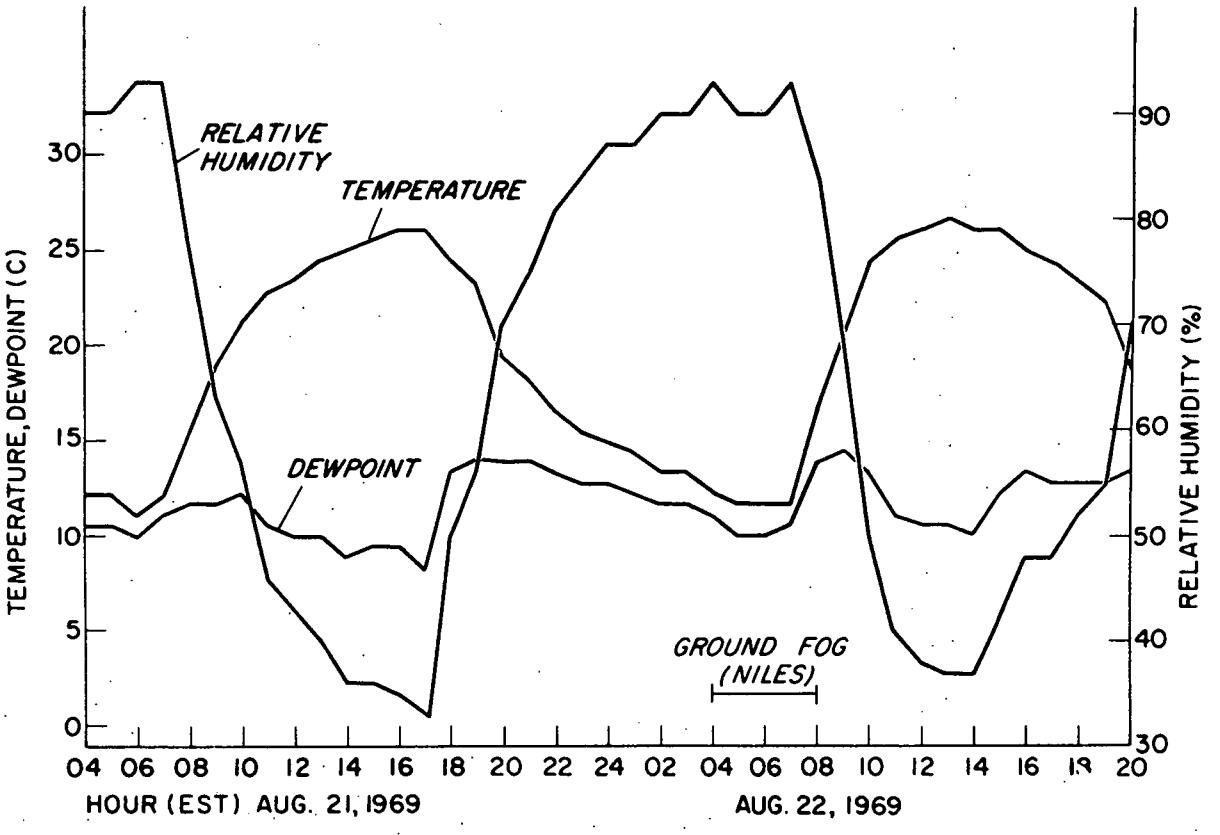

Figure VII-1 Relative Humidity, Temperature, and Dewpoint During Sampling

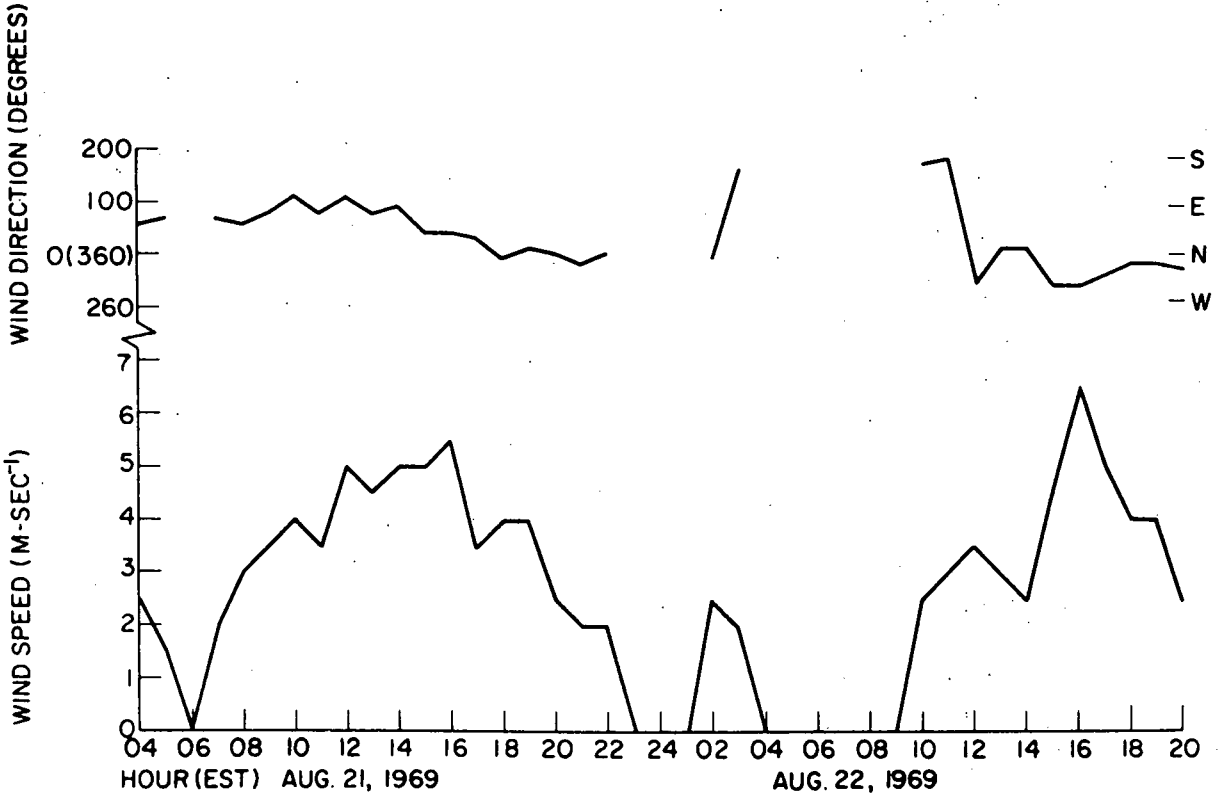

Figure VII-2 Wind Speed and Direction During Sampling

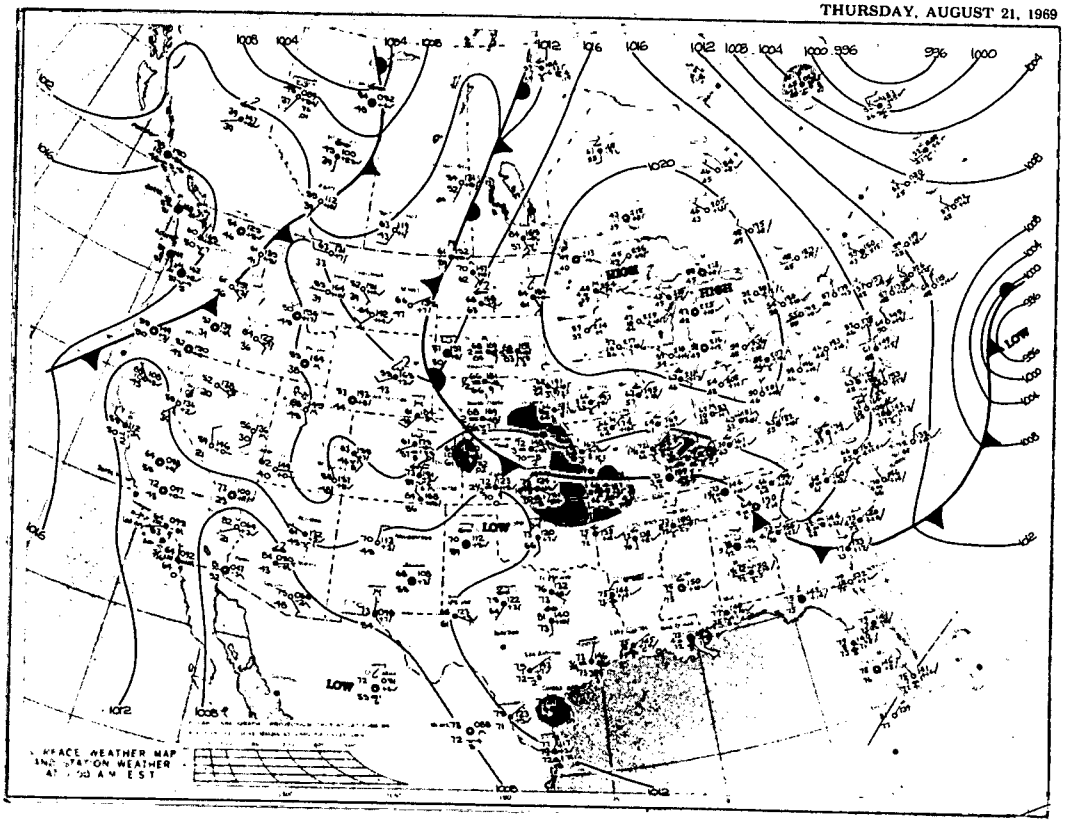

Figure VII-3 Surface Weather Map at 0700 EST 21 August 1969

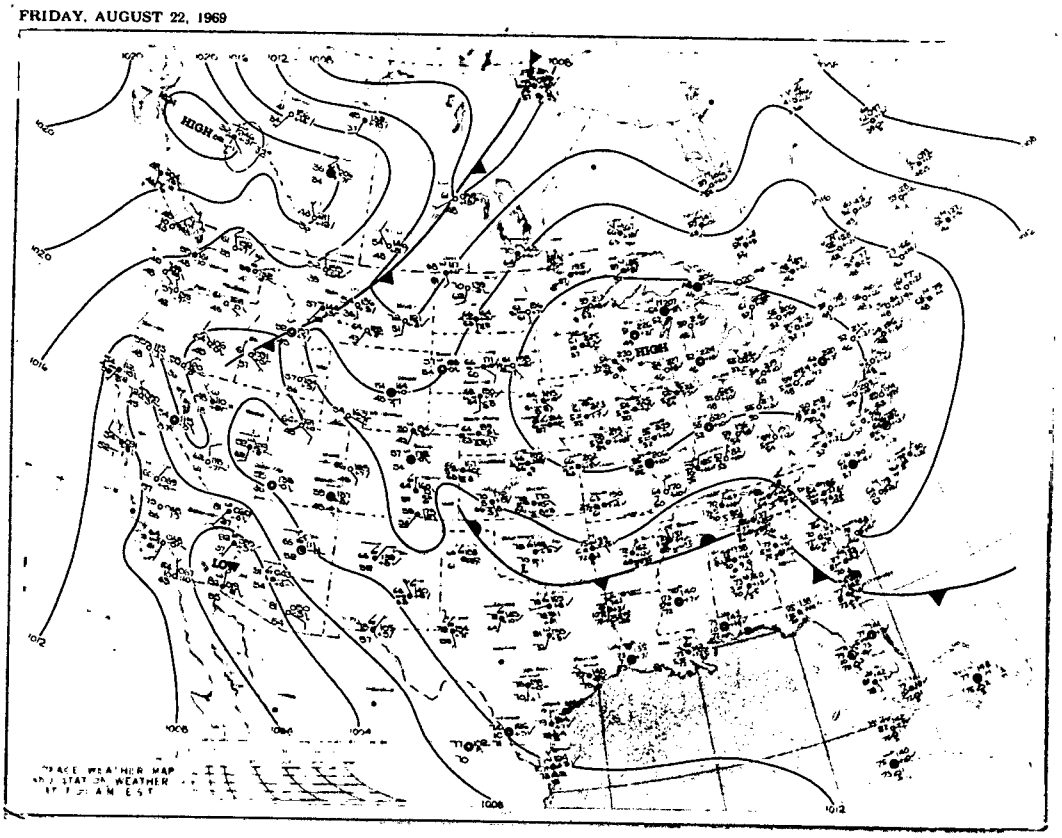

Figure VII-4 Surface Weather Map at 0700 EST 22 August 1969

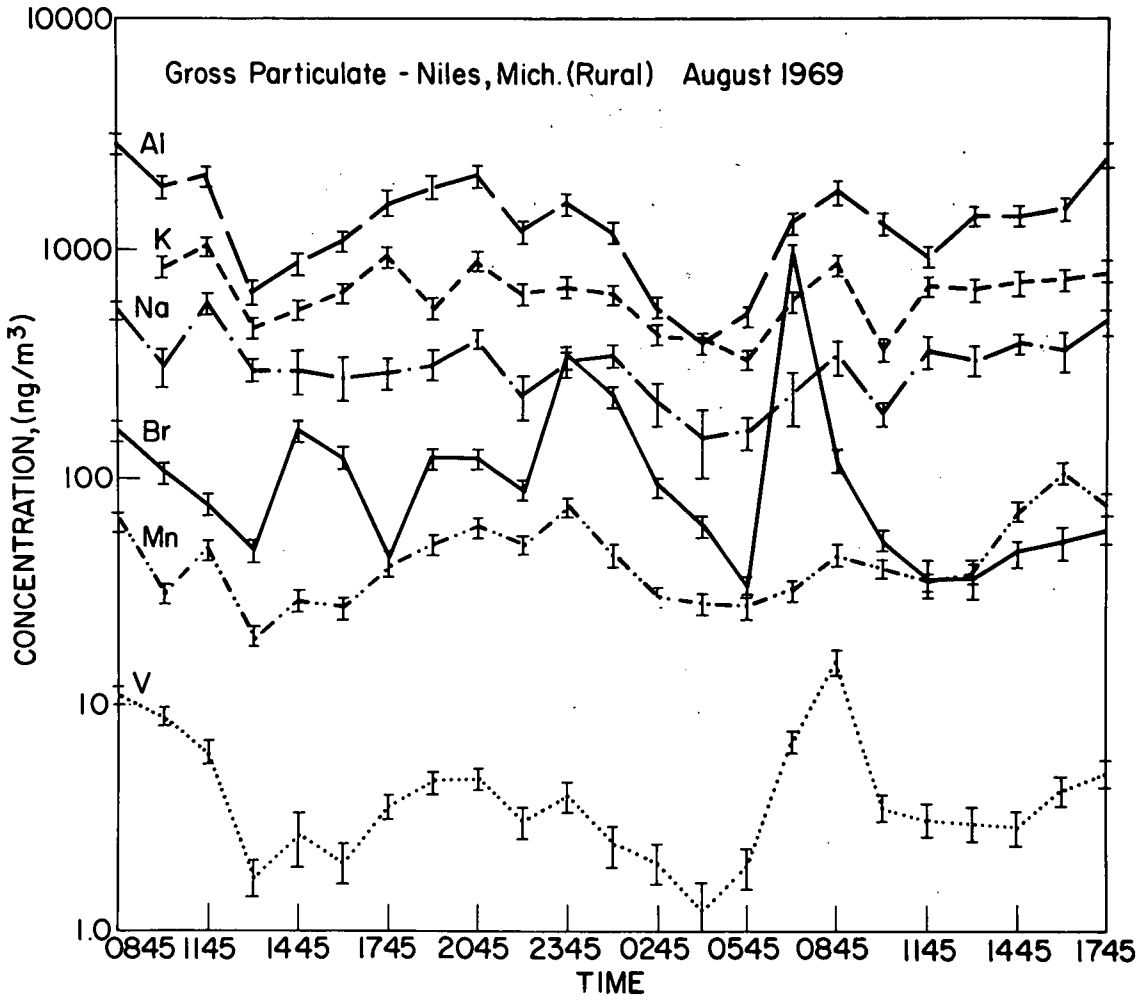

Figure VII-5 Concentration Variations of 6 Elements During Sampling

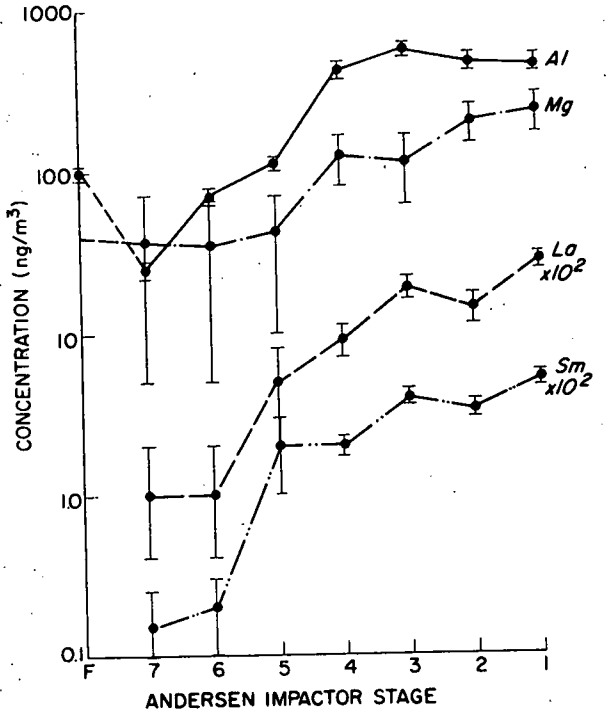

Figure VII-6 Particle Size Distribution of 4 Elements During Sampling

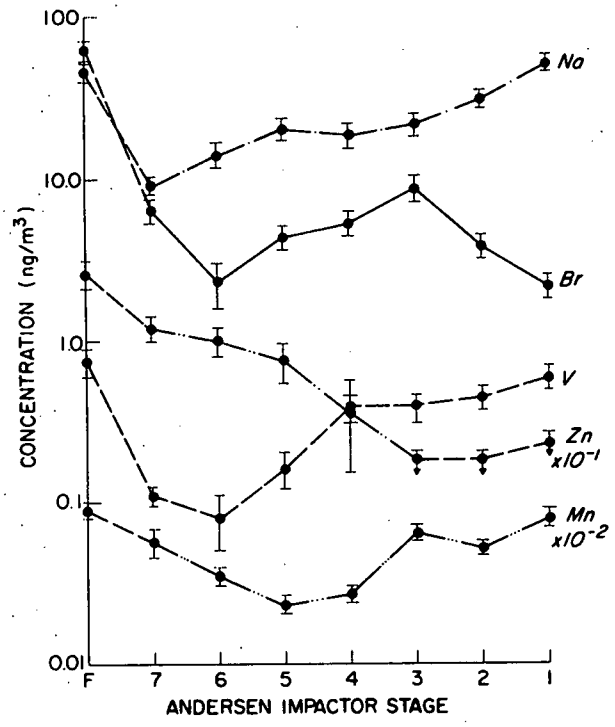

Figure VII-7 Particle Size Distribution of 5 Elements During Sampling

CHAPTER VIII

DIURNAL VARIATIONS II - LIVERMORE, CALIFORNIA*

Introduction

The determination of atmospheric aerosol trace element concentrations poses severe analytical problems because of the very low abundances of most elements. The consequent need for concentration is usually fulfilled by 24-hour sampling, which offers the additional advantage of encompassing the natural diurnal cycle, thereby yielding the most unbiased average for pollutant concentrations. The nature of diurnal variation cycles for trace elements is, however, of considerable interest. Unfortunately, because of the analytical difficulties introduced by the much smaller sample sizes little work has been done on trace element variations as a function of time. One study, by Rahn et al. (1971), has shown that in midwestern United States air some 19 elements can be determined in 90-minute samples taken on 25-mm diameter polystyrene filters, and most of these showed regular in-phase variations approaching and sometimes exceeding an order of magnitude in size.

---

*This work was carried out while the author was a summer employee during 1970 at Lawrence Radiation Laboratory, Livermore, California, and will be published under the authorship of K.A. Rahn, J.J. Wesolowski, W. John, and H.R. Ralston.

Livermore, California, site of one branch of the Lawrence Radiation Laboratory (LRL), offers a number of interesting possibilities with respect to trace element diurnal variations studies. It is located in the Livermore Valley, a small east-west oriented valley (∿16 x 10 km) considered to be part of the San Francisco Bay area but located to the east of the major bay basin and separated from it by a portion of the 500 meters high Pacific Coast Range. Since the direct flow of surface air from the bay basin to the valley is significantly hindered by these ridges air transport is mainly accomplished through natural passes on the western end of the valley, with two accompanying exits at the eastern end. Well-developed sea breezes occur nearly every summer day because of the temperature differential between the bay basin and inland areas, particularly the San Joaquin Valley, much larger than and somewhat inland from the Livermore Valley. Because of this well-known circulation cycle it was thought that diurnal studies might enable one to follow the influx of marine air by using the sodium and chlorine levels as natural tracers.

Because of the large meteorological, topographical and industrial source variations over the Bay Area there is no "typical" community or region. Although Livermore enjoys a rural setting (about 80 km southeast of San Francisco) it has had during the past few years a higher frequency of "adverse" oxidant days than any other location in the Bay Area. Moreover, there has been some speculation over the ratio of "local"

to "imported" smog, i.e., smog due to emissions in the San Francisco-Oakland area and advected into the Livermore Valley. By locating our trace element sampling unit next to the Livermore continuous gas monitoring station of the Bay Area Air Pollution Control District (BAAPCD), we hoped to see some correlations between the two.

Sample Collection

A pump was positioned on a tower in downtown Livermore, approximately 6 meters above ground, and samples were collected during a single 58-hour period from 1300 PST Tuesday, 21 July to 2300 PST Thursday, 23 July 1970. Each of the three days appeared at the time to be typical summer days, an impression confirmed by meteorological data taken at LRL, 5 km east of the sampler (Figure VIII-1). Winds were out of the westerly sector during the entire period, and varied from 1 to 15 mph. Temperature ranged from 58 to 84°F, and the relative humidity was at all times lower than 68 percent.

Each sample was 2 hours in duration, taken on 29 mm diameter Whatman No. 41 filter paper using a one-third hp vacuum pump operated at a constant flow rate of 1.5 cfm (43 lpm). This provided a sample size of 5.1 cubic meters collected at a linear velocity of 143 cm/sec, at which speed aerosol collection efficiencies exceed 98 percent down to diameters smaller than 0.1 μm (Lindeken et al., 1963).

Analytical Technique

Nondestructive neutron activation employing y-spectroscopy was used as the analytical tool because of its demonstrated sensitivity and specificity. A complete irradiation and counting sequence was developed (Table VIII-1), similar to the one of Dams et al. (1970). In preliminary work an analysis of 8 x 10-inch Whatman No. 41 hivol air filter samples of 24 to 48 hours duration taken in Livermore (at LRL) detected 34 elements. These are listed in Table I.

The greatly reduced sample size of a 2-hour diurnal sample limits the number of determinable elements to about 15. Elements with half lives longer than a few days are most affected because of the very low count rates obtained and the inability to lengthen counting times of routine application beyond a few hours. Included in this group are such interesting heavy elements as Fe, Co, Hg, Zn, Sb, Ni, Ba, Cr, and Se, most of which fall below the detection limit in samples of only a few cubic meters volume. Some, such as Sb and Ba, are better determined from shorter-lived isotopes.

Results

Useful results were obtained for 15 elements. Of these, the variations of 10 are plotted in Figure VIII-1. K, Cr, Ba, La, and Sm are omitted because of poorer statistics and variation patterns similar to the other elements. In general the elements Na, Cl, Al, Mn, and Br showed uncertainties of 10 to

20 percent, with uncertainties for Sm, Sc, and V in the 20 to 40 percent range, and the others somewhat higher and more variable. These differences can be seen in the smoothness of the curves, the first group generally showing the most regular variations. Certain irregularities in otherwise smooth patterns are, however, exhibited by several elements, such as the brief but sharp peaks at 0400 of 22 July shown by Al, Mn, Zn, V, and Sc, which appear to reflect real atmospheric composition changes.

Figure VIII-1 also shows variations of the gases CO, NO_2, and "oxidant" for the sampling period. These hourly averages were supplied by BAAPCD from the records of their continuous monitoring station in Livermore. Total hydrocarbon was also measured but was not plotted because its hourly average remained constant at 3 ppm during the period.

These data show the following principal features:

1) All trace elements measured undergo marked concentration changes during a diurnal cycle, typically varying by factors of 3 to 10 or more.
2) There appear to be only 3 fundamental types of cycles. These are listed below under 3), 4), and 5).
3) The cycle for Al, Mn, Fe, Zn, Sb, V, and Sc (Ba, Cr, La, and Sm behave similarly but are not plotted) peaks in the afternoon (1200-1400 PST) and reaches a minimum near or slightly past midnight (0000-0200 PST). The cyclic variations here are quite large, usually factors of 7-10.

4) The Cl-Na cycle is nearly 180° out of phase with the Al-Mn cycle, peaking in the night hours (approximately 0400 PST) and reaching its minimum in the afternoon (approximately 1400 PST). Cl varies by a factor of about 4, Na by a factor of 2-3. The Cl/Na ratio is in phase with this cycle, and at its maximum (1.6) nearly reaches the sea water Cl/Na ratio of 1.8.

5) The Br cycle is less well defined than the other two cycles. It shows peaks of 2000 PST each of the 3 evenings, as well as a peak on the first morning. The peak of the second morning is either absent entirely or else is hidden in the tail of a large concentration of Br found throughout the previous night.

6) The oxidant pattern has a single peak at 1400-1500 PST. Its cycle strongly resembles that of the Al-Mn group but lags it slightly and is somewhat shorter in duration.

7) Wind speed also is higher in daylight, peaking at approximately 1600 PST with minima at night.

8) Zn and Sb exhibit similar positive perturbations during 0600-1000 hours of the early morning of Thursday 23 July, with concentration increases of a factor of 3-5. Br may also show the variation, but not to such an extent and not in such a clear manner.

Discussion

The most outstanding trend shown by the trace metal data is the regular and apparently reproducible transition between two alternating composition regimes during each diurnal cycle. The "daytime" regime, beginning soon after sunrise and dying out around sunset, is markedly continental with its low Na and Cl content and its high for other elements. The night regime on the other hand seems marine in character with a reversal of the above concentrations.

The "continental" elements typified by Al and Mn show a diurnal cycle closely linked to wind speed, suggestive of local wind generation of soil and dust aerosols which are removed by fallout and impaction when the wind speeds decrease in the evenings. Such an hypothesis seems reasonable in view of the extremely dry California summers. It is to be noted that this diurnal pattern is out of phase with that observed for the same elements in the midwestern United States by Rahn et al. (1971), which were attributed to elevated pollution sources at a distance.

An alternative explanation for this diurnal pattern of the Al-Mn group can be seen in mixing patterns. If the air aloft contained these elements at levels comparable to the maximum observed at the surface, the increasing concentrations with wind speed in the morning might be due to the mixing of this overlying continental air aloft with the surface layer of marine air accumulated during the night.

These two conflicting hypotheses might be resolved by experiment. The first implies a strong particle size distribution change during a cycle, being more heavily weighted toward large particles during the day; the second suggests no such diurnal variation.

The contrast between the first and second nights tends to confirm the wind generation hypothesis. All the members of the Al-Mn group show considerably higher concentrations during the second night, when the wind averaged 3-5 mph compared with 1-3 mph for the first night.

Two of the elements in the Al-Mn category, namely Zn and Sb, show the basic pattern upon which is superimposed a single major excursion during the early morning hours of the third day, possibly indicative of a common pollution source. An areawide study of Northwest Indiana (Chapter VI) has shown both these elements to be among those with the strongest local sources, and a statistical analysis of these data by Dams et al. (1970) has shown a very high correlation between the areawide behavior of these two elements.

A third member of the Al-Mn group, V, often recognized to have a fuel combustion source, shows a deviation from the pattern at the end of the sampling period, where instead of falling by a factor of 5 it increased by a factor of 2.

Several features of the Cl-Na variation cycle strongly suggest a link with fresh marine air from the bay basin. The most obvious of these is the in-phase increase of both Cl and

Na during periods of decrease of the other elements (Br excluded), beginning in the late afternoon and early evening at or shortly after the westerly winds reach their peak speed. The order of magnitude higher Cl and Na concentrations relative to continental air of interior North America imply a recent marine origin for these elements. Further evidence for this hypothesis is found in the increasing Cl/Na ratio during the nights and its approach to the sea water value. The fact that the Cl/Na ratio approaches that of sea water at the time that the individual Cl and Na concentrations reach their maximum values suggests that the valley air near the surface at this time is essentially undiluted fresh marine air from the bay basin.

The valley air into which the fresh marine air from the west mixes is deficient in Cl. This result appears to be general, for preliminary results from 24-hour filters taken elsewhere in the Bay Area show a Cl/Na ratio considerably less than the sea water value. Though the Cl-deficiency of marine-associated air is well-known and generally attributed to loss into the gas phase, the present data indicate that <u>fresh</u> marine air, near the surface shows little or no Cl depletion.

The third distinct trace element pattern is displayed solely by Br. Its total variation of a factor of 3 is the smallest of the elements except Na, but regularities are still seen, as noted in (5) above. The morning maximum suggests

local sources, probably from automobile gasoline combustion (Br is commonly present in leaded gasolines). It is not clear whether the evening peak is from local or upwind bay pollution sources or both.

In order to lend coherence to the interpretation of the present trace element data we suggest the following provisional circulation model for the Livermore Valley. During the afternoon as the wind speed decreases the soil-generated aerosol (Al-Mn group) is removed by fallout and impaction, a fairly rapid process because of the large particle sizes involved. At the same time, as the surface air is being stabilized by cooling, fresh Na and Cl-rich marine air enters the valley and begins to replace the aged air. Because of the basic thermal stability of both bay basin and valley air, entrance to the valley is restricted to narrow passes and the flow proceeds slowly but steadily during the night, accounting for the prolonged gradual rise of Cl and Na levels. Shortly after sunrise, however, both Na and especially Cl levels drop, coinciding with the increase in Al-Mn group levels and wind speed. If, as is suggested, the overlying air mass is marine, then the increasing Al-Mn type levels would not be accounted for by vertical mixing, but must be soil derived. On the other hand, the sudden drop of Cl and Na levels and the drop of the Cl/Na ratio can be explained by mixing. Also, the timing of this drop (0800-1200 PST) suggest a link with the destruction of the nocturnal surface inversion and mixing with air between

approximately 100 m and 600 m rather than destruction of the subsidence inversion aloft. If this is true, then the Na and Cl-rich air would be confined to a low-level tongue in the bottom of the valley, an easily tested hypothesis. During the heating period of the morning, wind speeds increase and more soil aerosol is generated, and the diurnal cycle begins to repeat itself.

Relationships involving the gases are more ill-defined than for trace elements alone. For example, NO_2 should precede oxidant if they are photo-chemically related, but the Livermore data show the opposite sequence, a trend confirmed on the other days as well. CO variations are similar to those of NO_2 but not as pronounced, also often lacking a morning peak. There is, however, a reasonable correlation between Br, NO_2 and CO, suggesting similar or common sources. Particular features of note are the regularity and coincidence of evening peaks, and higher levels during the second night than during the first.

These relationships suggest that upstream or bay basin sources contribute heavily to Livermore smog and that a large part of the oxidant observed at Livermore has its origin in these upstream precursors. This is in agreement with the conclusions of a previous study of Livermore smog based on an examination of meteorological patterns (Crawford, 1968).

Though any conclusions from a single study such as this must be considered quite tentative, the highly cyclic nature

of the trace element concentration patterns observed for these three typical summer days suggest a corresponding regularity of the circulation pattern which is their cause. Details of the model may be checked by multipoint sampling in both the horizontal and vertical. In a more general sense, however, measurements of diurnal variations of trace elements have now been shown to be of value in providing valuable information leading to better understanding not only of sources and transport mechanisms of pollutants, but also of basic mesoscale meteorological processes.

Acknowledgements

We thank T. Crawford and H. Ellsaesser for helpful discussions and C. Maninger and E. Goldberg for their support of this work. We also thank the Bio-Medical Division for the use of their equipment.

TABLE VIII-1

Irradiation Time, Flux	Cooling Time	Counting Time	Elements Detected
2 minutes 2×10^{13} n/cm^2-sec	4 minutes	8 minutes	Al, V, Cu, Ti, Ca,* S*
	20 minutes	20 minutes	Na, Mg, Cl, Mn, Br, I, Ba
10 hours 4.5×10^{12} n/cm^2-sec	20-30 hours	40 minutes	Eu, Br, As, W. Ga, Zn, K, Cu, Na
	6-10 days	80 minutes	Sm, Au, Hg, La, Sb
	20-30 days	600-800 minutes	Fe, Cr, Co, Zn, Hg, Se, Ag, Sb, Ce, Eu, Sc, Th, Ni, Ta, Hf, Ba, Rb

*NOTE: Because of the small volume of the Ge detector no attempt was made to measure energies above 2000 keV. Thus S (3102 keV, 5.1 min) and Ca (3083 keV, 8.8 min) were not measured. Only an upper limit was obtained for Ni. In a more industrialized area one might also expect to detect In and Cd.

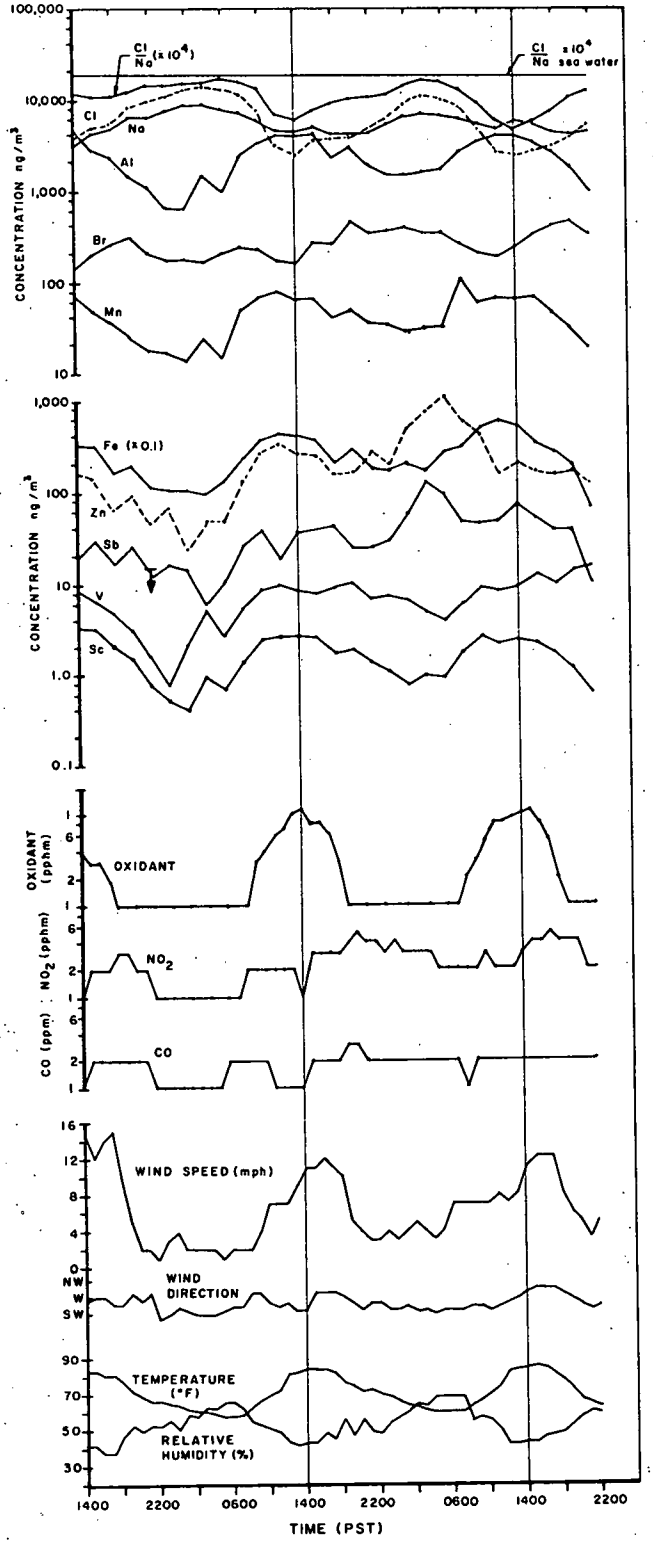

Figure VIII-1 Results of Measurements of Diurnal Variations of Aerosol

Trace Element Concentrations

PART III

REFLECTIONS

The principal objective of this work was to assess the impact of anthropogenic aerosol sources on the chemical composition of the aerosol of remote continental regions. While a complete answer to this problem has by no means been given, a start has been made for some elements. Most importantly, it appears that the analytical tools presently available may be sufficient to eventually resolve the question in much more detail.

It is now possible to sample air of the most remote regions of North America over periods of weeks and determine the concentrations and particle size distributions of some 30 trace elements. The careful use of Andersen cascade impactors with clean polyethylene impaction surfaces, clean filter paper such as Whatman No. 41, and neutron activation analysis virtually guarantees precise results for many elements. On the basis of results such as afforded by this study the elements can be classified according to source types, and inferences can be made about natural vs. anthropogenic sources.

Specifically, this investigation shows that evidence for anthropogenic (industrial) origins abounds in the samples of most regions studied. It was seen in all samples, even in those from the Northwest Territories, where the nearest possible

industrial sources are hundreds of kilometers distant, and highly scattered.

On the basis of evidence found for anthropogenic sources in the air of otherwise remote Twin Gorges and Algonquin, the remoteness problem, i.e., the impact of sources on the air of distant areas, emerges as an all-important one. Provided that the analytical method is sufficiently sensitive, the effects of anthropogenic sources in otherwise clean areas are seen to extend at least over hundreds of kilometers. Their possible effects in the thousands-of-kilometers range in an obvious extension of this work.

Analytical Techniques

The inherent strength of nondestructive neutron activation analysis is demonstrated by the present work. In general, these results also demonstrate the value of the application of a highly sensitive multielemental technique to even a few carefully-planned measurements. This is best seen here in the ARO case, where the presence and nature of a single strong pollution source was inferred from only two 3-week size distribution samples.

The present study by no means exhausts the full potential of this nondestructive technique. The utilization of still larger sample sizes may result in more elements being determined much more precisely.

A thorough chemical study of remote aerosols can profitably employ a combination of NNAA and other technqiues. Atomic absorption spectroscopy, anodic stripping voltammetry, and x-ray fluorescence are immediate possibilities. Each of these is strong in certain areas where NNAA is weak.

In addition to other techniques, other types of chemical measurements might offer valuable information. A thorough study of atmospheric geochemistry will ultimately require not only elemental concentrations but also a knowledge of actual compounds formed by these elements, information which the present technique does not provide.

Physical techniques also should not be overlooked: i.e., stereoscan electron microscopy combined with microprobe, etc. must add to knowledge about the particles in question.

Further Interpretation

The massive amount of data generated by a multielemental technique quickly creates a problem of interpretation. In certain sections of this work, particularly the Mackinac Island experiment, much further study remains to be made on the basic data. No comprehensiveness of interpretation is claimed for this work.

The Clean Air Problem

One of the principal results of this work is that the northernmost regions of Canada show significantly lower concentrations of trace elements than do Michigan or Indiana, and

that the concentrations decrease fairly smoothly with distance to the north and west. For the soil-derived elements some asymptotic behavior of the concentration profiles was suggested, indicating a possible approach to the background or at least to baseline conditions, but for many of the pollution elements a sharper continuing decrease was seen, meaning that more remote areas, such as over oceans, should show even lower concentrations of these elements. The problem of clean air, namely its nature and location, is therefore not resolved here except possibly for the soil elements.

Clean air is very elusive, both in practice and in theory. Several problems concerning clean air are illustrated by the results of this work. First, should clean air be sought at the surface, where local effects are clearly the largest, or is clean air the purest available in, say, the troposphere? In this regard it should be noted that the Jasper station, the only one of this study in a mountainous region (elevation 2000 m), shows aerosol/soil enrichment factors which for many anthropogenic elements are the lowest of the network.

Secondly, should clean air be limited to continental air, which will still show strong soil effects, or should it include marine air, which may be low in anthropogenic substances but high in sea salt? The answer to this will probably depend on the answer to the third problem, which is whether the criteria for clean air should refer simply to total particulate content or whether they should relate specifically to anthropogenic

substances and/or the identity of the materials forming the particles (marine vs. continental; automotive vs. industrial; forest fires vs. volcanoes; biologic vs. inorganic; etc.).

In light of the present work, the answer to the third problem seems obvious. Now that reliable multielemental methods are at hand, clean air should be defined in terms of the anthropogenic elements involved, some examples of which appear to be As, Se, Hg, Zn, Sb, etc., those elements predominantly found on small particles and having large aerosol/soil enrichments. On the other hand, the soil-derived elements such as Al, Fe, etc., cannot be ignored over continents, for there may also be pollution components in populated areas. These pollution components can be estimated by comparison with the corresponding concentrations of remote areas, but for clean air purposes the anthropogenic elements listed above seem to be the best indicators.

It is the opinion of this writer that clean air has at least a double connotation. Natural air is never clean - over oceans it contains sea salt and over continents it contains soil dust. The phrase "clean air" is used here to mean anthropogenically clean, that is, the state in which air would be found over both continents and oceans in the absence of human activities. Clearly, continental clean air will be very different in composition from marine clean air, and the determination of each requires separate experiments. This investigation approached continental clean air, but had nothing to do with marine clean air.

Follow-Up Experiments

The number of conclusions that can be drawn from an exploratory study such as the present one is severely limited. At the very least, confirmatory measurements need to be taken at or near the same locations before any strong statements about the representativeness of the reported numbers may be made. In addition, the variation of concentrations over other remote regions needs study. In particular, the Canadian East (Quebec) might profitable be included in a future survey. An interesting comparison would be with the western United States, both the mountainous and plains regions.

One problem worthy of some scrutiny is the magnitude of concentration variations on a smaller scale than observed here. These scales may range in size from tens of kilometers down to the micro scale. Stations ARO and TG give evidence for the importance of these variations, at least for industrially-derived elements. The magnitude of local variations of soil-derived elements remains unsettled, though the particle size distribution plots for the summer Canadian study suggest it to be small.

A major problem needing further investigation is the shift to L-type size distribution in remote areas of elements which by their abundance would seem still to be anthropogenic in origin. For example, Zn and Sb both showed this effect at Twin Gorges in summer, while at the less remote stations they were S- and M-type.

One possible explanation may lie in repeated cycles of cloud processes, effective even for the relatively insoluble compounds of these elements. Though this idea is very speculative, it suggests that closer attention to weather variables may be needed.

Several specific smaller experiments are suggested by these results. The first is a more thorough documentation of the industrial source at ARO, both because of its inherent interest and because of the possibilities for the use of this combination of elements and size distributions as a tracer or "signature" in mesoscale circulation studies. Such a documentation might be achieved by grid sampling around suspected sources, or single point sampling under varying wind directions.

A similar study might be undertaken around Twin Gorges, NWT, for there is again evidence of a strong pollution source here, probably in the Yellowknife region. Better knowledge of this source should allow future sample sites to be placed more nearly upwind, so as to give more meaningful background levels for the area.

The apparent aging of the marine aerosol as observed in the Twin Gorges winter samples might be further investigated. The Northwest Territories in winter appears to be an ideal natural laboratory for long-range transport studies of marine aerosol. If the Pacific Ocean is indeed the source of this aerosol, as seems most likely from the wind patterns aloft, the aerosol sampled at intermediate points between Twin Gorges and

the Pacific should be younger and show intermediate aging effects.

A number of improvements in sampling techniques are possible. For example, now that typical remote concentrations are known, it can be seen that the Andersen Samplers need to be run for months rather than weeks in order to accumulate sufficient sample to take full advantage of the neutron activation technique. Total filter samples could also be profitably run for more than the two weeks of this experiment. Future Andersen samples should be taken with backup filters where possible, because the clogging of the backup filters may not be as much of a problem as originally thought.

There exists a definite need for impactors having both fine particle size resolution as in the Andersen Sampler and higher flow rates, so that sampling times could be reduced considerably from the cumbersome weeks or months as at present. Also, better resolution in the smallest particle sizes would be desirable, especially below 0.1 μm. Hence new sampling techniques need to be used. The range and resolution of the Andersen sampler are definitely limited.

LIST OF REFERENCES

Andersen, A.A., "A Sampler for Respiratory Health Hazard Assessment," Amer. Ind. Hyg. Assoc. J., 27, 160 (1966).

Battan, L.S., The Unclean Sky, Doubleday & Company, Inc., Garden City, New York (1966).

Blanchard, D.C. and A.H. Woodcock, "Bubble Formation and Modification in the Sea and Its Meteorological Significance," TELLUS, 9, 145 (1957).

Brar, S.S., D.M. Nelson, J.R. Kline, P.F. Gustafson, E.L. Kanabrocki, C.E. Moore, and D.M. Hattori, "Instrumental Analysis for Trace Elements Present in Chicago Area Surface Air," J. Geophys. Res., 75 (15), 2939 (1970).

Cadle, R.D., Particle Size-Theory and Industrial Applications, Reinhold, New York (1965).

Callender, E., Dept. of Met. and Ocean., The Univ. of Mich., personal communication (1971).

Chow, T.J., J.L. Earl, and C.F. Bennett, "Lead Aerosols in Marine Atmosphere," Environ. Sci. Tech., 3, 737 (1969).

Commins, B.T. and R.E. Walter, "Observations from a Ten-Year Study of Pollution at a Site in the City of London," Atmos. Env., 1, 49 (1967).

Crawford, T., Chairman, The City of Livermore Air Pollution Control Study Committee (unpublished data) (1968).

Dams, R., K.A. Rahn, and J.W. Winchester, "Evaluation of Filter Materials and Impaction Surfaces for Nondestructive Neutron Activation Analysis of Aerosols," Env. Sci. Tech. (1971) (submitted).

Dams, R., J.A. Robbins, K.A. Rahn, and J.W. Winchester, "Nondestructive Neutron Activation Analysis of Air Pollution Particulates," Anal. Chem., 42, 861 (1970).

Dams, R., J.A. Robbins, K.A. Rahn, and J.W. Winchester, Quantitative Relationships Among Trace Elements over Industrialized N.W. Indiana, presented at the Symposium on the Use of Nuclear Techniques in the Measurement and Control of Environmental Pollution, Salzburg (1970).

Dingle, A.N., Dept. of Met. and Ocean., The Univ. of Mich., private communication (1970).

Duce, R.A., A.H. Woodcock, and J.L. Moyers, "Variation of Ion Ratios with Size Among Particles in Tropical Oceanic Air," TELLUS, 19, 369 (1967).

Egorov, V.V., T.N. Zhigalovskaya, and S.G. Malakhov, "Microelement Content of Surface Air Above the Continent and the Ocean," J. Geophys. Res., 75 (18), 3650 (1970).

Fitzgerald, J.S. and C.G. Detwiler, Knolls Atomic Power Lab. Rep. KAPL - 1088 (1954).

Flesch, J.P., C.N. Norris, and A.E. Nugent, Jr., "Calibrating Particulate Air Samplers with Monodisperse Aerosols," J. Amer. Indus. Hyg. Assoc., 28, 507 (1967).

Fletcher, N.H., The Physics of Rainclouds, Cambridge University Press, Cambridge, England (1966).

Friedlander, S.K., "Similarity Considerations for the Particle Size Spectrum of a Coagulating, Sedimenting Aerosol," J. Meteor., 17, 479 (1960).

Gillette, D.A., A Study of Aging of Lead Aerosols, Ph.D. Thesis, The Univ. of Mich. (1970).

Gillette, D.A. and I.H. Blifford, Jr., "Composition of Tropospheric Aerosols as a Function of Altitude," unpublished manuscript (1970).

Harkins, W.D. and R.E. Swain, "Papers on Smelter Smoke. I. The Determination of Arsenic and Other Solid Constituents of Smelter Smoke, with a Study of the Effect of High Stacks and Large Condensing Flues," J. Am. Chem. Soc., 29, 970 (1908).

Harrison, P.R., Area-wide Distribution of Lead, Copper, Cadmium and Bismuth in Atmospheric Particulates in Chicago and Northwest Indiana: A Multi-sample Application and Anodic Stripping Voltammetry, Ph.D. Thesis, The Univ. of Mich. (1970)

Hashimoto, Y. and Winchester, J.W., "Selenium in the Atmosphere," Env. Sci. and Tech., 1, 338 (1967).

Hewson, E.W., "Meteorological Measuring Techniques and Methods in Air Pollution Studies," in Industrial Hygiene and Toxicology, Vol. 3, L. Silverman (ed.), New York, Interscience

Hoffman, G.L., R.A. Duce, and W.H. Zoller, "Vanadium, Copper, and Aluminum in the Lower Atmosphere Between California and Hawaii," Env. Sci. Tech., 3(11), 1207 (1969).

Johnstone, H.F. and A.J. Moll, "Formation of Sulfuric Acid in Fogs," Ind. Eng. Chem., 52, 861 (1960).

Junge, C.E., Air Chemistry and Radioactivity, Academic Press, New York (1963).

Junge, C.E., "The Chemical Composition and Radioactivity of the Atmosphere," in Izdatelstvo "Mir" (English trans.) pp. 210-211 and p. 414, Moscow (1965).

Junge, C.E., "Comments on Concentration and Size Distribution Measurements of Atmospheric Aerosols and a Test of the Theory of Self-Preserving Distributions," J. Atmos. Sci., 26, 603 (1969).

Kleane, J.R. and E.M.R. Fisher, "Analysis of Trace Elements in Airborne Particulates by Neutron Activation and Gamma Ray Spectrometry," Atm.Env., 6, 603 (1968).

Kneip, T.J., M. Eisenbud, C.D. Strenhlow, and P.C. Freudenthal, Airborne Particulates in New York City, APCA Paper No. 69-166, 62nd National Convention, New York (1969).

Lee, J. and Jervis, R.E., "Detection of Pollutants in Airborne Particulates by Activation Analysis," Amer. Nuc. Soc. Trans., 11, 50 (1968).

Lee, J., R.K. Patterson, and J. Wagman, "Particle Size Distribution of Metal Components in Urban Air," Proc. of the Amer. Chem. Soc. (April 1967).

Lindeken, P.L., R.L. Morgin, and K.F. Petrock, "Collection Efficiency of Whatman 41 Filter Paper for Submicron Aerosols," Health Physics, 9, 305 (1963).

Lininger, R.L., R.A. Duce, J.W. Winchester, and W.R. Matson, "Chlorine, Bromine, Iodine, and Lead in Aerosols from Cambridge, Massachusetts," J. Geophys. Res., 71(10), 2457 (1966).

Lockhart, L.B. and R.L. Patterson, NRL Report 6054, U.S. Naval Research Laboratory, Washington, D.C. (1964).

Loucks, R.H., Particle Size Distributions of Chlorine and Bromine in Mid-Continent Aerosols From the Great Lakes Basin, Ph.D. Thesis, The Univ. of Mich. (1969).

Loucks, R.N. and J.W. Winchester, "Pollution Contributions to the Atmospheric Inventory of Chlorine and Bromine in Aerosols Over Continental U.S.A." Trace Substances in Environmental Health. III. Conference Proceedings, University of Missouri (1969).

Mason, B., Principles of Geochemistry, 3rd Ed., Wiley & Sons, Inc., New York (1966).

May, K.R., "The Cascade Impactor," J. Scientific Instruments, 22, 187 (1945).

Munn, R.E. and M. Katz, Int. J. Air Poll., 2(1), 51 (1959).

Murozumi, M., T.J. Chow, and C. Patterson, "Chemical Concentrations of Pollutant Lead Aerosols, Terrestrial Dusts, and Sea Salts in Greenland and Antarctic Snow Strata," Geochim. et Cosmochim. Acta., 33, 1247, (1969).

Nifong, G.D., Particle Size Distributions of Trace Elements in Pollution Aerosols, Ph.D. Thesis, The Univ. of Mich. (1970).

Ozolins, G. and C. Rehmann, Air Pollutant Emission Inventory of Northwest Indiana, A Preliminary Survey, 1966, National Center for Air Pollution Control Publication APTD-68-4 (1968).

Parkinson, T.F. and L.G. Grant, "Activation Analysis of Particulate Air Contaminants," Nature, 197, 479 (1963).

Pillay, K.K.S. and C.C. Thomas, Jr., Report WNY-046, Western New York Nuclear Research Center, Buffalo (1969).

Rahn, K.A., R. Dams, J.A. Robbins, and J.W. Winchester, "Diurnal Variations of Aerosol Trace Element Concentrations as Determined by Nondestructive Neutron Activation Analysis," Atm.Env. (1971) (in press).

Slade, D.H., Meteorology and Atomic Energy 1968," U.S. Atomic Energy Commission Publication No. TID-24190, Washington, D.C. (1968).

Smith, W.S. and N.F. Surprenant, Proc. ASTM, 53, 1122 (1953).

Spurny, K. and J. Fiser, "Bemerkung zur Mikorgravimetrischen Bestimmung der Aerosolkonzentration mit Hilfe von Filtrationsmethoden," Staub 30, 249 (1970).

Summers, P.W., "The Seasonal, Weekly, and Daily Cycles of Atmospheric Smoke Content in Central Montreal," J. Air Poll. Control Assoc., 16(8), 403 (1966).

U.S. Department of Health, Education, and Welfare, Meteorological Aspects of Air Pollution, Course conducted by Air Pollution Training Program, Cincinnati, Ohio (1965).

U.S. Department of Health, Education, and Welfare, Air Quality Data, National Air Pollution Control Administration Publication No. APTD 68-9 (1968).

Vinogradov, A.P., The Geochemistry of Rare and Dispersed Chemical Elements in Soils, 2nd Ed., Consultants Bureau, Inc., New York (1959).

Von Smoluchowski, M., "Drei Vortrage uber Diffusion Brownsche Molekularbewegung, und Koagulation von Kolloid Teilchen," Physik Zeitschrifte, 17, 557 (1916).

Weisman, B., O.H. Matheson, and M. Hirt, Atm.Env., 3, 1 (1969).

Weiss, H.V., M. Koide, and E.D. Goldberg, "Selenium and Sulfur in a Greenland Ice Sheet:Relation to Fossil Fuel Fuel Combustion," Science (in press) (1971).

Winchester, J.W. and R.A. Duce, "Coherence of Iodine and Bromine in the Atmosphere of Hawaii, Northern Alaska, and Massachusetts," Tellus, 18, 287 (1966).

Winchester, J.W. and R.A. Duce, "The Global Distribution of Iodine, Bromine and Chlorine in Marine Aerosols," Die Naturwissenschaften, 5, 110 (1967).

Winchester, J.W. and G.D. Nifong, Water Pollution in Lake Michigan by Trace Elements from Pollution Aerosol Fallout, Presented at the Great Lakes Symposium, American Chemical Society Annual Meeting, Minneapolis, Minn. (1969).

APPENDIX

APPENDIX 1a

EVALUATION OF FILTER MATERIALS AND IMPACTION SURFACES FOR NONDESTRUCTIVE NEUTRON ACTIVATION ANALYSIS OF AEROSOLS*

Introduction

The recent introduction of lithium-drifted germanium (Ge(Li)) semiconductor gamma-ray detectors has revolutionized the field of neutron activation analysis. The superior energy resolution characteristics of these diodes allow discrimination between gamma rays of energies within a few keV of each other, greatly reducing mutual interferences between elements and in many cases totally eliminating the need for post-irradiation chemical separations. The increased speed and enhanced specificity thus obtained combines with the proven sensitivity and multielemental nature of neutron activation analysis to make this technique an extremely powerful one in trace element analysis.

In addition, the elimination of chemical manipulations of the sample opens up the possibility of totally nondestructive analysis, i.e., where the sample is not removed from its collection matrix or changed in any way during analysis. Several advantages accompany nondestructivism: reduction of analytical uncertainties associated with sample preparation and post-irradiation chemistry, availability of the sample for analysis by other techniques and other laboratories, determination of isotopes with half-lives as short as seconds, and potential automation of the procedure.

The determination of trace element composition of aerosols is an ideal application for nondestructive neutron activation analysis. Its sensitivity is needed because of the very low atmospheric abundance of total aerosol (1 mg-m^{-3}-1 μg-m^{-3}, or 1 ppb-1 ppt by weight) and the consequently lower elemental levels (10^{3}-10^{-3} ng-m^{-3}). Its multielemental nature

*This article will be published under the authorship of R. Dams, K. A. Rahn, and J. W. Winchester.

and specificity aid in analysis of the chemically complex and highly variable composition of the aerosol. Furthermore, the speed of nondestructivism can be used to advantage, for the general difficulty of controlled sampling in the real atmosphere requires a large number of analyses before valid conclusions may be drawn.

A procedure for the nondestructive neutron activation analysis of aerosols has been developed in our laboratory and applied to a variety of atmospheric samples (Dams, Robbins, et al., 1970). These aerosol samples, which may be taken on highly pure filters or impaction surfaces, are irradiated twice in a nuclear reactor and are counted four times after decaying for periods of 3 minutes to 20 days. Some 30-33 elements may be detected in a given sample, with half-lives ranging from minutes to years. Analysis for short-lived isotopes is rapid - more than 10 elements may be determined within an hour of the time of receipt of the sample.

Table 1a-1 lists the determinable elements, their detection limits in typical urban 24-hour filter samples, and representative concentrations in a rural area (Niles, Michigan) and an urban site (East Chicago, Illinois). In samples where the collected aerosol is large relative to filter impurities the elemental detection limits are predominantly determined by interferences from other elements in the sample, the situation for most elements in the above urban samples. When sample durations become 1-2 hours or less (volumes of a few cubic meters of air) filter impurity levels become more important and indeed may become the limiting factor in determining the detection limits. Such short sampling times, however, are vital for diurnal variations studies, and have been shown to be feasible even for a rural area (Rahn, Dams, et al., 1971) where samples of 1.5 hours in duration were used to follow the variations of 15 trace elements during a 36-hour period. For this type of study, or for sampling in remote areas where elemental concentrations may be many times lower than in urban areas, impurity levels become a major consideration in the

selection of a filter material.

Parkinson and Grant (1963) evaluated impurity levels in three filter materials and found Whatman No. 42 to be the lowest in activatable elements, though they do not report individual concentrations. Keane and Fisher (1968) have used nondestructive neutron activation analysis and NaI(Tl) gamma-ray spectroscopy to determine 7 inorganic impurity levels in a number of the commoner filter types. Spurny and Fiser (1970) quote impurity levels for 7 elements in three filter papers, also as determined by activation analysis.

Physical Properties of Filters

The important physical properties of the commonly-used filter materials are well-known and have been thoroughly summarized elsewhere (Lockhart and Patterson, 1964). The principal ones include collection efficiency as a function of both particle size and flow rate, flow rate as a function of pressure drop across the filter (called (resistivity" below), and flow rate decrease during sampling due to the dust loading on the filter. Of secondary importance are tensile strength, thickness, weight, and hygroscopicity.

Most filters fall into one of two groups - the fibrous type which is composed of cellulose or synthetic organic fibers, and the membrane type which features circular pores of a highly reproducible diameter.

Experimental

Using the review of Lockhart and Patterson (1964) as a guide, we selected for chemical analysis a number of filters whose physical properties seemed suitable to our sampling purposes and which were expected to contain only low concentrations of interfering inorganic materials. Representatives of both the fibrous type and the membrane type were included (see Table 1a-2). These were analyzed by our nondestructive procedure discussed above, with the results shown in Table 1a-3. Elements which are generally determinable in aerosols but which do not appear in this table have concentrations in the filters which are below the detection limit, and in

practice are considered negligible (for Whatman No. 41, the cleanest filter tested, these include V, Cu, Zn, Mg, In, As, Ca, La, Sm, Eu, W, Au, Sc, Se, Ce, and Th). Because of the relatively high impurity levels in membrane filters EHWP047 and GA-6, analysis was restricted to those elements with short-lived isotopes.

Flow rates were measured in the 20x25 cm format (where filters of this size were available) using a General Metal Works high volume pump, Model GMWL 2000. For the 25 and 47 mm sizes flow rates were measured with a Gelman Twin Cylinder pump, having a free air capacity of 68 $l\text{-}min^{-1}$ and a maximum vacuum of 66 cm Hg. Table 1a-4 shows the results as flow rates over the exposed or "effective" surface of the filter.

In addition, the effect of dust loading on flow rate was investigated for W41, C, and HAWP in Ann Arbor, Michigan air, with the results listed in Table 1a-4.

Because some elements are found to be primarily associated with the smaller aerosol particle sizes, it is of interest to determine the degree of penetration, element by element, of actual aerosols through a filter. A 24-hour sampling experiment was performed with two 20x25 cm polystyrene filters placed on top of each other, a primary (upper) and a backup (lower) filter. A maximum of 5% of the Zn, 2.5% of the Br, 5% of the La, and 1% of the Al were found on the backup filter, with all the other elements essentially completely collected by the primary filter. It appeared, however, that sheets of this polystyrene were not very homogeneous, and the observed thickness difference of a factor of two may account for some of the penetration listed above.

Discussion

Inspection of the filter impurity levels of Table 1a-3 immediately shows DMS to have extremely high values of Cl, Br, Cu, and Zn, precluding sensitive determination of these elements in samples taken on this filter material. In addition, irradiation of the filter alone induces high enough activities (mostly from Cl and Br) to not only raise the

detection limits of at least 15 other elements by an order of magnitude (column 4 of Table 1a-6 does not include this additional interference) but also to saturate the counter. This filter is thus eliminated from further consideration for activation analysis purposes.

The impurity levels of two of the membranes, EHWP047 and GA-6, though not prohibitively high, are generally much higher than for the remainder of the filters. Unless very long samples are considered, the impurities here effectively restrict the application of these two materials to sampling in heavily polluted areas. The membrane filters HA and AA have lower concentrations of most elements, but Na, Cr, and Cu could pose problems. Most elements are very low in the polystyrene PS, but Ba and Cl are high enough to prohibit determination of them in samples. Fortunately, neither has a high enough neutron cross section to interfere significantly with the other elements. All the impurity levels of W41 compare favorably with PS, especially the Cl (30 times lower) and Ba.

Table 1a-4 displays the sharp contrast in physical properties between the fibrous and membrane types. The latter generally show high flow resistance, raising minimum sampling times by as much as a factor of 3. They have extremely high retentivities at all flow rates, even for small particles, and though the effect of dust loading on flow rates is considerable it is not enough to be a problem. Since retentivities are so nearly equal between the two pore sizes investigated, the 75% greater flow rate of the 0.8 μm type represents a real sampling advantage over the 0.45 μm size.

Of the fibrous filter group, the polystyrenes combine high flow rates, high retentivities, and a very small tendency to become clogged. Even at lower air velocities such as sometimes encountered in high volume sampling the elements associated with the smaller particles are retained with greater than 95% efficiency.

The cellulose filter (C) allows a very high flow rate

but has a poor filtering performance because of the very low retentivity of small particles. Its profitable use seems to be restricted to less critical applications in those heavily polluted areas where its virtual freedom from clogging can be employed to greatest advantage.

Whatman No. 41 also allows high flow rates, but has a somewhat lower retentivity than the polystyrenes or membranes. This difference is insignificant at high linear velocities (such as obtained through a 25 mm filter) but may become troublesome under other conditions. The effect of dust loading on flow rate is greater for W41 than for any of the other filters tested. The practical consequences of these properties will be treated in more detail below.

For a given filter type, Table 1a-4 also illustrates the effect of varying pump-filter combinations on flow rates per unit area. The pumps used here are representative of the common types currently in use. One type, the modified vacuum cleaner variety used with 20x25 cm high volume filter holders, provides very high total flow rates but must be used with low resistivity filters because of its small vacuum. The other type, such as is used with 25 and 47 mm diameter filter holders and some inertial impactors, provides a higher vacuum but its smaller free air capacity means lower absolute flow rates. These pumps are used most effectively when "purity" of sample, or high sample/blank ratio is desired rather than large total samples. For highly sensitive analytical methods such as neutron activation this "purity" of signal may be of greater importance than the larger but less "pure" signal from high volume pumps, especially for the shorter-lived isotopes whose detection limits are well below atmospheric concentrations and where absolute sample size is not so important. Indeed, Table 1a-4 reveals a threefold difference in flow rate per surface area between 25 mm and 20x25 cm sizes, making collection on the former preferable for the shorter sampling periods. Because they do not depend on air flow for their cooling, the high-vacuum pumps can also be equipped with high

resistivity filters for special applications.

One drawback to the small filters is that their effective surface area is considerably less than their total area. For example, using Gelman holders the unexposed edge zone is 25% of the total for a 25 mm filter and 45% for the 47 mm size. In contrast, the 20x25 cm size is large enough that samples for analysis can be cut wholly from the exposed interior.

Selection of a particular pump-filter combination is often dictated by the specific goal of the sampling, with the stringency of the filter impurity requirements increasing as the sample time decreases. For example, Table 1a-5 shows that for 24-hour samples on Whatman No. 41 paper there is little practical difference between a 20x25 cm sample and a 25 mm filter, for in each case the sample/blank ratios are well over 10 for most elements. Under these conditions a considerably less pure filter could satisfactorily be used. But when the sampling time is decreased to roughly 1 hour the differences in impurities and flow rates become much more critical.

The selection factors of flow rate, clogging, and impurity levels can be quantitatively combined into a "figure of merit," the sampling time needed to collect an amount of a given element equal to the amount present as impurity within the filter. Table 1a-6 gives these numbers for various filters and the atmospheric concentrations of the Niles, Michigan sample of Table 1a-1. Though corresponding numbers for remote or polluted urban locales may vary from these by a factor of 10 in either direction, the filter/filter ratios remain valid. Comparison of Column 2 with the others illustrates that the ultimate sensitivity of determination of several elements in very short period samples is often limited by the filter impurity levels rather than by interferences from other elements in the sample, examples being Cl, Br, Na, Cu, Al, Mn, Zn, and Sb.

In general, W41 shows the lowest values of the figure

of merit for most elements, with PS slightly higher (its Cl is much higher), and DMS, HAWP025, and AAWP025 considerably higher for most elements. For the two membranes HAWP025 and AAWP025 these high values are due in large part to their high resistivity and consequent low flow rates, while the high DMS values reflect actual impurity levels. From the standpoint of activation analysis the membranes have another disadvantage, for under irradiation they become increasingly brittle and highly susceptible to electrostatic charge induction. After a few hours' irradiation they are nearly impossible to handle, requiring dissolution in water or acid solution and nullifying the nondestructive aspect of the analysis. Because their essentially absolute collection efficiency down to at least a particle diameter of 0.3 μm does not seem to represent a significant sampling advantage over most of the other filters, we have abandoned the use of membrane filters.

Cellulose or Polystyrene?

The general requirements of activation analysis and our special interest in short-period samples narrow down the original list of possible filters to two types, the tightly-bound cellulose (W41) and the polystyrene (PS). Though the highly pure PS is apparently no longer available on a routine basis, there is no reason in principle why it cannot be made, and so will be considered further below.

Subsequent testing of another cellulose filter, TFA 810 (The Staplex Company, New York), has shown it to be very similar to W41 in physical and chemical properties. It thus may serve as an effective substitute when the somewhat cleaner W41 is not available. In the following discussion W41 will be considered the representative of the tightly-bound cellulose filters, which as a class will be referred to simply as "cellulose."

Though the figure of merit listings suggest W41 as the best filter choice, other physical properties seem to recommend polystyrene. In particular, the comparative DOP efficiencies of Lockhart and Patterson (1964) show W41 to drop

as low as 61% collection efficiency (at 0.3 μm diameter) at 7.3 cm-sec^{-1} face velocity (where Microsorban is still 99.87% efficient), while rising to 99.98% at 283 cm-sec^{-1}. This evidence may not be as clear-cut as it seems, though, for 3 other studies of W41 efficiencies exist, with somewhat conflicting results (Smith and Surprenant (1953), Fitzgerald and Detwiler (1954), Lindeken, Morgin, et al. (1963)). The lowest efficiency was found by Smith and Surprenant, 23% for 0.3 μm DOP at 10 cm-sec^{-1}. Fitzgerald and Detwiler used 0.35 μm duralumminum at this same velocity, obtaining an efficiency of 91%. The most detailed measurements, those of Lindeken, Morgin, et al., were obtained with solid polystyrene latex aerosols over a wide range of diameters and flow rates, with all efficiencies found to be greater than 74%. This solid aerosol was chosen to better simulate the natural aerosol than could liquid DOP, and may account for the higher efficiencies found. Lockhart and Patterson and Lindeken, Morgin, et al. agree on the rapid increase of efficiency with flow rate, and at typical actual sampling velocities of greater than 35 cm-sec^{-1} (and usually greater than 70 cm-sec^{-1}) they both give values in excess of 90%.

Informative as they are, we feel that the above arguments are somewhat unrealistic, however, because they are based on numbers obtained using clean filters rather than the dust-loaded filters of an actual sample. Another measurement of Lindeken, Morgin, et al. showed a very rapid increase in the collection efficiency of W41 with time, presumably because of plugging of air passages by the collected particles. Under their laboratory conditions, which seem nearly comparable to atmospheric sample accumulation rates, initial efficiencies of 75% would rise to greater than 95% in approximately 30 minutes, suggesting that in practice the results obtained with cellulose and polystyrene filters should be nearly indistinguishable.

To check this we collected simultaneous 24-hour 47 mm PS and W41 filter samples in one of the most industrialized

areas of East Chicago, Indiana, results of which are shown in Table 1a-7. Of 30 elements listed, 25 agreed to within one standard deviation, and in the case of Cl the discrepancy is due to its high impurity levels in the PS. For 25 elements (Cl, S, W, and Hg not included) the W41/PS atmospheric concentration ratios averaged 1:02 ± 0.05, lending weight to the idea that little or no efficiency differences can be seen in actual sampling. In the case of shorter-period samples where the dust loading may not increase the W41 efficiencies to such an extent, we prefer to use a 25 mm filter size. Collection velocities here are usually much larger than with the 47 mm size, bringing even the initial efficiencies into the 95%-or-greater range.

Another potential problem of cellulose is its well-known hygroscopicity. For applications involving weighing, these filters must be equilibrated at constant relative humidity before weighing. That this can be successfully implemented on a routine basis is demonstrated by the experience of the Bay Area Air Pollution Control District of San Francisco, which uses W41 for all its total particulate sampling.

The thinness of cellulose as compared to polystyrene or glass fiber makes small-sized thickness inhomogeneities more important, and definite variations in light transmittance trough a clean filter can be seen. These, however, are of a size scale very small relative to irradiation aliquots, and our experience has not shown them to be a problem. For 24-hour high volume filters the smallest piece needed for irradiation is approximately 1 cm^2 (for the short irradiation), and reproducibilities here are usually 10-20% or better.

On the positive side, the thinness of cellulose offers some distinct advantages over polystyrene. Since physical size of the irradiation aliquot is limited by flux gradients in the reactor core and the need to simultaneously irradiate several samples and a standard, the 5-6-fold increase in packaging efficiency offered by cellulose over polystyrene represents a real gain for the long-lived isotopes, where activities

are lowest and sample size is the limiting factor in many elemental sensitivities.

Another advantage of the cellulose filters is their high tensile strength. Not only is routine rough handling during sampling possible, but much of this tensile strength remains after irradiation. The polystyrenes, on the other hand, are quite fragile and require delicate handling, a property somewhat inconsistent with any proposed wide-scale use by local agencies. In particular, the polystyrenes cannot be used for total particulate determinations because of the loss of some edge material upon removal from the filter holder after sampling. This property alone eliminates them from consideration for general use.

Summary - Need for a Standard Filter

According to our experience, reasonable criteria for the selection of a single filter for use in all situations are: minimum impurities, maximum flow rate, and ease of handling both before and after irradiation. Of the filters presently available, Whatman No. 41 (or TFA 810) seems to best meet these requirements. Though it is not an ideal filter, particularly in its hygroscopic and dust loading properties, compensations for these features can satisfactorily be made. Practical tests, both by our laboratory and others, have shown the utility of this filter under all types of sampling conditions.

Now that the means for high-precision trace element analysis of atmospheric particulates are commensurate with the increasing interest in this field, we feel it imperative that local agencies begin regular sampling on inorganically pure filters, in order to establish a national stockpile for future analysis. Such a stockpile now exists, but the vast majority of these samples are on glass fiber filters, all varieties of which introduce high blanks into the nondestructive process and render the samples useless in this regard. We feel that a national stockpile should be accumulated on a standard filter type, and that the need to begin the

stockpile supersedes the lack of an ideal filter. Cellulose should be adopted temporarily until the development of a clearly superior type, an event likely to be at least several years in the future. Sampling at the local level could then be divided between cellulose and glass fiber filters. Unfortunately, since local sampling is normally used only for total particulate determination, and cellulose is more difficult to use and no better for this purpose, the work of local agencies would be complicated with the promise of little or no immediate gain for them. But in the long run the creation of a national reservoir of potential trace element data would seem to be worth such inconveniences, and might spur the development of a new filter type.

Impaction Surfaces

A growing number of atmospheric samples are being taken with inertial impactors, for size distribution both of total particulate and individual elements. A major part of our trace element work has been done with Andersen Samplers, 7-stage cascade devices where the aerosol particles impact onto circular plates some 9.6 cm in diameter. For nondestructive purposes we have found it convenient to cover the plates with a thin polyethylene sheet, which then becomes the actual impaction surface. The polyethylene circle with its impacted aerosol is then analyzed by the same procedure described above for the filters.

Since air does not pass through these circles, physical properties such as collection efficiency, flow rate, and clogging are removed from consideration, the only remaining important one being durability of the material under prolonged irradiation. On the other hand, elemental impurity levels become even more important because of:

1) the relatively low flow rates for impactors (28 lpm for the Andersen Sampler, for example)
2) the partitioning of the sample among several stages
3) the large collection area per stage.

Of the common organic materials which might be used for

collection surfaces, we have found Mylar and Teflon to be unsatisfactory. The Teflon becomes quite brittle under long irradiations, and the Mylar has large Mn and Sb impurity levels.

The best material we have found is polyethylene. Impurities here seem to be associated with the bulk of the material rather than the surface, making the thinnest sheeting the best. After analysis of different lots from different manufacturers we have settled on Durethene 12010 (Sinclair-Koppers Company, Chicago, Illinois), thickness 0.001." Impurity levels for this material are listed in Table 1a-7. As was the case for the filters, long-period samples have detection limits determined primarily by mutual elemental interferences, while for shorter samples the impurity levels for a few elements may become limiting. The low flow rates and sample division mentioned above serve to lengthen the sampling times needed to achieve the same precision as with filters. Another difference from the filters is that the elemental interferences vary greatly from stage to stage because of the variation of size distribution patterns for the elements.

This polyethylene withstands irradiations of 3×10^{17} n-cm^{-2}, and though it is more brittle after irradiation it can still be easily handled. Impurity levels are low enough to allow sampling times of less than a day, though other considerations have led us to adopt sample durations of 2-3 weeks.

Another feature of thin sheets such as these is their easy implementation to total particulate measurements. Since the mass of material per stage will be very small, a collection surface which is to be weighed before and after sampling should itself have as little mass as possible. The glass or stainless steel surfaces included in impactors are heavy enough to cause large errors when determining the difference between these two large numbers, but use of polyethylene greatly eases this situation. In addition, polyethylene has no hygroscopicity problems.

Table 1a-1. Nondestructive Activation Analysis of Aerosols

Element	$t_{irradiation}$	$t_{cooling}$	$t_{counting}$, Second	Detection limit, ng	Concentration, ng/m^3 air: Niles, Michigan[a]	Concentration, ng/m^3 air: East Chicago Indiana[b]
Al	5 min.	3 min.	400	40	800	1,000
V	5 min.	3 min.	400	1	3	10
Cu	5 min.	3 min.	400	100	30	900
Ti	5 min.	3 min.	400	200	100	100
S	5 min.	3 min.	400	25,000	---	10,000
Ca	5 min.	3 min.	400	1,000	900	4,000
Mg	5 min.	15 min.	1000	3,000	800	1,000
Br	5 min.	15 min.	1000	20	70	50
Cl	5 min.	15 min.	1000	500	---	---
Mn	5 min.	15 min.	1000	3	30	100
Na	5 min.	15 min.	1000	200	200	300
In	5 min.	15 min.	1000	0.2	0.02	0.05
K	5 hours	20-30 hours	2000	75	400	1,000
Zn	5 hours	20-30 hours	2000	200	50	3,000
Br	5 hours	20-30 hours	2000	25	50	70
As	5 hours	20-30 hours	2000	40	0.05	10
Ga	5 hours	20-30 hours	2000	10	---	1
La	5 hours	20-30 hours	2000	2	1	6
Sm	5 hours	20-30 hours	2000	0.05	0.1	0.4
Eu	5 hours	20-30 hours	2000	0.1	0.04	0.1
Sb	5 hours	20-30 hours	2000	30	1	30
W	5 hours	20-30 hours	2000	5	---	6
Au	5 hours	20-30 hours	2000	1	0.1	---
Sc	5 hours	20-25 days	4000	0.3	0.5	3
Cr	5 hours	20-25 days	4000	20	10	100
Co	5 hours	20-25 days	4000	2	0.3	3
Fe	5 hours	20-25 days	4000	1,500	600	10,000
Ni	5 hours	20-25 days	4000	1,500	---	---
Zn	5 hours	20-25 days	4000	100	60	2,000
Se	5 hours	20-25 days	4000	---	---	2
Ag	5 hours	20-25 days	4000	10	---	3
Sb	5 hours	20-25 days	4000	8	2	30
Ce	5 hours	20-25 days	4000	20	2	10
Hg	5 hours	20-25 days	4000	10	---	4
Th	5 hours	20-25 days	4000	3	0.4	1

[a] Average concentrations over 36 hours, 21-22 August 1969, 1.5 m above ground, wind variable <1 m/sec. at rural location 5 km from Niles, Michigan.

[b] Average concentrations over 24 hours, 11 June 1969, 3 m above ground, wind south 5-10 m/sec, in industrial ~1 km from Lake Michigan.

Table 1a-2. Filter Material Investigated

Filter Material	Manufacturer's Name	(Key)	Manfacturer	Specifications	Comments
Polystyrene	Microscrban	(PS)	Delbag Luftfilter (Germany)	----	No longer available
Polystyrene	Microsorban	(DMS)	Delbag Luftfilter (Germany)	----	Presently available
Cellulose-organic binder	Whatman No. 41	(W41)	W. and R. Balston Ltd. (England)	----	Tightly woven
Cellulose	----	(C)	C. H. Dexter and Sons (USA)	----	Loosely woven
Membrane cellulose esters	MF-Millipore	(HAWP025)	Millipore Filter Corp. (USA)	Pore size 0.45 um, diameter 25mm	----
Membrane cellulose esters	MF-Millipore	(HAWP047)	Millipore Filter Corp. (USA)	Pore size 0.45 um, diameter 47mm	----
Membrane cellulose esters	MF-Millipore	(AAWP025)	Millipore Filter Corp. (USA)	Pore size 0.8 um, diameter 25mm	----
Membrane cellulose esters	MF-Millipore	(AAWP047)	Millipore Filter Corp. (USA)	Pore size 0.8 um, diameter 47mm	----
Membrane cellulose acetate	Cellotate	(EHWP047)	Millipore Filter Corp. (USA)	Pore size 0.5 um, diameter 47mm	----
Membrane cellulose triacetate	Metricel	(GA-6)	Gelman Instrument Co. (USA)	Pore size 0.45 um, diameter 47mm	----

Table 1a-3 Filter Impurity Levels (ng/cm^2)

	PS	DMS	W41	C	HAWP025	HAWP047	AAWP025	AAWP047	EHWP047	GA-6
Cl	3,000	27,000	100	300	1,000	1,000	1,700	1,000	1,800	600
Br	25	1,000	5	20	4	3	< 5	< 2	6	4
S	---	±30,000	---	6,000	---	---	4,800	---	---	---
Na	80	90	150	700	600	330	520	400	1,800	2,200
K	20	8	15	200	130	100	120	100	---	---
Mg	<200	< 1,500	< 80	2,400	< 300	< 200	400	200	---	---
Ca	300	300	140	3,800	670	250	500	370	570	1,250
Ba	7,000	< 500	< 100	< 100	< 100	< 100	< 100	< 100	---	---
Al	20	20	12	200	20	10	15	10	60	740
Sc	0.04	< 0.01	< 0.05	0.2	< 0.05	< 0.01	< 0.01	< 0.05	---	---
Ce	< 0.4	< 1	< 0.5	< 0.3	< 0.5	< 1	< 0.5	< 0.3	---	---
La	< 0.2	< 0.1	< 0.2	< 0.3	< 0.1	< 0.2	< 0.5	< 0.2	---	---
Ti	10	70	10	50	15	5	10	< 10	---	---
Fe	100	85	40	300	40	< 300	80	40	---	---
Mn	1	2	0.5	80	7	2	2.5	2	6	2
Co	0.2	0.2	0.1	0.8	0.2	< 1	0.4	0.1	---	---
Ni	25	< 25	< 10	60	< 8	< 50	14	< 20	---	---
Ag	< 2	< 2	2	3	< 4	---	< 3	< 1	---	---
Cu	10	320	< 4	90	20	40	85	60	25	30
Zn	60	515	< 25	30	25	20	10	7	---	---
Sb	2.5	1	0.15	0.5	0.5	3	0.4	1	---	---
Cr	5	2	3	12	15	14	20	15	---	---
Hg	3	1	0.5	3	< 0.4	< 1	< 1	0.5	---	---
V	0.06	< 0.6	< 0.03	0.5	< 0.06	0.09	< 0.2	< 0.05	< 0.05	< 0.05

(-) not determined

Table 1a-4. Selected Physical Properties of Filters

Filter material	PS	DMS	W41	C	HAWP025	HAWP047	AAWP025	AAWP047	EHWP047	GA-6
Flow rate ($l\text{-}min.^{-1}\text{-}cm^{-2}$) 20x25 cm (effective surface 400 cm^2)	4.5	4.5	4.5	6	---	---	---	---	---	---
Flow rate ($l\text{-}min.^{-1}\text{-}cm^{-2}$) 47 mm diameter (effective surface 9.62 cm^2)	6.5	6.5	6.5	7	---	2.6	---	4.8	2.6	2.6
Flow rate ($l\text{-}min.^{-1}\text{-}cm^{-2}$) 25 mm diameter (effective surface 3.68 cm^2)	12	13	13	17	4.3	---	7.3	---	---	---
Retention (%) of 0.3 μm D.O.P. aerosol*** (25mm diameter)	99.96	99.95	99.7	--->	99.98	---	99.97	---	---	---
Retention (%) of 0.3 μm D.O.P. aerosol*** (20x25 cm)	99.8	99.7	91	80**	---	---	---	---	---	---
Volume filtered at 10% reduction in flow*** (m^3_{air}/cm^2_{filter})	48	35	2.0 2.8*	>50*	4.1*	4.1*	6.3	6.3	---	---
Thickness (mm)***	---	---	0.25	---	---	---	---	---	---	---
Tensile strength ($kg\text{-}cm^{-1}$)***	0.15	0.15	1.41	---	---	---	0.29	0.29	---	---

*Determined by the authors in Ann Arbor, Michigan
**Determined by Brar et al. (1969) for total particulate by weight in Chicago
***Determined by Lockhart and Patterson (1964)

Table 1a-5. Sample/blank Ratios for 25mm Diameter W41 Filters, using Niles, Michigan Concentrations

Element	Conc. (ng/m^3)	(Sample/Blank)* 1 hr sample	4 hr sample	24 hr sample
Cl	100**	0.6**	2.3**	12**
Br	70	8	33	160
Na	200	0.8	3	16
K	400	16	62	310
Ca	900	4	15	75
Al	800	40	160	800
Ti	100	6	23	120
Fe	600	9	35	180
Mn	30	35	140	700
Co	0.3	1.8	7.0	35
Sb	2	8	31	160
Cr	10	2	8	40
V	3	>60	>230	>1200
Cu	30	>4	>17	>80
Zn	60	>1.4	>5.6	>28

*For {47mm diameter / 20x25 cm} multiply by {0.37 / 0.46}

**From cascade impactor data of same period.

Table 1a-6. Sampling Times to Equal Blank Values or Detection Limits

Element	Sampling time at Niles in hours on 25mm filter disc to equal:						
	Detection Limit	PS Blank	DMS Blank	W41 Blank	C Blank	HAWP025 Blank	AAWP025 Blank
Cl	2	60	500	1.7	4	50	50
Br	0.15	0.8	29	0.15	0.4	0.35	---
Na	0.5	1	0.9	1.5	5	18	9
K	0.1	0.1	0.04	0.085	0.8	2.2	1
Mg	1.5	---	---	---	4	---	1.5
Ca	0.5	0.7	0.6	0.25	5.5	3.8	1.7
Al	0.02	0.05	0.04	0.025	0.3	0.15	0.06
Ti	0.6	0.2	1	0.1	0.5	0.7	0.35
Fe	1	0.3	0.25	0.1	0.6	0.35	0.4
Mn	0.05	0.08	0.15	0.035	4	1.5	0.3
Co	2.8	1.5	1	0.6	3.3	3.5	4
Cu	2	1	25	---	5	5	12
Zn	0.7	2.5	18	---	0.75	2.5	0.6
Sb	2	3.5	1.5	0.2	0.5	2	1
Cr	0.8	1	0.35	0.5	1.5	7.8	6

(-) If for the blank value only a higher limit was found or if it was not determined.

Table 1a-7. Polystyrene-Cellulose Efficiency Comparison

Element	Atmospheric Concentration (ng/m^3)		Concentration Ratio
	Polystyrene	Whatman No. 41	What. No. 41/ Poly.
Cl	4400 (500)*	7500 (500)	1.70
Br	350 (90)	500 (50)	1.43
S	15 (15)	43 (25)	2.87
Na	900 (150)	1300 (200)	1.44
K	4000 (400)	4200 (200)	1.05
Mg	730 (400)	760 (150)	1.04
Ca	4100 (800)	3900 (500)	0.95
Al	2300 (400)	2800 (200)	1.22
Ga	4.5 (1.0)	4.6 (1.5)	1.02
Sc	4.9 (0.6)	3.4 (0.5)	0.69
Ce	17 (3)	12 (2)	0.71
La	4.6 (0.5)	4.6 (0.5)	1.00
Sm	0.67 (0.10)	0.67 (0.10)	1.00
Eu	0.18 (0.04)	0.13 (0.03)	0.72
Ti	170 (50)	280 (80)	1.65
Fe	22,000 (4,000)	15,000 (3,000)	0.68
Mn	240 (40)	280 (30)	1.12
Co	3.9 (0.5)	2.9 (0.4)	0.74
Ni	55 (55)	70 (60)	1.27
W	1.5 (0.7)	< 2	----
Ag	3 (3)	2.5 (2.0)	0.83
Cu	130 (20)	160 (20)	1.23
Zn	4400 (200)	4300 (200)	0.98
As	29 (7)	35 (8)	1.21
Sb	21 (5)	21 (5)	1.00
Cr	90 (15)	70 (15)	0.78
Hg	1.7 (1.1)	< 1.6	----
V	58 (5)	66 (5)	1.14
Se	16 (3)	14 (3)	0.88
Th	1.0 (0.2)	0.8 (0.2)	0.80

*Large filter impurity correction

Table 1a-8. Impurity levels in Durethene polethylene, No. 12010

Element	Concentration ($ng\text{-}cm^{-2}$)
Cl	8 (2)
Br	1.0 (0.5)
Na	2.5 (0.4)
K	1.2 (0.3)
Mg	8 (6)
Al	6.8 (1.0)
Sc	< 0.006
Ce	< 0.009
La	< 0.04
Ti	11 (6)
Fe	< 11
Mn	0.10 (0.02)
Co	0.02 (0.01)
Ni	< 1.3
Ag	< 0.3
Cu	1.0 (0.5)
Zn	2 (1)
Sb	0.04 (0.01)
Cr	< 0.3
Hg	< 0.1
V	0.010 (0.003)

APPENDIX 1b

REMARKS ON SAMPLING TECHNIQUES

A number of special problems arise in sampling for eventual analysis by nondestructive neutron activation techniques. Sampling procedures are often dependent on the specific analytical technique, and it is important to bear in mind that the following discussion is concerned solely with problems related to NNAA.

The Andersen Sampler

From the standpoint of nondestructive neutron activation analysis, sampling with the Andersen impactor for elements with short-lived isotopes is easy. Any 24-hour sample will do quite well for the first and second counts (short irradiation) and nearly as well for the third count (long irradiation). But the fourth count (long-lived isotopes) is very difficult here, simply because the sample mass is not great enough to provide adequate decay rates (see results of sample A1, Table 5-2).

The reasons for this are twofold: the low flow rate of the Andersen Sampler (28 lpm is optimum) and division of the sample among the seven stages and filter.

To alleviate this problem the total counts accumulated in the long-lived spectrum must be increased by more than an order of magnitude over the number obtained from the standard 24-hour sample. Possible solutions include increasing irradiation time, counting time, or sample size. Irradiation time cannot be significantly increased, for it is already at the limit for polyethylene (5 hours in the core). Other methods of encapsulation, such as quartz tubing, are much more time-consuming and complicated, though they remain an option. Counting time can perhaps be doubled or tripled from the nominal 4000 seconds, but the number of samples needing processing precludes an order-of-magnitude increase.

The third approach was therefore incorporated, namely,

a great increase in the sample size. This was first tried in the Mackinac Island Experiment (3-week samples), with high-quality size distributions for such interesting long-lived elements as Fe, Co, Cr, Hg, Se, Zn, Sc, and Sb being obtained for the first time. These results were so satisfactory that the 3-week period was adopted for the duration of the remote sampling.

Long-term samples have other advantages over the 24-hour variety. Because of their fewer numbers they decrease the analytical burden, and the average values obtained may well be more significant for most elements than the more variable daily averages. In addition, the experimenter planning a small number of long samples is encouraged to focus his efforts on optimization of sampling and analysis rather than on needless repetition of shorter samples

As discussed in Chapter II, the disadvantage of the long-period sample is the elimination of the backup filter. Though this sacrifice is necessary in the midwestern U.S., it may be possible to circumvent it in the more remote regions. Future experiments should investigate this matter further.

Diurnal Studies

The essence of a diurnal variations study lies in revealing the extent of concentration variations in as much detail as possible. Since atmospheric concentration changes may occur with time scales of minutes or tens of minutes (fumigation, for example), short sample times constitute the primary goal. But shorter samples have lower sample/blank ratios on the filter paper, and times shorter than about 1 hour introduce large uncertainties for those elements with significant blanks. In addition, the smaller mass collected reduces the decay rates, most critically affecting the medium- and long-lived isotopes.

Our results have shown that for sample times on the order of 1-2 hours with a 25 mm filter and Gelman Twin Cylinder pump the elements Mn, Al, V, Br, Na, Cl, K, and Sm may

be reliably determined in midwestern rural areas, in approximately that order of decreasing sensitivity. It is important to note that this list only contains two elements (K,Sm) which come from counts other than the first two, and these elements are among the least well-determined of the better ones. No long-lived elements are on this list.

There is a temptation to try to extend the list by increasing the sample times to 4 hours or so. This may well add some elements, but at the price of time resolution. It is the feeling of this writer that the time resolution aspects of a diurnal experiment supersede the number of elements followed, especially because 1) the above list is nearly always found, and 2) our results have shown that a great deal of parallelism usually exists in the behavior of the elements, so that some of the better-determined ones can serve effectively as indicators for others. For example, determination of the rare earths is not so important when Al is also found, for they all seem to have the soil (or industrial soil dust) as their principal source. Zn will parallel Sb in most cases, and As and In will usually be parallel.

On the other hand, there is no inherent limitation to this small list of well-determined elements. Larger pumps and larger filters can collect greater samples in the same time (the linear air velocity should remain as high as for the 25 mm filter) and should allow routine determination of several of the more sensitive long-lived elements.

Nondestructive Neutron Activation Analysis of Air Pollution Particulates

R. Dams,[1] J. A. Robbins, K. A. Rahn, and J. W. Winchester[2]

Dept. of Meteorology & Oceanography and Great Lakes Research Division, University of Michigan, Ann Arbor, Mich. 48104

A nondestructive and computer assisted neutron activation analytical procedure for the determination of up to 33 elements in air pollution particulates has been designed and tested in studies of samples taken in and near the Northwest Indiana industrial area. Samples are counted after (1) 3 minutes, (2) 15 minutes, (3) 20–30 hours, and (4) 20–30 days following neutron irradiation for (1) Ca, Ti, V, Cu, Al, S, (2) Na, Mg, Mn, In, Cl, Br, I, (3) K, La, Sm, Eu, Cu, Zn, W, Au, Ga, As, Sb, Br, (4) Sc, Ce, Th, Cr, Fe, Co, Ni, Ag, Zn, Hg, Sb, Se using a Ge(Li) detector.

ELEMENTAL ANALYSIS of pollution aerosols requires a precise yet sensitive method if the results are to be used for study of source identification or atmospheric transport processes. For studies involving large numbers of samples speed and ease of analysis are necessary, and selectivity in the detection of many elements at the nanogram to microgram level is desirable in order to permit sampling of only a few cubic meters of air. Zoller and Gordon (*1*) have presented a discussion of the principles and merits of nondestructive neutron activation analysis in this application, together with an outline of a procedure and results of several analyses of Cambridge, Massachusetts, air pollution particulate samples for more than 20 elements. In this paper we present a procedure which extends the method to 33 elements and utilizes a computer data processing technique offering a good compromise between speed, accuracy, and economy. A thorough test of reproducibility of the procedure is presented by the results of replicate determinations of samples taken in East Chicago, Indiana, and Niles, Michigan.

The National Air Sampling Network (*2*) has used an emission spectrographic technique to analyze for 16 elements—Be, Bi, Cd, Co, Cr, Cu, Fe, Mn, Mo, Ni, Pb, Sb, Sn, Ti, V, Zn—using a procedure involving ashing and extracting in nitric acid. The method requires skilled operators, is not highly sensitive, and is often limited by high blank values for several elements. Of the reported values 45% are given only as upper limits. When the high neutron fluxes of nuclear reactors are used, neutron activation analysis is an extremely sensitive method and no blanks due to chemical reagents are introduced. Several authors (*3–5*) have applied NaI γ spectrometry coupled with radiochemistry for resolution of the γ spectra to the determination of several elements in aerosols. High resolution Ge(Li) detectors greatly extend the scope of nondestructive activation analysis so that a very large number of isotopes can be counted simultaneously. If computer assisted, this technique can become almost completely automated. Several authors (*1*, *6–8*) have used Ge(Li) detectors for destructive or nondestructive analysis of aerosols.

Sampling Procedure. Aerosols may be sampled by passing air through a filter which allows a high flow rate and at the same time has good particle retentivity down to 0.1 μm size. Glass fiber filters have often been used for the analysis of organics, sulfate, nitrate, and total particulate, but this filter must be ruled out for nondestructive activation analysis because of its high concentrations of trace metals. Although it is not an ideal filter, polystyrene (*9*) was used in the present investigation, combining a good filtering performance with fairly low blank values. However, the sensitivity of a number of elements, such as Cl, Na, Al, Ca, Mn, Zn, and Sb, is still limited by the magnitude of the blank (*9*), and values for Cl are not reported in the test results described below for this reason.

Insofar as pumps are concerned, those in common use for air pollution monitoring are low vacuum, high volume types used with 20 × 25 cm (8 × 10 inch) filters. In the present investigation, however, high vacuum, low free air capacity pumps equipped with 25 mm (or 47 mm) diameter holders were also used. Where the high volume pumps generate a flow rate of 4.5 l./min-cm^2 the high vacuum pumps and 25 mm holders reach 12 l./min-cm^2. In spite of the fact that the latter holder has an unexposed waste zone at the edge of the filter (25% of the total area) which decreases the signal to blank ratio somewhat, this figure is still twice as high as for the high volume sampler.

Nondestructive Neutron Activation Analysis. A procedure for the nondestructive analysis of air pollution particulate matter for up to 33 elements in solid form has been developed, though it can also be used for the analysis of other types of environmental samples as well.

For the analysis of elements giving rise to short-lived isotopes, each sample in our procedure is packaged in a polyethylene vial, then placed in a rabbit which carries it through a pneumatic tube to a position near the core of the Ford Nuclear Reactor on the campus of the University of Michigan, where it is irradiated for five minutes at a flux of 2×10^{12} neutrons/cm^2 sec. At the end of this period it rapidly returns to the laboratory where it is manually transferred to a counting vial and carried to the counting room. At three minutes

[1] Present address, Institute for Nuclear Research, University of Ghent, Ghent, Belgium.

[2] Present address, Dept. of Oceanography, Florida State University, Tallahassee, Fla. 32306

(1) W. H. Zoller and G. E. Gordon, ANAL. CHEM., 42, 256 (1970).
(2) U. S. Public Health Service, Air Quality Data from the National Air Sampling Networks and Contributing State and Local Networks, 1966 Edition, Durham, N. C., 1968.
(3) S. S. Brar, D. M. Nelson, E. L. Kanabrocki, C. E. Moore, C. D. Burnham, and D. M. Hattori, Proceedings 1968 International Conference "Modern Trends in Activation Analysis," Gaithersburg, Maryland, 1969, p 43.
(4) R. M. Loucks, J. W. Winchester, W. R. Matson, and M. A. Tiffany, Proceedings 1968 International Conference "Modern Trends in Activation Analysis," Gaithersburg, Maryland, 1969, p 36.
(5) J. R. Keane and E. M. R. Fisher, *Atmospheric Environ.*, 2, 603 (1968).
(6) N. D. Dudey, L. E. Ross, and V. E. Noshkin, Proceedings 1968 International Conference "Modern Trends in Activation Analysis," Gaithersburg, Maryland, 1969, p 55.
(7) G. L. Hoffman, R. A. Duce, and W. H. Zoller, *Environ. Sci. Technol.*, 3, 1207 (1969).
(8) K. K. S. Pillay and C. C. Thomas, Jr., Report WNY-046, Western New York Nuclear Research Center, Buffalo, 1969.
(9) R. Dams, K. Rahn, and J. W. Winchester, unpublished data, 1970.

Reprinted from ANALYTICAL CHEMISTRY, Vol. 42, Page 861, July 1970

Table I. Nuclear Properties and Measurement of Short-Lived Isotopes

Element	Isotope	Half-life	$t_{irradiate}$	$t_{cool.}$	$t_{count.}$	Gamma-rays used, keV
Al	^{28}Al	2.31 min.	5 min.	3 min.	400 sec.	1778.9
S	^{37}S	5.05 min.	"	"	"	3102.4
Ca	^{49}Ca	8.8 min.	"	"	"	3083.0
Ti	^{51}Ti	5.79 min.	"	"	"	320.0
V	^{52}V	3.76 min.	"	"	"	1434.4
Cu	^{66}Cu	5.1 min.	"	"	"	1039.0
Na	^{24}Na	15 hr.	"	15 min.	1000 sec.	1368.4; 2753.6
Mg	^{27}Mg	9.45 min.	"	"	"	1014.1
Cl	^{38}Cl	37.3 min.	"	"	"	1642.0; 2166.8
Mn	^{56}Mn	2.58 hr.	"	"	"	846.9; 1810.7
Br	^{80}Br	17.6 min.	"	"	"	617.0
In	^{116m}In	54 min.	"	"	"	417.0; 1097.1
I	^{128}I	25 min.	"	"	"	442.7

Table II. Nuclear Properties and Measurement of Long-Lived Isotopes

Element	Isotope	Half-life	$t_{irradiate}$	$t_{cool.}$	$t_{count.}$	Gamma-rays used, keV
K	^{43}K	12.52 hr.	2–5 hr.	20–30 hr.	2000 sec.	1524.7
Cu	^{64}Cu	12.5 hr.	"	"	"	511.0
Zn	^{69m}Zn	13.8 hr.	"	"	"	438.7
Br	^{82}Br	35.9 hr.	"	"	"	776.6; 619.0; 1043.9
As	^{76}As	26.3 hr.	"	"	"	657.0; 1215.8
Ga	^{72}Ga	14.3 hr.	"	"	"	630.1; 834.1; 1860.4
Sb	^{122}Sb	2.75 day	"	"	"	564.0; 692.5
La	^{140}La	40.3 hr.	"	"	"	486.8; 1595.4
Sm	^{153}Sm	47.1 hr.	"	"	"	103.2
Eu	^{152m}Eu	9.35 hr.	"	"	"	121.8; 963.5
W	^{187}W	24.0 hr.	"	"	"	479.3; 685.7
Au	^{198}Au	2.70 day	"	"	"	411.8
Sc	^{46}Sc	83.9 day	"	20–30 day	4000 sec.	889.4; 1120.3
Cr	^{51}Cr	27.8 day	"	"	"	320.0
Fe	^{59}Fe	45.1 day	"	"	"	1098.6; 1291.5
Co	^{60}Co	5.2 yr.	"	"	"	1173.1; 1332.4
Ni	^{58}Co	71.3 day	"	"	"	810.3
Zn	^{65}Zn	245 day	"	"	"	1115.4
Se	^{75}Se	121 day	"	"	"	136.0; 264.6
Ag	^{110m}Ag	253 day	"	"	"	937.2; 1384.0
Sb	^{124}Sb	60.9 day	"	"	"	602.6; 1690.7
Ce	^{141}Ce	32.5 day	"	"	"	145.4
Hg	^{203}Hg	46.9 day	"	"	"	279.1
Th	^{233}Pa	27.0 day	"	"	"	311.8

after irradiation a count of 400 seconds live-time duration is begun, and this is followed by a count of 1000 seconds live-time starting 15 minutes after irradiation. Both these and subsequent counts are performed on a 30 cm^3 Ge(Li) detector coupled to a 4096 channel analyzer. The detector is housed in an iron shield and operated in an air conditioned room at a gain setting of 1 keV/channel. The observed resolution is 2.5 keV FWHM for the ^{60}Co 1332 keV photopeak and a peak to Compton ratio of 18/1. Table I shows the isotopes determined by the first two counts.

All spectra are recorded on 7-track magnetic tape for future data analysis and can also be printed on paper tape. Conversion of counting rates under the various peaks to concentrations is accomplished by subjecting a few standard solutions containing well-known mixtures of these same elements to the same irradiation and counting sequence. To avoid possible errors due to coincidence summing or to broadening of peaks at high counting rates, sample sizes are generally adjusted to make counting rates of sample and standard of comparable magnitude.

Though all the short irradiations are performed at the same site in the reactor and under conditions of nearly constant power, small corrections for variations of both the neutron flux and rabbit placement from irradiation to irradiation are accomplished by co-irradiation of a titanium metal foil flux monitor with each sample. It is counted for 20 seconds at 13 minutes after the end of irradiation, between the two sample counts. If the analysis rate does not exceed one sample in 40 minutes, the same flux monitor may be used repeatedly, with less than 1% of the original 5.8-minute ^{51}Ti remaining in the next count. Net counting rates of the sample spectrum are normalized to an arbitrary Ti activity, equivalent to a reference neutron flux. Experimentally we have found that during one 20-day reactor operating cycle the standard deviation of the flux as determined by means of this flux monitor was 3%. However, variations of up to 8% were experienced between the neutron flux at the irradiation site during different reactor cycles.

The same sample, or another portion of the same air filter, is then irradiated at a higher flux (1.5×10^{13} neutrons/cm^2 sec) for 2–5 hours in the reactor core. Each is individually heat sealed in a polyethylene tube and irradiated together with eight others plus a standard mixture of elements in a polyethylene bottle, 4 cm in diameter, lowered into the reactor pool. Cooling of the samples during irradiation is achieved by allowing the pool water to circulate through several holes cut in the container bottle. Standards are prepared by depositing 100 μl each of two well-balanced mixtures of the appropriate

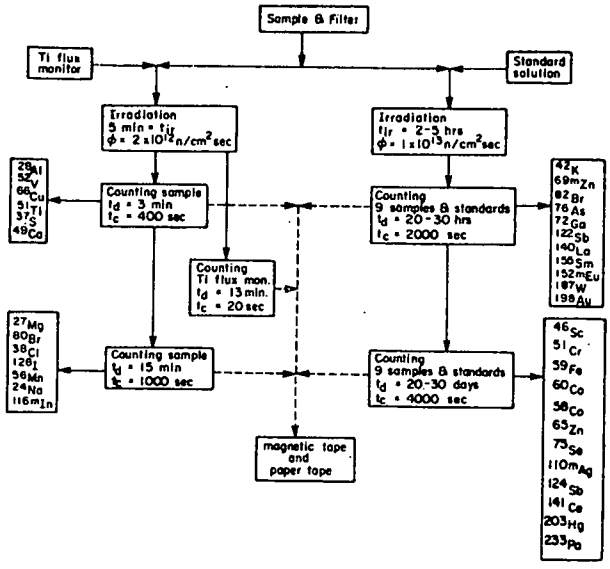

Figure 1. Irradiation-counting scheme

elements onto a highly pure substrate (ashless filter paper) and allowing to dry, then sealing immediately inside polyethylene tubes. After irradiation, the samples and standards are transferred to clean containers and counted once for 2000 seconds live-time after 20–30 hours of cooling and then for 4000 seconds live-time after 20–30 days of cooling. Table II shows elements determined from these counts. Horizontal and vertical flux gradients at the irradiation site in the core have been measured, and errors due to thermal neutron flux gradients over the bottle dimensions appear to be less than 5% provided the samples are confined to a single horizontal layer of vertically oriented tubes at the bottom of the bottle and the bottle is rotated 180° at half of the irradiation time. Fast neutron flux gradients at this site are about twice as large as thermal gradients, but the only fast neutron reaction used in our procedure is in the determination of nickel, ^{58}Ni (n,p) ^{58}Co.

The entire irradiation and counting procedure is illustrated in Figure 1, and Tables I and II list the γ transitions used. Sometimes the most prominent photopeak of an isotope cannot be used because of interferences by neighboring peaks of other isotopes. Examples of unusable peaks include 844 keV of ^{27}Mg (846 keV ^{56}Mn) and 559 keV of ^{76}As (555 keV ^{82}Br and 564 keV ^{122}Sb). The monoenergetic ^{203}Hg (279.1 keV) is interfered with by ^{75}Se (279.6 keV), but a correction based on the spectrum of pure ^{75}Se can be applied because the interference is usually less than 20% of the ^{203}Hg activity in the air pollution samples we have analyzed so far. The measurement of ^{64}Cu (511.0 keV) is interfered with by external pair production of high energy γ-rays. In typical samples 15-hour ^{24}Na is the most important source of high energy γ-rays after a decay period of 20 hours, and a correction, usually less than 10%, can be applied to the apparent ^{64}Cu activity.

The ratio of thermal to fast neutron flux was determined at both irradiation sites using the reactions ^{31}P (n,γ) ^{32}P and ^{32}S (n,p) ^{32}P. The ratios obtained were 7.5 for pneumatic tube and 4.5 for pool irradiation sites. Interferences by threshold reactions were calculated and checked experimentally, with the finding that in typical aerosol samples the only reaction affecting a calculated concentration by more than 2% is ^{27}Al (n,p) ^{27}Mg. Once the aluminum concentration is know, the appropriate correction can be applied to the magnesium concentration.

Automated Data Reduction. In order that our nondestructive neutron activation analysis procedure should be applicable to large numbers of samples, such as in routine monitoring, some sort of automatic data reduction is necessary. We feel that accuracy as well as speed is increased by elimination of many human errors, but we have also found that human judgment should be retained in the examination of the data and in devising procedures for checking data quality.

In the present investigation a computer program was developed and used to do the following: (1) qualitatively determine the presence of isotopes, (2) calculate net peak areas, (3) convert areas to weights of trace elements, (4) subtract analytical blanks due to filter materials, (5) calculate concentrations of trace elements in the originally sampled air.

The Program. The magnetic tape on which up to 100 γ-ray spectra, each of 4096 channels, are stored is submitted to the IBM 360/67 computer together with a Fortran IV program typed on cards. The program makes an inventory of the tape and creates a new compact error-free version, providing a list with position and tagword of each spectrum on the final tape.

Initially an approximate energy calibration of the spectrometer is required. On this basis the program can refine and update the calibration for each spectrum by comparing the observed positions of some prominent peaks with the true γ-ray energies, present as a data library in the program. This calibration fit can in principle be a polynomial of any order, but usually a linear or at most quadratic fit suffices.

The main program for obtaining trace element concentrations from spectra requires a data set specifying γ transition energies of expected peaks. From this and the above energy calibration an approximate peak location is computed. The channel with the greatest number of counts is sought in a 7-channel interval centered on this calculated location. If this channel occurs at the end of the search interval, such as if the expected peak is masked by the edge of a nearby large peak, it fails to qualify as a peak and the program moves on to the next peak search; otherwise it is taken as the actual peak location. The net peak area is evaluated by summing counts

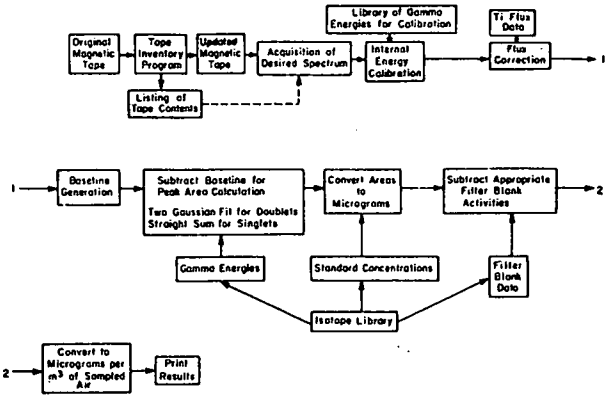

Figure 2. A simplified flow diagram of automated spectrum analysis

over an interval of seven channels centered about the actual peak position and subtracting base-line counts. The estimate of the base line under peaks is accomplished by a regression technique as described by Ralston and Wilcox (*10*). Not all maxima found within the scan interval are associated with real peaks. Included in the output is a measure of the statistical significance of each net peak area which enables the user to assess data quality at a glance.

Further data sets are provided in the program. For the short counts (Table I) these include conversion factors from peak areas to concentrations (calculated from standard short lived spectra), and for the longer count data (Table II) they include concentrations of the elements in the standards, filter blank values, and isotope half lives. Apart from the above data sets, the program requires only one card per spectrum, containing information about the irradiation and count type, filter type and fraction of sample irradiated, whether the sample is a standard, flux monitor, or unknown, and finally factors used in converting weights of elements to concentrations in air, expressed in any desired units.

If the spectrum is a flux monitor, only one net peak area is determined (320 keV ^{51}Ti). This value is used to normalize all peak areas of the unknown (400 and 1000 second counts) to a reference neutron flux. In an unknown sample the peak areas are converted to weights. If the spectrum is from a long count (2000 or 4000 seconds), peak areas are compared to those of the standard and after decay corrections (arising because sample and standard are not counted at the same time after irradiation) weights of the trace elements are calculated. Appropriate blanks are subtracted, followed by division by volume of air sampled to give concentrations. A detailed error analysis gives standard deviations of concentrations based on counting statistics and uncertainties in blank and standard values. Figure 2 shows schematically the outline of the computer program.

In its present form the program does not resolve doublets. A Gaussian fit treating these cases has been tried successfully in some cases but the increased running time and consequent expense does not justify its inclusion as a permanent feature of the program. For similar reasons the computer technique is supplemented by manual calculations for ^{76}As, ^{72}Ga, ^{122}Sb, and ^{187}W where very small photopeaks are located on tails of neighboring large peaks. Processing of one 4096 channel spectrum takes about 15 seconds of computer time, and the turnaround time at the University of Michigan Computing Center for analysis of a full magnetic tape of up to about 100 spectra may be as short as one hour.

Table III. Sensitivities for Determination of Trace Elements in Aerosols

		Neutron activation		Emission spectrography
Element	Decay time[a]	Detection limit (μg)	Minimum concentration in urban air (μg/m³) 24-hour sample	minimum concentration in urban air (μg/m³) 24-hour sample
Al	3 min.	0.04	0.008	...
S	"	25.0	5.0	...
Ca	"	1.0	0.2	...
Ti	"	0.2	0.04	0.0024
V	"	0.001	0.002	0.0032
Cu	"	0.1	0.02	0.01
Na	15 min.	0.2	0.04	...
Mg	"	3.0	0.6	...
Cl	"	0.5	0.1	...
Mn	"	0.003	0.0006	0.011
Br	"	0.02	0.004	...
In	"	0.0002	0.00004	...
I	"	0.1	0.02	...
K	20–30 hr.	0.075	0.0075	...
Cu	"	0.05	0.005	0.01
Zn	"	0.2	0.02	0.24
Br	"	0.025	0.0025	...
As	"	0.04	0.004	...
Ga	"	0.01	0.001	...
Sb	"	0.03	0.003	0.040
La	"	0.002	0.0002	...
Sm	"	0.00005	0.000005	...
Eu	"	0.0001	0.00001	...
W	"	0.005	0.0005	...
Au	"	0.001	0.0001	...
Sc	20–30 day	0.003	0.000004	...
Cr	"	0.02	0.00025	0.0064
Fe	"	1.5	0.02	0.084
Co	"	0.002	0.000025	0.0064
Ni	"	1.5	0.02	0.0064
Zn	"	0.1	0.001	0.24
Sc	"	0.01	0.0001	...
Ag	"	0.1	0.001	...
Sb	"	0.08	0.001	0.040
Ce	"	0.02	0.00025	...
Hg	"	0.01	0.0001	...
Th	"	0.003	0.00004	...

[a] Decay time before counting. See Tables I and II.

Sensitivity. The sensitivity for the different elements is often determined by the composition of the sample because it may be limited by the degree of interference from other substances. Column 3 of Table III shows the sensitivity

(10) H. R. Ralston and G. E. Wilcox, Proceedings 1968 International Conference "Modern Trends in Activation Analysis," Gaithersburg, Maryland, 1969, p 1238.

Table IV. Elements Detected in Suspended Particulate from East Chicago, Indiana, ng/m³

Element	1st Anal.[a]	2nd Anal.[a]	3rd Anal.[a]	4th Anal.[a]	Mean[b]
Ca	7700 (1200)	6600 (1000)	6650 (1000)		7000 (700)
Ti	225 (60)	165 (55)	170 (60)		190 (40)
V	20 (1.4)	16.1 (1.2)	18.2 (1.3)		18.1 (1.5)
Cu	1020 (100)	1050 (100)	1140 (100)		1070 (80)
Al	2370 (150)	1980 (130)	2200 (150)		2175 (170)
S	11,000 (9,000)	...	15,000 (9,000)		13,000 (8,000)
Na	485 (36)	405 (35)	470 (40)		455 (40)
Mg	2600 (750)	1650 (700)	2850 (800)		2400 (600)
Mn	245 (14)	222 (12)	305 (17)		255 (40)
In	0.13 (0.07)	0.06 (0.06)	0.11 (0.07)		0.10 (0.05)
Br	81 (9)	74 (9)	94 (10)		83 (9)
K	1510 (100)	1380 (70)	1600 (160)	1210 (120)	1415 (150)
La	5.8 (0.7)	6.0 (0.5)	6.5 (0.6)	5.6 (0.7)	5.9 (0.4)
Sm	0.53 (0.06)	0.35 (0.04)	0.47 (0.04)	0.39 (0.05)	0.41 (0.05)
Eu	0.165 (0.03)	0.12 (0.03)	0.17 (0.05)	0.10 (0.03)	0.135 (0.02)
Cu	1150 (150)	1125 (150)	1200 (150)	1100 (150)	1150 (100)
Zn	1440 (150)	1370 (140)	1420 (140)	1365 (140)	1400 (100)
W	7.6 (2)	5.0 (1)	5.6 (1)	5.2 (2)	5.8 (1)
Ga	1.3 (0.7)	1.4 (0.6)	1.2 (0.8)	1.3 (0.7)	1.3 (0.4)
As	14.5 (0.7)	8 (2.5)	14 (2)	12.5 (3)	12 (3)
Sb	25 (3)	24 (3)	30 (3)	23 (4)	25 (2)
Br	63 (7)	68 (6)	77 (8)	60 (7)	67 (4)
Sc	3.8 (0.3)	3.2 (0.5)	2.1 (0.2)		3.1 (0.5)
Ce	15.2 (2.0)	14.2 (2.0)	8.6 (1.5)		13 (3)
Th	1.4 (0.3)	1.2 (0.5)	...		1.3 (0.4)
Cr	137 (10)	112 (15)	88 (10)		113 (20)
Fe	17,000 (1200)	13,500 (1000)	10,500 (1000)		13,800 (3000)
Co	3.35 (0.3)	2.6 (0.2)	1.9 (0.2)		2.6 (0.6)
Ni	...	<60	...		<60
Ag	3.1 (2.5)	1.8 (2.0)	2.2 (2.4)		2.4 (1.5)
Zn	2210 (240)	1450 (150)	1430 (140)		1690 (300)
Hg	5.3 (1.4)	4.4 (1.3)	...		4.8 (1.0)
Sb	43 (4)	28 (3)	23 (3)		32 (9)
Se	3.0 (0.8)	4.6 (1.4)	...		3.8 (1.0)

[a] Standard deviations are based on counting statistics of sample, blank, and standard.
[b] Standard deviations are based on dispersion of replicate analyses.

obtained by the present procedure for the analysis of typical inland aerosol samples, expressed in weights of the elements. The sensitivity obtained by the National Air Sampling Network (*2*) applying emission spectrography and using 90 cm² (14 inch²) of a 24-hour high volume sample is expressed in concentrations of the elements in urban air (column 5). For convenience the sensitivities obtained by the present neutron activation technique were also converted to concentrations in urban air (column 4) when counting irradiated samples after the decay times indicated, where 0.8, 0.8, 1.6, and 13 cm² of the filter were used for the four counts, respectively, corresponding approximately to 5, 5, 10, and 80 m³ of air collected during 24 hours by a high volume sampler. The sensitivities obtainable in non-urban areas are better for both methods. It should be borne in mind that the sensitivities given are not fixed values for all urban aerosols because they also depend to a certain extent on the composition of the sample.

APPLICATION

We have applied our procedure to a study of the composition of aerosols collected in the southern Lake Michigan basin. As an example the data given in Tables IV and V are drawn from results of a one-day area-wide survey of the Northwest Indiana region, June 11, 1969, a full account of which will be published separately. Each sample was 24 hours in length, taken on a polystyrene 20 × 25 cm (8 × 10 inch) filter. The East Chicago, Indiana, location was chosen to be illustrative of a heavily polluted industrial area, whereas the Niles, Michigan, station is in a rural location some 100 km to the ENE. During the sampling period the sky was generally overcast (0.6–0.9 fractional cloud cover), and scattered traces of rain fell in the metropolitan area but not at the rural location. Winds were nearly constant from the south at 5–10 m/sec during the 24 hours.

Tables IV and V show that the concentrations of 30 elements in total were investigated, and 4 of these (Cu, Zn, Sb, Br) were duplicated in different counts. Each analysis was replicated from two to four times. Standard deviations are given both for the single measurements as returned by the computer (based on counting statistics and uncertainties in blanks and standards) and for the mean of the values reported (based on the dispersion of the replicate analyses).

DISCUSSION

Tables IV and V show the 29 elements that can be determined, even though some of these are present only in very low concentrations. Although a much smaller amount of the filter is used, the sensitivities compare favorably with those obtained by emission spectrography as performed by the National Air Sampling Network (*2*). For most elements at least ten times better sensitivity is obtained; exceptions are Ti and Ni. In another application, which will be published elsewhere, we found that, after a sampling time of only 90 minutes in a rural location, 15 elements could routinely be determined. In an industrial or urban area the same number of elements may be detected after a much shorter sampling time.

For some elements the sensitivity is limited by the purity of the filter paper, *e.g.*, Cl, Br, Na, and Zn. For at least 15

Table V. Elements Detected in Suspended Particulate from Niles, Michigan, ng/m³

Element	1st Anal.[a]	2nd Anal.[a]	3rd Anal.[a]	4th Anal.[a]	Mean[b]
Ca	600 (200)	1100(300)	1150 (280)		1000 (200)
Ti	105 (35)	105 (35)	150 (40)		120 (25)
V	5.0 (0.5)	5.2 (0.5)	4.9 (0.5)		5.0 (0.3)
Cu	250 (30)	290 (35)	325 (37)		290 (30)
Al	1100 (100)	1240 (8)	1280 (85)		1200 (70)
S	9,000 (6,000)	9,000 (6,000)	16,000 (8,000)		11,000 (5,000)
Na	140 (18)	180 (20)	175 (20)		170 (20)
Mg	350 (400)	680 400)	...		500 (300)
Mn	58 (3)	62 (4)	67 (5)		62 (4)
In	0.04 (0.03)	0.04 (0.03)	0.03 (0.03)		0.04 (0.03)
Br	34 (4)	28 (4)	34 (5)		32 (3)
K	740 (40)	930 (50)	660 (30)	700 (30)	750 (100)
La	1.4 (0.2)	1.7 (0.2)	1.1 (0.2)	1.0 (0.2)	1.3 (0.3)
Sm	0.26 (0.01)	0.30 (0.01)	0.21 (0.02)	0.20 (0.02)	0.24 (0.03)
Eu	0.05 (0.017)	0.065 (0.021)	0.045 (0.009)	0.06 (0.010)	0.055 (0.008)
Cu	260 (35)	260 (35)	245 (35)	305 (35)	270 (25)
Zn	124 (33)	186 (40)	132 (20)	113 (20)	140 (20)
W	0.4 (0.2)	0.2 (0.2)	0.55 (0.2)	0.4 (0.2)	0.4 (0.1)
Ga	1.1 (0.6)	1.0 (0.6)	0.7 (0.4)	0.9 (0.4)	0.9 (0.4)
As	4.4 (2)	5.2 (2)	4.8 (2)	4.0 (2)	4.6 (2)
Sb	5.4 (1)	7.0 (1)	5.7 (1)	4.7 (0.8)	5.8 (0.6)
Br	46 (2)	55 (3)	35 (2)	38 (2)	43 (5)
Sc	1.2 (0.1)	1.2 (0.1)			1.2 (0.1)
Ce	0.77 (0.1)	0.86 (0.1)			0.82 (0.10)
Th	0.28 (0.04)	0.26 (0.04)			0.27 (0.03)
Cr	9.1 (0.8)	10.0 (0.8)			9.5 (0.8)
Fe	1900 (100)	1840 (100)			1900 (100)
Co	1.0 (0.1)	0.90 (0.08)			0.95 (0.10)
Ni	...	...			...
Ag	<1	<1			<1
Zn	185 (10)	172 (10)			180 (10)
Hg	2.0 (0.6)	1.7 (0.6)			1.9 (0.3)
Sb	6.6 (0.7)	6.1 (0.05)			6.3 (0.5)
Se	2.5 (0.6)	2.5 (0.6)			2.5 (0.5)

[a] Standard deviations are based on counting statistics of sample, blank, and standard.
[b] Standard deviations are based on dispersion of replicate analyses.

Table VI. Ratios of Concentrations Found, East Chicago/Niles

3 & 15 min. decay		20–30 hr decay		20–30 day decay	
Ca	7.0 ± 1.5	K	1.9 ± 0.3	Sc	2.6 ± 0.4
Ti	1.6 ± 0.6	La	4.5 ± 1.2	Ce	16.0 ± 4.0
V	3.6 ± 0.4	Sm	1.7 ± 0.3	Th	4.8 ± 1.4
Cu	3.7 ± 0.4	Eu	2.5 ± 0.4	Cr	12.0 ± 2.0
Al	1.8 ± 0.2	Cu	4.3 ± 0.6	Fe	7.3 ± 1.6
S	1.1 ± 0.8	Zn	10.0 ± 2.0	Co	2.7 ± 0.6
Na	2.7 ± 0.3	W	14.5 ± 4.5	Ag	>2.4 ± 1.5
Mg	4.8 ± 3.0	Ga	1.4 ± 0.7	Zn	9.4 ± 1.7
Mn	4.1 ± 0.7	As	2.6 ± 1.3	Hg	2.5 ± 0.7
In	2.5 ± 2.0	Sb	4.3 ± 0.5	Sb	5.1 ± 1.5
Br	2.6 ± 0.4	Br	1.5 ± 0.2	Se	1.5 ± 0.2

elements the sensitivity is affected by the composition of the sample. The abundant elements Al, Na, and Br give rise to a large amount of radioactivity, and other elements may be difficult to detect in their presence. It appears that the large amount of V found by Zoller and Gordon (*1*) in their samples caused a limitation on sensitivity in their short runs. A destructive technique involving chemical separations may improve the sensitivity for some elements, *e.g.*, Cu, Zn, Ga, As, Se, Ce, Sm, Eu, W, Au, Hg, but the nondestructive sensitivities for these elements appear to be adequate for the 24-hour samples from urban and rural areas we have examined. Some increase in sensitivity may be achieved by increasing the counting time or the neutron dose, although some chemical separations may still be required to detect elements such as Sr, Mo, Cd, I, and additional rare earths.

By close examination of Tables IV and V it can be seen that, although only trace quantities are determined, from 10^{-3} to 10^{-10} gram, the reproducibility of the determinations is quite adequate, for the differences are generally within the calculated standard deviations (67% confidence level) of the single values. These standard deviations are high (>40%) only when the concentrations determined are near the limit of detection. In cases where the determination of an element is duplicated in different counts or in irradiations of different portions of the air filter sample, good agreement is usually obtained. This includes the reproducibility of the chemical analysis, the accuracy in measurement of the filter area taken for analysis and the possible nonuniform air-flow through the filter. We conclude that for the determination of most elements an accuracy of 25% can readily be obtained from one analysis. This is sufficient for many monitoring purposes.

A test of the adequacy of the analytical precision obtained is given in Table VI showing the ratios of concentrations found in East Chicago to those in Niles, together with the standard deviations of the ratios. In nearly every case the ratio is significantly greater than unity, and in general the ratio is not statistically the same for every element. A study involving a number of sampling locations over a wide area may lead to the identification of local sources characteristic for

each element or group of elements. Such an investigation is now in progress in our laboratory.

ACKNOWLEDGMENT

We are grateful to S. S. Brar of the Argonne National Laboratory and to personnel of the division of air pollution control of the city of East Chicago, Indiana, for collection of the sample described in Table IV.

RECEIVED for review February 11, 1970. Accepted April 21, 1970. This work was supported in part by U.S.A.E.C. Contract AT(11-1)-1705, U.S.P.H.S. Grant AP-00585, N.S.F. Grant GA-811, and the University of Michigan. Contribution No. 174 from the Department of Meteorology and Oceanography and No. 127 from the Great Lakes Research Division, University of Michigan.

APPENDIX 2b

REMARKS ON THE ANALYTICAL TECHNIQUE

Any nondestructive analytical technique is a compromise, for a conscious decision is made to accept the inevitable interferences from other elements in the absence of post-irradiation chemical separations. Fortunately, Ge(Li) semiconductors reduce these interferences to tolerable levels for many elements. Further compromise is introduced when the nondestructive approach is made multielemental, as in this investigation, for the irradiation - cooling - counting sequence can then only be optimized for groups of elements rather than for any specific ones.

The strong point of our analytical scheme is the short irradiation sequence. Small sample sizes are least critical here, because of the rapid decay of the short-lived isotopes. Aluminum (^{28}Al, 1779 keV, largest peak in the spectrum up to 10 minutes after irradiation) presents an interference, but is largely decayed at 15 minutes after irradiation, when the second (1000 second) count begins. The short counts are easily replicated when maximum accuracy is desired.

The necessity for streamlining the short count procedure was recognized as its potential for routine applications began to emerge. It was for this reason that the fixed schedule of irradiation and counting times of Appendix 2a was developed. Chemical standards are run in this sequence, along with a Ti flux monitor, and once the appropriate mass/counts conversion factors have been reproducibly established they remain valid over a long period. The flux monitor rather than the standards are then run with the samples, reducing the number of spectral peaks generated by nearly one-half, a substantial gain in efficiency. This technique also allows longer counts on the short-lived isotopes, for a standard need not be counted each time. This is especially important for the shortest-lived species, where counting time is

clearly at a premium.

These gains are not without their price, however, for flexibility in irradiation, cooling, and counting times is lost, as well as variability in counting geometry, for the entire sequence must exactly reproduce that of the standards. We have found, though, that by carefully choosing the sample size almost every irradiation can be made to give useable activities, so that the above disadvantages do not seem serious in practice.

A simple modification of the technique has added important sensitivity for several elements. The first count is dominated by ^{28}Al activity, but this decays so rapidly that by the start of the second count sample activities are well below optimum levels. When sufficient sample is available, we now irradiate 4 times as much as before, and perform the first count in a position recessed so that the original activity remains the same. For the second count the sample is returned to the close position, giving 4 times the previous activity and significantly improving borderline elements such as I, In, and Mg.

There are two major weak spots in our technique, the third and fourth counts. The third count is dominated heavily by ^{24}Na activity, often resembling a pure ^{24}Na spectrum. Elements determined here would show greatly improved sensitivity in the absence of the Na, but in nondestructive applications this cannot be accomplished. For expendable samples, though, post-irradiation removal of Na by a hydrated antimony pentoxide (HAP) column may be desirable.

The fourth count, of long-lived isotopes, also requires special attention when maximum precision is desired. A combination of large sample sizes and long irradiation and counting times is required to make its precision comparable to the short counts, but, as discussed in Appendix 1b, problems often arise here. The easiest type of sample to accommodate is the 24-hour "hivol" 8x10 in filter paper (Whatman No. 41), where irradiation of 12 in^2 for 3-5 hours at a flux of 1.5×10^{13}

n/cm^2-sec is just suitable for counting times of 4000 seconds. (Contrast this with the 1/4 in^2 sample needed for optimum short counts.) When these large sample sizes are not available, counting times may profitably be extended, though not on a routine basis.

APPENDIX 3

TABLE 3-1: MACKINAC ISLAND FILTERS (ng/m^3)

	MIF1	MIF2	MIF3	$\overline{MIF}$
Na	150(25)	90(10)	130(20)	120
Mg	60(50)	55(25)	35(30)	50
Al	200(20)	140(20)	220(30)	190
Cl	90(60)	55(55)	52(50)	66
K	110(20)	130(20)	120(20)	120
Ca	140(40)	160(30)	240(30)	180
Sc	0.15(0.02)	0.14(0.02)	0.13(0.02)	0.14
Ti	21(6)	16(5)	22(5)	20
V	1.6(0.2)	2.0(0.2)	1.6(0.2)	1.7
Cr	3.4(0.4)	2.0(0.2)	1.6(0.2)	2.3
Mn	22(3)	14(2)	18(2)	18
Fe	540(60)	570(60)	390(40)	500
Co	0.22(0.03)	0.22(0.03)	0.16(0.02)	0.20
Ni	< 5	< 5	< 5	< 5
Cu	10(2)	18(3)	12(2)	13
Zn	50(5)	60(6)	40(4)	50
Ga	0.4(0.1)	0.3(0.1)	0.3(0.1)	0.3
As	11(2)	8(1)	12(2)	10
Se	1.3(0.5)	1.5(0.3)	0.9(0.3)	1.2
Br	12(2)	15(3)	14(2)	14
Ag	< 0.4	< 0.4	< 0.3	< 0.4
In	0.004(0.003)	0.012(0.003)	0.013(0.003)	0.010
Sb	1.2(0.2)	1.4(0.2)	0.9(0.1)	1.2
I	1.1(0.2)	1.0(0.3)	1.0(0.3)	1.0
La	0.23(0.04)	0.16(0.06)	0.19(0.05)	0.19
Ce	0.36(0.10)	0.30(0.09)	0.26(0.07)	0.31
Sm	0.013(0.004)	0.029(0.006)	0.025(0.005)	0.22
Eu	0.006(0.004)	0.007(0.003)	0.009(0.003)	0.007
W	0.1(0.1)	< 0.15	0.08(0.06)	0.1
Hg	0.3(0.2)	0.1(0.1)	< 0.1	0.1
Th	0.07(0.01)	0.04(0.01)	0.04(0.01)	0.05

TABLE 3-2: ANN ARBOR ANDERSEN SAMPLE AA1 (ng/m^3)

	7	6	5	4	3	2	1
Na	20(2)	35(4)	27(3)	37(4)	65(7)	70(7)	100(10)
Mg	5(9)	9(15)	13(13)	19(14)	18(17)	14(16)	< 23
Al	5(1)	7(1)	16(2)	79(8)	160(20)	150(20)	150(20)
Cl	14(2)	20(3)	12(2)	41(5)	88(9)	100(10)	170(20)
K	33(4)	24(3)	14(2)	26(3)	40(4)	26(3)	41(5)
Ca	6(3)	8(4)	11(3)	37(10)	74(16)	67(16)	180(30)
Sc	0.005(0.002)	0.009(0.002)	0.018(0.003)	0.077(0.010)	0.16(0.02)	0.093(0.010)	0.14(0.07)
Ti	1.3(1.4)	2.8(1.5)	1.8(0.9)	8.5(2.5)	12(3)	11(3)	15(3)
V	0.70(0.07)	0.57(0.06)	0.33(0.04)	0.45(0.05)	0.55(0.06)	0.38(0.05)	0.41(0.05)
Cr	0.42(0.10)	0.70(0.10)	0.82(0.11)	1.3(0.2)	1.6(0.2)	1.0(0.2)	2.0(0.2)
Mn	5.9(0.6)	11(2)	7.2(0.8)	5.6(0.6)	4.4(0.5)	2.6(0.3)	4.2(0.5)
Fe	30(10)	54(10)	87(15)	180(20)	320(40)	190(20)	400(40)
Co	0.045(0.020)	0.036(0.020)	0.030(0.010)	0.073(0.015)	0.19(0.04)	0.095(0.025)	0.14(0.04)
Ni	1(1)	1(1)	< 1.5	1.5(1.5)	< 2.5	< 2	< 2
Cu	1.8(0.2)	1.7(0.3)	1.7(0.4)	4.5(0.5)	11(2)	13(2)	110(20)
Zn	12(2)	17(2)	25(3)	49(5)	95(10)	70(8)	150(20)
Ga	0.18(0.03)	0.09(0.02)	0.03(0.03)	0.11(0.02)	0.16(0.03)	0.14(0.03)	0.11(0.11)
As	1.1(0.2)	0.72(0.18)	0.70(0.15)	0.81(0.20)	0.61(0.20)	0.40(0.25)	0.57(0.39)
Se	0.25(0.04)	0.25(0.04)	0.12(0.03)	0.09(0.04)	0.10(0.07)	0.06(0.04)	< 0.05
Br	17(3)	14(2)	10(1)	12(2)	13(2)	8(1)	6(1)
Ag	< 0.07	< 0.05	0.08(0.08)	0.08(0.09)	< 0.07	0.06(0.06)	0.10(0.10)
In	0.0056 (0.0010)	0.0098 (0.0016)	0.0084 (0.0014)	0.0044 (0.0013)	0.0052 (0.0013)	0.0023 (0.0011)	0.0017 (0.0014)
Sb	0.75(0.08)	0.65(0.10)	0.37(0.05)	0.30(0.03)	0.30(0.04)	0.12(0.02)	0.16(0.03)
I	0.43(0.11)	-	0.15(0.07)	0.13(0.07)	< 0.06	-	-
La	0.21(0.03)	0.25(0.03)	0.35(0.04)	0.47(0.05)	0.39(0.04)	0.11(0.03)	0.11(0.03)
Ce	0.18(0.05)	0.11(0.05)	0.08(0.04)	0.28(0.05)	0.53(0.08)	0.30(0.10)	0.40(0.10)
Sm	0.014(0.002)	0.008(0.003)	0.006(0.002)	0.011(0.003)	0.024(0.003)	0.017(0.003)	0.019(0.004)
Eu	0.0018 (0.0012)	< 0.0015	< 0.0015	0.0025 (0.0015)	0.0043 (0.0020)	0.0025 (0.0015)	< 0.0070
W	0.01(0.03)	0.03(0.03)	0.04(0.03)	0.06(0.04)	0.15(0.06)	0.16(0.06)	0.23(0.09)
Hg	0.17(0.09)	0.09(0.07)	0.10(0.08)	< 0.07	< 0.10	< 0.07	0.12(0.10)
Th	0.003(0.004)	0.003(0.004)	0.004(0.003)	0.017(0.004)	0.034(0.004)	0.010(0.005)	0.030(0.010)

TABLE 3-3: MACKINAC ISLAND ANDERSEN SAMPLE MI1 (ng/m^3)

	7	6	5	4	3	2	1
Na	9(1)	13(2)	22(3)	10(1)	10(1)	7(1)	7(1)
Mg	-	5(5)	< 9	< 5	(5)	3(4)	< 6
Al	1.6(0.2)	3.4(0.4)	14(2)	27(3)	39(4)	30(3)	25(3)
Cl	1.2(0.4)	0.4(0.4)	1.2(0.4)	3.0(0.4)	2.7(0.4)	3.0(0.4)	4.5(0.5)
K	13(2)	14(2)	13(2)	10(1)	11(2)	10(1)	9(1)
Ca	5(2)	4(2)	10(3)	18(4)	23(5)	24(5)	25(5)
Sc	0.003(0.001)	0.003(0.001)	0.012(0.002)	0.018(0.003)	0.028(0.006)	0.020(0.003)	0.014(0.002)
Ti	1.2(0.7)	< 0.3	1.4(0.8)	1.8(0.9)	1.8(1.0)	3.0(0.8)	2.8(0.8)
V	0.24(0.03	0.17(0.01)	0.14(0.02)	0.15(0.02)	0.15(0.02)	0.09(0.01)	0.075(0.011)
Cr	0.17(0.03)	0.27(0.03)	0.33(0.04)	0.21(0.04)	0.27(0.04)	0.11(0.03)	0.19(0.03)
Mn	2.3(0.3)	2.2(0.3)	2.4(0.3)	1.1(0.2)	1.1(0.2)	0.59(0.06)	0.54(0.06)
Fe	40(5)	70(10)	86(10)	65(8)	70(10)	42(6)	36(6)
Co	0.017(0.005)	0.019(0.010)	0.024(0.010)	0.022(0.010)	0.030(0.008)	0.027(0.010)	0.025(0.008)
Ni	< 0.3	-	-	-	-	-	-
Cu	1.2(0.2)	1.3(0.2)	2.0(0.3)	1.4(0.2)	1.9(0.2)	1.1(0.2)	1.0(0.1)
Zn	3.6(0.4)	5.2(0.6)	5.5(0.6)	3.0(0.4)	2.3(0.4)	1.5(0.2)	1.7(0.2)
Ga	0.058(0.013)	0.020(0.010)	0.018(0.010)	0.019(0.010)	0.029(0.015)	0.015(0.010)	0.013(0.007)
As	2.3(0.3)	1.7(0.2)	1.5(0.2)	0.34(0.08)	0.23(0.07)	0.20(0.06)	0.11(0.06)
Se	0.11(0.04)	0.086(0.018)	0.050(0.015)	0.030(0.015)	0.013(0.013)	0.013(0.011)	0.012(0.010)
Br	1.8(0.3)	1.2(0.2)	1.1(0.2)	0.55(0.10)	0.60(0.06)	0.41(0.09)	0.22(0.05)
Ag	< 0.02	< 0.04	0.02(0.02)	0.035(0.030)	0.030(0.030)	< 0.035	< 0.035
In	0.0010 (0.0005)	0.0020 (0.0005)	0.003(0.001)	0.0010 (0.0004)	0.0010 (0.0003)	0.0010 (0.0004)	0.0010 (0.0004)
Sb	0.18(0.02)	0.11(0.01)	0.09(0.02)	0.055(0.008)	0.055(0.008)	0.03(0.01)	0.04(0.01)
I	0.20(0.05)	0.15(0.04)	0.026(0.026)	0.018(0.019)	0.026(0.020)	0.016(0.014)	0.034(0.016)
La	< 0.01	0.0097 (0.0100)	0.020(0.013)	0.040(0.010)	0.038(0.009)	0.028(0.008)	0.019(0.007)
Ce	0.03(0.02)	0.02(0.02)	0.044(0.020)	0.080(0.030)	0.10(0.02)	0.06(0.02)	0.06(0.02)
Sm	0.0006 (0.0011)	< 0.0012	0.0014 (0.0002)	0.0040 (0.0010)	0.0060 (0.0010)	0.0052 (0.0008)	0.0033 (0.0008)
Eu	< 0.0005	0.0004 (0.0006)	<0.0010	0.0008 (0.0005)	0.0010 (0.0005)	0.0012 (0.0005)	0.0006 (0.0004)
W	< 0.01	< 0.012	< 0.017	0.021(0.012)	0.015(0.011)	0.019(0.011)	0.009(0.009)
Hg	< 0.02	< 0.03	< 0.03	< 0.03	0.03(0.03)	< 0.035	< 0.04
Th	0.001(0.001)	0.001(0.001)	0.002(0.001)	0.004(0.002)	0.004(0.002)	0.004(0.002)	0.003(0.002)

TABLE 3-4: ANN ARBOR ANDERSEN SAMPLE AA2 (ng/m^3)

	7	6	5	4	3	2	1
Na	15(2)	16(2)	50(5)	77(8)	210(30)	290(30)	610(70)
Mg	-	<13	27(21)	12(20)	18(29)	55(30)	90(10)
Al	2.9(0.3)	4.7(0.5)	39(4)	97(10)	190(20)	170(20)	200(20)
Cl	5(1)	6(1)	22(3)	98(10)	280(30)	420(50)	900(90)
K	30(3)	31(4)	65(7)	30(3)	32(4)	26(3)	41(5)
Ca	8(3)	9(3)	33(11)	73(17)	190(20)	200(40)	290(60)
Sc	0.0021 (0.0008)	0.0034 (0.0010)	0.029(0.004)	0.071(0.009)	0.39(0.05)	0.11(0.02)	0.16(0.02)
Ti	1(1)	1(1)	3(3)	6(3)	19(4)	14(2)	18(7)
V	1.1(0.2)	0.93(0.10)	1.2(0.2)	0.67(0.07)	0.86(0.09)	0.55(0.06)	0.53(0.08)
Cr	0.07(0.04)	0.45(0.06)	0.96(0.15)	0.96(0.15)	1.0(0.2)	0.93(0.14)	1.2(0.2)
Mn	3.3(0.4)	4.3(0.5)	13(2)	5.2(0.6)	3.8(0.4)	2.6(0.3)	3.5(0.4)
Fe	18(4)	43(5)	150(20)	160(20)	280(30)	240(30)	350(40)
Co	0.014(0.002)	0.023(0.003)	0.054(0.006)	0.062(0.007)	0.12(0.02)	0.087(0.009)	0.11(0.02)
Ni	-	-	-	-	-	-	-
Cu	1.2(0.2)	1.7(0.3)	5.6(1.0)	5.7(0.7)	11(2)	10(3)	25(6)
Zn	6(1)	17(2)	74(10)	120(20)	270(40)	210(30)	300(40)
Ga	0.18(0.02)	0.17(0.02)	<0.10	0.15(0.04)	0.10(0.08)	<0.10	<0.25
As	1.2(0.3)	1.4(0.3)	2.8(0.3)	0.8(0.3)	<0.5	<0.5	0.6(0.4)
Se	0.27(0.03)	0.48(0.05)	0.53(0.06)	0.099(0.017)	0.077(0.028)	0.019(0.021)	0.046(0.006)
Br	10(2)	8(2)	16(2)	11(2)	12(2)	8(1)	8(1)
Ag	0.020(0.007)	0.019(0.010)	0.047(0.018)	0.013(0.021)	<0.040	<0.040	0.050(0.040)
In	0.010(0.001)	0.015(0.002)	0.033(0.003)	0.009(0.002)	0.008(0.002)	0.003(0.002)	0.005(0.003)
Sb	0.50(0.07)	0.82(0.10)	1.1(0.2)	0.52(0.07)	0.62(0.08)	0.54(0.07)	0.33(0.04)
I	0.36(0.10)	0.33(0.10)	0.29(0.12)	-	-	0.33(0.07	0.39(0.18)
La	0.08(0.02)	0.05(0.02)	0.14(0.03)	0.19(0.03)	0.19(0.04)	0.13(0.05)	0.25(0.16)
Ce	0.07(0.01)	0.10(0.02)	0.20(0.03)	0.24(0.04)	0.45(0.06)	0.32(0.05)	0.40(0.05)
Sm	0.009(0.002)	0.005(0.002)	0.046(0.005)	0.037(0.004)	0.17(0.02)	0.20(0.02)	0.45(0.05)
Eu	0.0016 (0.0011)	0.0015 (0.0012)	0.0009 (0.0023)	0.0028 (0.0024)	0.0083 (0.0075)	0.0052 (0.0051)	0.013(0.018)
W	<0.02	< 0.02	<0.04	<0.04	<0.05	<0.06	0.30(0.20)
Hg	0.058(0.023)	0.054(0.038)	0.064(0.038)	<0.035	<0.013	0.065(0.035)	<0.03
Th	< 0.003	<0.004	< 0.003	0.020(0.005)	0.021(0.009)	0.026(0.006)	0.035(0.004)

TABLE 3-5: MACKINAC ISLAND ANDERSEN SAMPLE MI2 (ng/m^3)

	7	6	5	4	3	2	1
Na	11(2)	21(3)	33(4)	14(2)	14(2)	7(1)	6(1)
Mg	< 6	6(7)	12(7)	4(5)	7(5)	3(4)	7(4)
Al	1.9(0.2)	5.3(0.6)	22(3)	25(3)	42(5)	35(4)	25(3)
Cl	0.4(0.4)	0.6(0.5)	1.2(0.4)	1.3(0.4)	3.8(0.5)	2.7(0.4)	4.2(0.5)
K	22(3)	12(2)	13(2)	8(1)	12(2)	8(1)	6(1)
Ca	2.4(1.1)	6.8(2.0)	21(5)	29(6)	24(6)	38(7)	33(6)
Sc	0.0022 (0.0007)	0.0029 (0.0006)	0.014(0.002)	0.019(0.002)	0.025(0.003)	0.021(0.003)	0.016(0.002)
Ti	< 0.15	0.3(0.4)	1.6(1.0)	3.5(0.9)	2.6(1.1)	1.6(0.9)	2.1(0.8)
V	0.32(0.04)	0.26(0.03)	0.21(0.03)	0.16(0.02)	0.19(0.02)	0.12(0.02)	0.08(0.01)
Cr	0.22(0.03)	0.23(0.03)	0.23(0.03)	0.11(0.03)	0.15(0.02)	0.24(0.03)	0.11(0.02)
Mn	2.1(0.3)	2.5(0.3)	2.0(0.2)	0.9(0.1)	1.0(0.1)	0.6(0.1)	0.5(0.1)
Fe	24(3)	46(5)	74(8)	51(6)	57(6)	43(5)	39(4)
Co	0.022(0.003)	0.011(0.002)	0.021(0.003)	0.019(0.004)	0.022(0.003)	0.019(0.003)	0.015(0.002)
Ni	-	-	-	-	-	-	-
Cu	1.0(0.3)	1.1(0.2)	1.6(0.3)	0.8(0.2)	1.1(0.2)	0.6(0.1)	0.4(0.1)
Zn	7.5(0.8)	6.9(0.7)	7.9(0.8)	2.5(0.3)	2.0(0.3)	1.1(0.2)	1.3(0.2)
Ga	0.05(0.03)	< 0.01	0.01(0.01)	0.03(0.01)	0.03(0.01)	0.01(0.01)	0.01(0.01)
As	0.89(0.09)	1.8(0.2)	0.97(0.10)	0.34(0.06)	0.27(0.17)	0.12(0.03)	0.08(0.02)
Se	0.47(0.05)	0.13(0.02)	0.065(0.008)	0.021(0.007)	0.023(0.006)	0.019(0.007)	0.010(0.006)
Br	1.7(0.2)	1.4(0.2)	0.84(0.10)	0.38(0.04)	0.50(0.05)	0.32(0.04)	0.15(0.02)
Ag	-	-	-	-	-	-	-
In	0.0025 (0.0005)	0.0056 (0.0007)	0.0058 (0.0006)	0.0015 (0.0004)	0.0011 (0.0004)	0.0006 (0.0003)	0.0004 (0.0003)
Sb	0.56(0.07)	0.16(0.02)	0.13(0.02)	0.059(0.007)	0.044(0.005)	0.067(0.007)	0.036(0.005)
I	0.19(0.05)	0.14(0.04)	0.016(0.025)	0.015(0.017)	0.014(0.018)	0.017(0.015)	0.029(0.015)
La	0.046(0.008)	0.022(0.012)	0.049(0.012)	0.047(0.008)	0.046(0.008)	0.024(0.006)	0.022(0.005)
Ce	0.14(0.02)	< 0.02	0.082(0.010)	0.074(0.010)	0.072(0.008)	0.060(0.009)	0.045(0.009)
Sm	0.016(0.001)	0.007(0.001)	0.024(0.001)	0.0050 (0.0008)	0.0073 (0.0008)	0.0039 (0.0006)	0.0036 (0.0005)
Eu	0.0008 (0.0005)	0.0008 (0.0005)	< 0.0008	0.0012 (0.0005)	0.0015 (0.0005)	0.0006 (0.0004)	0.0009 (0.0004)
W	0.026(0.011)	0.012(0.009)	< 0.012	< 0.009	0.010(0.005)	< 0.006	< 0.005
Hg	0.030(0.018)	0.022(0.013)	0.014(0.014)	0.022(0.013)	0.007(0.012)	< 0.009	0.013(0.011)
Th	< 0.002	0.0022 (0.0016)	0.0061 (0.0020)	0.0034 (0.0018)	0.0079 (0.0015)	0.0048 (0.0020)	0.0046 (0.0016)

TABLE 3-6: EAST CHICAGO CENTRAL FIRE STATION ANDERSEN SAMPLE CFS1 (ng/m^3)

	7	6	5	4	3	2	1
Na	55(6)	72(8)	78(8)	100(10)	150(20)	190(20)	300(30)
Mg	10(30)	15(35)	30(40)	45(40)	160(40)	100(50)	160(60)
Al	16(2)	11(2)	45(5)	150(20)	210(30)	230(30)	300(30)
Cl	26(3)	110(20)	170(20)	190(20)	230(30)	300(30)	450(50)
K	22(3)	34(4)	38(4)	55(6)	52(6)	54(6)	66(7)
Ca	15(8)	15(15)	45(25)	200(40)	230(50)	360(60)	440(70)
Sc	0.01(0.02)	0.02(0.03)	0.04(0.02)	0.11(0.02)	0.10(0.01)	0.13(0.02)	0.31(0.04)
Ti	3(5)	2(5)	5(5)	6(6)	8(6)	14(4)	10(7)
V	6.2(0.7)	3.1(0.4)	3.1(0.4)	5.7(0.6)	4.7(0.5)	3.7(0.4)	3.8(0.4)
Cr	0.7(0.5)	0.2(0.5)	3.2(0.6)	3.0(0.5)	2.0(0.5)	3.9(0.5)	5.3(0.6)
Mn	8.1(0.9)	14(2)	13(2)	11(2)	8.0(0.8)	7.5(0.8)	13(2)
Fe	30(50)	40(50)	310(60)	300(60)	330(60)	420(60)	660(70)
Co	0.06(0.10)	0.12(0.10)	0.08(0.10)	0.23(0.10)	0.15(0.10)	0.25(0.10)	0.39(0.10)
Ni	-	-	-	-	-	-	-
Cu	2.5(0.5)	3.0(0.6)	3.6(0.7)	3.9(0.8)	3.6(0.7)	3.3(0.6)	4.3(1.0)
Zn	55(20)	150(30)	250(50)	160(30)	65(8)	37(5)	30(5)
Ga	0.11(0.06)	0.14(0.07)	0.21(0.10)	0.38(0.20)	0.17(0.09)	0.14(0.08)	0.13(0.11)
As	1.7(0.5)	2.3(0.6)	3.6(0.8)	1.4(0.5)	0.6(0.4)	< 0.5	< 0.5
Se	< 0.40	0.12(0.23)	0.20(0.28)	0.37(0.22)	0.15(0.18)	0.11(0.18)	0.26(0.19)
Br	9(1)	10(1)	16(2)	27(3)	14(2)	11(2)	9(1)
Ag	-	-	-	-	-	-	-
In	0.040(0.004)	0.080(0.010)	0.10(0.01)	0.060(0.010)	0.020(0.005)	0.003(0.003)	< 0.020
Sb	2.1(0.3)	4.7(0.5)	7.9(0.8)	6.7(0.8)	2.7(0.3)	1.9(0.2)	1.5(0.2)
I	< 1	< 1	< 1	< 1	< 1	< 1	(1)
La	< 0.03	0.05(0.03)	0.28(0.04)	0.85(0.09)	0.43(0.05)	0.40(0.07)	0.45(0.09)
Ce	< 0.4	< 0.2	< 0.3	0.47(0.21)	0.39(0.18)	0.26(0.18)	0.96(0.19)
Sm	< 0.005	< 0.004	0.013(0.004)	0.051(0.006)	0.037(0.004)	0.035(0.005)	0.022(0.006)
Eu	< 0.001	0.002(0.002)	0.003(0.002)	0.003(0.002)	0.003(0.002)	0.011(0.003)	0.014(0.004)
W	< 0.05	0.02(0.05)	0.08(0.06)	0.08(0.08)	< 0.10	< 0.10	< 0.10
Hg	< 0.4	< 0.2	0.19(0.24)	0.64(0.20)	0.52(0.18)	0.42(0.17)	0.21(0.18)
Th	< 0.05	< 0.03	0.02(0.03)	0.05(0.03)	0.07(0.02)	0.02(0.02)	0.03(0.03)

TABLE 3-7: EAST CHICAGO MARKSTOWN PARK ANDERSEN SAMPLE MKT1 (ng/m^3)

	7	6	5	4	3	2	1
Na	47(5)	32(3)	66(7)	97(10)	170(20)	150(20)	190(20)
Mg	< 60	25(25)	45(35)	45(30)	90(50)	55(40)	170(50)
Al	8(1)	15(2)	76(8)	200(20)	300(30)	220(30)	210(30)
Cl	10(2)	20(2)	92(10)	96(10)	210(30)	200(20)	290(30)
K	41(8)	49(8)	47(8)	46(9)	64(9)	59(9)	92(12)
Ca	< 15	< 15	40(15)	170(40)	280(50)	290(50)	390(70)
Sc	< 0.003	< 0.004	0.06(0.02)	0.09(0.02)	0.15(0.02)	0.18(0.02)	0.20(0.02)
Ti	< 10	< 10	< 11	7(6)	20(8)	13(6)	12(6)
V	9.9(1.0)	3.6(0.4)	5.2(0.6)	6.2(0.7)	8.6(0.9)	4.6(0.5)	3.0(0.3)
Cr	0.7(0.5)	0.9(0.5)	2.8(0.6)	3.8(0.5)	5.0(0.6)	4.2(0.5)	6.5(0.7)
Mn	7(1)	7(1)	15(2)	15(2)	16(2)	10(1)	14(2)
Fe	40(70)	40(70)	210(70)	240(70)	460(80)	570(80)	920(100)
Co	0.04(0.09)	0.04(0.09)	0.12(0.09)	0.10(0.10)	0.26(0.09)	0.14(0.09)	0.34(0.09)
Ni	-	-	-	-	-	-	-
Cu	26(6)	47(12)	94(25)	69(15)	40(10)	23(6)	40(10)
Zn	65(20)	95(15)	150(20)	80(10)	42(6)	25(4)	21(4)
Ga	0.34(0.09)	0.12(0.08)	0.12(0.10)	0.17(0.10)	0.14(0.12)	0.16(0.12)	< 0.20
As	1.3(0.5)	1.7(0.4)	2.8(0.5)	1.0(0.6)	1.2(0.6)	0.5(0.7)	0.3(1.0)
Se	0.7(0.2)	0.1(0.2)	< 0.3	< 0.3	< 0.2	< 0.2	0.2(0.2)
Br	26(3)	11(2)	10(1)	11(2)	9.5(1.0)	6.8(0.7)	5.8(0.6)
Ag	-	-	-	-	-	-	-
In	0.006 (0.002)	0.010 (0.002)	0.030 (0.003)	0.012 (0.003)	0.005 (0.004)	0.006 (0.003)	0.004 (0.003)
Sb	1.7(0.2)	1.4(0.2)	4.5(0.5)	1.4(0.2)	1.2(0.2)	0.72(0.13)	0.80(0.13)
I	0.7(0.3)	< 0.9	< 0.9	< 0.9	< 0.9	< 0.9	< 0.9
La	0.1(0.1)	0.2(0.1)	1.8(0.2)	3.1(0.4)	2.0(0.2)	1.1(0.2)	1.9(0.2)
Ce	0.1(0.2)	0.2(0.2)	1.3(0.2)	2.4(0.3)	1.8(0.2)	0.8(0.2)	1.3(0.2)
Sm	< 0.01	0.02(0.01)	0.06(0.01)	0.09(0.01)	0.07(0.01)	0.05(0.01)	0.09(0.01)
Eu	< 0.01	0.01(0.01)	0.01(0.01)	0.01(0.01)	0.01(0.01)	0.01(0.01)	< 0.01
W	0.08(0.07)	0.09(0.07)	0.07(0.07)	0.06(0.07)	0.14(0.09)	< 0.10	< 0.13
Hg	0.25(0.24)	< 0.30	0.16(0.24)	0.21(0.22)	0.19(0.22)	< 0.22	< 0.22
Th	0.01(0.02)	0.02(0.02)	0.02(0.02)	0.03(0.03)	0.07(0.02)	0.05(0.02)	0.07(0.02)

TABLE 3-8: TWIN GORGES FILTERS (ng/m^3)

	TGF1	TGF2	TGF3	TGF4	TGF
Na	29(3)	14(2)	11(2)	18(3)	18(2)
Mg	24(24)	18(18)	9(9)	13(8)	16(9)
Al	100(10)	49(5)	41(5)	76(8)	66(7)
Cl	16(2)	8(1)	7(1)	7(1)	9(1)
K	56(6)	69(7)	33(5)	59(6)	54(6)
Ca	80(15)	40(10)	13(2)	29(10)	40(5)
Sc	0.061(0.007)	0.062(0.007)	0.019(0.002)	0.035(0.004)	0.044(0.005)
Ti	9.4(1.5)	5.6(1.0)	2.0(0.8)	4.3(1.5)	5.3(0.7)
V	0.31(0.04)	0.32(0.04)	0.07(0.02)	0.16(0.03)	0.21(0.03)
Cr	1.1(0.2)	0.59(0.06)	0.39(0.05)	0.28(0.10)	0.59(0.06)
Mn	2.5(0.3)	1.5(0.2)	0.7(0.1)	1.3(0.2)	1.5(0.2)
Fe	110(20)	65(7)	45(5)	65(11)	71(8)
Co	0.076(0.009)	0.048(0.007)	0.018(0.006)	0.028(0.007)	0.042(0.005)
Ni	< 2	< 1.5	< 0.8	< 1.5	< 2
Cu	1.5(1.0)	1.0(0.2)	0.4(0.1)	0.7(0.1)	0.9(0.3)
Zn	7.0(1.5)	5.5(1.0)	1.2(0.3)	1.5(0.5)	3.8(0.5)
Ga	0.02(0.02)	0.044(0.018)	0.019(0.019)	0.021(0.021)	0.026(0.010)
As	0.15(0.15)	0.40(0.10)	0.27(0.08)	0.43(0.07)	0.31(0.06)
Se	0.042(0.022)	0.034(0.015)	0.025(0.018)	0.071(0.017)	0.043(0.011)
Br	0.20(0.02)	0.19(0.02)	0.70(0.15)	1.1(0.11)	0.54(0.06)
Ag	< 0.15	< 0.10	< 0.10	< 0.10	< 0.15
In	0.0027(0.0027)	0.0007(0.0010)	< 0.0009	0.0013(0.0013)	0.0013(0.0008)
Sb	0.090(0.014)	0.030(0.010)	0.36(0.04)	0.027(0.012)	0.13(0.02)
I	0.31(0.07)	0.30(0.05)	0.12(0.03)	0.09(0.03)	0.20(0.03)
La	0.084(0.009)	0.10(0.01)	0.062(0.007)	0.12(0.02)	0.09(0.010)
Ce	0.35(0.04)	0.25(0.03)	0.14(0.02)	0.21(0.04)	0.24(0.03)
Sm	0.012(0.002)	0.017(0.002)	0.008(0.001)	0.014(0.002)	0.013(0.002)
Eu	0.0015(0.0015)	0.0021(0.0007)	0.0016(0.0007)	0.0017(0.0005)	0.0017(0.0005)
W	< 0.02	0.023(0.023)	< 0.015	0.025(0.025)	0.016(0.016)
Hg	0.059(0.069)	< 0.06	< 0.06	0.11(0.15)	0.06(0.06)
Th	0.080(0.008)	0.045(0.005)	0.033(0.004)	0.050(0.010)	0.052(0.006)

TABLE 3-9: JASPER AND MACKINAC ISLAND FILTERS (ng/m^3)

	JF1	JF2	JF3	$\overline{JF}$	$\overline{MIF}$
Na	36(4)	31(4)	41(5)	36(4)	44(5)
Mg	51(25)	58(20)	51(20)	53(13)	470(50)
Al	130(20)	175(20)	230(30)	150(20)	230(30)
Cl	14(2)	14(2)	12(2)	13(2)	35(4)
K	99(10)	110(15)	110(15)	110(20)	150(20)
Ca	70(30)	220(30)	160(30)	150(20)	1200(200)
Sc	0.064(0.007)	0.062(0.007)	0.12(0.02)	0.082(0.009)	0.12(0.02)
Ti	5(1)	12(3)	8(4)	8(3)	11(11)
V	0.31(0.04)	0.33(0.04)	0.35(0.05)	0.33(0.04)	1.8(0.2)
Cr	0.54(0.17)	0.18(0.16)	0.55(0.19)	0.32(0.11)	0.91(0.19)
Mn	4.3(0.5)	5.9(0.6)	5.6(0.6)	5.3(0.6)	9.2(1.0)
Fe	130(20)	240(30)	280(30)	220(30)	250(30)
Co	0.052(0.008)	0.053(0.008)	0.072(0.009)	0.059(0.06)	0.17(0.02)
Ni	<2	<2	3(2)	<2	<3
Cu	2.4(0.3)	5.9(0.6)	3.0(0.4)	3.8(0.4)	10(3)
Zn	4.8(0.5)	2.5(2.0)	8.4(0.9)	5.2(0.8)	22(4)
Ga	0.030(0.020)	0.040(0.040)	0.056(0.030)	0.042(0.020)	0.15(0.04)
As	0.28(0.20)	0.25(0.25)	0.29(0.15)	0.27(0.12)	3.2(0.4)
Se	0.050(0.023)	0.032(0.021)	0.012(0.023)	0.033(0.013)	0.67(0.07)
Br	2.1(0.3)	1.7(0.3)	2.3(0.3)	2.0(0.2)	7.2(1.0)
Ag	<0.15	<0.15	<0.15	<0.15	<0.5
In	<0.003	<0.003	<0.003	<0.003	0.024(0.004)
Sb	0.08(0.02)	0.17(0.03)	0.15(0.02)	0.13(0.02)	0.40(0.04)
I	0.30(0.08)	0.13(0.08)	0.20(0.08)	0.21(0.06)	<0.2
La	0.16(0.02)	0.097(0.025)	0.090(0.040)	0.12(0.02)	0.17(0.03)
Ce	0.18(0.07)	0.11(0.06)	0.46(0.07)	0.25(0.04)	0.41(0.08)
Sm	0.015(0.002)	0.017(0.002)	0.019(0.002)	0.017(0.002)	0.030(0.004)
Eu	0.0019(0.0019)	0.0053(0.0006)	0.0040(0.0019)	0.0037(0.0010)	0.0080(0.0008)
W	0.04(0.04)	0.04(0.04)	0.025(0.025)	0.035(0.021)	0.30(0.10)
Hg	0.29(0.20)	<0.2	<0.25	0.17(0.09)	0.38(0.22)
Th	0.033(0.013)	<0.015	0.066(0.015)	0.036(0.008)	0.018(0.012)

TABLE 3-10: PRINCE ALBERT FILTERS (ng/m^3)

	PAF1	PAF2	PAF3	PAF4	$\overline{PAF}$
Na	51(10)	73(9)	20(2)	27(3)	43
Mg	35(20)	120(30)	20(20)	55(15)	60
Al	130(20)	230(30)	120(20)	140(20)	150
Cl	8(2)	14(2)	9(2)	15(2)	11
K	80(15)	170(20)	70(7)	130(20)	112
Ca	100(30)	200(40)	90(20)	130(30)	130
Sc	0.12(0.02)	0.21(0.03)	0.051(0.006)	0.10(0.01)	0.12
Ti	10(10)	11(4)	7(3)	9(3)	9
V	0.35(0.08)	0.68(0.08)	0.29(0.04)	0.36(0.05)	0.42
Cr	2.2(0.3)	1.5(0.2)	0.23(0.09)	0.56(0.17)	1.1
Mn	5.3(0.7)	8.6(0.9)	4.3(0.5)	5.4(0.6)	5.9
Fe	200(20)	280(30)	85(15)	140(20)	180
Co	0.094(0.010)	0.13(0.02)	0.028(0.006)	0.089(0.011)	0.085
Ni	< 2	<2	<1	3(2)	<2
Cu	2.0(0.5)	0.75(0.10)	0.21(0.03)	0.61(0.07)	0.9
Zn	30(25)	11(2)	3(1)	9(2)	13
Ga	<0.035	0.06(0.06)	<0.03	0.047(0.010)	0.085
As	0.25(0.25)	0.66(0.12)	<0.2	0.27(0.06)	0.32
Se	0.039(0.023)	0.13(0.03)	0.031(0.014)	0.054(0.028)	0.063
Br	1.5(0.6)	2.6(0.3)	1.5(0.2)	4.0(0.5)	2.9
Ag	< 0.2	< 0.2	0.12(0.10)	< 0.2	< 0.2
In	0.0037(0.0037)	0.0026(0.0020)	< 0.0020	< 0.0018	0.0020
Sb	0.085(0.018)	0.22(0.03)	0.14(0.02)	0.19(0.03)	0.16
I	0.090(0.090)	0.24(0.08)	0.098(0.098)	0.089(0.089)	0.13
La	0.09(0.04)	0.17(0.02)	0.06(0.01)	0.10(0.03)	0.10
Ce	0.31(0.05)	0.57(0.06)	0.14(0.03)	0.27(0.06)	0.32
Sm	0.014(0.003)	0.027(0.004)	0.014(0.002)	0.018(0.004)	0.018
Eu	0.0034(0.0010)	0.0046(0.0024)	0.0021(0.0004)	0.0042(0.0005)	0.0036
W	< 0.03	< 0.05	< 0.03	< 0.03	< 0.03
Hg	0.31(0.18)	< 0.2	< 0.15	< 0.30	< 0.3
Th	0.040(0.009)	0.058(0.011)	0.019(0.006)	0.042(0.012)	0.040

TABLE 3-11: RIDING MOUNTAIN FILTERS (ng/m^3)

	RMF1	RMF2	RMF3	RMF4	$\overline{RMF}$
Na	58(8)	67(9)	61(8)	39(5)	56
Mg	160(50)	120(30)	140(40)	110(30)	130
Al	270(30)	390(40)	390(40)	280(30)	330
Cl	140(15)*	39(5)	19(3)	25(3)	28
K	150(40)	190(20)	180(20)	180(20)	175
Ca	320(50)	280(40)	470(60)	360(60)	360
Sc	0.13(0.02)	0.15(0.02)	0.24(0.03)	0.14(0.02)	0.16
Ti	7(7)	20(5)	11(11)	10(4)	12
V	0.59(0.06)	0.91(0.10)	0.86(0.09)	0.57(0.10)	0.73
Cr	1.1(0.2)	0.80(0.15)	1.1(0.2)	0.69(0.14)	0.92
Mn	5.8(0.6)	7.7(0.8)	13(2)	8.3(1.0)	8.7
Fe	220(30)	270(30)	360(40)	250(30)	270
Co	0.11(0.02)	0.095(0.011)	0.14(0.02)	0.11(0.02)	0.11
Ni	< 2	< 2	< 3	< 2	< 2
Cu	7.0(2.0)	4.0(3.0)	3.5(0.5)	3.1(0.5)	4.4
Zn	22(4)	15(2)	12(2)	13(2)	15
Ga	0.060(0.030)	0.057(0.020)	0.065(0.065)	0.042(0.042)	0.056
As	0.47(0.05)	0.28(0.28)	0.64(0.20)	0.40(0.40)	0.45
Se	0.10(0.02)	0.16(0.03)	0.27(0.03)	0.19(0.03)	0.18
Br	1.6(0.2)	4.9(0.5)	2.5(0.3)	3.3(0.4)	3.1
Ag	< 0.2	< 0.2	< 0.3	< 0.2	< 0.2
In	0.0033(0.0033)	< 0.0035	0.0044(0.0044)	0.0021(0.0021)	0.0029
Sb	0.13(0.02)	0.13(0.02)	0.16(0.03)	0.42(0.05)	0.21
I	0.25(0.25)	< 0.25	0.15(0.15)	0.20(0.10)	0.18
La	0.17(0.04)	0.25(0.04)	0.19(0.03)	0.16(0.03)	0.19
Ce	0.33(0.05)	0.37(0.05)	0.17(0.06)	0.37(0.05)	0.31
Sm	0.030(0.003)	0.041(0.005)	0.039(0.004)	0.032(0.005)	0.035
Eu	0.0086(0.0020)	0.0098(0.0025)	0.0081(0.0015)	0.0062(0.0010)	0.0082
W	0.05(0.04)	< 0.05	< 0.04	< 0.04	< 0.05
Hg	0.28(0.18)	0.80(0.20)	< 0.3	0.37(0.18)	0.41
Th	0.037(0.010)	0.063(0.011)	0.085(0.014)	0.047(0.010)	0.058

*Not used in averaging.

TABLE 3-12: ALGONQUIN FILTERS (ng/m^3)

	AROF1	AROF2	AROF3	AROF4	$\overline{AROF}$
Na	68(7)	66(7)	80(8)	61(7)	69
Mg	40(40)	40(40)	50(30)	40(40)	40
Al	270(30)	230(30)	280(30)	190(20)	240
Cl	5(1)	5(1)	4(1)	3(1)	4
K	180(20)	190(20)	160(20)	140(20)	170
Ca	240(30)	150(20)	175(25)	100(20)	160
Sc	0.19(0.02)	0.13(0.02)	0.17(0.02)	0.09(0.01)	0.14
Ti	17(4)	17(4)	16(5)	11(5)	15
V	2.7(0.3	1.0(0.1)	1.8(0.2)	2.3(0.3)	1.9
Cr	2.5(0.3)	2.5(0.3)	1.4(0.2)	1.2(0.2)	1.9
Mn	13(2)	13(2)	12(2)	11(2)	12
Fe	330(40)	270(30)	380(40)	250(30)	310
Co	0.16(0.02)	0.16(0.02)	0.20(0.02)	0.11(0.02)	0.16
Ni	4.8(2.5)	8.1(2.4)	< 3.5	4.0(1.1)	5.0
Cu	6.0(1.0)	8.0(1.0)	10(3)	7.5(1.0)	7.9
Zn	47(5)	37(4)	40(4)	36(4)	40
Ga	0.11(0.03)	0.17(0.04)	0.16(0.03)	0.14(0.02)	0.14
As	2.8(0.3)	4.6(0.5)	6.6(0.7)	4.8(0.5)	4.7
Se	0.56(0.06)	0.68(0.07)	0.72(0.08)	0.58(0.06)	0.63
Br	7.5(1.0)	4.5(0.5)	4.2(0.5)	6.5(1.0)	5.7
Ag	< 0.2	< 0.3	< 0.4	< 0.2	< 0.4
In	0.058(0.008)	0.018(0.002)	0.037(0.004)	0.044(0.005)	0.039
Sb	0.90(0.10)	0.43(0.05)	0.60(0.06)	0.47(0.05)	0.60
I	0.30(0.30)	0.26(0.10)	0.22(0.10)	0.32(0.10)	0.27
La	0.30(0.05)	0.32(0.04)	0.32(0.04)	0.25(0.04)	0.30
Ce	0.82(0.10)	0.54(0.07)	0.91(0.10)	0.50(0.05)	0.69
Sm	0.049(0.005)	0.054(0.006)	0.062(0.007)	0.041(0.005)	0.051
Eu	0.0092(0.0010)	0.0096(0.0020)	0.010(0.003)	0.0070(0.0040)	0.0090
W	0.075(0.008)	0.030(0.010)	0.025(0.025)	0.036(0.036)	0.041
Hg	0.16(0.30)	0.37(0.19)	0.18(0.21)	0.05(0.08)	0.19
Th	0.078(0.020)	0.039(0.011)	0.078(0.013)	0.028(0.005)	0.056

TABLE 3-13: NILES FILTERS (ng/m^3)

	NF1	NF2	NF3	NF4	$\overline{NF}$
Na	110(10)	100(10)	160(20)	130(20)	120
Mg	190(50)	70(70)	180(100)	210(30)	160
Al	510(60)	360(40)	810(90)	630(70)	580
Cl	44(8)	29(3)	40(4)	72(8)	46
K	280(30)	240(30)	440(50)	410(50)	340
Ca	800(150)	530(100)	670(70)	610(70)	650
Sc	0.44(0.05)	0.36(0.04)	0.62(0.07)	0.55(0.06)	0.49
Ti	30(30)	16(16)	60(15)	33(6)	35
V	3.2(0.4)	2.2(0.3)	5.9(0.6)	3.0(0.3)	3.6
Cr	3.7(0.4)	3.1(0.4)	4.7(0.5)	3.9(0.4)	3.8
Mn	43(5)	32(4)	50(5)	41(5)	41
Fe	920(100)	700(70)	1100(150)	1100(150)	950
Co	0.29(0.03)	0.24(0.03)	0.44(0.05)	0.40(0.04)	0.34
Ni	3(4)	< 5	< 8	< 7	< 7
Cu	10(4)	10(4)	19(4)	22(5)	15
Zn	90(15)	210(30)	100(15)	120(20)	130
Ga	0.31(0.08)	0.22(0.03)	0.56(0.12)	0.32(0.20)	0.35
As	7.1(0.8)	3.7(0.7)	4.6(0.8)	3.1(0.4)	4.6
Se	0.73(0.08)	0.84(0.09)	1.0(0.10)	0.96(0.10)	0.89
Br	40(4)	75(8)	150(20)	110(20)	94
Ag	< 0.5	< 0.5	< 0.9	< 0.7	< 0.7
In	0.014(0.005)	0.009(0.009)	0.018(0.010)	0.027(0.004)	0.017
Sb	1.6(0.2)	1.4(0.2)	2.5(0.3)	2.0(0.2)	1.9
I	< 0.5	< 0.5	0.58(0.20)	< 0.4	< 0.5
La	0.91(0.10)	0.51(0.06)	0.72(0.08)	0.91(0.10)	0.76
Ce	2.1(0.3)	1.3(0.2)	1.8(0.2)	1.4(0.2)	1.6
Sm	0.076(0.010)	0.076(0.009)	0.15(0.02)	0.13(0.02)	0.11
Eu	0.017(0.003)	0.011(0.003)	0.028(0.003)	0.020(0.003)	0.019
W	0.08(0.08)	0.08(0.08)	0.15(0.15)	0.16(0.10)	0.12
Hg	0.82(0.29)	0.65(0.28)	< 0.5	0.56(0.35)	0.61
Th	0.085(0.017)	0.056(0.016)	0.18(0.03)	0.13(0.02)	0.11

TABLE 3-14: TWIN GORGES ANDERSEN SAMPLE TG1 (ng/m^3)

	7	6	5	4	3	2	1
Na	1.4(0.2)	0.5(0.1)	2.5(0.3)	5.0(0.5)	4.3(0.5)	6.4(0.7)	29(3)
Mg	2.5(2.5)	4.6(3.5)	< 4	< 3	5.2(3.3)	4.3(3.4)	21(7)
Al	5.7(0.6)	3.4(0.4)	9.3(1.0)	18(2)	20(2)	28(3)	85(9)
Cl	< 0.25	0.20(0.22)	0.27(0.23)	0.45(0.24)	0.25(0.24)	0.35(0.25)	6.1(0.7)
K	3.8(0.4)	1.6(0.2)	4.5(0.5)	10(1)	10(1)	15(2)	37(4)
Ca	2(1)	2(1)	5(2)	10(3)	16(3)	19(4)	70(10)
Sc	0.0013 (0.0003)	0.0011 (0.0002)	0.0037 (0.0004)	0.0091 (0.0010)	0.0088 (0.0009)	0.0095 (0.0010)	0.031(0.004)
Ti	< 0.25	<0.25	<0.25	2.1(0.6)	1.6(0.6)	1.4(0.7)	9.1(1.0)
V	0.012(0.002)	0.016(0.002)	0.039(0.004)	0.046(0.007)	0.056(0.009)	0.042(0.009)	0.11(0.02)
Cr	<0.05	< 0.05	0.05(0.04)	0.09(0.04)	0.03(0.04)	0.68(0.07)	1.6(0.2)
Mn	0.050(0.005)	0.065(0.007)	0.15(0.02)	0.31(0.04)	0.47(0.05)	0.59(0.06)	1.5(0.2)
Fe	3(2)	5(2)	9(2)	11(2)	12(2)	16(2)	40(4)
Co	0.0050 (0.0010)	0.0039 (0.0010)	0.0054 (0.0011)	0.0070 (0.0011)	0.0095 (0.0011)	0.015(0.002)	0.041 (0.002)
Ni	<0.2	<0.2	<0.3	<0.3	<0.3	<0.3	<0.4
Cu	0.025(0.007)	0.039(0.010)	0.29(0.07)	0.10(0.04)	0.10(0.04)	0.16(0.02)	0.13(0.05)
Zn	0.21(0.06)	0.08(0.06)	0.20(0.06)	0.24(0.07)	0.33(0.07)	0.65(0.07)	2.4(0.3)
Ga	0.0026 (0.0009)	<0.0011	0.0028 (0.0011)	0.0038 (0.0034)	0.0022 (0.0028)	< 0.0040	0.0112 (0.0068)
As	0.023(0.008)	0.021(0.006)	0.046(0.010)	0.054(0.020)	0.039(0.020)	0.014(0.024)	0.023(0.008)
Se	<0.007	0.013(0.007)	<0.0	<0.008	<0.008	< 0.008	<0.009
Br	0.29(0.04)	0.12(0.03)	0.08(0.03)	0.10(0.03)	0.14(0.03)	0.15(0.03)	0.19(0.04)
Ag	<0.02	<0.02	<0.03	<0.03	<0.03	<0.02	<0.02
In	<0.0002	<0.0002	<0.0002	<0.0002	<0.0002	<0.0004	<0.0004
Sb	0.0070 (0.0023)	0.0058 (0.0022)	0.0090 (0.0024)	0.013(0.003)	0.012(0.003)	0.0080 (0.0030)	0.023 (0.004)
I	0.021(0.007)	0.018(0.008)	0.011(0.008)	0.024(0.010)	<0.016	0.030(0.013)	0.13(0.03)
La	0.0042 (0.0013)	0.0036 (0.0009)	0.0063 (0.0018)	0.027(0.004)	0.024(0.003)	0.037 (0.004)	0.094 (0.010)
Ce	<0.020	<0.030	<0.020	0.096(0.016)	0.050(0.015)	0.077(0.014)	0.19(0.02)
Sm	0.0006 (0.0001)	0.0005 (0.0001)	0.0009 (0.0001)	0.0029 (0.0003)	0.0026 (0.0003)	0.0045 (0.0005)	0.012 (0.002)

TABLE 3-14--Continued

	7	6	5	4	3	2	1
Eu	0.00011 (0.00010)	<0.00012	0.00042 (0.00022)	0.00080 (0.00028)	0.00016 (0.00025)	0.00045 (0.00030)	0.0019 (0.0005)
W	0.0012 (0.0008)	<0.0010	0.0021 (0.0016)	<0.0030	<0.0030	0.0048 (0.0021)	<0.0065
Hg	0.09(0.04)	<0.05	0.03(0.04)	0.02(0.04)	0.05(0.05)	0.04(0.04)	0.08(0.05)
Th	0.003(0.003)	<0.003	0.007(0.003)	0.014(0.003)	0.009(0.003)	0.010 (0.003)	0.031 (0.004)

TABLE 3-15: JASPER ANDERSEN SAMPLE J1 (ng/m^3)

	7	6	5	4	3	2	
Na	2.9(0.3)	4.0(0.4)	7.8(0.8)	5.0(0.5)	8.5(0.9)	5.8(0.6)	-
Mg	< 2	<2.5	5(3)	5(3)	5(4)	21(4)	-
Al	2.4(0.3)	4(1)	16(2)	18(2)	29(3)	43(2)	-
Cl	0.35(0.21)	0.31(0.21)	1.2(0.3)	1.0(0.2)	5.4(0.6)	1.7(0.3)	-
K	3.4(0.4)	2.2(0.3)	5.4(0.6)	9(1)	19(2)	27(3)	-
Ca	2(1)	4(1)	11(2)	13(4)	31(6)	48(7)	-
Sc	0.0003 (0.0002)	0.0014 (0.0003)	0.0059 (0.0007)	0.0080 (0.0010)	0.013 (0.002)	0.018 (0.002)	-
Ti	< 0.2	< 0.2	0.13(0.27)	0.13(0.56)	0.63(0.70)	3.4(0.9)	-
V	0.022(0.003)	0.012(0.002)	0.024(0.004)	0.039(0.007)	0.044(0.009)	0.086(0.011)	-
Cr	0.039(0.009)	0.030(0.008)	0.038(0.011)	0.045(0.009)	0.075(0.010)	0.095(0.012)	-
Mn	0.11(0.02	0.19(0.02)	0.32(0.02)	0.43(0.05)	0.69(0.07)	1.1(0.2)	-
Fe	10(2)	20(2)	18(2)	18(2)	23(3)	32(4)	-
Co	0.0032 (0.0009)	0.0030 (0.0009)	0.0074 (0.0010)	0.0082 (0.0010)	0.0098 (0.0011)	0.015 (0.002)	-
Ni	< 0.2	< 0.2	<0.2	< 0.3	<0.3	<0.3	
Cu	0.30(0.10)	0.093(0.030)	0.16(0.05)	0.098(0.030)	0.14(0.04)	0.15(0.05)	-

TABLE 3-15--Continued

	7	6	5	4	3	2	
Zn	0.30(0.08)	0.22(0.06)	0.23(0.06)	0.20(0.06)	0.60(0.08)	1.3(0.1)	-
Ga	0.0023 (0.0014)	< 0.0025	< 0.0030	0.0031 (0.0021)	0.010(0.004)	0.010(0.003)	-
As	0.031(0.010)	< 0.020	0.033(0.015)	0.024(0.012)	< 0.025	< 0.030	-
Se	< 0.0080	< 0.0080	< 0.0080	< 0.0060	0.007(0.006)	0.011(0.007)	-
Br	0.47(0.06)	0.12(0.02)	0.09(0.02)	0.13(0.03)	0.15(0.03)	0.16(0.03)	-
Ag	< 0.02	< 0.03	< 0.02	< 0.03	< 0.03	< 0.03	-
In	0.0003 (0.0002)	0.0003 (0.0002)	< 0.0002	< 0.0002	< 0.0003	< 0.0003	
Sb	0.015(0.003)	0.010(0.003)	0.014(0.003)	0.012(0.003)	0.0030 (0.0020)	0.0040 (0.0030)	-
I	0.054(0.009)	0.010(0.008)	< 0.010	< 0.012	< 0.015	< 0.016	-
La	0.0020 (0.0016)	0.0032 (0.0019)	0.010(0.003)	0.0095 (0.0021)	0.022(0.004)	0.028(0.004)	-
Ce	0.0062 (0.0044)	0.020(0.005)	0.023(0.005)	0.033(0.005)	0.038(0.006)	0.065(0.007)	-
Sm	0.0002 (0.0001)	0.0005 (0.0001)	0.0013 (0.0002)	0.0015 (0.0002)	0.0040 (0.0004)	0.0049 (0.0005)	-
Eu	0.00010 (0.00008)	0.00020 (0.00025)	0.00050 (0.00028)	0.00040 (0.00020)	0.00090 (0.00035)	0.00082 (0.00035)	-
W	0.0016 (0.0010)	< 0.0020	< 0.0025	< 0.0025	0.0035 (0.0036)	< 0.0040	-
Hg	0.057(0.021)	0.058(0.019)	0.051(0.021)	0.028(0.021)	< 0.045	< 0.05	-
Th	0.0009 (0.0006)	0.0006 (0.0005)	0.0012 (0.0006)	0.0021 (0.0006)	0.0060 (0.0008)	0.0043 (0.0008)	

TABLE 3-16: RIDING MOUNTAIN ANDERSEN SAMPLE RM1 (ng/m^3)

	7	6	5	4	3	2	1
Na	1.7(0.2)	2.2(0.3)	6.0(0.6)	4.5(0.5)	7.4(0.8)	11(2)	52(6)
Mg	3(3)	1(2)	1(4)	6(4)	24(6)	35(8)	110(25)
Al	2.5(0.3)	4(0.5)	17(2)	23(3)	47(5)	77(8)	350(40)
Cl	<0.4	<0.4	0.3(0.3	1.4(0.4)	3.2(0.5)	3.9(0.5)	15(2)
K	3(1)	3(1)	9(1)	20(2)	36(4)	29(3)	150(20)
Ca	2(2)	6(2)	18(4)	45(8)	63(10)	86(13)	280(40)
Sc	0.0036 (0.0008)	0.0049 (0.0009)	0.017(0.002)	0.024(0.003)	0.051(0.006)	0.067(0.007)	0.31(0.04)
Ti	<0.3	<0.3	0.4(0.4)	1.6(0.8)	1.1(1.1)	0.9(1.4)	17(4)
V	0.017(0.003)	0.015(0.003)	0.045(0.006)	0.053(0.010)	0.11(0.02)	0.12(0.02)	0.47(0.06)
Cr	<0.06	0.09(0.06)	0.09(0.06)	0.17(0.06)	0.24(0.08)	0.39(0.07)	1.3(0.2)
Mn	0.10(0.02)	0.13(0.02)	0.48(0.05)	0.70(0.07)	1.5(0.2)	2.1(0.3)	6.6(0.7)
Fe	15(3)	5(3)	25(4)	35(5)	69(7)	78(8)	390(40)
Co	0.015(0.004)	0.014(0.004)	0.024(0.004)	0.023(0.005)	0.031(0.006)	0.047(0.005)	0.17(0.02)
Ni	<0.6	<0.6	<0.7	<0.8	<0.9	<0.8	<1.8
Cu	0.066(0.010)	0.089(0.011)	0.16(0.05)	0.15(.05)	0.23(0.06)	0.19(0.05)	0.85(0.20)
Zn	0.9(0.1)	1.2(0.5)	1.8(0.9)	3.7(1.5)	1.1(1.1)	1.8(0.5)	7.1(3.5)
Ga	<0.003	<0.003	<0.005	0.004(0.005)	0.008(0.006)	<0.015	0.069 (0.026)
As	0.080(0.017)	0.088(0.015)	0.10(0.02)	0.030(0.021)	0.032(0.036)	<0.075	<0.16
Se	0.069(0.012)	0.043(0.012)	0.024(0.012)	0.007(0.012)	0.009(0.016)	0.018(0.013)	0.042 (0.020)
Br	0.29(0.05)	0.14(0.03)	0.11(0.03)	0.28(0.05)	0.26(0.05)	0.22(0.05)	0.49(0.09)
Ag	<0.05	<0.06	<0.06	<0.07	<0.08	<0.08	0.41(0.13)
In	0.0001 (0.0002)	0.0005 (0.0002)	0.0009 (0.0003)	0.0005 (0.0004)	<0.0003	<0.0007	<0.0015
Sb	0.094(0.008)	0.12(0.02)	0.16(0.01)	0.065(0.009)	0.080(0.015)	0.050(0.010)	0.13(0.02)
I	0.022(0.010)	<0.015	0.024(0.015)	0.018(0.017)	<0.016	0.07(0.03)	0.05(0.07)
La	<0.002	0.004(0.002)	0.017(0.003)	0.022(0.003)	0.026(0.005)	0.044(0.007)	0.23(0.03)
Ce	<0.025	<0.030	0.053(0.024)	0.072(0.025)	0.14(0.03)	0.15(0.03)	0.70(0.05)
Sm	0.0003 (0.0001)	0.0003 (0.0001)	0.0015 (0.0002)	0.0028 (0.0003)	0.0052 (0.0006)	0.0063 (0.0007)	0.038 (0.004)

TABLE 3-16--Continued

	7	6	5	4	3	2	1
Eu	<0.0001	0.0001 (0.0001)	0.0003 (0.0002)	0.0006 (0.0002)	0.0007 (0.0003)	0.0011 (0.0005)	0.0099 (0.0016)
W	<0.0020	< 0.0020	< 0.0030	0.0075 (0.0026)	0.0043 (0.0044)	< 0.008	0.035 (0.018)
Hg	0.090(0.060)	0.078(0.059)	< 0.07	< 0.08	< 0.08	0.054(0.070)	0.16(0.11)
Th	< 0.004	< 0.004	0.003(0.004)	0.007(0.004)	0.014(0.005)	0.035(0.005)	0.082 (0.010)

TABLE 3-17: ALGONQUIN ANDERSEN SAMPLE ARO1 (ng/m^3)

	7	6	5	4	3	2	1
Na	1.7(0.2)	4.4(0.5)	10(1)	12(2)	12(2)	11(2)	14(2)
Mg	<2.5	3(4)	< 7	14(7)	< 8	8(6)	12(6)
Al	4(1)	7(1)	19(2)	31(4)	43(5)	51(6)	82(9)
Cl	0.15(0.15)	0.30(0.20)	0.13(0.30)	0.09(0.25)	0.70(0.25)	0.66(0.25)	4.9(0.5)
K	4(1)	8(1)	16(2)	18(2)	28(3)	30(3)	39(4)
Ca	1(1)	4(3)	6(2)	16(5)	21(5)	30(6)	38(7)
Sc	0.0012 (0.0003)	0.0012 (0.0004)	0.0085 (0.0009)	0.015(0.002)	0.023(0.003)	0.031(0.004)	0.035 (0.004)
Ti	< 0.25	0.22(0.51)	0.71(0.68)	1.4(0.9)	2.0(1.0)	2.9(1.1)	4.7(1.3)
V	0.21(0.03)	0.41(0.05)	0.21(0.03)	0.15(0.02)	0.13(0.02)	0.11(0.02)	0.083 (0.016)
Cr	0.052(0.017)	0.11(0.02)	0.18(0.03)	0.13(0.02)	0.13(0.02)	0.11(0.02)	0.17(0.02)
Mn	0.35(0.04)	1.3(0.2)	2.7(0.3)	1.6(0.2)	1.2(0.2)	1.1(0.2)	1.2(0.2)
Fe	5(1)	14(2)	31(4)	34(4)	39(4)	51(6)	54(6)
Co	0.0045 (0.0010)	0.011(0.002)	0.010(0.002)	0.013(0.002)	0.018(0.002)	0.023(0.003)	0.029 (0.003)
Ni	< 0.2	<0.3	<0.4	<0.3	0.20(0.26)	0.56(0.27)	<0.4

TABLE 3-17--Continued

	7	6	5	4	3	2	1
Cu	0.20(0.05)	0.63(0.10)	1.5(0.2)	0.85(0.10)	0.60(0.10)	0.60(0.10)	0.56(0.10)
Zn	1.8(0.2)	5.3(0.6)	15(2)	6.9(0.7)	2.5(0.4)	1.8(0.2)	2.6(0.3)
Ga	0.0080 (0.0019)	0.019(0.004)	0.014(0.005)	0.020(0.006)	0.021(0.006)	0.015(0.007)	0.022 (0.007)
As	0.30(0.03)	0.92(0.10)	2.0(0.2)	0.80(0.08)	0.37(0.05)	0.16(0.05)	0.11(0.05)
Se	0.060(0.006)	0.14(0.02)	0.14(0.02)	0.033(0.004)	0.013(0.004)	0.019(0.004)	0.022 (0.004)
Br	0.44(0.06)	0.92(0.12)	0.52(0.06)	0.14(0.03)	0.28(0.05)	0.24(0.05)	0.33(0.08)
Ag	< 0.02	< 0.02	< 0.02	< 0.02	0.02(0.02)	0.02(0.02)	< 0.02
In	0.0033 (0.0004)	0.0081 (0.0009)	0.037(0.004)	0.016(0.002)	0.0062 (0.0008)	0.0017 (0.0005)	0.0013 (0.0005)
Sb	0.058(0.006)	0.20(0.02)	0.23(0.03)	0.10(0.01)	0.047(0.005)	0.033(0.004)	0.040 (0.004)
I	0.016(0.009)	0.006(0.016)	0.020(0.022)	< 0.025	0.011(0.021)	0.036(0.020)	< 0.021
La	0.0048 (0.0016)	0.011(0.003)	0.031(0.004)	0.054(0.006)	0.069(0.007)	0.062(0.007)	0.10(0.01)
Ce	0.015(0.007)	0.010(0.008)	0.044(0.010)	0.094(0.010)	0.14(0.02)	0.14(0.02)	0.14(0.02)
Sm	0.0007 (0.0001)	0.0009 (0.0002)	0.0032 (0.0004)	0.0068 (0.0007)	0.011(0.002)	0.011(0.002)	0.016 (0.002)
Eu	< 0.0001	0.0003 (0.0002)	0.0009 (0.0003)	0.0004 (0.0003)	0.0017 (0.0004)	0.0017 (0.0004)	0.0036 (0.0006)
W	0.0047 (0.0014)	0.0081 (0.0024)	0.0080 (0.0035)	< 0.0050	0.011(0.005)	0.005 (0.005)	< 0.006
Hg	0.032(0.016)	0.028(0.022)	0.047(0.024)	0.012(0.018)	0.047(0.018)	0.011(0.018)	< 0.02
Th	< 0.0015	< 0.0020	< 0.0020	0.0074 (0.0016)	0.011(0.016)	0.012(0.002)	0.011 (0.002)

TABLE 3-18: MACKINAC ISLAND ANDERSEN SAMPLE MI3 (ng/m^3)

	7	6	5	4	3	2	1
Na	3.5(0.4)	5.6(0.6)	8.7(0.9)	7.0(0.7)	8.0(0.8)	6.0(0.6)	9.1(1.0)
Mg	< 4	7(4)	5(4)	14(4)	28(7)	80(9)	230(30)
Al	3.1(0.3)	12(2)	18(2)	33(4)	51(6)	53(6)	79(8)
Cl	0.4(0.2)	0.4(0.2	0.2(0.2)	0.4(0.2)	2.5(0.4)	3.8(0.4)	6.8(0.7)
K	13(2)	23(3)	23(3)	11(2)	34(4)	29(3)	59(6)
Ca	4(2)	3(2)	8(3)	26(5)	100(15)	200(20)	540(60)
Sc	0.0002 (0.0003)	0.0016 (0.0004)	0.0058 (0.0006)	0.013(0.002)	0.025(0.003)	0.026(0.003)	0.044 (0.005)
Ti	< 0.3	< 0.8	< 1.0	1.2(0.7)	3.4(1.2)	2.5(1.2)	3.8(1.6)
V	0.47(0.05)	0.23(0.03)	0.11(0.02)	0.12(0.02)	0.19(0.02	0.15(0.02)	0.15(0.02)
Cr	0.17(0.03)	0.16(0.03)	0.16(0.03)	0.11(0.03)	0.17(0.03)	0.14(0.03)	0.16(0.03)
Mn	0.6(0.1)	1.4(0.2)	1.5(0.2)	0.8(0.1)	1.1(0.2)	1.0(0.1)	1.7(0.2)
Fe	9(2)	19(2)	29(3)	30(3)	47(5)	37(4)	70(7)
Co	0.015(0.002)	0.014(0.002)	0.011(0.002)	0.014(0.002)	0.023(0.003)	0.022(0.003)	0.037 (0.004)
Ni	< 0.3	< 0.3	< 0.3	< 0.3	< 0.4	< 0.4	< 0.5
Cu	0.30(0.04)	< 0.008	0.34(0.05)	0.30(0.10)	0.38(0.05)	0.16(0.05)	0.33(0.05)
Zn	2.7(0.3)	5.3(0.6)	5.6(0.6)	2.5(0.3)	2.5(0.3)	1.6(0.4)	3.0(0.5)
Ga	0.062(0.009)	0.045(0.007)	0.023(0.005)	0.008(0.004)	0.025(0.007)	0.008(0.006)	0.015 (0.010)
As	1.5(0.2)	1.7(0.2)	0.95(0.10)	0.30(0.04)	0.28(0.05)	0.14(0.03)	0.21(0.06)
Se	0.12(0.02)	0.15(0.02)	0.059(0.006)	0.018(0.004)	0.008(0.004)	0.019(0.004)	0.008 (0.005)
Br	1.4(0.2)	1.5(0.2)	0.44(0.06)	0.42(0.06)	0.91(0.11)	0.53(0.07)	0.84(0.11)
Ag	< 0.02	< 0.02	< 0.02	< 0.02	0.017(0.020)	< 0.02	< 0.03
In	0.0014 (0.0003)	0.0023 (0.0004)	0.0042 (0.0006)	0.0015 (0.0003)	< 0.0005	0.0003 (0.0005)	0.0009 (0.0006)
Sb	0.12(0.02)	0.16(0.02)	0.096(0.010)	0.034(0.004)	0.036(0.004)	0.060(0.006)	0.035 (0.004)
I	0.052(0.014)	0.051(0.018)	0.012(0.017)	< 0.015	0.020(0.024)	< 0.025	0.018 (0.029)

TABLE 3-18--Continued

	7	6	5	4	3	2	1
La	0.014(0.003)	0.011(0.004)	0.028(0.005)	0.031(0.004)	0.068(0.007)	0.038(0.006)	0.098 (0.010)
Ce	0.012(0.011)	0.032(0.011)	0.021(0.011)	0.040(0.010)	0.067(0.010)	0.062(0.010)	0.12(0.02)
Sm	0.0011 (0.0003)	0.0005 (0.0002)	0.0026 (0.0003)	0.0033 (0.0004)	0.0073 (0.0008)	0.0058 (0.0006)	0.014 (0.002)
Eu	<0.0003	<0.0003	0.0002 (0.0003)	0.0002 (0.0003)	0.0020 (0.0005)	0.0004 (0.0005)	0.0026 (0.0007)
W	0.0092 (0.0030)	0.0092 (0.0036)	0.012(0.004)	0.0038 (0.0028)	0.0091 (0.0053)	0.0022 (0.0041)	0.016 (0.007)
Hg	0.14(0.05)	<0.06	0.036(0.046)	0.022(0.041)	0.024(0.042)	0.101(0.042)	0.091 (0.045)
Th	0.0023 (0.0019)	<0.0020	<0.0020	0.0040 (0.0018)	0.0043 (0.0018)	0.0087 (0.0019)	0.012 (0.002)

TABLE 3-19: NILES ANDERSEN SAMPLE N1 (ng/m^3)

	7	6	5	4	3	2	1
Na	11(2)	10(1)	34(4)	36(4)	49(5)	26(3)	31(4)
Mg	14(12)	<10	<14	<13	58(26)	62(18)	84(20)
Al	5(1)	12(2)	78(8)	110(20)	220(30)	190(20)	230(30)
Cl	1.3(0.4)	0.7(0.4)	1.5(0.5)	3.5(0.5)	15(2)	12(2)	13(2)
K	31(3)	20(2)	46(5)	45(5)	80(8)	78(8)	93(10)
Ca	5(4)	7(3)	37(8)	60(15)	220(40)	200(40)	270(50)
Sc	0.0034 (0.0010)	0.0089 (0.0010)	0.053(0.006)	0.082(0.009)	0.14(0.02)	0.13(0.02)	0.16(0.02)
Ti	<1	<1	1(2)	6(3)	17(5)	13(6)	21(10)
V	0.36(0.04)	0.15(0.02)	0.31(0.04)	0.39(0.04)	0.58(0.06)	0.53(0.07)	0.62(0.07)
Cr	0.42(0.08)	0.36(0.07)	0.56(0.08)	0.46(0.07)	0.73(0.08)	0.62(0.07)	1.6(0.2)

TABLE 3-19--Continued

	7	6	5	4	3	2	1
Mn	4.1(0.5)	2.8(0.3)	4.7(0.5)	3.5(0.4)	6.3(0.7)	5.0(0.5)	6.1(0.7)
Fe	30(3)	36(5)	120(20)	130(20)	210(30)	190(20)	270(30)
Co	0.021(0.003)	0.018(0.002)	0.045(0.005)	0.062(0.007)	0.10(0.01)	0.093(0.010)	0.16(0.02)
Ni	<0.8	<0.8	<1.0	<1.0	<1.0	<0.9	<0.8
Cu	1.0(0.3)	0.7(0.1)	1.5(0.5)	1.6(0.2)	1.8(0.3)	1.2(0.2)	1.2(0.2)
Zn	16(2)	15(2)	35(4)	14(2)	9(2)	7(2)	6(2)
Ga	<0.015	0.024(0.010)	0.023(0.018)	0.021(0.016)	0.043(0.019)	0.046(0.025)	0.063 (0.024)
As	0.93(0.12)	0.27(0.08)	0.51(0.13)	0.13(0.12)	0.60(0.17)	0.51(0.17)	0.10(0.10)
Se	0.42(0.05)	0.14(0.02)	0.14(0.02)	0.068(0.010)	0.053(0.010)	0.019(0.009)	0.015 (0.010)
Br	12(2)	2.9(0.4)	4.6(0.6)	4.8(0.6)	8.1(1.0)	5.1(0.6)	2.8(0.4)
Ag	<0.06	<0.08	<0.06	<0.05	<0.05	<0.05	<0.07
In	0.0073 (0.0014)	0.0079 (0.0012)	0.015 (0.002)	0.0037 (0.0011)	0.0063 (0.0021)	<0.0025	<0.0030
Sb	0.50(0.05)	0.24(0.03)	0.22(0.03)	0.11(0.02)	0.14(0.02)	0.11(0.02)	0.10(0.02)
I	0.096(0.053)	<0.05	<0.06	<0.05	<0.10	<0.12	<0.14
La	0.19(0.02)	0.03(0.01)	0.21(0.02)	0.19(0.02)	0.27(0.02)	0.16(0.03)	0.18(0.03)
Ce	0.21(0.03)	0.07(0.04)	0.26(0.03)	0.25(0.03)	0.36(0.04)	0.33(0.04)	0.51(0.06)
Sm	0.0037 (0.0013)	0.0026 (0.0009)	0.020(0.002)	0.017(0.002)	0.036(0.004)	0.031(0.004)	0.031 (0.004)
Eu	<0.0010	<0.0008	0.0051 (0.0015)	0.0051 (0.0015)	0.0060 (0.0024)	0.0073 (0.0021)	0.0056 (0.0021)
W	0.050(0.013)	0.010(0.009)	0.027(0.017)	0.042(0.019)	0.040(0.020)	0.029(0.017)	0.044 (0.025)
Hg	0.09(0.19)	0.20(0.15)	0.21(0.17)	0.10(0.15)	0.50(0.17)	0.23(0.15)	0.40(0.17)
Th	<0.006	<0.007	0.015(0.005)	0.021(0.005)	0.026(0.005)	0.036(0.005)	0.042 (0.006)

TABLE 3-20: TWIN GORGES ANDERSEN SAMPLE TG2 (ng/m^3)

	7	6	5	4	3	2	1
Na	1.9(0.2)	21(3)	99(10)	100(10)	50(5)	12(2)	4.3(0.5)
Mg	<1.5	3(3)	15(7)	<12	<10	6(4)	1(2)
Al	0.29(0.03)	0.36(0.04)	2.9(0.3)	4.6(0.5)	10(1)	9.9(1.0)	10(1)
Cl	<0.15	<0.2	61(7)	150(20)	79(8)	16(2)	2.7(0.3)
K	0.50(0.18)	1.9(0.8)	12(3)	8.1(4.8)	5.4(1.7)	6.8(0.7)	6.0(0.6)
Ca	0.3(0.4)	1.3(0.5)	14(6)	10(10)	8(8)	8(4)	6.2(1.6)
Sc	0.0002 (0.0001)	0.0003 (0.0001)	0.0009 (0.0002)	0.0020 (0.0002)	0.0036 (0.0004)	0.0041 (0.0005)	0.0044 (0.0005)
Ti	< 0.1	< 0.2	<0.6	< 0.9	<0.8	0.6(0.3)	0.7(0.3)
V	0.0065 (0.0008)	0.051(0.006)	0.062(0.007)	0.067(0.009)	0.11(0.02	0.039(0.004)	0.031 (0.004)
Cr	0.014(0.015)	0.028(0.007)	0.059(0.008)	0.14(0.02)	0.24(0.03)	0.24(0.03)	0.33(0.04)
Mn	0.031(0.004)	0.072(0.008)	0.17(0.02)	0.10(0.01)	0.14(0.02)	0.11(0.02)	0.11(0.02)
Fe	24(7)	70(12)	170(20)	130(20)	130(20)	130(20)	160(20)
Co	0.0018 (0.0007)	0.0025 (0.0008)	0.0043 (0.0009)	0.0056 (0.0010)	0.0071 (0.0009)	0.0058 (0.0009)	0.010 (0.001)
Ni	<0.1	<0.15	<0.2	<0.2	<0.2	<0.2	<0.2
Cu	<0.04	<0.08	0.4(0.4)	0.9(0.6)	<0.6	0.3(0.2)	0.2(0.2)
Zn	0.08(0.04)	0.33(0.05)	0.85(0.10)	0.52(0.07)	0.37(0.05)	0.25(0.05)	0.38(0.05)
Ga	0.006(0.002)	<0.015	0.077(0.048)	<0.09	0.020(0.017)	0.018(0.008)	0.005 (0.004)
As	0.018(0.012)	0.14(0.06)	< 0.3	<0.7	0.22(0.11)	0.045(0.044)	0.025 (0.019)
Se	0.007(0.002)	0.026(0.003)	0.019(0.003)	0.007(0.003)	< 0.003	<0.003	<0.003
Br	0.12(0.02)	0.57(0.08)	0.61(0.13)	1.1(0.2)	0.15(0.06)	0.090(0.029)	0.058 (0.016)
Ag	< 0.008	< 0.015	0.018(0.011)	<0.015	<0.015	<0.02	<0.02
In	< 0.0001	0.0001 (0.0001)	0.0008 (0.0004)	0.0024 (0.0006)	<0.0004	<0.0002	<0.0003
Sb	0.006(0.001)	0.013(0.002)	0.020(0.002)	0.012(0.002)	0.011(0.002)	0.012(0.002)	0.011 (0.002)
I	0.023(0.004)	0.11(0.02)	0.12(0.02)	0.063(0.028)	< 0.030	0.020(0.010)	<0.006

TABLE 3-20--Continued

	7	6	5	4	3	2	1
La	0.0013 (0.0019)	< 0.01	< 0.04	< 0.05	0.007(0.016)	0.018(0.007)	0.026 (0.004)
Ce	0.004(0.002)	0.005(0.003)	0.005(0.003)	0.016(0.003)	0.022(0.003)	0.026(0.003)	0.034 (0.004)
Sm	0.0004 (0.0001)	< 0.0007	0.0044 (0.0031)	0.0075 (0.0048)	0.0018 (0.0012)	0.0032 (0.0005)	0.0024 (0.0003)
Eu	< 0.0002	0.0003 (0.0005)	< 0.0030	< 0.0050	< 0.0015	0.0010 (0.0004)	0.0002 (0.0002)
W	< 0.0025	< 0.009	< 0.04	0.074(0.045)	< 0.02	< 0.0070	0.0018 (0.0028)
Hg	0.008(0.006)	< 0.012	< 0.009	< 0.008	< 0.008	0.006(0.007)	0.015 (0.007)
Th	0.0004 (0.0003)	< 0.0004	< 0.0007	0.0069 (0.0007)	0.0047 (0.0005)	0.0085 (0.0009)	0.0093 (0.0010)

TABLE 3-21: TWIN GORGES ANDERSEN SAMPLE TG3 (ng/m^3)

	F	7	6	5	4	3	2	1
Na	4.5(0.7)	0.3(0.2)	9.6(1.0)	36(4)	32(3)	16(2)	4.5(0.5)	2.4(0.3)
Mg	< 8	7(4)	6(6)	< 11	15(14)	15(9)	< 6	7.1(4.4)
Al	1.2(0.2)	0.8(0.2)	1.9(0.2)	2.1(0.3)	5.1(0.6)	4.9(0.5)	4.1(0.5)	6.4(0.7)
Cl	6.3(0.9)	< 0.8	< 0.9	< 0.9	51(6)	27(2)	6.0(1.0)	1.0(0.8)
K	2.1(0.6)	0.8(0.3)	5.1(0.7)	8.3(1.8)	2.6(1.6)	4.7(0.9)	1.7(0.5)	3.6(0.4)
Ca	2.0(3.0)	1.7(2.0)	5.0(3.0)	4.0(3.0)	< 5	3.0(3.0)	5.3(4.1)	5.0(3.0)
Sc	-	-	-	-	-	-	-	-
Ti	< 0.4	< 0.5	< 0.5	< 0.5	< 0.7	< 0.5	< 0.5	< 0.5
V	0.073 (0.008)	0.024 (0.004)	0.14(0.02)	0.067 (0.008)	0.032 (0.007)	0.016 (0.005)	0.008 (0.004)	0.004 (0.005)
Cr	-	-	-	-	-	-	-	-

TABLE 21--Continued

	F	7	6	5	4	3	2	1
Mn	0.10(0.01)	0.12(0.02)	0.26(0.03)	0.27(0.03)	0.37(0.04)	0.20(0.02)	0.06(0.01)	0.10(0.01)
Fe	-	-	-	-	-	-	-	-
Co	-	-	-	-	-	-	-	-
Ni	-	-	-	-	-	-	-	-
Cu	<0.3	<0.2	0.6(0.3)	0.6(0.3)	0.7(0.5)	0.8(0.4)	0.4(0.3)	<0.3
Zn	-	-	-	-	-	-	-	-
Ga	0.014 (0.006)	0.009 (0.003)	0.011 (0.006)	<0.02	<0.02	0.011 (0.008)	0.011 (0.005)	<0.005
As	0.03(0.04)	0.04(0.02)	0.27(0.06)	0.31(0.14)	0.53(0.13)	0.75(0.09)	0.33(0.05)	0.07(0.03)
Se	-	-	-	-	-	-	-	-
Br	0.85(0.12)	0.43(0.09)	1.2(0.2)	0.72(0.13)	0.38(0.10)	0.35(0.09)	0.29(0.08)	0.20.0.07)
Ag	-	-	-	-	-	-	-	-
In	<0.0005	<0.0003	<0.0005	<0.0005	<0.0008	<0.0006	<0.0003	<0.0003
Sb	-	-	-	-	-	-	-	-
I	0.16(0.03)	0.02(0.02)	0.12(0.03)	0.06(0.03)	<0.04	<0.03	0.02(0.02)	0.02(0.01)
La	<0.007	<0.003	<0.008	<0.020	<0.020	0.009 (0.009)	0.009 (0.005)	0.012 (0.004)
Ce	-	-	-	-	-	-	-	-
Sm	<0.0004	<0.0002	<0.0004	<0.0015	<0.0010	0.0006 (0.0005)	0.0009 (0.0005)	0.0012 (0.0003)
Eu	<0.0004	<0.0002	0.0008 (0.0004)	<0.0015	<0.0010	0.0008 (0.0005)	<0.0003	<0.0002
W	<0.007	0.010 (0.003)	<0.008	<0.020	0.026 (0.015)	0.023 (0.008)	<0.005	<0.005
Hg	-	-	-	-	-	-	-	-
Th	-	-	-	-	-	-	-	-

TABLE 3-22: ALGONQUIN ANDERSEN SAMPLE ARO2 (ng/m^3)

	7	6	5	4	3	2	1
Na	8.8(0.9)	16(2)	39(4)	21(3)	8.1(0.9)	3.8(0.4)	2.2(0.3)
Mg	< 6	<10	<13	9(8)	< 6	< 4	4(4)
Al	23(3)	38(4)	72(8)	43(5)	34(4)	20(2)	16(2)
Cl	< 0.3	0.5(0.4)	6.8(0.8)	7.4(0.8)	3.3(0.5)	1.5(0.3)	1.4(0.3)
K	6.6(0.7	6.7(0.7)	12(2)	6.6(1.2)	3.6(0.6)	3.6(0.5)	5.3(0.6)
Ca	4.5(2.0)	< 4	< 5	11(5)	5.0(3.0)	7.0(3.0)	5.5(3.0)
Sc	0.0012 (0.0004)	0.0017 (0.0005)	0.0058 (0.0006)	0.0081 (0.0009)	0.0065 (0.0007)	0.0051 (0.0006)	0.0045 (0.0005)
Ti	<1	<1.5	< 2	<1.3	<1.2	<0.9	1.0(0.4)
V	1.2(0.2)	0.46(0.05)	0.33(0.04)	0.26(0.03)	0.14(0.02)	0.072(0.011)	0.027 (0.006)
Cr	0.20(0.02)	0.20(0.02)	0.38(0.04)	0.24(0.03)	0.14(0.02)	0.09(0.02)	0.09(0.02)
Mn	1.2(0.2)	1.4(0.2)	2.3(0.3)	1.1(0.2)	0.59(0.06)	0.32(0.04)	0.22(0.03)
Fe	32(4)	44(5)	80(8)	62(7)	42(5)	25(3)	15(2)
Co	0.010(0.002)	0.010(0.002)	0.013(0.002)	0.016(0.002)	0.015(0.002)	0.011(0.002)	0.011 (0.002)
Ni	0.3(0.3)	<0.3	0.5(0.4)	< 0.3	< 0.3	< 0.3	< 0.3
Cu	1.3(0.4)	2.0(0.5)	4.5(0.8)	2.7(0.6)	1.3(0.2)	0.8(0.4)	0.3(0.1)
Zn	3.2(0.4)	6.1(0.7)	12(2)	4.5(0.6)	1.8(0.2)	1.2(0.2)	1.0(0.2)
Ga	0.018(0.006)	0.009(0.008)	0.053(0.024)	< 0.015	0.012(0.006)	<0.005	<0.005
As	0.31(0.04)	0.40(0.06)	1.2(0.2)	0.15(0.08)	0.076(0.035)	0.028(0.024)	0.027 (0.020)
Se	0.11(0.02)	0.080(0.010)	0.10(0.01)	0.032(0.006)	0.010(0.005)	< 0.006	< 0.008
Br	1.3(0.3)	0.79(0.15)	0.54(0.20)	0.34(0.15)	0.35(0.15)	0.24(0.10)	0.13(0.06)
Ag	< 0.03	< 0.03	< 0.04	< 0.03	< 0.03	< 0.05	<0.02
In	0.0052 (0.0007)	0.018(0.002)	0.039(0.004)	0.0071 (0.0009)	0.0008 (0.0005)	0.0005 (0.0003)	0.0004 (0.0003)
Sb	0.085(0.009)	0.069(0.007)	0.068(0.007)	0.023(0.004)	0.019(0.003)	0.011(0.003)	0.005 (0.003)
I	0.13(0.02)	0.05(0.03)	< 0.05	< 0.04	< 0.03	< 0.02	< 0.02
La	< 0.0070	0.012(0.007)	< 0.030	0.0095 (0.0120)	0.0085 (0.0052)	0.0042 (0.0038)	0.012 (0.003)

TABLE 3-22--Continued

	7	6	5	4	3	2	1
Ce	0.013(0.007)	0.013(0.007)	0.032(0.007)	0.047(0.007)	0.016(0.006)	0.028(0.006)	0.016 (0.006)
Sm	0.0005 (0.0004)	0.0016 (0.0005)	0.0031 (0.0017)	0.0021 (0.0008)	0.0017 (0.0004)	0.0014 (0.0003)	0.0013 (0.0002)
Eu	<0.0004	<0.0004	<0.0016	0.0018 (0.0008)	0.0007 (0.0004)	<0.0004	<0.0002
W	<0.006	<0.008	<0.025	<0.015	<0.005	<0.004	0.011 (0.003)
Hg	0.03(0.03)	0.05(0.03)	0.01(0.03)	0.01(0.02)	0.03(0.02)	0.03(0.02)	0.03(0.02)
Th	0.0011 (0.0010)	<0.0012	0.0012 (0.0011)	0.0018 (0.0009)	0.0017 (0.0008)	0.0005 (0.0008)	0.0002 (0.0007)

TABLE 3-23: MACKINAC ISLAND ANDERSEN SAMPLE MI4 (ng/m^3)

	7	6	5	4	3	2	1
Na	8.6(0.9)	16(2)	28(3)	16(2)	14(2)	6.5(0.7)	6.5(0.7)
Mg	<6	10(7)	<8	4(6)	5(6)	7(5)	37(7)
Al	2.7(0.3)	4.6(0.5)	17(2)	31(4)	48(5)	33(4)	41(5)
Cl	<0.5	0.7(0.5)	<0.5	1.7(0.5)	3.2(0.6)	2.5(0.5)	2.3(0.5)
K	9.1(1.0)	10(1)	8.5(1.4)	7.4(1.0)	15(2)	10(1)	15(2)
Ca	3(3)	2(2)	10(4)	<10	35(10)	39(8)	110(20)
Sc	<0.0006	0.0018 (0.0007)	0.0083 (0.0009)	0.014(0.002)	0.028(0.003)	0.017(0.002)	0.020 (0.002)
Ti	0.5(0.4)	<0.5	1.1(0.5)	0.8(0.9)	4.4(1.1)	1.3(1.0)	3.9(1.1)
V	0.26(0.03)	0.11(0.02)	0.11(0.02)	0.10(0.01)	0.13(0.02)	0.10(0.01)	0.07(0.02)
Cr	0.27(0.03)	0.17(0.03)	0.21(0.03)	0.19(0.03)	0.19(0.03)	0.12(0.03)	0.08(0.03)
Mn	1.3(0.2)	1.3(0.2)	1.1(0.2)	0.80(0.08)	0.98(0.10)	0.72(0.08)	0.90(0.10)
Fe	15(3)	18(3)	35(4)	38(4)	67(7)	40(4)	39(4)

TABLE 3-23--Continued

	7	6	5	4	3	2	1
Co	0.024(0.004)	0.019(0.003)	0.026(0.004)	0.039(0.004)	0.062(0.007)	0.049(0.005)	0.0039 (0.004)
Ni	<0.5	<0.5	<0.7	<0.5	1.9(0.5)	0.6(0.4)	0.3(0.4)
Cu	1.2(0.2)	1.3(0.2)	1.6(0.3)	1.2(0.3)	1.5(0.5)	1.1(0.3)	0.8(0.2)
Zn	4.7(0.5)	7.1(0.8)	11(2)	3.2(0.4)	2.2(0.3)	1.4(0.2)	2.3(0.3)
Ga	0.024(0.008)	0.019(0.010)	<0.015	0.011(0.009)	0.020(0.009)	<0.007	0.009 (0.005)
As	3.1(0.4)	2.4(0.3)	1.4(0.2)	0.33(0.07)	0.58(0.08)	0.31(0.06)	0.17(0.05)
Se	0.56(0.06)	0.38(0.04)	0.18(0.02)	0.040(0.009)	0.032(0.010)	0.023(0.009)	0.021 (0.009)
Br	1.5(0.2)	0.85(0.12)	0.78(0.12)	0.71(0.11)	0.87(0.13)	0.61(0.09)	0.38(0.07)
Ag	<0.1	<0.1	<0.1	<0.1	<0.1	<0.1	<0.1
In	0.0064 (0.0008)	0.020(0.002)	0.024(0.003)	0.0036 (0.0006)	0.0024 (0.0005)	0.0024 (0.0005)	0.0021 (0.0005)
Sb	0.10(0.01)	0.091(0.010)	0.075(0.008)	0.029(0.006)	0.031(0.006)	0.021(0.006)	0.028 (0.006)
I	0.13(0.03)	0.11(0.03)	0.042(0.026)	0.026(0.020)	0.037(0.022)	<0.025	<0.025
La	0.006(0.007)	0.009(0.009)	0.029(0.012)	0.028(0.009)	0.041(0.009)	0.025(0.006)	0.034 (0.006)
Ce	<0.18	0.020(0.012)	0.043(0.013)	0.051(0.011)	0.085(0.012)	0.044(0.011)	0.046 (0.011)
Sm	0.0022 (0.0007)	0.0008 (0.0008)	0.0005 (0.0010)	0.0035 (0.0007)	0.0041 (0.0007)	0.0055 (0.0006)	0.0046 (0.0005)
Eu	<0.0010	<0.0010	<0.0010	0.0011 (0.0006)	0.0006 (0.0005)	<0.0004	0.0013 (0.0003)
W	<0.010	<0.010	<0.015	<0.014	<0.009	<0.006	<0.010
Hg	0.39(0.08)	0.13(0.07)	0.07(0.07)	0.11(0.05)	<0.08	0.10(0.06)	0.06(0.05)
Th	<0.0020	<0.0020	0.0018 (0.0019)	0.0041 (0.0017)	0.0068 (0.0018)	0.0044 (0.0017)	0.0090 (0.0018)

APPENDIX 4

Table 4-1 Trace Element Concentrations in Nanogram/m^3 of Air Sampled at 25 Stations.

Station Number	1	2	3	4	5	6	7	8	9	10
S*	15(6)	11(6)	16(10)	8(5)	14(8)	13(8)	9(6)	14(7)	11(7)	7(5)
Ca	5450(600)	3000(1000)	4700(600)	3100(800)	3000(600)	7000(700)	5300(800)	2300(400)	3050(500)	5000(1100)
Al	2450(300)	2250(500)	2350(300)	1550(200)	1800(200)	2175(170)	2120(270)	1400(90)	1375(70)	1450(200)
V	9.8(0.9)	8.2(1)	9.1(1)	16.8(3.0)	11.3(1.0)	18.1(1.5)	9.8(1.0)	6.3(1.0)	6.2(0.5)	5.2(0.7)
Cu	130(20)	33(15)	93(10)	195(20)	100(15)	1100(100)	210(15)	3100(200)	3100(200)	4000(250)
Ti	280(50)	170(35)	200(40)	135(50)	155(35)	190(40)	185(40)	190(35)	260(40)	155(30)
In	0.12(0.06)	0.08(0.05)	0.11(0.05)	0.07(0.04)	0.12(0.05)	0.10(0.05)	0.09(0.06)	0.04(0.04)	<0.05	0.04(0.03)
Br	180(20)	170(30)	180(25)	95(15)	75(8)	75(8)	130(15)	67(5)	55(7)	40(4)
Mn	390(50)	150(30)	177(30)	215(40)	300(45)	255(40)	208(12)	125(6)	105(12)	83(5)
Mg	1500(700)	1500(500)	1200(400)	900(400)	1300(500)	2400(600)	1750(500)	780(300)	1250(400)	1650(400)
Na	500(50)	370(100)	300(40)	225(18)	270(55)	455(55)	335(50)	210(15)	215(50)	160(20)
Sm	0.46(0.06)	0.48(0.06)	0.36(0.05)	0.37(0.04)	0.38(0.03)	0.41(0.08)	0.32(0.04)	0.22(0.04)	0.27(0.03)	0.26(0.04)
Zn	750(70)	350(25)	255(25)	740(70)	390(35)	1540(150)	1120(100)	250(20)	460(70)	320(50)
Sb	14(1)	6.5(1)	5.2(0.5)	28(5)	15(2)	28(4)	32(3)	7.0(0.7)	13(3)	5.3(0.5)
W	<0.8	0.8(0.3)	0.5(0.3)	0.8(0.3)	0.7(0.3)	5.6(1)	1.0(0.3)	0.5(0.25)	0.7(0.3)	0.5(0.3)
Ga	<1.0	0.9(0.3)	<0.5	0.8(0.4)	0.8(0.4)	1.3(0.4)	1.3(0.5)	0.7(0.4)	0.8(0.4)	0.8(0.4)
Eu	0.14(0.02)	0.11(0.04)	0.095(0.03)	0.115(0.015)	0.10(0.01)	0.135(0.02)	0.10(0.015)	0.10(0.02)	0.08(0.015)	0.07(0.02)
As	3(2)	3(1)	3(2)	7(3)	2(1)	12(3)	8.5(2)	2(1)	6.8(1.5)	3.5(1.2)
K	1860(200)	1500(150)	1370(130)	1200(150)	1260(160)	1415(150)	1390(150)	1040(140)	990(70)	800(40)
La	4.4(0.3)	5.2(0.8)	3.5(0.6)	3.2(0.4)	3.7(0.5)	5.9(0.4)	2.7(0.5)	2.5(0.5)	2.3(0.3)	2.5(0.3)
Co	2.4(0.2)	1.2(0.1)	1.35(0.15)	1.65(0.1)	1.4(0.15)	2.6(0.6)	1.8(0.2)	0.92(0.10)	1.5(0.1)	1.3(0.1)
Fe	9900(400)	4550(200)	5500(300)	7300(400)	7250(400)	13,800(3000)	8300(600)	4000(600)	6000(300)	4000(200)
Sc	3.1(0.3)	1.85(0.1)	2.0(0.2)	2.3(0.2)	2.2(0.2)	3.1(0.5)	1.9(0.2)	1.3(0.1)	2.0(0.1)	1.7(0.1)
Cr	66(4)	26(3)	38(4)	58(3)	69(5)	113(20)	55(5)	21(2)	79(4)	79(4)
Hg	4.9(0.9)	3.5(1)	2.8(1)	1.4(0.4)	1.9(0.6)	4.8(1.0)	1.5(0.5)	2.8(1.0)	1.9(0.5)	2.0(0.4)
Se	2.9(0.6)	3.6(1.3)	2.4(1.0)	2.3(0.5)	3.4(0.6)	3.8(1.0)	2.9(0.6)	1.8(0.5)	2.1(0.5)	1.8(0.3)
Th	0.85(0.25)	0.48(0.1)	0.62(0.10)	0.58(0.10)	0.70(0.10)	1.3(0.4)	0.48(0.10)	0.28(0.10)	0.46(0.05)	0.45(0.06)
Ce	10.7(1.0)	8.3(0.5)	7.2(1.0)	8.1(1.0)	7.6(0.8)	13(3)	5.5(0.5)	5.1(1.0)	2.5(0.2)	2.1(0.2)
Ag	1.7(1.5)	1.4(1.3)	1.3(1.1)	2(1.5)	1.7(1.2)	2.4(1.5)	<2	3.0(1.2)	5(2)	3(2)
Ni	<50	<40	25(25)	30(20)	<50	<40	<80	30(25)	<30	<20

*$\mu g/m^3$

Table 4-1 (cont.)

Station Number	11	12	13	14	15	16	17	18	19
S*	9(4)	8(3)	15(7)	8(4)	9(3)	6(4)	10(5)	6(4)	3(3)
Ca	2900(300)	1700(200)	3600(1000)	2100(100)	2250(250)	1500(300)	4330(400)	1430(400)	1410(200)
Al	2200(250)	1675(150)	2400(300)	1900(250)	2600(250)	1650(150)	2090(150)	1770(140)	1590(100)
V	5.5(0.4)	5.3(1.5)	8.6(1.0)	4.3(1.2)	6.6(0.5)	4.0(1.0)	17.3(0.8)	4.5(0.4)	4.8(0.3)
Cu	170(10)	32(10)	75(15)	240(60)	150(40)	75(10)	32(10)	26(5)	182(15)
Ti	185(35)	130(30)	190(50)	150(30)	240(35)	150(50)	145(25)	150(25)	120(25)
In	0.07(0.04)	0.05(0.04)	0.15(0.06)	0.04(0.03)	<0.05	<0.05	0.04(0.03)	0.04(0.03)	0.04(0.03)
Br	45(6)	57(8)	300(30)	68(7)	52(7)	51(6)	37(5)	26(3)	35(5)
Mn	112(10)	92(12)	270(40)	98(10)	130(10)	92(15)	101(10)	85(5)	63(3)
Mg	700(400)	1000(400)	2700(400)	620(400)	1000(500)	1000(500)	1350(400)	800(300)	530(300)
Na	300(20)	270(30)	380(40)	255(20)	305(25)	225(50)	360(30)	305(15)	290(20)
Sm	0.28(0.04)	0.44(0.05)	0.42(0.03)	0.25(0.03)	0.23(0.04)	0.17(0.02)	0.45(0.05)	0.33(0.02)	0.38(0.02)
Zn	100(12)	160(30)	290(25)	135(20)	115(20)	130(15)	315(20)	135(20)	280(20)
Sb	2.25(0.4)	3.8(0.6)	4.1(0.5)	2.5(0.5)	3.0(0.8)	3.0(0.5)	11.5(1.0)	2.2(0.3)	2.7(0.4)
W	0.25(0.2)	1.2(0.4)	1.2(0.5)	<0.4	0.4(0.3)	0.3(0.3)	0.5(0.3)	0.5(0.5)	<0.5
Ga	0.7(0.3)	1.8(1.0)	0.25(0.15)	0.55(0.3)	0.5(0.3)	3.5(1.0)	0.8(0.3)	0.9(0.4)	0.7(0.4)
Eu	0.085(0.015)	0.085(0.010)	0.09(0.01)	0.08(0.01)	0.08(0.02)	0.06(0.01)	0.095(0.01)	0.07(0.01)	0.085(0.015)
As	4(3)	6.5(3)	7(3)	4(2)	3.5(1.5)	4(3)	3(2)	3(2)	2.7(2)
K	905(65)	1300(150)	1090(60)	1000(60)	990(110)	730(90)	1250(70)	1050(85)	1320(80)
La	1.7(0.3)	2.2(0.4)	2.4(0.3)	1.8(0.3)	1.5(0.3)	0.9(0.1)	4.4(0.4)	2.2(0.2)	2.6(0.2)
Co	0.47(0.10)	0.84(0.08)	1.15(0.15)	0.60(0.1)	0.55(0.06)	0.70(0.10)	1.3(0.1)	0.8(0.1)	0.90(0.07)
Fe	2025(150)	2940(250)	12,000(1000)	2050(200)	1420(120)	2290(300)	3300(300)	2700(180)	3000(150)
Sc	0.92(0.1)	1.4(0.2)	1.8(0.2)	1.1(0.2)	0.95(0.1)	1.1(0.1)	1.9(0.1)	1.3(0.1)	1.4(0.11)
Cr	9(1)	13(0.7)	33(4)	10.2(2)	6.2(0.8)	8.6(0.8)	18(1.5)	8.7(0.5)	9.0(0.6)
Hg	0.8(0.3)	1.5(0.4)	1.5(0.6)	1.6(1.0)	1.5(0.5)	1.2(0.3)	0.9(0.5)	0.8(0.4)	1.8(0.5)
Se	0.8(0.5)	2.3(1.0)	1.1(0.4)	1.7(0.3)	1.5(0.6)	1.8(0.5)	1.4(0.5)	1.1(0.4)	1.5(0.3)
Th	0.17(0.02)	0.42(0.04)	0.43(0.10)	0.25(0.05)	0.22(0.04)	0.34(0.04)	0.52(0.04)	0.42(0.06)	0.47(0.04)
Ce	2.4(0.2)	4.2(0.8)	7.2(1.0)	3.0(0.3)	2.5(0.4)	3.1(0.6)	3.3(0.2)	1.8(0.2)	1.8(0.1)
Ag	<1	<1	<1.5	<1	<1	0.9(0.8)	<1.5	<1	<1
Ni	<20	<20	14(15)	<30	<20	<20	<25	<25	16(12)

*$\mu g/m^3$

Table 4-1 (cont.)

Station Number	21	22	23	24	26A	30
S*	17(8)	7(6)	10(8)	18(10)	15(7)	11(5)
Ca	3900(1000)	2260(400)	1950(400)	3400(1000)	2650(600)	1000(200)
Al	3000(600)	2260(400)	1960(150)	3100(300)	1850(150)	1200(70)
V	8.2(1.0)	6.9(1.0)	6.2(0.8)	10.2(1.0)	5.9(0.4)	5.0(0.3)
Cu	95(15)	75(30)	860(60)	43(15)	290(25)	280(25)
Ti	265(80)	195(35)	180(35)	225(50)	165(25)	120(25)
In	0.09(0.06)	0.04(0.04)	0.08(0.06)	0.05(0.04)	0.05(0.03)	0.04(0.03)
Br	70(12)	32(7)	27(6)	61(12)	75(7)	37(6)
Mn	145(20)	115(20)	82(10)	160(20)	106(7)	62(4)
Mg	1150(500)	1200(600)	800(600)	1350(600)	800(400)	500(300)
Na	325(60)	275(70)	230(40)	405(30)	255(40)	170(20)
Sm	0.65(0.20)	0.31(0.03)	0.36(0.06)	0.43(0.07)	0.38(0.05)	0.24(0.03)
Zn	195(15)	135(15)	260(40)	190(15)	190(20)	160(20)
Sb	5.2(0.5)	5.0(0.8)	4.6(1.1)	5.9(0.7)	5.0(0.5)	6.0(0.5)
W	1.3(0.7)	0.5(0.2)	1.2(0.6)	0.75(0.3)	0.8(0.3)	0.4(0.2)
Ga	2.9(1.3)	0.8(0.3)	0.7(0.4)	0.65(0.25)	1.0(0.3)	0.9(0.4)
Eu	0.17(0.03)	0.08(0.02)	0.10(0.02)	0.10(0.01)	0.08(0.02)	0.055(0.010)
As	8(4)	5(2.5)	6(3)	8(3)	3.5(1.0)	4.6(2.0)
K	1810(110)	1190(100)	1025(70)	1510(150)	1110(130)	750(100)
La	3.6(0.5)	1.8(0.2)	0.9(0.3)	2.6(0.5)	2.1(0.3)	1.3(0.3)
Co	1.6(0.15)	0.76(0.1)	0.7(0.3)	1.35(0.20)	1.0(0.1)	0.95(0.10)
Fe	5375(200)	2050(200)	2050(200)	3150(250)	2300(100)	1900(100)
Sc	2.55(0.15)	1.25(0.15)	1.1(0.2)	1.7(0.2)	1.3(0.1)	1.2(0.1)
Cr	18.2(0.8)	10.3(1.5)	9.6(1.6)	13.3(1.8)	11.5(0.6)	9.5(0.8)
Hg	3.45(0.5)	2.1(0.6)	4.8(1.4)	3.5(1.0)	2.0(0.4)	1.9(0.3)
Se	4.4(1.2)	2.5(0.5)	3.4(2.0)	2.8(1.0)	2.5(0.3)	2.5(0.5)
Th	0.68(0.07)	0.29(0.10)	0.28(0.10)	0.40(0.10)	0.29(0.03)	0.27(0.03)
Ce	7.0(0.6)	2.9(0.4)	2.3(0.8)	4.5(0.5)	1.4(0.1)	0.82(0.10)
Ag	<0.5	<1	<4	1.7(1.0)	<1	<1
Ni	<15	<30	<15	250(250)	20(15)	<25

*$\mu g/m^3$

APPENDIX 5

TABLE 5-1: COLLECTION DATA FOR MISCELLANEOUS SAMPLES

Sample	Type	Location	Dates	Volume, m^3	Comments
A1	Andersen Sampler	Niles, Michigan	3/6/69-4/6/69	85	
A2	"	"	14/8/69-16/8/69	82.5	Hot, hazy, humid
A4	"	"	19/8/69-21/8/69	81.2	Warm, dry
NJ1	47 mm filter, Microsorban	Hasbrouck Heights, New Jersey	25/12/69-28/12/69	249	Snow during most of collection
M1	20 x 25 m filter, Microsorban	Marietta, Ohio	17/12/69-18/12/69	2140	Snow
M2	"	"	18/12/69-19/12/69	2040	Snow
M3	"	"	19/12/69-20/12/69	2700	-
M4	"	"	19/12/69-20/12/69	2860	-

TABLE 5-2: ANDERSEN SAMPLE A1 (ng/m^3)

	7	6	5	4	3	2	1
Na	5.1(0.6)	5.7(0.6)	5.7(0.6)	3.2(0.4)	7.3(0.8)	5.4(0.6)	13(2)
Mg	<4	<4	<5	9(5)	28(8)	70(20)	48(20)
Al	17(2)	9(1)	18(2)	30(3)	41(5)	50(5)	57(6)
Cl	4.1(0.8)	8.0(1.2)	7.7(1.2)	3.1(1.2)	8.7(1.2)	4.0(0.8)	4.0(0.8)
K	25(3)	19(2)	22(3)	18(2)	46(5)	41(5)	61(7)
Ca	8(8)	14(7)	22(9)	33(9)	77(15)	80(20)	140(30)
Sc	<0.02	<0.02	0.04(0.02)	<0.03	0.04(0.02)	0.05(0.02)	0.11(0.03)
Ti	-	-	-	-	-	-	-
V	0.12(0.02)	0.07(0.02)	0.12(0.02)	0.10(0.03)	0.18(0.02)	0.18(0.02)	0.09(0.02)
Cr	<1	<1	<1	2(1)	5(1)	2(1)	5(1)
Mn	1.5(0.2)	2.2(0.3)	1.9(0.2)	0.7(0.1)	2.1(0.3)	1.3(0.2)	1.7(0.2)
Fe	-	-	-	-	-	-	-
Co	-	-	-	-	-	-	-
Ni	-	-	-	-	-	-	-
Cu	<1	1.2(0.6)	1.2(0.6)	7(1)	<1	6(1)	<1
Zn	22(10)	28(3)	36(10)	35(5)	26(4)	23(8)	18(10)
Ga	-	-	-	-	-	-	-
As	-	-	-	-	-	-	-
Se	<0.6	0.5(0.5)	0.5(0.5)	1.2(0.8)	1.2(0.8)	<0.8	1.2(0.8)
Br	1.7(0.2)	1.5(0.3)	0.96(0.20)	0.80(0.20)	0.64(0.20)	0.28(0.15)	0.04(0.04)
Ag	-	-	-	-	-	-	-
In	0.004(0.001)	0.012(0.004)	0.006(0.002)	<0.002	<0.002	<0.002	<0.002
Sb	-	-	-	-	-	-	-
I	-	-	-	-	-	-	-
La	0.01(0.01)	0.04(0.02)	0.13(0.02)	0.12(0.02)	0.18(0.04)	0.04(0.02)	0.12(0.02)
Ce	-	-	-	-	-	-	-
Sm	0.0038(0.0005)	<0.0030	0.0038(0.0035)	<0.0035	0.0067(0.0042)	0.0097(0.0038)	0.0061(0.0035)
Eu	-	-	-	-	-	-	-
W	-	-	-	-	-	-	-
Hg	-	-	-	-	-	-	-
Th	-	-	-	-	-	-	-

TABLE 5-3: ANDERSEN SAMPLE A2 (ng/m^3)

	F	7	6	5	4	3	2	1
Na	36(4)	14(2)	25(3)	44(5)	19(2)	31(4)	33(4)	42(5)
Mg	<38	<30	<42	95(44)	65(35)	200(60)	-	-
Al	46(5)	27(3)	37(4)	93(10)	270(30)	450(50)	520(60)	400(40)
Cl	<60	7(3)	15(4)	6(4)	17(4)	30(5)	25(6)	32(6)
K	-	-	-	-	-	-	-	-
Ca	-	-	-	-	-	-	-	-
Sc	-	-	-	-	-	-	-	-
Ti	3(3)	<3	3(3)	<3	7(4)	23(6)	22(10)	22(10)
V	0.31(0.04)	1.0(0.1)	0.77(0.08)	0.53(0.06)	0.57(0.06)	1.2(0.2)	0.68(0.13)	0.65(0.1)
Cr	-	-	-	-	-	-	-	-
Mn	2.6(0.3)	6.3(0.7)	14(2)	13(2)	5.7(0.6)	8.4(0.9)	5.9(0.6)	5.9(0.6)
Fe	-	-	-	-	-	-	-	-
Co	-	-	-	-	-	-	-	-
Ni	-	-	-	-	-	-	-	-
Cu	2.3(1.7)	2.1(1.4)	3.6(1.7)	<2	<3	8(5)	13(7)	7(7)
Zn	-	-	-	-	-	-	-	-
Ga	-	-	-	-	-	-	-	-
As	-	-	-	-	-	-	-	-
Se	-	-	-	-	-	-	-	-
Br	22(3)	8.6(0.9)	8.0(0.8)	6.1(0.7)	5.2(0.6)	9.1(1.0)	2.9(0.7)	3.0(0.7)
Ag	-	-	-	-	-	-	-	-
In	<0.003	<0.003	0.005(0.004)	0.004(0.004)	0.004(0.003)	<0.005	-	-
Sb	-	-	-	-	-	-	-	-
I	3(2)	3(2)	<4	3(3)	2(2)	<4	-	-
La	-	-	-	-	-	-	-	-
Ce	-	-	-	-	-	-	-	-
Sm	-	-	-	-	-	-	-	-
Eu	-	-	-	-	-	-	-	-
W	-	-	-	-	-	-	-	-
Hg	-	-	-	-	-	-	-	-
Th	-	-	-	-	-	-	-	-

TABLE 5-4: ANDERSEN SAMPLE A4 (ng/m^3)

	F	7	6	5	4	3	2	1
Na	130(20)	18(2)	10(1)	13(2)	14(2)	23(3)	41(5)	58(6)
Mg	120(60)	<30	<24	29(25)	51(26)	130(40)	180(70)	200(70)
Al	72(8)	14(2)	14(2)	44(5)	100(10)	230(30)	320(40)	400(40)
Cl	<60	22(3)	6(3)	11(3)	12(3)	16(3)	47(5)	39(5)
K	-	-	-	-	-	-	-	-
Ca	-	-	-	-	-	-	-	-
Sc	-	-	-	-	-	-	-	-
Ti	81(4)	<2	<2	4(2)	<2	14(4)	25(6)	24(7)
V	0.81(0.09)	0.09(0.02)	0.10(0.02)	0.26(0.03)	0.31(0.04)	0.57(0.06)	0.63(0.08)	0.67(0.09)
Cr	-	-	-	-	-	-	-	-
Mn	4.2(0.5)	-	-	-	-	5.4(0.6)	7.3(0.8)	9.2(1.0)
Fe	-	-	-	-	-	-	-	-
Co	-	-	-	-	-	-	-	-
Ni	-	-	-	-	-	-	-	-
Cu	4(3)	2(1)	<1	<2	<2	<3	8(5)	5(5)
Zn	-	-	-	-	-	-	-	-
Ga	-	-	-	-	-	-	-	-
As	-	-	-	-	-	-	-	-
Se	-	-	-	-	-	-	-	-
Br	110(20)	6.4(0.7)	4.4(0.5)	6.8(0.7)	7.1(0.8)	9.5(1.0)	7.3(0.8)	3.8(0.6)
Ag	-	-	-	-	-	-	-	-
In	-	-	-	-	-	-	-	-
Sb	-	-	-	-	-	-	-	-
I	7(4)	<2	<2	<2	<2	<2	<4	<4
La	-	-	-	-	-	-	-	-
Ce	-	-	-	-	-	-	-	-
Sm	-	-	-	-	-	-	-	-
Eu	-	-	-	-	-	-	-	-
W	-	-	-	-	-	-	-	-
Hg	-	-	-	-	-	-	-	-
Th	-	-	-	-	-	-	-	-

TABLE 5-5: NEW JERSEY AND OHIO FILTERS (ng/m^3)

	NJ1	M1	M2	M3	M4
Na	600(60)	290(40)	170(20)	130(20)	520(70)
Mg	180(200)	<800	<125	200(70)	<3000
Al	680(70)	3200(400)	740(100)	800(80)	2600(300)
Cl	470(70)	-	-	-	-
K	270(30)	980(100)	350(40)	250(30)	2700(300)
Ca	420(140)	650(200)	300(100)	340(70)	570(300)
Sc	0.70(0.07)	2.5(0.3)	0.74(0.08)	0.62(0.07)	3.5(0.4)
Ti	190(50)	250(100)	90(25)	90(20)	250(250)
V	65(7)	8.6(1.0)	4.1(0.5)	3.2(0.4)	17(2)
Cr	9.0(1.0)	110(20)	14(2)	59(6)	1700(200)
Mn	10(1)	950(100)	38(5)	37(4)	3500(400)
Fe	1500(200)	3800(400)	1200(200)	800(80)	5100(600)
Co	1.1(0.2)	2.0(0.2)	0.59(0.06)	0.55(0.06)	4.3(0.5)
Ni	28(10)	<25	<12	<10	<30
Cu	40(4)	42(10)	65(10)	22(5)	120(30)
Zn	94(10)	220(30)	170(20)	120(20)	450(60)
Ga	0.8(0.3)	2.5(0.5)	1.0(0.3)	0.5(0.2)	3.5(1.0)
As	<3	16(4)	9(2)	5.2(1.0)	40(8)
Se	1.4(0.6)	5.8(1.0)	3.2(1.0)	1.4(0.3)	11(2)
Br	100(20)	77(8)	70(10)	40(8)	190(20)
Ag	<2	<1	<1	<1	<2
In	0.036(0.013)	0.08(0.09)	0.04(0.01)	0.04(0.01)	0.3(0.3)
Sb	2.1(0.3)	4.0(0.4)	5.4(0.6)	2.5(0.3)	11(2)
I	-	-	<1	<1	-
La	1.2(0.2)	2.2(0.3)	1.2(0.2)	0.66(0.15)	2.2(0.5)
Ce	2.1(0.3)	7.1(0.8)	1.4(0.3)	1.3(0.2)	14(2)
Sm	0.15(0.04)	0.50(0.05)	0.16(0.02)	0.12(0.02)	0.71(0.10)
Eu	0.045(0.020)	0.10(0.03)	0.032(0.008)	0.022(0.005)	0.17(0.06)
W	0.6(0.3)	<0.4	0.32(0.15)	<0.15	2.8(0.7)
Hg	0.6(0.2)	0.2(0.6)	<0.5	0.3(0.3)	2(1)
Th	0.18(0.02)	0.89(0.25)	0.21(0.10)	0.31(0.10)	1.1(0.4)